Author:
Sosa Madrid, Martha Laura L

Title:
Creating hierachical particle assemblies using organo-clays

composites with anionic polymers

Creating hierarchical particle assemblies using organo-clays: composites with anionic polymers

Martha Laura Sosa Madrid

A dissertation submitted to the University of Bristol in accordance with the requirements for award of the degree of Doctor of Philosophy in the Faculty of Science.

School of Chemistry

September 2021

[Word Count: 29 353]

Abstract

Anionic polymers such as polyacrylic acid and alginates are used in dentistry for various purposes. This research investigated how properties of such systems can be modified and potentially improved by addition of clay nanofillers. Natural clay samples were used as well as different samples of the modified clay to achieve improved mechanical properties on materials such as glass ionomer cements (GICs) and hydrogels.

Clay particles (montmorillonite (MMT) platelets, size < 1 µm) were treated with different length chains of ω-amino carboxylic acids (ω-aa): 12-aminododecanoic acid (ADA), 6-aminohexanoic acid (AHA) and γ-aminobutyric acid (GABA); there has been evidence that such amino acids help dispersion into polymer matrix. Different routes for treating the clay were investigated and the best results were obtained using elevated temperature and low pH.

The matrix of GICs consists of polymers such as polyacrylic acid (PAA) and such polymers interact well with clay. The addition of ω-aa modified clays was found to increase the compressive strength of the GICs by ~70 %.

Another major problem with dental materials was addressed, currently there is no available material that offers effective, lasting protection against bacterial colonisation. For this reason, the same clay (MMT) was treated with chlorhexidine (CHX) to create a system that would retain its antimicrobial properties, or even could serve as a slow release system depending on the amount of CHX added. CHX intercalated into MMT was found to be bound strongly with very slow or no release.

Additionally, a novel nanofiller system was proposed which could offer both enhanced strength and antimicrobial properties, by adding the modified clays described above into an alginate hydrogel structure. The Young's modulus was determined by compressing gel beads; inclusion of clay particles resulted in an increase in modulus (between 33 and 69%) but the surface modification with ω-amino acids did not result in a significant difference.

Acknowledgments

I would like to thank my supervisors Jeroen S. Van Duijneveldt, Michele E. Barbour and Annela Seddon for their expertise, guidance, and patience to deal with the melodramatic events occurred in parallel to my attempts to finish this research. I could have not made it happen without your support. You have not only taught me science you have also been an example of what I should aspire to be like one day.

I am grateful to Dr Natalie Pridmore and Dr Hazel Sparkes for training and assistance with the powder X-ray diffraction. To Dr Jeon-Charles Eloi for assistance and access to Scanning Electron Microscopy and Rafael Moreno for helping with his brilliant knowledge about hydrogels. To Rob Richardson and Annela Seddon for carrying out small angle X-ray scattering measurements on my behalf.

I am thankful for the full-time PhD funding from CONCyTEP, CONACyT and to the University of Bristol Disability Services for the support offered to endure hardships.

To the BCFN crew and my multiple group mates in JSvD lab and the Dental School, especially to Sai, Alex H. and Matt for listening to my multiple complaints, for the laughs and tears shared; to Andy, for the food talks; and to Sian, Sara, Sarah, James, for the help with anything I seemed to not know "how to". Thank you very much!

To my friends, if I have to make a list of reasons it would be longer than the thesis itself, so I'll try to keep it short. To the ones around the world, thanks for reading my messages or taking my calls at funny hours: Zoey, Claudia, Oly, Scar, Lino, Vini, Evelyn, Irving, Mel, Gerardo, Anthony, Xiomara, Juan, Curtis, Alina; to the ones in the UK, thanks for being part of my life: Guille, Perla, Sandra, Benny, Fer, Ange, Jacek, Beedie, Ramunas, Will B., Ivett, Emily, Monica.

To the Eldridges for welcoming me into their family. Special mention to Alex, for dealing with me on my good and bad days, for the food, the talks, the tea but overall thanks for always holding my beloved hair at the right moment.

I could express many times and, in several ways, how grateful I am to my family, but it will never be enough! To my dad, thanks for your support even after I told you I wasn't becoming an Economist, I just love science way too much. To my mum, for being the best human being on earth, sorry for making you worry too much while being too far away. To my brother… for everything, I always took you for granted until we were kilometres apart. To Danna †, Robin †, Tugui and Olaf, because the world without unconditional pet's love would not be the same. I love you all!

I would like to extend this thanks to all the people that helped me these last years to not lose my mind, I have become a stronger person after all, but it wouldn't have been possible without you. To my mentor, Alison, thanks for opening my eyes to realise that I shouldn't be

my worst enemy. To my social prescribing rep, Will S. for the referrals and sessions to improve my wellbeing.

Finally, to every single person that came to my rescue when everything seemed to go wrong, if I have forgotten your name, sorry, I am on meds that make my mind foggy, however, I can assure you my gratitude goes to you too.

"Es difícil volar cuando esperas la caída, es difícil soñar cuando no ves la salida… Y aunque ahora el mundo gire en otra dirección, eres tú quién le da sentido a lo que dicte tu dormido corazón, ¡no todo está perdido!"

- Jorge Ruiz (Maldita Nerea)*, La respuesta no es la huida.*

Author's Declaration

I declare that the work in this dissertation was carried out in accordance with the requirements of the University's Regulations and Code of Practice for Research Degree Programmes and that it has not been submitted for any other academic award. Except where indicated by specific reference in the text, the work is the candidate's own work. Work done in collaboration with, or with the assistance of, others, is indicated as such. Any views expressed in the dissertation are those of the author.

SIGNED: ....Martha Laura Sosa Madrid............. DATE: ....27/09/2021................

Table of Contents

List of Figures

List of Tables

Chapter 1 Introduction

1.1 Clay

1.1.1 Montmorillonite

Over the years clays have been the subject of many academic studies but also find practical use in several applications. The clay mineral used in the research presented within this thesis is montmorillonite (MMT), which is the main component of the rock type bentonite.

Montmorillonite is a 2:1 aluminosilicate, meaning it is composed of an octahedral aluminium oxide layer between two tetrahedral silicon oxide layers, see Figure 1.1. It is naturally hydrophilic because of the presence of hydrated inorganic counterions (Na^+ or Ca^{2+}) in the interlayer space[1].
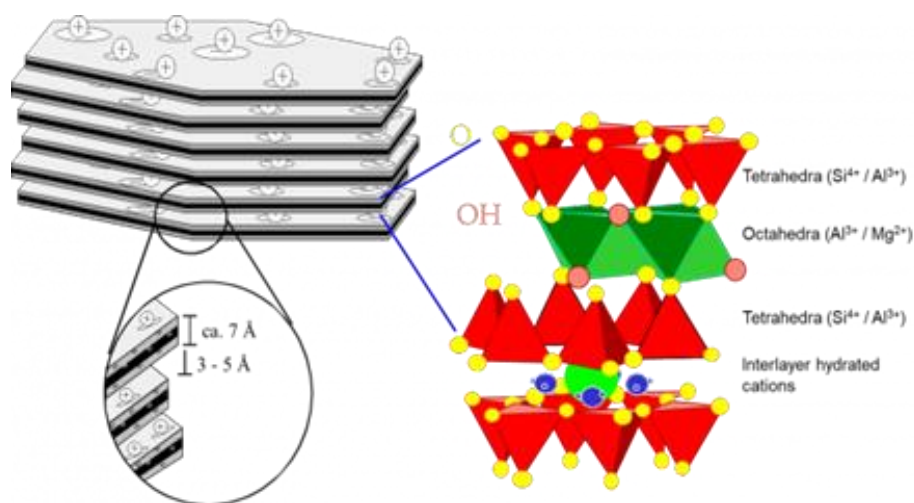
Figure 1.1 Bentonite clay structure[2].

Since the interaction between the anionic charge in the octahedral layer and the cation on top of the silicate layer is closer related to an exchange of charges, the existing cations can be exchanged for other cations of similar charge to generate organically treated clays[3]. Conversely it is also immiscible with many non-ionic organic polymers since the latter are essentially hydrophobic[1]. However, there are ways to overcome this limitation, one of them

is by attaching polar functional groups to either the mineral surface or the polymer chain, this is due to its ability to take up positively charged organic compounds. Common modifiers used for the organic modification of clays are quaternary ammonium cations[4], diamines[5], and amino acids[6].

There are two types of organic cation-exchange: one by replacing the inorganic counterions of the clay with short-chain compact cationic species, and the other by the intercalation of long chain alkylammonium or quaternary ammonium ions with an alkyl chain at the end. The latter one is also known as organoclay[1].

One well known application for these organoclays is their addition as nanofillers into composite materials as it has been found to enhance various material properties. The effectiveness of fillers depends on their physical-mechanical properties that are determined by the degree of their dispersion in the matrix as well as the filler particle size and shape[1]. However, not every modification works the same for all surfaces, and hence the development of different techniques is necessary[7].

1.2   Dental Materials

Over the years dentistry has been focusing on the preservation and enhancement of oral health, this by preventing cavities and diseases as well as rehabilitating defects such as missing, or damaged hard and soft tissues. Hence the importance of keep developing different materials that would facilitate the work.

All dental materials fall under four main groups: metals, ceramics, polymers and composites. According to their purpose, dental materials can be classified as:

- Preventive: toothpaste, mouthwash, fissure sealants, fluoride products, etc.
- Restorative: amalgams, metals (gold, silver), ceramics, calcium hydroxide, resins, etc.
- Auxiliary: waxes, acrylic resins, porcelain, finishing and polishing abrasives[8].

The interest in producing new dental filling materials emerged because of the necessity to improve the quality and diminish the risk of using environmentally unfavourable materials as is the case of amalgams made with an alloy of mercury, silver, tin and copper[9].

It is challenging to find alternative restoration materials because it is hard to get all the properties that made amalgams popular in the first place: their low cost, durability[10], strength, easy application[11], and antimicrobial effect[12].

Another reason to look for alternatives is that amalgams are not an aesthetical material, thereupon other products that look more like the natural teeth are preferred these days. That is the case of the ceramic inlays, composite resins and glass ionomer cements. However, none of these materials have been able to match the properties of amalgams. They need to be replaced after a certain amount of time being used as they start to wear away due to use, and some also decay around the margins (periphery) of the filling. In addition, dental materials available now do not offer effective, lasting protection against bacterial colonisation.

1.2.1 Glass ionomer cements (GICs)

Glass ionomer cements (GIC) are a composite material that could serve as a preventive dental material, but it is mainly used for restoration due to its characteristics. GICs are prepared by mixing powder with liquid to produce a plastic mass that after some time sets to a rigid solid.

Although none of the commercially available glass-ionomer cements are chemically identical, they have many features in common and also, they can be found in different presentations: powder-liquid, anhydrous cements and capsules[13].

The powder part of a GIC consists of alumina-silica based glass filler particles containing calcium fluoride, while its liquid part contains polyacrylic and tartaric acid[8]. The setting of the GICs is based on neutralization, see equation (1.1) of the polyacid by the basic glass with the formation of metal polyacrylate units, which has been demonstrated by various techniques, including electron probe microanalysis[14] [15], infrared spectroscopy[16], Fourier-transform infrared spectroscopy[17], ^{13}C NMR spectroscopy[18], and pH change[19] [20]. This setting process involves three overlapping stages: dissolution, gelation and hardening.

$$MO \cdot SiO_2 + H_2A \rightarrow MA + SiO_2 + H_2O \qquad (1.1)$$

Glass   Acid   Salt   Silica gel
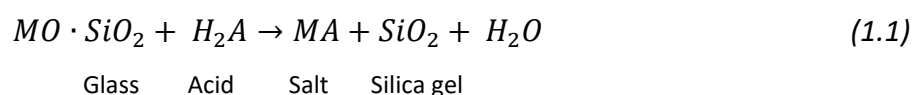
In the dissolution process, see Figure 1.2a, the acid reacts with the outer layer of glass, the layer is depleted in calcium, aluminium, sodium and fluorine ions and a silica gel remains. Then, the initial set, called gelation, takes place, the calcium ions react readily with carboxyl groups of the acid. Figure 1.2b shows this phase of the setting process which demonstrates calcium ions cross-link polyacid molecules. Then, the aluminium ions, which form a part of the glass network that is more difficult to break down, are finally released. When compared with calcium ions, the trivalent nature of aluminium ions makes a higher degree of cross-linking of polymer molecules occur (Figure 1.2c). Thus, the formation of the aluminium salt bridges provides the final strength to the cement. The hardening phase normally last 7 days. The final structure is as shown in Figure 1.2d, and is composed of glass particles, which are surrounded by a silica gel in a cross-linked polyacrylic acid (PAA) matrix. It is the aluminium and calcium ions that will eventually form the salt matrix[21].
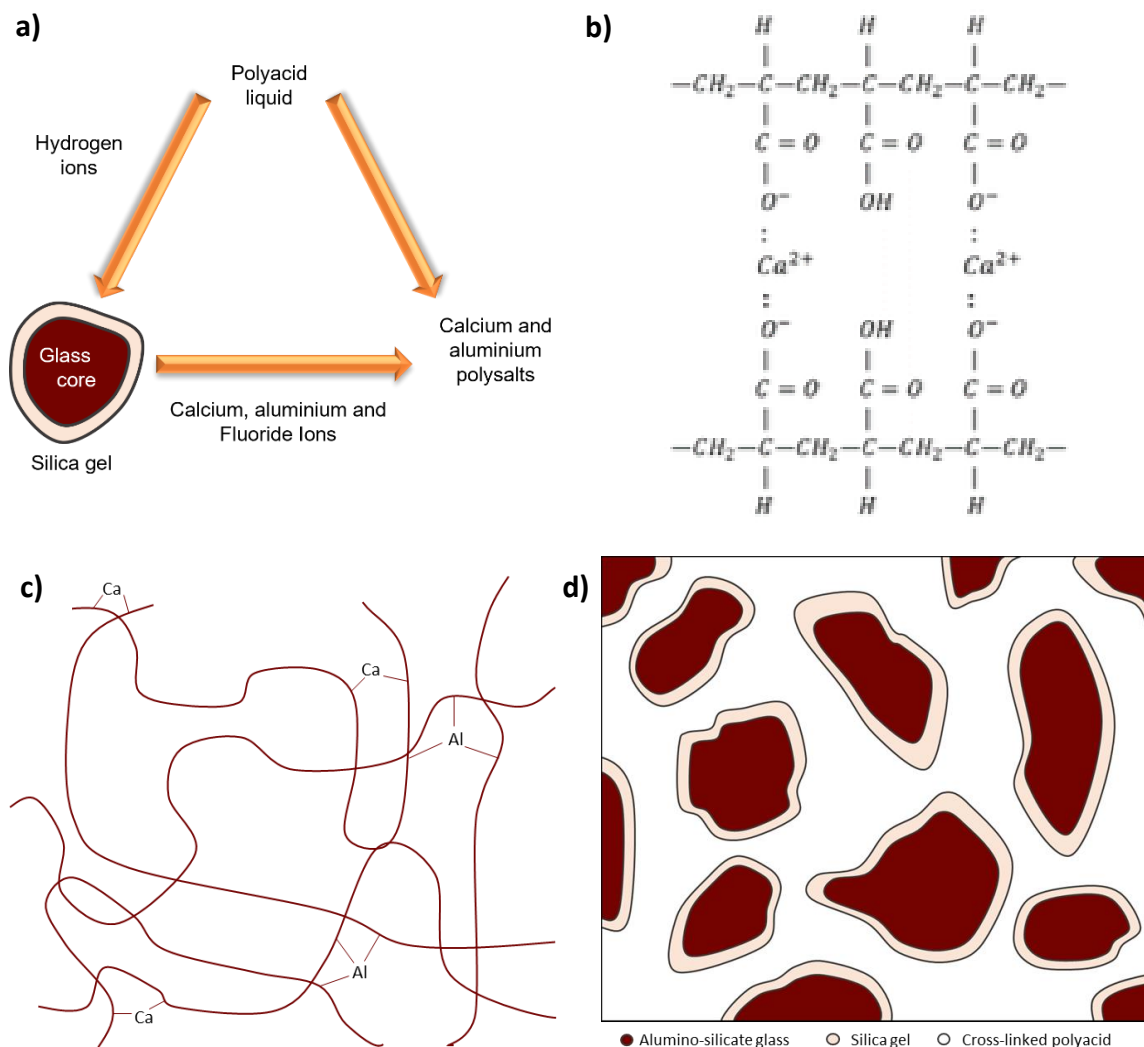
Figure 1.2. Setting process of a Glass Ionomer Cement (GIC). a) Dissolution, b) Gelation, c) Hardening and d) Final structure of the material.

The reason why GICs have become one of the accepted dental restorative and adhesive materials is because of their favourable handling and clinical properties, of these properties one of the most remarkable is the thermal compatibility with tooth enamel and dentine due to their similarity in the thermal expansion coefficients with the tooth structure, adhesion to moist tooth structure and base metals, low cytotoxicity and biocompatibility[22]. Furthermore, GICs are easier to work with than some other dental materials, such as silicate and zinc phosphates[23].

However, GICs present relatively poor physical properties, it means that they tend to be quite brittle. Properties such as compressive and tensile strength are low, limiting their possible use in some larger posterior load-bearing restorations[24]. Although in some cases when used as

restorative materials, glass ionomer cements will acquire enhanced loads when their powder:liquid mixing ratio is increased, they are unfortunately quite weak to withstand the masticatory forces in the posterior area of the mouth.

There are different parameters that could affect the effectiveness of dental materials, such is the case of the mechanical properties, such as, compressive strength (CS), diametral-tensile strength (DTS), flexural strength (FS), flexural modulus (Ef), as well as the working time (WT) and the setting times (ST) at determined temperature (usually room temperature) [25] [26] [27] [28].

In the case of GIC one of the most important is the powder:liquid ratio. It has been reported that changes in this ratio will impact the stiffness of the mix, setting rate, compressive strength, superficial hardness, resistance to aqueous attack[29] and porosity distribution[30]. Another parameter is the setting time itself; this depends on the product used, but it is important to give it enough time to set after the mixing and packing so it can offer its best strength[31]. Although some GICs have showed that their compressive strength continues increasing over a period of 100 days[29], this depends in the polymeric acid matrix of the material and it seems to be better in those based on polyacrylic acid[32].

There have been some projects where GICs have been mixed with different materials to try improving their mechanical properties such is the case of N-vinylpyrrolidone containing polyacids, nano-hydroxy and fluoroapatite[33], or the addition of 1-methacryloylpyrrolidone-2-carboxylic acid[34] or the addition of other filer particles like glass fibre reinforcement[35].

1.3 Chlorhexidine

Chlorhexidine (CHX) is an antimicrobial agent that could be bacteriostatic and bactericidal depending on; the concentration used, pH, temperature and time of contact of the solution with oral structures. CHX binds with hard and soft tissues in the oral cavity, and it could be slowly released over time, making it efficient against gram-positive and gram-negative bacteria as well as yeasts and some viruses. It can be found in three forms: digluconate, diacetate, both water soluble and hydrochloride salts that is poorly soluble in water. It is commonly used in commercial dental products that are available to the general public such as mouthwash, toothpaste, gels, sprays, varnishes and even chewing gums[36].

Its wide use in medical and dental applications make this substance interesting to study, additionally, it builds on recent work where slow release chlorhexidine technologies have been developed and implemented to dental materials[23][37][38][39].

1.4 Project aims

The aim of this project was to explore hierarchical structures and their applications in specific composite materials used in dentistry, in this instance a glass ionomer cement and a hydrogel.

The approach comprised the modification of a natural clay, montmorillonite (MMT), with ω-amino carboxylic acids (ω-aa), in order to determine whether this makes any significant change in the final structure. Other types of amino acids were not considered as candidates due to the particularity of the groups and charges present in their composition, while all amino acids have the same basic structure what ω-amino carboxylic acids provide is a C chain with the end groups $-NH_2$ and -COOH, respectively. The only amino acid with these characteristics is glycine, which has been reported to be used in dental materials however, its structure is too simple as it consists of only one C linking the end groups. Additionally, considering that the cost of ω-aa and glycine is very similar, the focus of this research project went to the use of only ω-amino carboxylic acids.

Three ω-aa were selected to measure the significance of using different length chains: 12-aminododecanoic acid, 6-aminohexanoic acid and γ-aminobutyric acid. The selection criteria of the length were based on the literature for the longest one whilst the other two are ratios of a half and a third, respectively, in order to establish if the chain length influences the mechanical properties that we are aiming for, as well as their biocompatibility.

GICs were picked as one option to explore, as their matrix consists of polymers such as polyacrylic acid (PAA), and such polymers are known to interact well with clays, therefore the addition of a clay structure could benefit the properties presented by the dental material itself.

Furthermore, the opportunity of developing new materials to address another major problem (antimicrobial resistance) was addressed by creating a system that might have useful antimicrobial properties. As clay minerals interact readily with amines, their interaction with

7

chlorhexidine (CHX), a common antimicrobial agent, may result in a nanofiller offering a combination of strength enhancement and slow release of antimicrobial. The release test reported below was designed to determine the ability of this clay treated with different chlorhexidine concentrations to release CHX in aqueous environments.

Lastly, clay modified hydrogel (sodium alginate) beads were prepared as an alternative potential route to hierarchical structured materials. Whilst chemically GICs and alginate gels are similar in the sense of consisting of organic polyacids with ionic crosslinks, their mechanical properties are very different indeed. Our hope and intention were to use the hydrogel beads as an alternative (and hopefully, more accessible route) to quantifying the interaction between the clays and the polymer.

1.5   Thesis Overview

This thesis consists of 6 chapters. Chapter 2 shows the methods followed to produce the modified organo-clays, using three different length chain ω-amino carboxylic acid (12-aminododecanoic acid, 6-aminohexanoic acid and γ-aminobutyric acid) and a natural clay (montmorillonite), how they were characterised using various techniques and the comparison between the original clay and the resulted materials.

Chapter 3 presents the first proposed application of the modified clays, in this instance by adding it into a glass ionomer cement matrix to then test if the mechanical properties of this dental materials have been positively or negatively affected, different parameters were considered to achieve an increase in the compressive strength of the dental cements.

In chapter 4, the same natural clay (montmorillonite) was treated but this time with an antimicrobial compound (chlorhexidine). Several characterisation techniques were used along with a release test in order to analyse how the chlorhexidine contained in the matrix would behave if these modified clays were added into aqueous environments.

Chapter 5 is the final experimental chapter, and it focuses on another application of the modified clays. Samples of the different clays made in chapter 2 and 4 were added into alginate hydrogels. Their composition and mechanical properties were characterised.

Chapter 6 provides a general conclusion of the results obtained within the research, as well as addressing some suggestions for further work.

Finally, some additional information regarding details of the several samples prepared in the previous chapters is presented in Appendix form.

Chapter 2 Modified Clays

2.1 Introduction

There has been a growing interest in creating composites with improved properties, and different methods have been tested. One of these methods proposes the addition of a filler that will interact with the matrix of the composite material, the result depending on the filler's characteristics. One class of potential filler materials are clay minerals, following a suitable surface modification with organic molecules, because of the advantages that clays have shown.

In particular work has been done using montmorillonites due to the large surface area they offer, the fact that they can be saturated with cations, how relatively easy it is to measure the distance between plates using XRD and how this helps to understand the packing of the adsorbed molecules by considering their stericity.[40]

How the organic molecule interacts with the clay mineral varies depending on several factors, such as, considering if the cation-exchange mechanism is pH sensitive, how many proton-accepting groups the molecule has, the chain length or the amount of C atoms of the molecules.[40]

In 1985 the first polymer clay nanocomposite was created at Toyota Central R&D Labs, Inc. and it opened a wide range of new application opportunities for automotive, electric and food industries.[41] In 1990, the first clay-based polymer nanocomposite was used for industrial purposes[42]. One of the approaches pioneered by Toyota involved modifying the clay first using amino-dodecanoic acid (ADA) – prior to further processing in the monomer intercalation method[43]. See Figure 2.1. This inspired the clay modification routes explored in the present work.
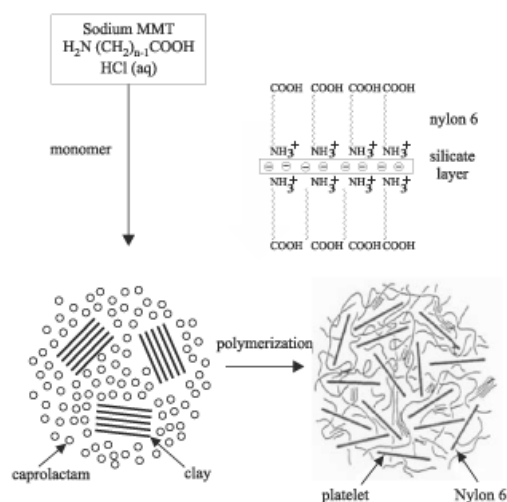
Figure 2.1. Montmorillonite treated with caprolactam followed by polymerisation. Scheme that represents the arrangement of the ω-amino carboxylic acids chains on the surface of a montmorillonite platelet.[44]

The results described in the Toyota patents[43][45][42] corresponding to these previous approaches demonstrate how the formation of nanocomposites, made by the addition of amino carboxylic acids followed by polymerisation, helped to improve mechanical properties, such as Young's modulus, thermal expansion, heat distortion temperature and shear stress response.

This technique was not only followed by Toyota, inspired by their process Nanocor® commercialised a Nylon-6 nanocomposite. They took 12-aminododecanoic acid (ADA) modified montmorillonite and incorporated this into Nylon-6 by in situ polymerization. The process involves polymerization after mixing the monomer (or oligomer) with the organically modified clay; the advantage of doing it this way is that the ADA links with the polymer chains during the polymerisation[46], see Figure 2.2.
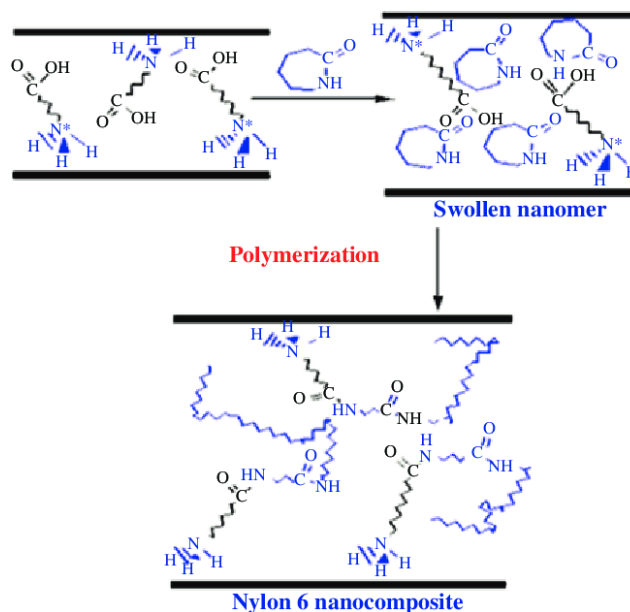
Figure 2.2. In situ polymerisation to produce Nylon-6 nanocomposite.[46]

The fact that the ADA helps the clay to interact with the polymers is of interest to us as our intention is to add modified clays to other materials that may also be able to interact favourably with the acid functionality of the amino acid, specifically glass ionomer cement (GIC) matrix and the sodium alginate hydrogel.

In this chapter we explore different preparation methods of montmorillonite clay modified with ω-amino carboxylic acids (ω-aa). We employ different concentrations of ω-aa, as well as three different length chains of ω-amino carboxylic acids (ADA, AHA and GABA). The modified clay samples were then analysed using elemental analysis and X-ray scattering and diffraction, to determine which was the most effective and efficient route for obtaining the modified clays.

2.2   Materials and Methods

2.2.1 Clay functionalisation with ω-amino carboxylic acids (ω-aa)

The clay used was Wyoming montmorillonite, SWy-2 (MMT), which was purchased from the Clay Minerals Society source clays repository at Purdue University. Its molecular formula is

$(Si_{7.94}Al_{0.06})$-$(Al_{2.88}Fe_{0.5}Mg_{0.62})O_{20}(OH)_4Na_{0.68}$[47], and the cation exchange capacity (CEC) of this clay is 84 mmol / 100 g[48]. The ω-amino carboxylic acids used were: 12-aminododecanoic acid (ADA) (95% Sigma Aldrich UK), 6-aminohexanoic acid (AHA) (≥98.5% Sigma Aldrich UK and 99+% ACROS Organics) and γ-aminobutyric acid (GABA) (97 % Sigma-Aldrich). Hydrochloric acid 35% (HCl) was used (GPR Rectapur®, VWR Chemicals) and deionised water (Millipore MilliQ).

For imaging purposes some of the samples were labelled with Acridine Orange (AO w/Zn), pure, ca. 55% dye content, from ACROS Organics. This dye product also contained $ZnCl_2$ (to aid solubility). In order to avoid the Zn^{2+} ions interfering with the clay surface chemistry, later experiments were carried out with the base form of the dye that has no salt added, Acridine Orange base (AO), 75% dye content, from Sigma-Aldrich.

2.2.1.1 Sample preparation following different routes

For most of the modified clay samples, an initial suspension was made by adding 10 g of clay to 1 L of deionised water and left to mix with the help of a magnetic stirrer for 24 hours to ensure dispersion. At this point, the clay powder may still contain some impurities with a larger particle size, such as quartz, and therefore the suspension was allowed to stand for 3 hours to allow the large particles to settle. The supernatant was kept as stock clay suspension, the average amount of clay remaining in the solution was ~8 g.

For the samples that were dyed, acridine orange corresponding to 1% of the clay mass was added to the clay suspension and it was left in stirring for ~2 hours.

For most of the modified clay samples the Cationic Exchange Capacity (CEC) of the clay was taken into account when designing the preparation protocol. This CEC refers to the number of exchangeable cations and is traditionally expressed in units of mmol per 100 g of clay. The cation exchange capacity of the clay used in this research project (SWy-2 MMT) corresponds to 84 mmol /100 g. However, a small number of other samples were prepared aiming to attain a certain concentration (i.e., 0.02 M or 0.35 M) at the end of the treatment.

Two main routes were followed, the first being a "neutral" treatment referring to just mixing the clay with the ω-aa without the intervention of any other factors and the "acid" treatment, as its name implies utilises an acid (as well as heating) during the mixing process, see Figure 2.3.
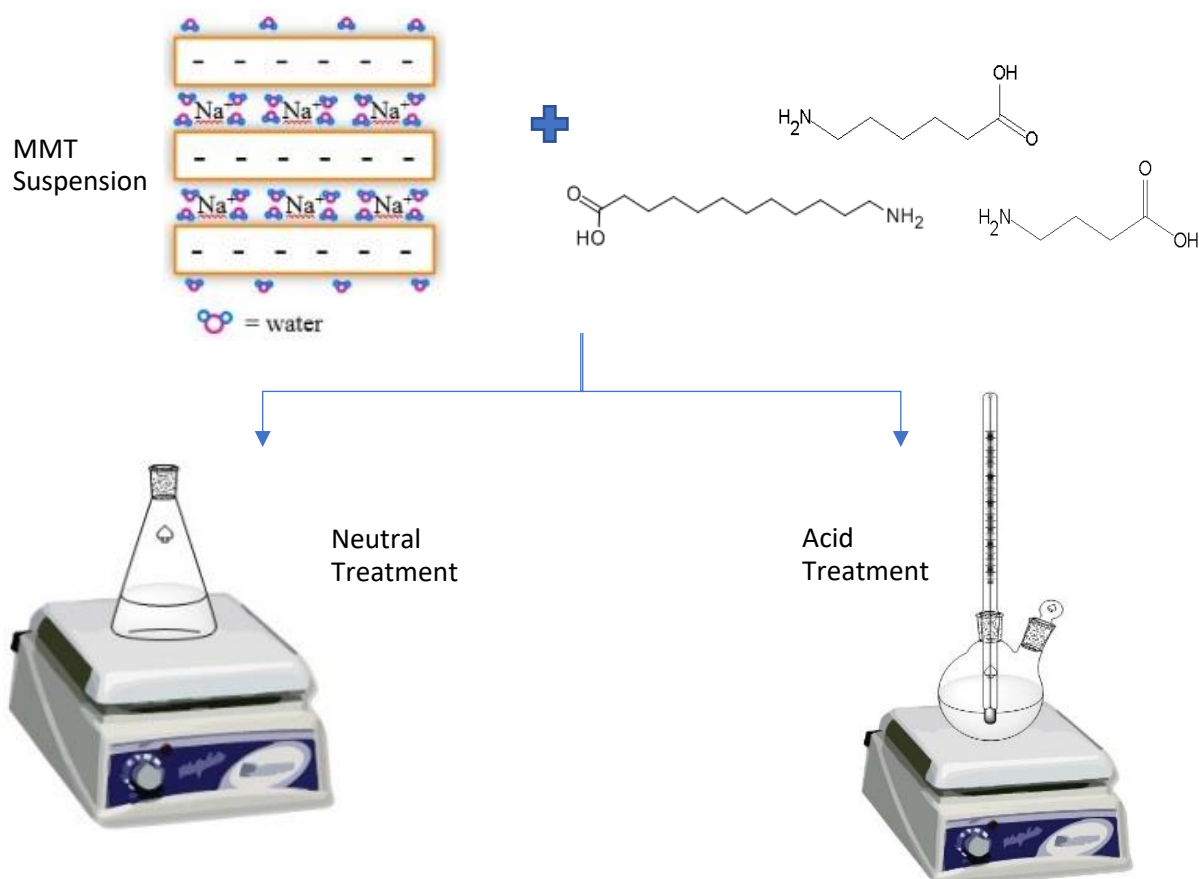
Figure 2.3 Scheme of clay treatment with ω-amino carboxylic acids.

The resulting product from both routes were either dried at 60 °C under vacuum during ~12h or freeze dried using an Alpha 1-2 LD Plus Martin Christ freeze dryer, using a chamber temperature around -55 °C.

Using a magnetic stirrer to mix the clay suspension with the respective ω-amino carboxylic acid during 24 h at room temperature (RT). After this time the suspension obtained was centrifuged at 10k rpm for 40 minutes in a Sorvall Legend-T, decanted, and dried. Some samples were dried at 60 °C under vacuum overnight (~12h) and some other samples were frozen and freeze dried. The product of some samples needed to be ground using a pestle and mortar to get a powder sample.

Besides the name given to this treatment, the pH of the clay sample is not neutral, it was denoted this way due to the lack of further modification to the natural pH of the clay which could be as high as 9 – 10 when dispersed in water. The treatment would not be impacted by this pH, therefore, it is important to highlight that the label "neutral" refers to the lack of any additional substance in the sample preparation.

In Table 2.1 a further description of how each sample was prepared is given.

Table 2.1. Process to prepare the modified clay by neutral treatment.

Sample	Description			
	Clay content (in solution)	ω-aa content	Dye 1% w/w	Drying technique
MMT+AO+ADA 24h	~2 g MMT 250 ml	6 CEC (~2.19 g)	AO w/Zn (~0.02 g)	~60°C under vacuum overnight
MMT+AO+AHA 24h	~2 g MMT 250 ml	3 CEC (~0.66 g)	AO w/Zn (~0.02 g)	~60°C under vacuum overnight
MMT+AO+5x AHA 24h	~1.5 g MMT ~250 ml	19.8 CEC (~3.28 g)	AO (~0.015 g)	~60°C under vacuum overnight
MMT+AO+5x GABA 24h	~2 g MMT 250 ml	5 CEC (~0.87 g)	AO (~0.02 g)	Freeze dried
MMT+ADA 24h	~2 g MMT 250 ml	3 CEC (~1.08 g)	-	Freeze dried

MMT+AHA 24h	~2 g MMT 250 ml	3 CEC (~0.66 g)	-	Freeze dried
MMT+GABA 24h	~2 g MMT 250 ml	3 CEC (~0.52 g)	-	Freeze dried

2.2.1.1.2 Acid Treatment

For some of the samples a dispersion of 6 g MMT in 180 ml of deionised water was made and they were not subjected to a further cleaning step, mainly to keep the concentration fixed. The procedure of this treatment was inspired by the one described by Usuki in 2005[49], the main difference is that for the purposes of this chapter's objective, the procedure was stopped before the polymerisation steps as the intention was to get chains of ω-aa intercalated between the clay platelets.

This method consists of preparing 2 solutions. Solution A (MMT dispersed in water) is stirred at 80 °C. Meanwhile, solution B is prepared by heating water up to 80 °C, adding the ω-amino carboxylic acids while stirring and then the concentrated HCl.

Solution B was added to solution A with vigorous stirring for 5 minutes. Then it was filtered using vacuum (Buchner funnel), followed by 2 washes with hot deionized water (80 °C). After the washing step, the samples with dye were dried in the vacuum oven, whilst for the samples without dye the sediment was frozen and freeze dried. The product of some samples that formed clumps after the drying process needed to be ground using a pestle and mortar to get a fine powder sample.

The solutions were prepared as shown in Table 2.2. Also, as mentioned in the methodology, samples with added dye and without it were prepared.

Table 2.2. Process to prepare the modified clay by acid treatment.

Sample	Solution A		Solution B			
	Clay content (in solution)	Dye 1% w/w	ω-aa content	HCl (ml)	Water (ml)	Drying technique
MMT+AO+ADA HCl	~2 g MMT 250 ml	AO w/Zn (~0.02 g)	11.5 CEC (~4.15 g)	1.67	55.55	~60°C under vacuum overnight
MMT+AO+ADA HCl	~6 g MMT 180 ml	AO (0.06 g)	2.8 CEC (~3.08 g)	1.2	40	~60°C under vacuum overnight
MMT+AO+AHA HCl	~1.5 g MMT ~190 ml	AO (~0.015 g)	11.4 CEC (~1.88 g)	1.67	55.55	~60°C under vacuum overnight
MMT+AO+3x AHA HCl	~2 g MMT 250 ml	AO (~0.02 g)	35.4 CEC (~7.8 g)	1.67	55.55	~60°C under vacuum overnight
MMT+AO+GABA HCl	~2 g MMT 250 ml	AO (~0.02 g)	5.2 CEC (~0.9 g)	1.67	55.55	Freeze dried
MMT+ADA HCl	~6 g MMT 180 ml	-	2.8 CEC (~3.08 g)	1.2	40	Freeze dried
MMT+AHA HCl	~6 g MMT 180 ml	-	2.8 CEC (~1.88 g)	1.2	40	Freeze dried
MMT+GABA HCl	~6 g MMT 180 ml	-	2.8 CEC (~1.48 g)	1.2	40	Freeze dried
MMT+3x AHA HCl	~2 g MMT 250 ml	-	34.4 CEC (~7.58 g)	~1.7	~56	Freeze dried
MMT+3x GABA HCl	~2 g MMT 250 ml	-	34.4 CEC (~5.96 g)	~1.7	~56	Freeze dried

2.2.2 Characterisation

2.2.2.1 Fourier-transform Infrared Spectroscopy (FT-IR)

These data were obtained using a Perkin-Elmer Spectrum 100 FT-IR (PerkinElmer, Waltham, MA, USA) with an Attenuated Total Reflection attachment that allows a powder to be tested, at the teaching labs within the School of Chemistry. The samples were analysed in powder form and tests run in the wavenumber range from 400 to 4000 cm^{-1} and 600 to 4000 cm^{-1} respectively, with a resolution of 8 cm^{-1}.

This technique was considered useful as a preliminary test to corroborate if the ω-amino carboxylic acids treatment was giving different results compared with the neutral treatment. The test confirms the presence of ω-aa in the sample and, also, potentially provides information on how the ω-aa interacts with the clay (through peaks shifting for instance, compared to the pure compounds).

2.2.2.2 X-Ray Powder Diffraction (XRD)

This analysis was performed using a Bruker (Billerica, USA) D8 Advance Powder X-ray Diffractometer (Cu Kα radiation, λ = 1.54 Å) at 2θ values of 5°–40° and 4°-25°, with a step size of 0.05°. Two different sample holders were used, see Figure 2.4.

Figure 2.4. On the left, sample holder made of silicon used for smaller amount of sample and on the right, sample holder made of plastic for larger amount of powder.

This technique was considered at first instance because the concern of keeping the integrity of the clay after the treatment with acid due to the data reported in the literature[50] about how some types of clays during the process of acid activation obtain certain amounts of amorphous silica.

The data obtained with this technique had to be corrected for a background due to the sample holder. This was done using the software EVA (DIFFRAC[PLUS] Evaluation Package Release 2007).

The equation (2.1) was used to calculate the d spacing of the peaks based on Bragg's law where λ is the incident wavelength, d is the spacing between the planes of same (hkl) in the crystal lattice and θ is the angle between the incident ray and the crystal plane. This allows to estimate how the molecules of the substance added interact within the layers of the clay structure.

$$d = \frac{\lambda}{2 \sin \theta} \qquad (2.1)$$

2.2.2.3   Small Angle X-Ray Scattering (SAXS)

These measurements were performed using a GANESHA 300 XL (Xenocs) SAXS system with an adjustable sample to detector distance. X-rays were generated using a sealed tube generator with a Cu anode (X-ray wavelength 1.54 Å). Samples were run in Medium Angle ($0.015 < Q < 0.65$ Å^{-1}) and Wide Angle ($0.07 < Q < 2.8$ Å^{-1}). Samples were loaded either as suspensions in solution into 1.5mm borosilicate glass capillaries (Capillary Tube Supplies Ltd.), see Figure 2.5a, or as powders in between two 7 μm thick mica sheets, held in a custom-built stainless-steel holder, see Figure 2.5b.
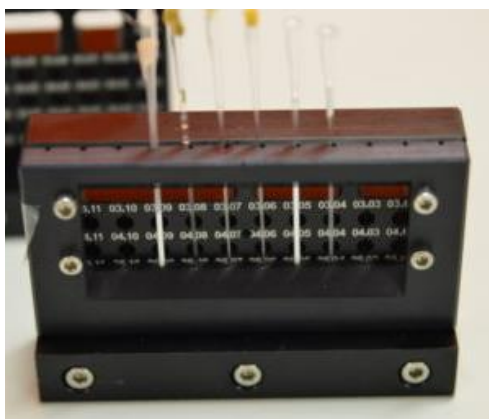
a)   b)

Figure 2.5. Sample holders. a) Capillary sample stage. b) Sandwich cell holders.

The d-spacing measured by SAXS was found by selecting each peak and using the equation (2.2), where q is the position of the peak in intensity and d is the layer spacing between the clay particles in Å.

$$d = \frac{2\pi}{q}$$ (2.2)

2.2.2.4 Elemental Analysis (EMA)

Data was obtained in two different facilities. Half of the samples were analysed at the microanalytical laboratory within the School of Chemistry, the other half of the samples were sent to OEA Laboratories Limited (Cornwall, United Kingdom). All samples were submitted as a powder.

This method was chosen as a primary test to check if the ω-amino carboxylic acid was present in the modified clay, since this process is an easy quantitative analysis. The data obtained with this technique helped to check how much the organic content of the samples increased when the ω-amino carboxylic acids were added.

2.3 Results

2.3.1 Clay functionalisation with ω-amino carboxylic acids

2.3.1.1 Effect of neutral treatment at room temperature (24h)

During the washing step for the samples without dye it was very noticeable how three layers were formed (Figure 2.6). For the purpose of obtaining a clean "clay + ω-aa" sample, both the white top layer and the clear middle layer were removed.

The white top layer is likely to consist (mostly) of unadsorbed ω-aa. The volume of the white top layer depended on the ω-amino carboxylic acid used: ADA > AHA > GABA, which makes sense as the ADA is least water soluble.

Figure 2.6. Sample of MMT+ADA 24h after being centrifuged for cleaning purposes.

The layer at the bottom that corresponded to the clean modified clay sample was then taken out to then be freeze dried and pulverized in order to be characterised.

2.3.1.2 Effect of treatment via acid (HCl)

During the washing step for the samples with shorter chain amino acids the filtering step was quite difficult (GABA>AHA>ADA). The short-chain ω-aa modified samples remained rather

hydrophilic resulting in a fine dispersion of the modified particles that would quickly block the filter, see Figure 2.7.

Figure 2.7. Sample of MMT+GABA 3x HCl being filtered for cleaning purposes.

Once the washes were done, the resulting product was taken to the freeze dryer and pulverized to obtain the powder samples to be characterised. These were the samples that were then used to mix with the different materials in the following chapters of this thesis.

2.3.2 Characterisation

2.3.2.1 Fourier-transform Infrared Spectroscopy (FT-IR)

Figure 2.8 shows the distinctive absorption peaks for montmorillonite. These are situated around 3600 cm^{-1} (-OH of *Al-OH* and *Si-OH*), 3400 cm^{-1} (most likely to be the -OH stretching of the water in the interlayer)[51], the one around 1630 cm^{-1} (suggests water of hydration in the adsorbent)[52], around 1100 cm^{-1} – 1000 cm^{-1} and 600 cm^{-1} – 500 cm^{-1} (the stretching bands of Si-O-Si and Si-O-Al respectively) and between 950 - 800 cm^{-1} (due to the Al-Al-OH, Al-Fe-OH and Al-Mg-OH interactions).[53] [54] [55] [56]
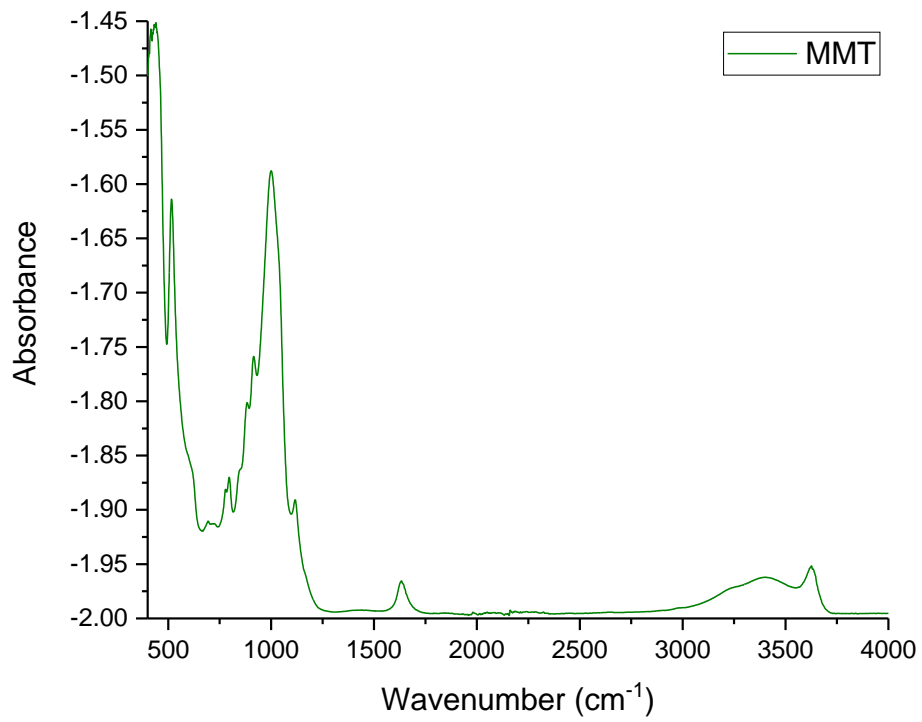
Figure 2.8. FT-IR spectrum of Montmorillonite.

In Figure 2.9, the spectrum shows the main peaks for ADA which are around $3000 - 2800 \text{cm}^{-1}$ for the carboxylic acids and around $1700 - 1300 \text{ cm}^{-1}$ that correspond to the amines.
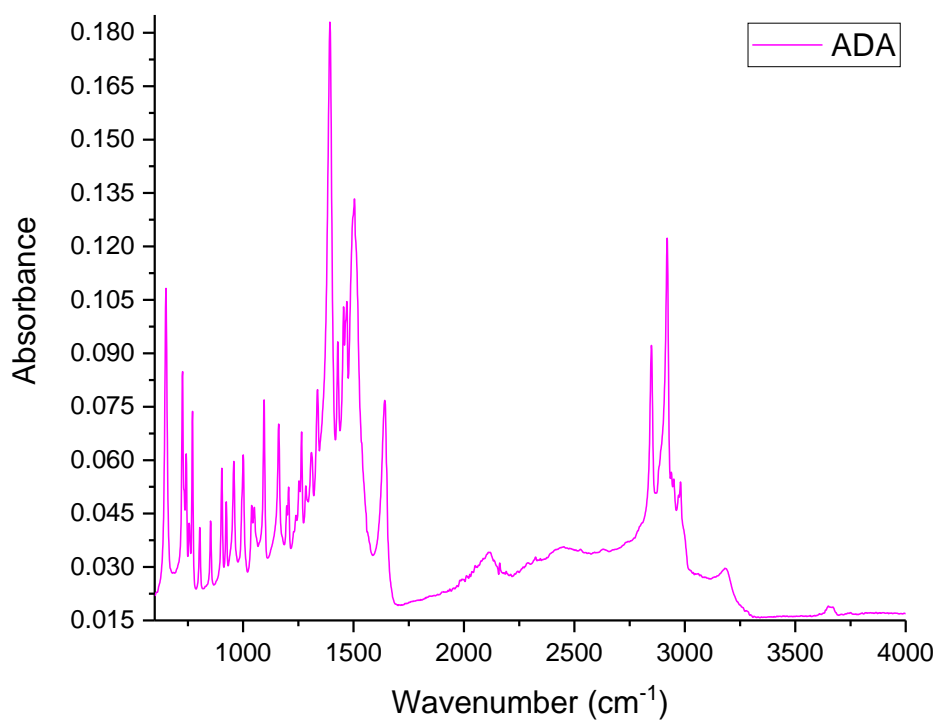
Figure 2.9. FT-IR spectrum of 12-aminododecanoic acid.

In Figure 2.10, the spectrum for AHA shows peaks around 1300 cm^{-1} and 3000 cm^{-1} correspond respectively to C-N and N-H. While the signals between 1500 cm^{-1} and 1550 cm^{-1} are attributed to the symmetric and asymmetric stretching vibrations of uncoordinated COO^{-} terminal groups.
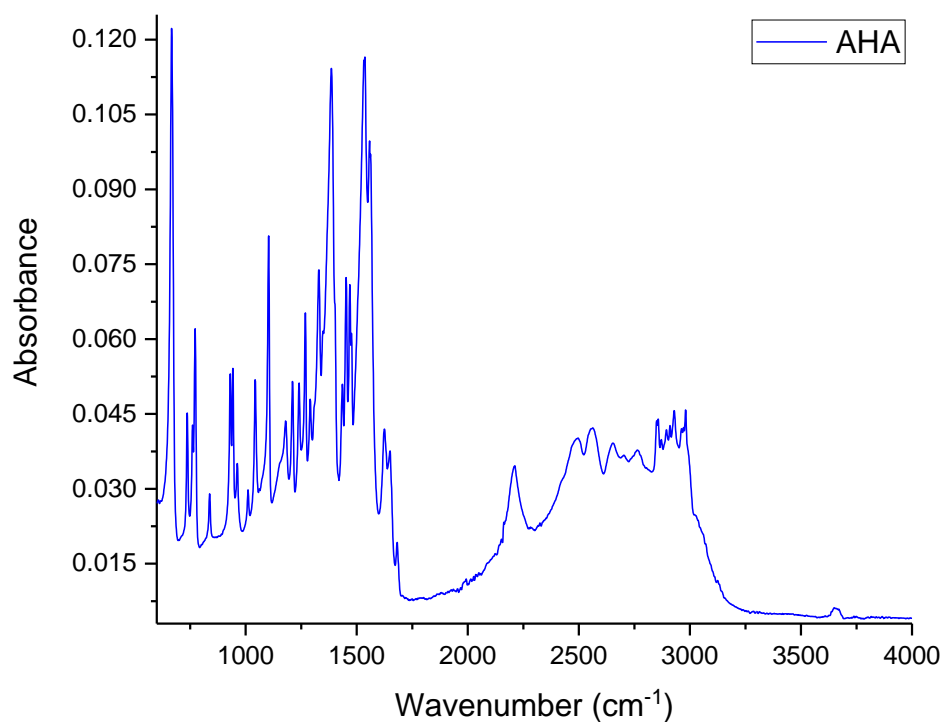
Figure 2.10. FT-IR spectrum of 6-aminohexanoic acid.

The last of the precursors is GABA and its spectrum shown in   Figure 2.11 presents the C-H stretching around 2900 cm^{-1} and 3000 cm^{-1} correspond to the CH_2 group. The NH_3^+ stretching bands are broader and weaker than those arising from the uncharged NH_2 groups. This spectrum shows a very broad band around 3000 cm^{-1} corresponding to NH_3^+ symmetric stretching mode. The COO^- vibrations are observed as intense bands between 500 cm^{-1} to 1000 cm^{-1}.
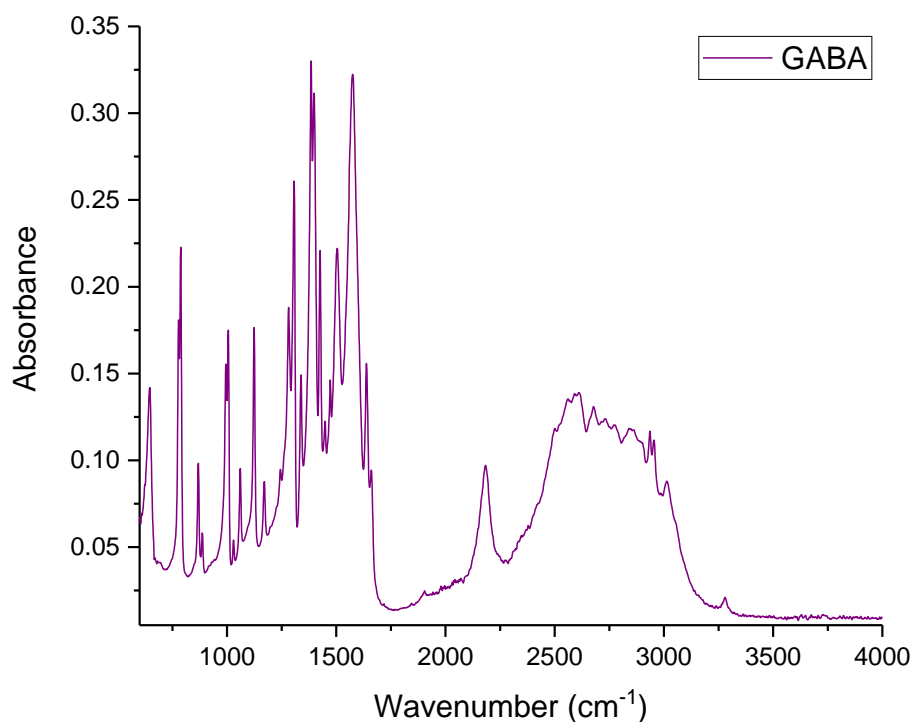
Figure 2.11. FT-IR spectrum of γ-aminobutyric acid.

Figure 2.12 shows the IR spectra of clay samples modified using the neutral route. All spectra are dominated by the montmorillonite peaks, however there are some weaker peaks as well indicating presence of ω-aa in the ADA treated sample. As will be discussed below this is consistent with this sample having by far the highest organic content of the three. The peaks are rather weak however so we will not attempt a more detailed analysis of peak shifts here.
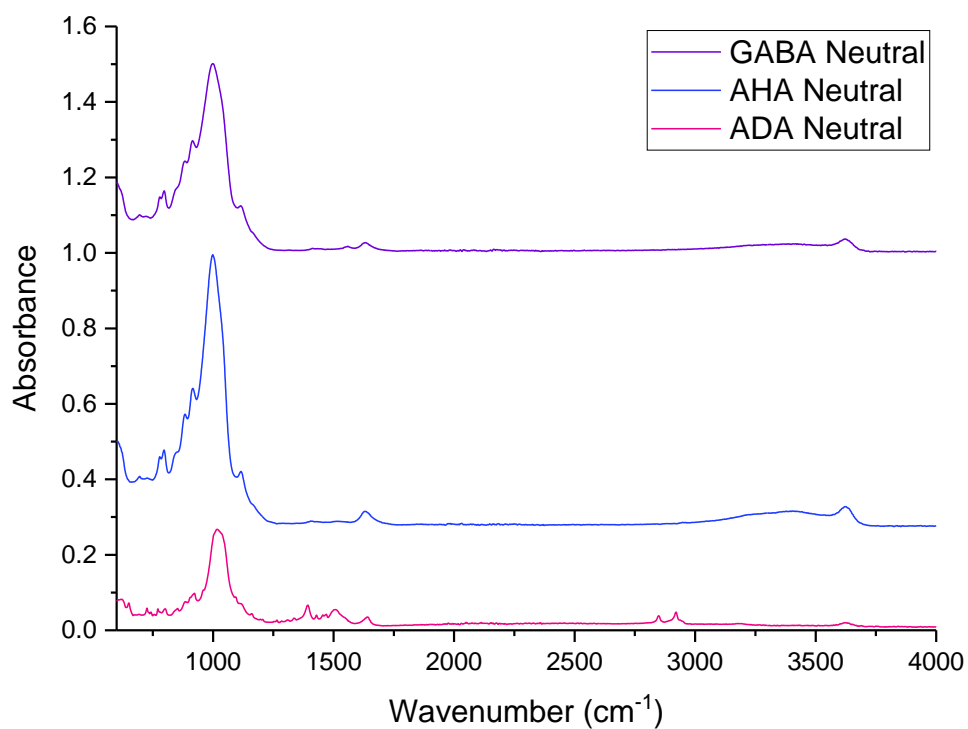
Figure 2.12. FT-IR of modified clays by neutral treatment with the three different ω-aa. Spectra have been shifted for easy comparison.

Meanwhile, Figure 2.13 shows the IR spectra of clays modified using the acid route. Weak ω-aa peaks can be seen in all spectra, which is consistent with the organic content of these samples discussed below.
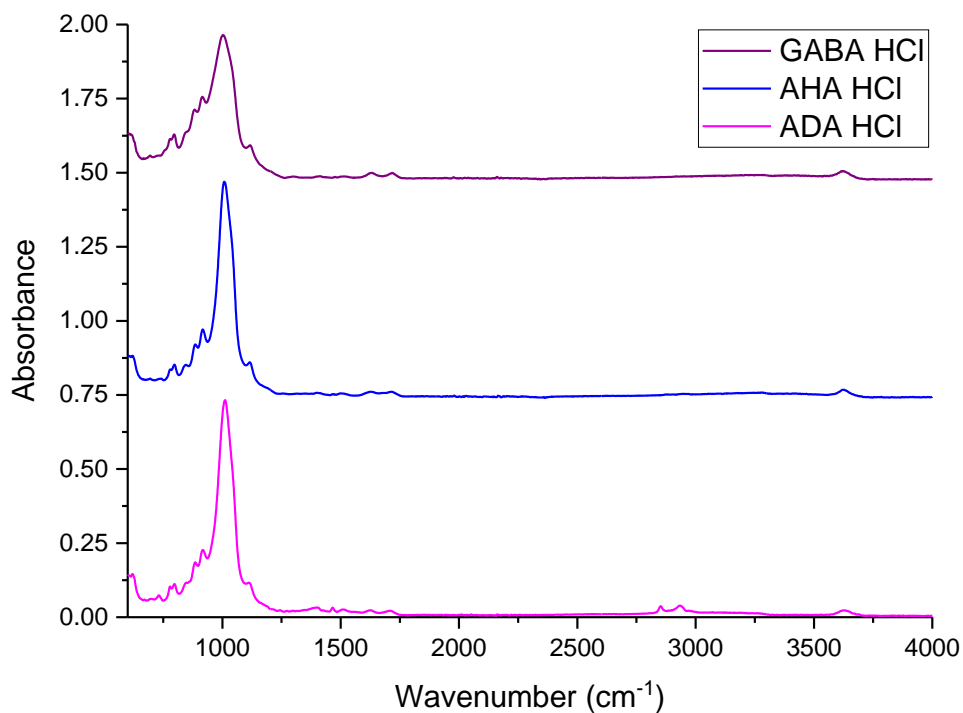
Figure 2.13. FT-IR of modified clays by acid treatment with the three different ω-aa. Spectra have been shifted for easy comparison.

For the clay samples that were dyed, the spectra obtained are presented for completeness in Figure 2.14. It is not clear why the clay signal varies in intensity as much as it does; peaks associated with the organic components are hard to discern.
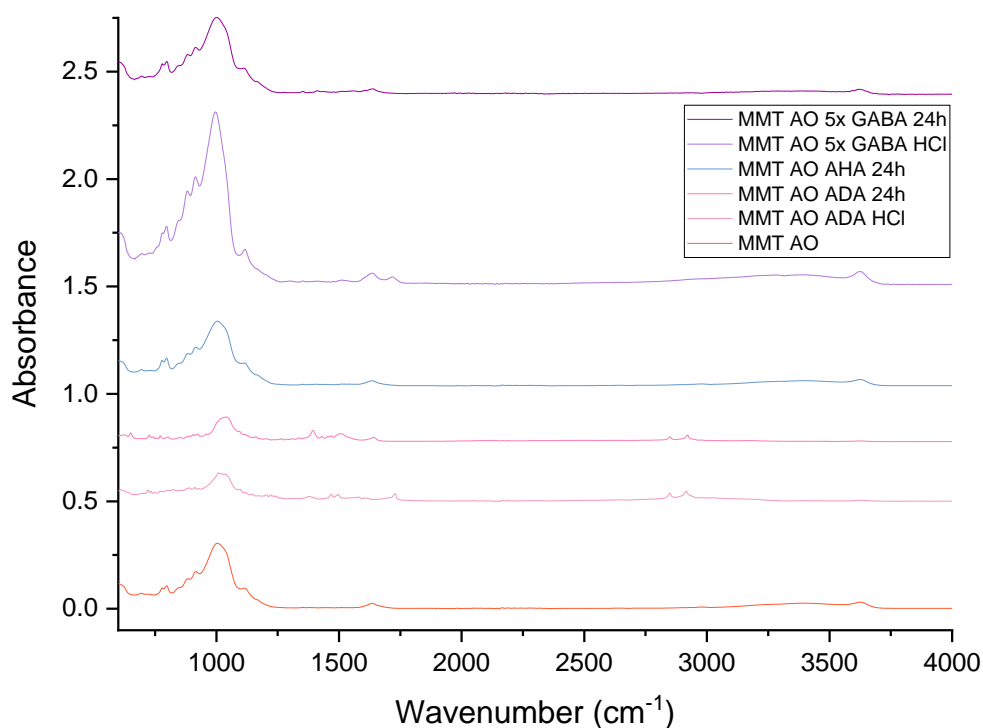
Figure 2.14. FT-IR of the different treatment dyed samples + modified clays + ω-aa. Spectra have been shifted for easy comparison.

2.3.2.2 X-Ray Powder Diffraction (XRD)

The following data will be used to compare the different modified clay samples to highlight the changes in the clay structure.

Figure 2.15 shows the spectra of the clay and the ω-amino carboxylic acids precursors. The intensity of the d_{001} peak (around 5°) in the original clay sample (MMT) is very low, in fact, the reason why the data of each precursor had to be plotted separately was to be able to highlight this peak in the MMT spectra.
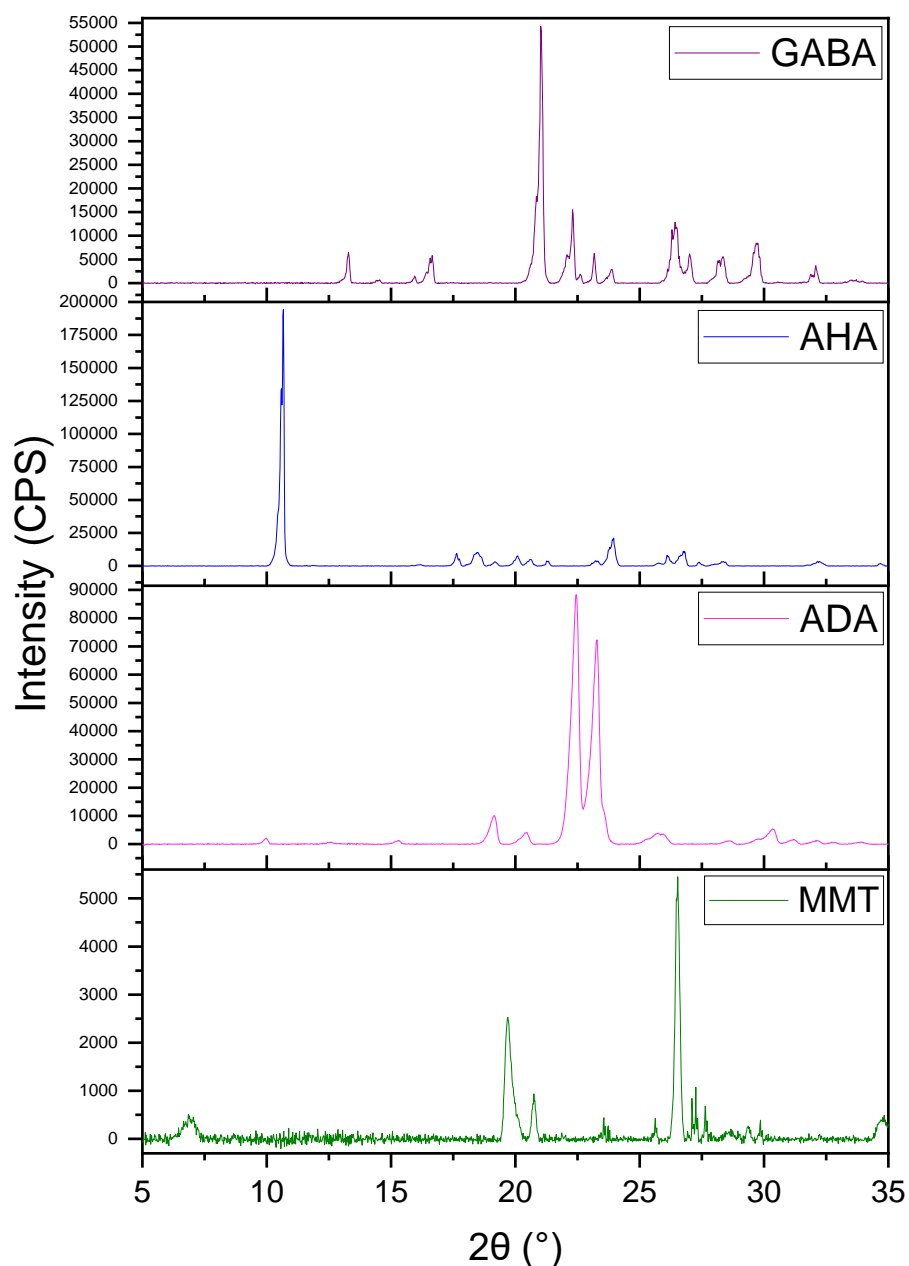
Figure 2.15. XRD of precursors.

The peaks present in the spectra for the modified clays by neutral treatment (24h) are a combination of the individual precursor's spectra, they keep presenting the signal for MMT around 20° but also other peaks, although this is more evident for the ADA and GABA samples. All these mean that our resulting modified clays contain clay as well as ω-aa, and the main feature to observe is the increment on the intensity of the d_{001} peak of the clay (see Figure 2.16). This suggests that the chains of ω-aa are interacting with the clay structure, with the resulting clay-organic sandwich layered structure giving a strong X-ray signal. Incorporation

of the ω-aa also results in an increase of the d-spacing (lowering of the peak angle) which will be discussed in more detail below.
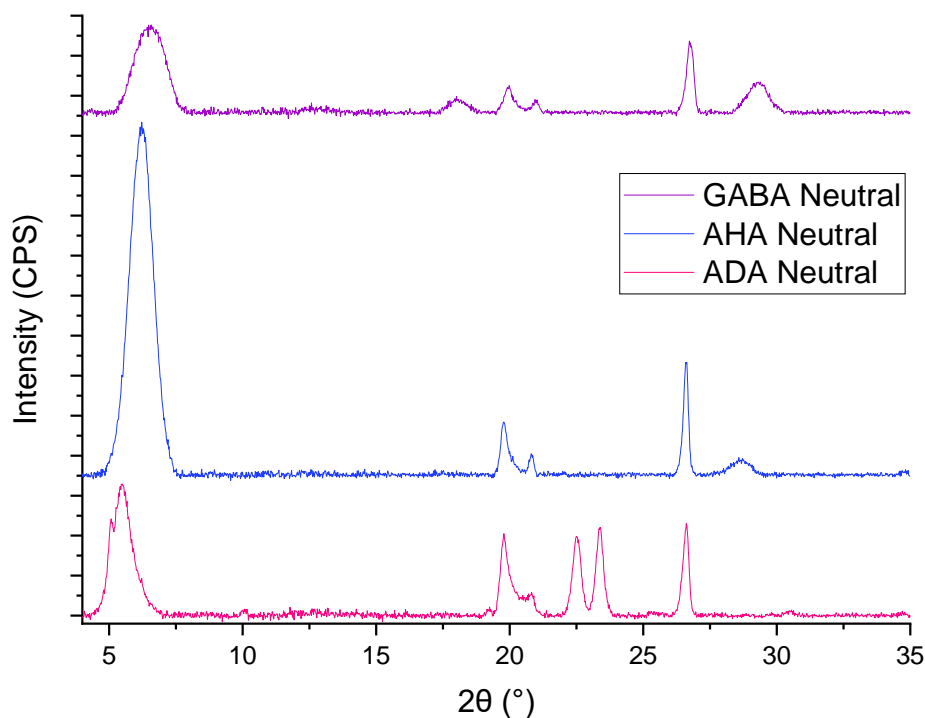
Figure 2.16. XRD of modified clays by neutral treatment with the three different ω-aa. Data shifted for clarity.

However, in Figure 2.17, the spectra for the modified clays treated with acid present noticeably fewer peaks than those of the neutral treated clays. Again, if we focus on the d_{001} peak, it can be seen how not only the intensity of it has increased but also it gets very well defined (sharp), this suggest that the clay layer structure is becoming better defined and / or the number of clay layers in a particle becomes higher. Altogether this indicates that the intercalation of ω-aa into the clay structure is more effective in this case, with little ω-aa remaining present outside the clay stacks.
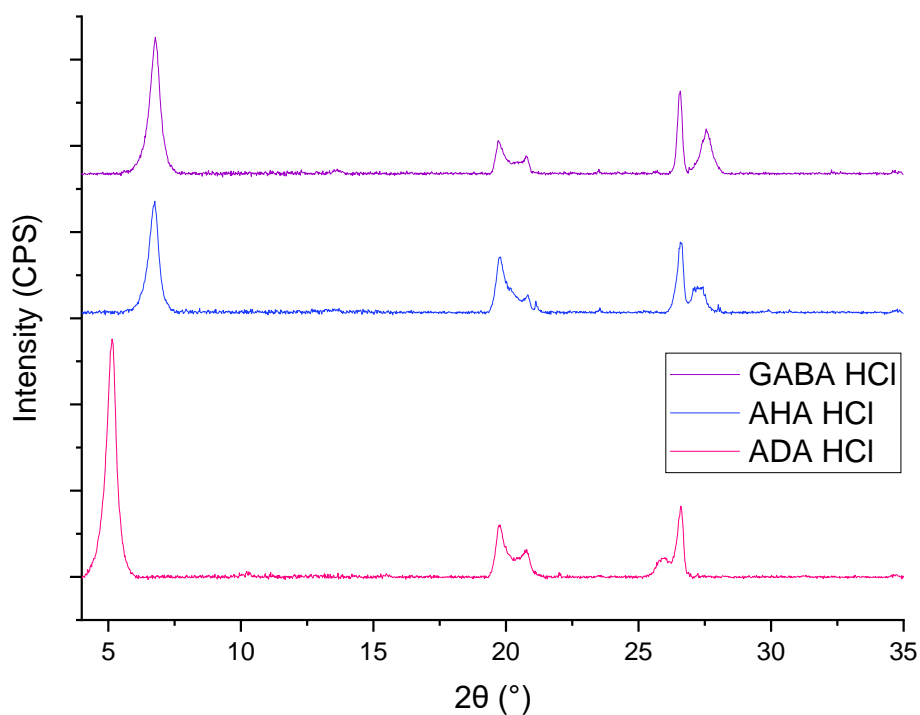
Figure 2.17. XRD of modified clays by neutral treatment with the three different ω-aa. Data shifted for clarity.

2.3.2.3 Small Angle X-Ray Scattering (SAXS)

With this technique it is possible to focus on the d_{001} peak that was already seen with the XRD spectra but as it was very close to the limits of detection, this technique will be useful to prove if the data was accurate.

In Figure 2.18 the scattering data of the precursors is shown. All the peaks were measured to calculate their correspondent d spacing that can be seen in the first column of Table 2.3.
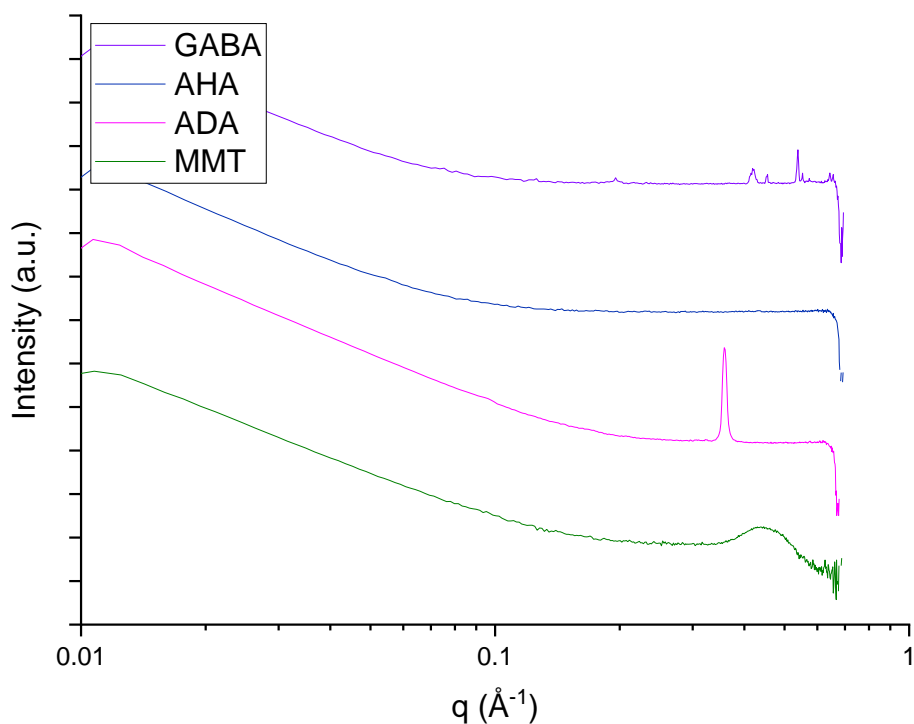
Figure 2.18. SAXS spectra of all precursors. Successive curves are shifted for clarity; graph in logarithmic scale, note that each tick mark in the Y axis represents one order of magnitude.

Table 2.3. Peak position of all samples and precursors.

Precursor	d spacing (Å)	Clay Sample	d spacing (Å)	Clay Sample with dye	d spacing (Å)
MMT	14.3 (broad)			MMT + AO	24.9 (broad) 13.68 (broad)
ADA	17.6 (sharp)	MMT + ADA Neutral	17.5 (sharp) 14.7 (broad)	MMT + AO ADA Neutral	17.5 (sharp) 16.8 (broad)
		MMT + ADA HCl	17.1 (sharp)	MMT + AO ADA HCl	18.5 (sharp) 17.2 (sharp)
				MMT + AO w/o Zn ADA HCl	16.6 (sharp)
AHA	No visible peak	MMT + AHA Neutral	12.7 (broad)	MMT + AO AHA Neutral	13.7 (broad)
				MMT + AO 5x AHA Neutral	16.3 (broad) 13.3 (sharp)
		MMT + AHA HCl	12.8 (sharp)	MMT + AO AHA HCl	13.0 (sharp)

		MMT + 3x AHA HCl	13.2 (broad)		
GABA	32.1 (sharp) 15.1 (sharp) 15.0 (sharp) 14.9 (sharp) 13.8 (sharp) 11.7 (sharp) 11.4 (sharp) 11.0 (sharp) 9.8 (sharp) 9.6 (sharp)	MMT + GABA Neutral	21.7 (broad) 12.5 (broad)	MMT + AO w/o Zn 5x GABA Neutral	13.2 (sharp)
		MMT + GABA HCl	12.8 (sharp)	MMT + AO w/o Zn 5x GABA HCl	12.7 (sharp)
		MMT + 3x GABA HCl	12.9 (sharp)		

Samples prepared with clay and ω-amino carboxylic acids using the 2 different treatment methods (neutral and acid) but without the addition of dye are compared to the spectra of the precursor MMT (green line), this can be seen in Figure 2.19, Figure 2.20 and Figure 2.21. The correspondent d spacings can be found in the second column of Table 2.3.
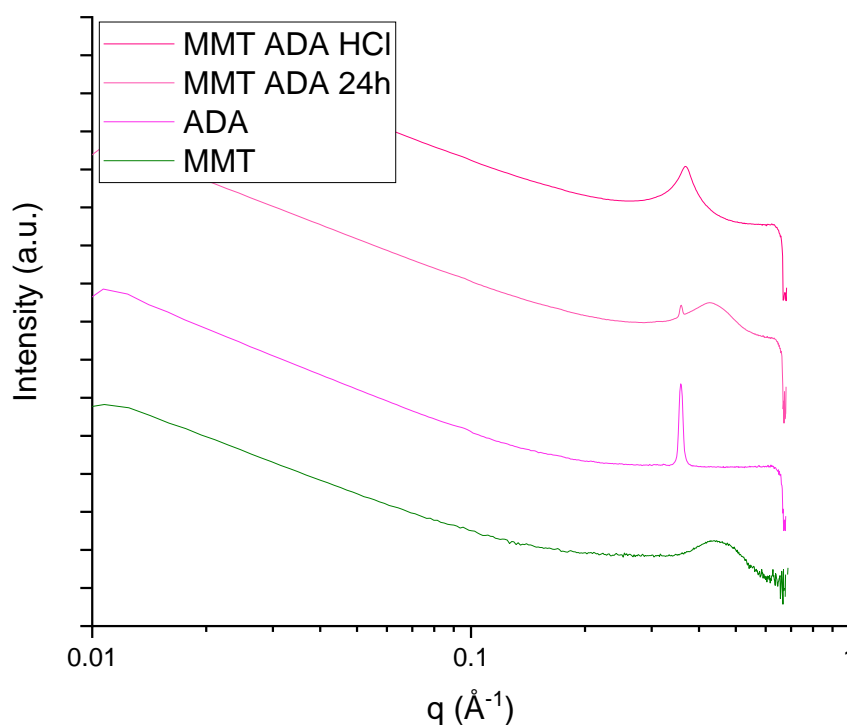
Figure 2.19. SAXS spectra of clay samples with clay and ADA. Y axis as in Fig. 2.18. Data shifted for clarity.

Figure 2.19 shows how the two peaks present on the modified clay after neutral treatment (MMT ADA 24h) appear almost in the same place of the peaks that correspond to the precursors, suggesting that by using this treatment the final product is either a mix of both clay and ω-aa that is not completely interacting or an excess of the ω-aa in the clay structure. On the other hand, the peak present on the modified clay after the acid treatment it becomes sharper and displaces to the left compared to the MMT itself, this suggest that the ω-aa is intercalating in between the clay platelets creating a better ordered structure.
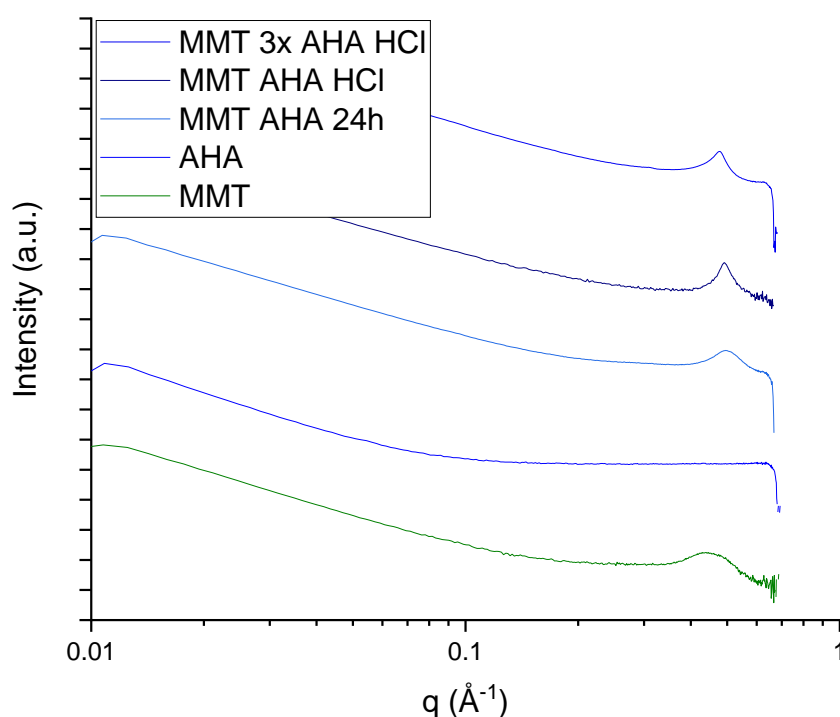
Figure 2.20. SAXS spectra of clay samples with clay and AHA. Y axis as in Fig. 2.18. Data shifted for clarity.

Figure 2.20 summarises SAXS data on samples treated with AHA. The main scattering peak for AHA in the pure form falls outside the q range studied here (see also Figure 2.15), so the data only inform us about the ordering of the clay platelets. The sample obtained using the neutral treatment (MMT AHA 24h) presents a very broad peak while the ones treated with acid are sharper. In this case, an excess of the ω-aa was added using the acid treatment to assess the capacity of the clay platelets to catch more organic molecules in the structure however, the peak lost a bit of the sharpness, suggesting that even if the ω-aa was intercalating the organisation of the structure was being slightly compromised.
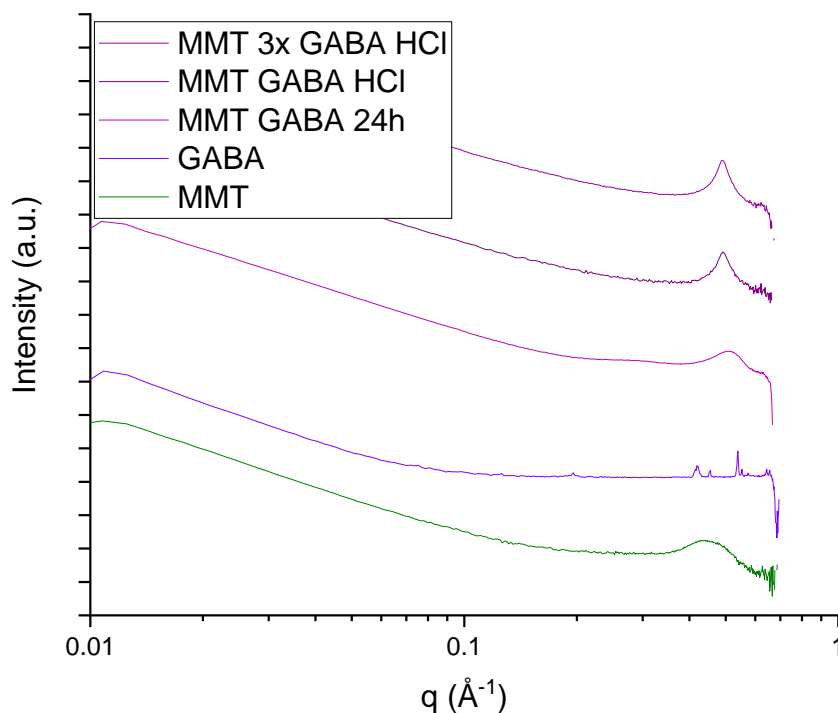
Figure 2.21. SAXS spectra of clay samples with clay and GABA. Y axis as in Fig. 2.18. Data shifted for clarity.

Finally, Figure 2.21 summarises results for treatment with GABA. The neutral treatment once more results in a broad scattering peak while the acid treatment seems to give a better intercalation. In this case the excess of ω-aa (GABA) added during this last treatment does not seem to affect the structure; it may be that it is easier to wash away any excess GABA during processing.

As explained in section 2.2.1 clay was initially dyed using acridine orange for imaging purposes, however, when the clay powders where run in SAXS, it could be seen how the dye was interacting with the clay particles, the clay sample with dye presented two peaks, see Figure 2.22a. Also, 2 dyes were used, one contained a bit of Zn and the other did not, these was detectable with this technique and can be seen in Figure 2.22b where an example of the modified clays with dyes varied compared to the clay sample that only contains the ω-aa.
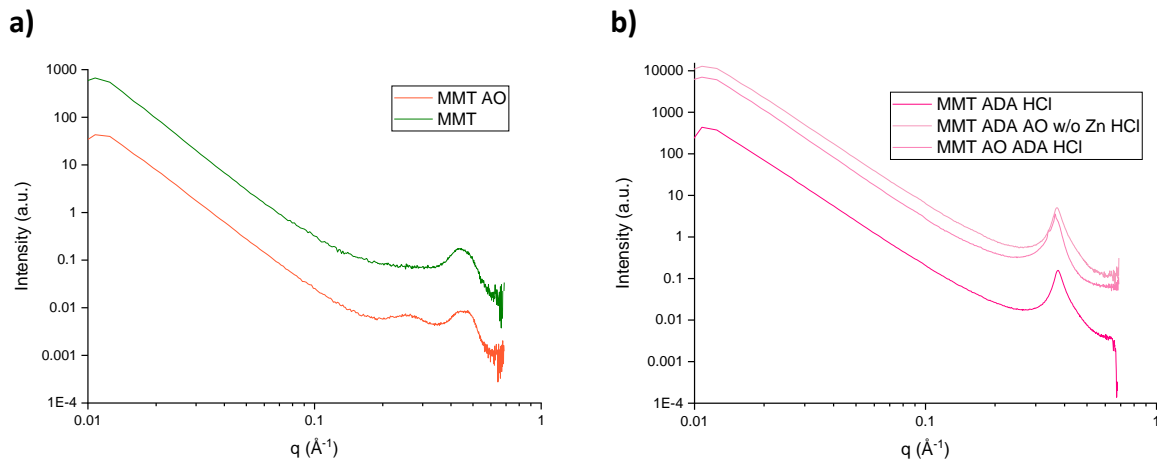
Figure 2.22. SAXS spectra of a) clay with and without dye and b) Clay samples with and without dye (MMT + ADA HCl). Y axis as in Fig. 2.18. Data shifted for clarity.

Thus, the spectra of the several combinations of dyed clay samples prepared using the different ω-aa are presented below. Samples with dye are compared to the base spectra of MMT+AO (orange line), as we can see in Figure 2.23, Figure 2.24 and Figure 2.25. All the peaks were measured to calculate their correspondent d spacing; this information can be found in the third column of Table 2.3.

As can be seen any of the peaks look as sharp as the ones presented previously, suggesting the clay ordering has not been affected by addition of the (small amount of) dye. The intention of adding the dye was to be able to verify via fluorescence microscopy that the modified clay was being well dispersed into the glass ionomer cement (GIC) to prepare the specimens that will be presented in Chapter 3. The results presented here show that the dye can indeed be used in this way.
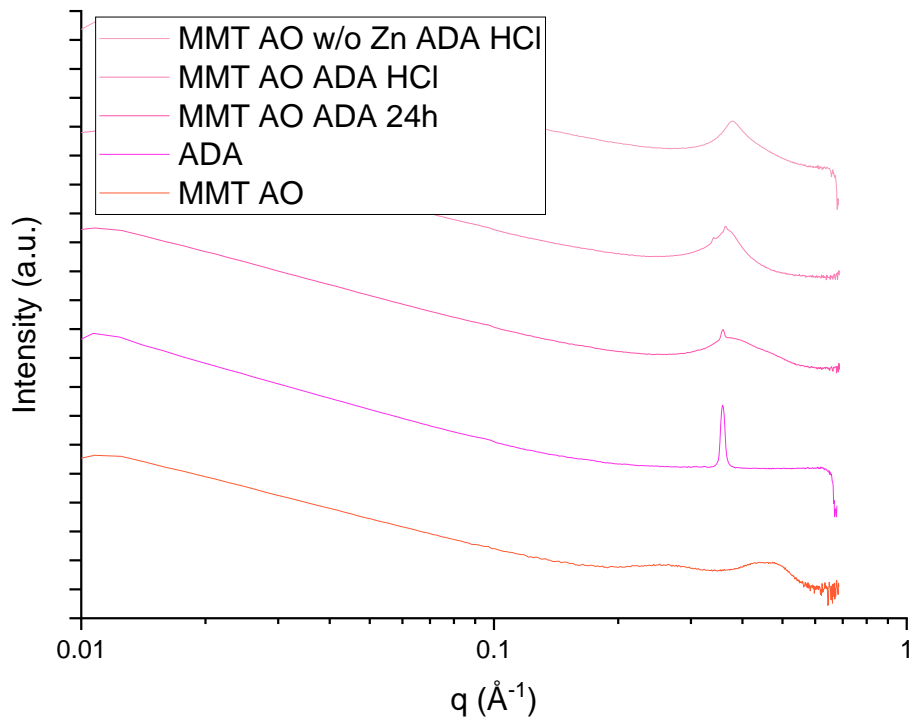
Figure 2.23. SAXS spectra of clay samples with clay, dye and ADA. Y axis as in Fig. 2.18. Data shifted for clarity.
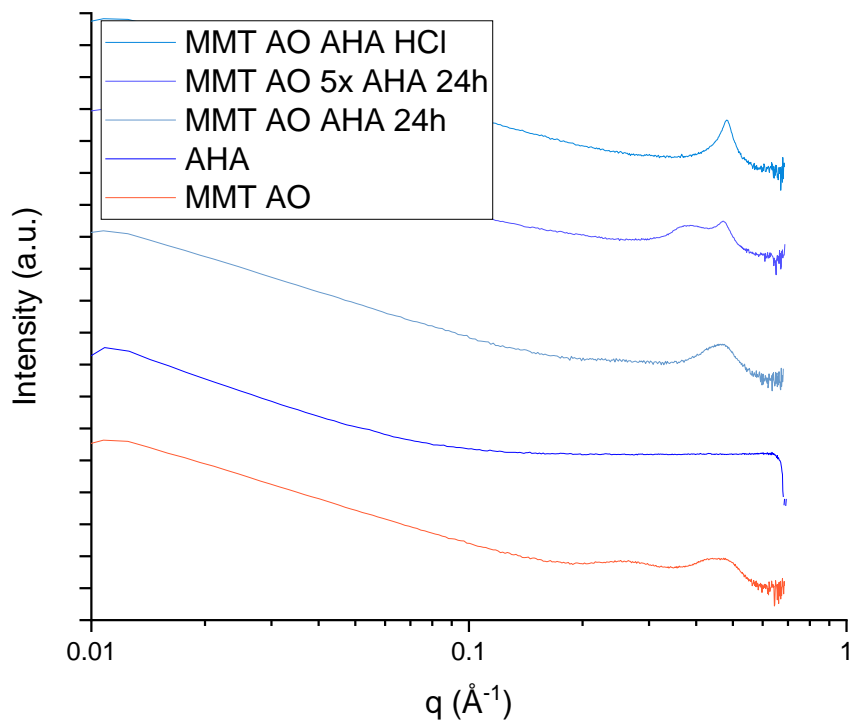
Figure 2.24. SAXS spectra of clay samples with clay, dye and AHA. Y axis as in Fig. 2.18. Data shifted for clarity.
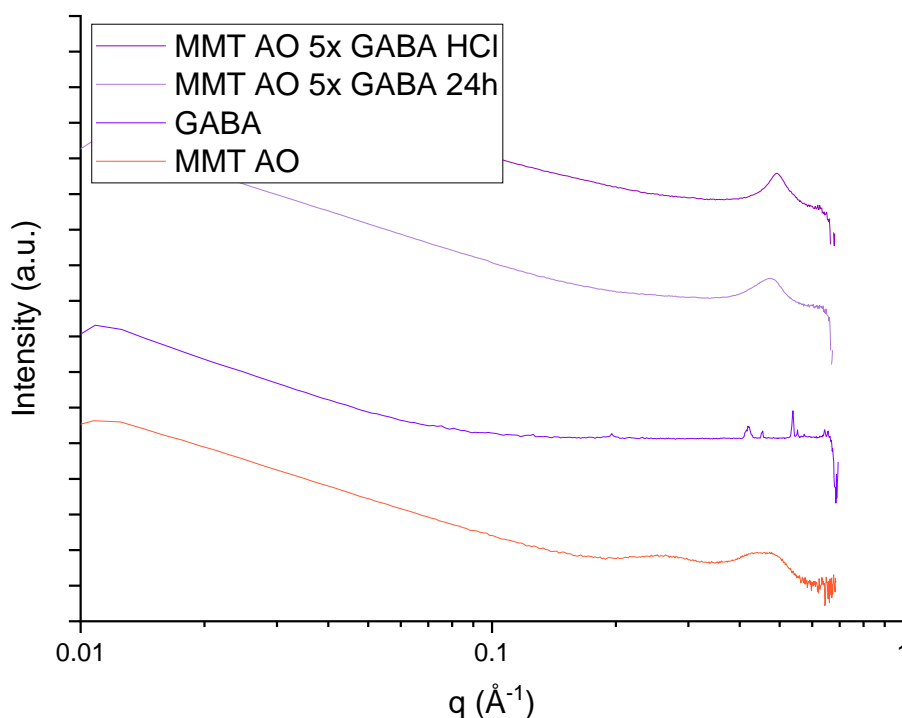
Figure 2.25. SAXS spectra of clay samples with clay, dye and GABA. Y axis as in Fig. 2.18. Data shifted for clarity.

2.3.2.4   Elemental Analysis (EMA)

This technique shows the organic content (%N, %C, %H or %CNH) obtained for the treated clays, with values for the precursors, as well as the samples using the labelled clay with fluorescent dye (Acridine Orange), so the amount of each element present in them could be compared.

Table 2.4 presents the data of the clay as a precursor, the first line shows the MMT as received, and the second line corresponds to the clay suspension with 1% AO added.

Table 2.4. EMA data for clay samples before any treatment with ω-aa.

Sample	Experimental Value		
	N %	C %	H %
MMT		0.3	1.3
MMT+AO	0.1	1.7	1.2

In Table 2.5, the experimental value of the organic content of each sample is compared with its theoretical value. With the ω-amino carboxylic acids it is basically the same values while with the two different Acridine Orange dyes it varies but this could be due to the presence of impurities, as neither of the two are 100% pure dye.

Table 2.5. EMA data of all ω-aa and dyes.

Sample	Experimental Value			Theoretical Value		
	N %	C %	H %	N %	C %	H %
ADA	6.6	66.7	11.5	6.5	66.8	11.6
AHA	10.8	54.6	9.9	10.6	54.8	9.9
GABA	13.6	46.8	8.5	13.6	46.6	8.7
AO	8.3	40.4	4.7	11.3	55.1	5.4
AO s/Zn	13.7	66.9	6.3	15.8	76.9	7.2

In Table 2.6, the experimental value (%CNH) of the organic content for treated clay samples is shown, however in the case of the first set of samples it could not easily be interpreted because it is not possible to determine how much of the organic content corresponds to the dye and how much to the ω-amino carboxylic acid. On the other hand, for the samples with no dye the data for the experimental value of the organic content of each sample (%CNH) is shown and from this the adsorbed amount of ω-aa was determined. These results will be discussed in the next section.

Table 2.6. EMA data of all modified clays, with and without dye.

Clay Sample with dye	Experimental Value %CNH	Clay Sample	Experimental Value %CNH	Adsorbed Amount (meq/100gclay)
MMT + AO ADA Neutral	50.2	MMT + ADA Neutral	32.0	281
MMT + AO ADA HCl	37.2	MMT + ADA HCl	17.6	121

40

MMT + AO w/o Zn ADA HCl	16.2			
MMT + AO AHA Neutral	4.4	MMT + AHA Neutral	3.6	38
MMT + AO 5x AHA Neutral	14.2			
MMT + AO AHA HCl	6.9	MMT + AHA HCl	7.5	85
	9.8	MMT + 3x AHA HCl	15.2	192
MMT + AO w/o Zn 5x GABA Neutral	5.9	MMT + GABA Neutral	3.2	48
MMT + AO w/o Zn 5x GABA HCl	6.6	MMT + GABA HCl	5.2	79
		MMT + 3x GABA HCl	6.4	99

2.4 Discussion

As can be seen in the previous sections, clays can easily be modified by adsorption of small organic species, however the results do depend on the processing route followed. As a further, graphic example of this, when adding Acridine Orange to the samples, it was noticed that depending on the ω-amino carboxylic acid used to treat the clay and the conditions (either neutral or acid treatment) the colour of the product varies dramatically, see Figure 2.26, presumably as a result of the degree of protonation of the AO dye.
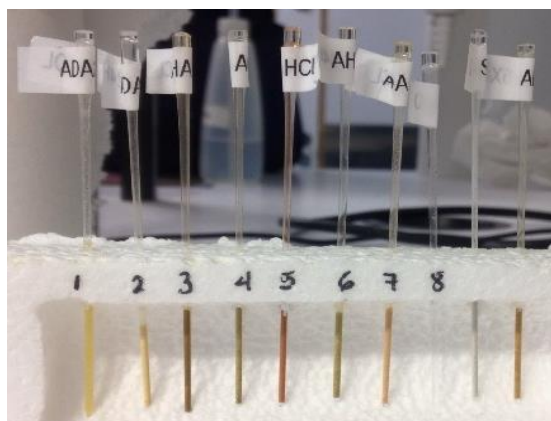
Figure 2.26. a) Different samples for SAXS characterisation ADA, AHA, MMT and AO. b) On the left is MMT + GABA HCl and on the right is MMT + GABA Neutral, both containing the same concentration of ω-aa and AO.

In the SAXS data presented above it can be seen how for MMT there is no well-defined d_{001} peak, however this changes already after the addition of 1% AO, indicating that this is able to intercalate between the platelets, resulting in a better-defined layered structure. This observation led to the preparation of samples without dye to compare the structure of the clay samples.

The difference between drying techniques was based on the explanation given in the Handbook of Clay Science, originally from Lagaly, 1987[57], see Figure 2.27.
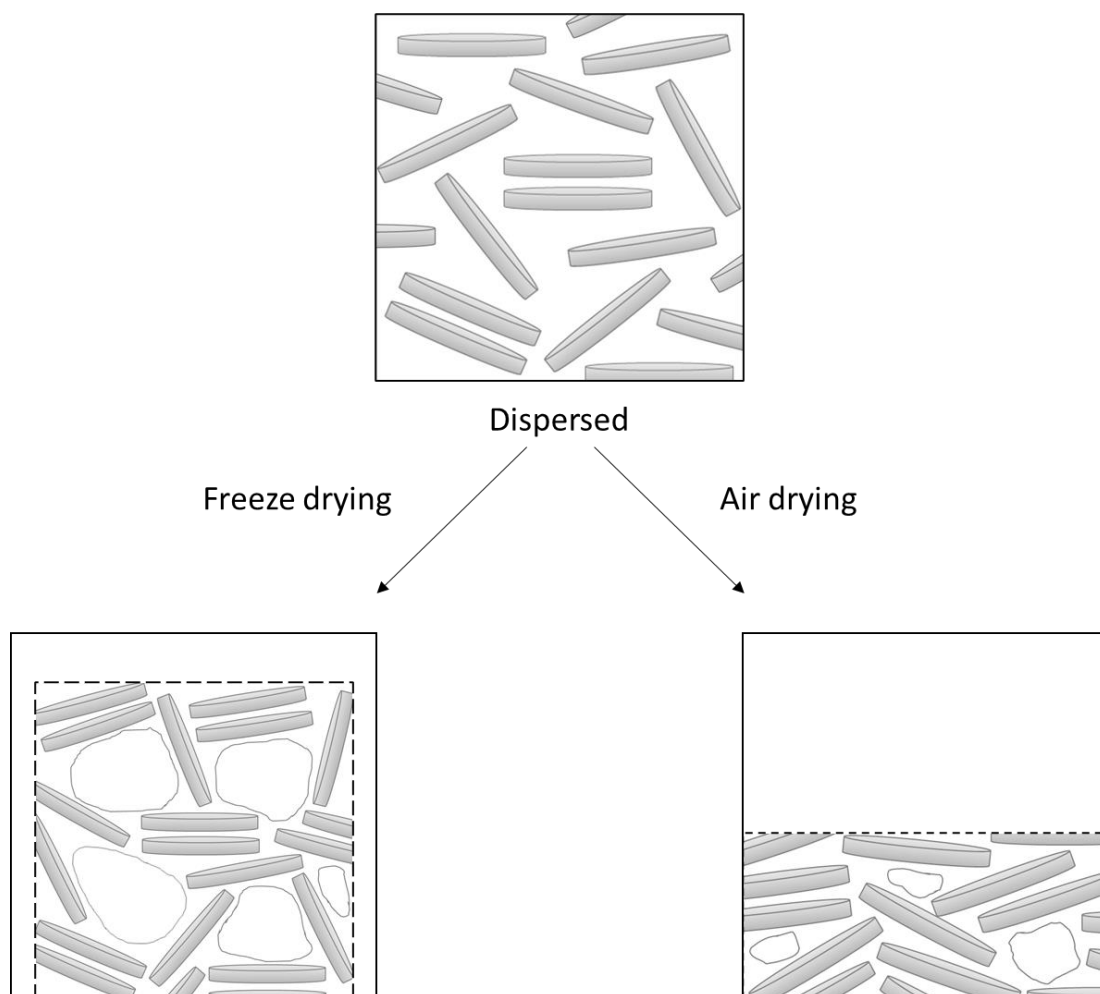
Figure 2.27. Aggregation of clay mineral particles.

Having all the data about the different samples and to avoid any interference due to the presence of dye, it was decided to prepare a new batch of samples following the conditions that produced the best results. For these samples no Acridine Orange was added, and the final product was freeze dried to facilitate redispersal. The characterisation results have been included above.

Comparing the FT-IR spectra of the modified clays with the pure precursors, we can observe that the signals in the range of the carboxylic acids and amines remain although we can notice some displacements on the peaks. At the same time, the absorption band for MMT in the region between 950 - 800 cm^{-1} also remains visible. Even if this technique does not let us extract further detail of how much of each compound is present in the sample, there are

noticeable differences in the peak intensities for the clays treated via the acid and neutral routes.

The most interesting feature in the XRD spectra (section 2.3.2.2) and the SAXS (section 2.3.2.3) is the emphasize the changes that occur to the d_{001} peak (around 5°), this corresponds to the arrangement of the platelets in the clay structure. As mentioned in those sections, although the rest of the peaks present in each spectra help to prove that the ω-amino carboxylic acids have been successfully incorporated into the clay samples, the definition (how sharp) of the d_{001} peak suggests a better arrangement of the ω-aa chains for the samples that were treated under the acid route. The presence of the extra peaks in the spectra that corresponds to the neutral treatment may suggest the excess of the ω-aa in the structure.

Our intentions were to create a well intercalated structure, see Figure 2.28, that would help to improve mechanical properties when added to other materials so having an excess of ω-aa could be counterproductive.
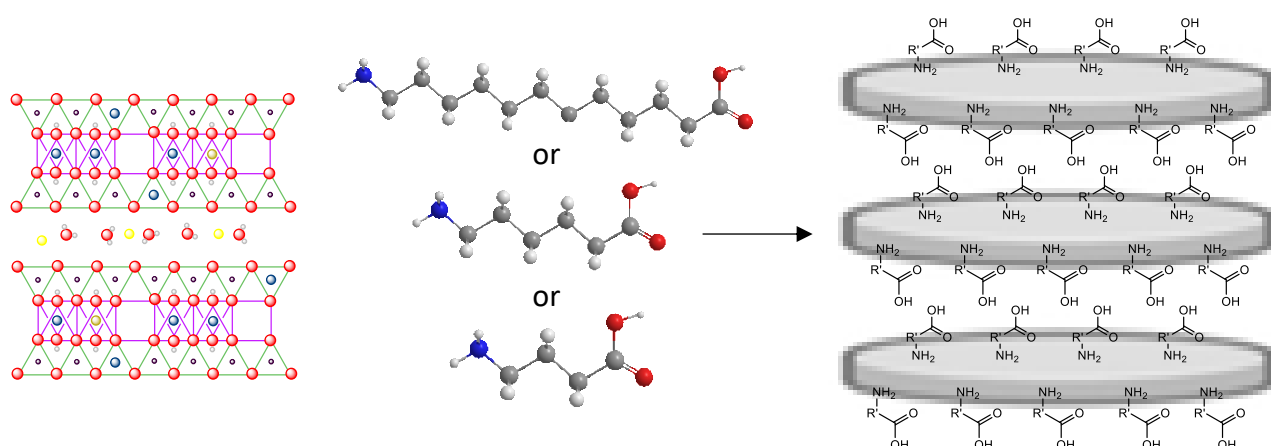
Figure 2.28. Scheme of desired clay + ω-amino carboxylic acid structure.

In general, one would expect a "good" treatment with amino acid to give a 1:1 exchange onto the clay, with a maximum attainable corresponding to the CEC of around 84 meq / 100 g of the ω-aa adsorbed between the sheets. A lower coverage would suggest an unsatisfactory treatment method, whereas a higher value would indicate an excess of ω-aa being present. This excess (over and above the CEC) may then either be absorbed between the sheets – or the ω-aa may be present separately outside the clay stacks.

A milliequivalent (meq) is a measure of the quantity of ions in an electrolyte fluid. One milliequivalent is one thousandth of one mole of charges.

For GABA we can see that only the acid treatment route resulted in a good coverage with ω-aa, of around 1 CEC.

For AHA we have a similar result, with treatment with one CEC equivalent of ω-aa resulting in an effective coverage of around 1 CEC. For the sample made with threefold excess of ω-aa, a significantly higher amount of ω-aa remains after the treatment (192 meq / 100 g). Inspection of Table 2.3 however suggests that most of the additional AHA has not been absorbed between the clay sheets, as there is only a very small increase of d-spacing compared to the preceding sample.

Finally, we turn to samples treated with a threefold excess of ADA – either using the neutral route or the acid treatment route. The neutral and acid methods resulted in samples with a similar d-spacing (17.5 and 17.1 Å respectively). The sample prepared via the neutral route did however contain a lot more ω-aa (see Table 2.6) – presumably this reflects an excess of ADA present outside the clay stacks therefore (which makes sense as the ADA is not water soluble and therefore will not have been washed away during treatment). We can also see scattering peaks associated with ADA crystals in this sample (see Figure 2.15 and Figure 2.16). For the acid treated sample, these peaks are absent altogether (Figure 2.17). The coverage amounts to just over 1 CEC (121 meq / 100 g clay).

Altogether the acid treatment method is producing the most robust and successful treatment of the clay samples, with variable results for the neutral treatment route.

2.5 Conclusion

As we could see, by following two different treatment routes the results varied, for the purposed pursued in this project, the acid treatment offered a better outcome. This is because the samples with neutral treatment suggest presenting an excess of ω-amino carboxylic acids in their structure, this is supported by the evidence given by each characterisation technique.

Having an excess of ω-aa would not be ideal considering that the modified clay samples are intended to be used in the preparation of other materials, and any excess could lead to a different response when mixing with the dental cements (GICs) in chapter 3, the antimicrobial (CHX) in chapter 4 or the hydrogel (Alg) in chapter 5.

It could be said that the best route to follow for each ω-aa to get a good coverage and minimum or not excess at all is the acid treatment, with no dye and freeze dried.

However, AO dye could still be added in case to need imaging data of the modified clays, as it was intended for checking the dispersion of our clay particles in the dental cements, and ω-aa can still be added afterwards to the structure.

Chapter 3 Investigating the Effects of Modified Clay Particles on the Mechanical Properties of Dental Glass Ionomer Cements

3.1 Introduction

It is of high interest to develop viable alternatives to dental amalgam filling materials and the main challenge is to get a different material with all the advantages that amalgam offers such as durability and cost[10]. Glass ionomer cements (GICs) are one promising alternative product that offer benefits such as prolonged fluoride release and adhesion to dental hard tissues; however, their applications are limited due to their low strength and brittleness[24].

The use of clays as fillers to reinforce GICs is motivated by their similitude on their hydrophilic nature of both materials. Also, molecules with carboxylic acid groups at one end are able to bond to the tooth structure[58]. Thus, the aim of the work described in this chapter was to evaluate the use of results of adding organic modified clays as a strengthening agent in GICs.

As mentioned in Chapter 1 it is of utmost importance to keep in mind the different parameters that could affect the properties of GICs such as the powder:liquid ratio[29][30] and the setting time[31] so the cement specimens can reach their best strength. There must be sufficient liquid – in the case of the formulation used here, water – to adequately wet the surface of the particles in the GIC. Given the clay additive is a fine particulate and thus has a high specific surface area in comparison to the powdered GIC components, and in addition it was necessary to mill the powders increasing the surface area still, it was anticipated that the powder:liquid ratio may need to be adjusted to account for this higher resultant net surface area.

An interesting contribution was reported by Fleming, their work's purpose was to reinforce a restorative GIC with a commercial montmorillonite (MMT) clay treated with 12-aminododecanoic acid (ADA) to assess the potential of the resulted dental material as a filling. They got interesting results upon the addition of different weight percentages of ADA-MMT, because it presented a significant increase in the mean compressive fracture strength of the GIC. They also reported an increase of the interlayer spacing between the clay sheets (using

X-ray analysis), implying that there was an enhanced opportunity for the poly-acrylic acid chains of the GIC to diffuse into the MMT galleries[26 59].

An earlier short project attempted to reinforce GICs by incorporating well-dispersed MMT and sepiolite clay into a GIC by suspending the clay in the aqueous portion of the GIC[60]. However, mechanical properties deteriorated upon addition of clay in that study when clay was added in the water phase. Other studies of incorporation of novel functional components into GICs have revealed that to incorporate particles in the aqueous phase has a detrimental effect on the mechanical properties, compared with incorporating particles in the powder phase[23 61 62]. For that reason, the mixing process in this project was made in powder form and the decision of use ball milling as the mixing technique was taken following the protocol used in other dental cement projects in the research group[62 63].

3.2   Materials and Methods

3.2.1 Incorporation of modified clay powders into GICs

A commercial glass ionomer cement (GIC) was used. This product comprises a powder composed of fluoroaluminosilicate glass, freeze dried polyacrylic acid and tartaric acid which is mixed with deionised water (ChemFil® Superior LYG, Dentsply DeTrey, Konstanz, Germany).

The modified clays used in this chapter were montmorillonite SWy-2 (MMT) which was functionalised by adding different chain lengths of ω-amino carboxylic acids: 12-aminododecanoic acid (ADA), 6-aminohexanoic acid (AHA) and γ-aminobutyric acid (GABA) following the route of the acid treatment, being freeze dried and stored in vials to be used later for the purposes of this chapter. To ensure that the mixing was sufficient to attain homogeneous distribution of the modified clay into the GICs specimens, one of the clay samples was fluorescently labelled with Acridine Orange (AO). Thus, the modified clays used correspond to the samples MMT+AO+ADA HCl, MMT+ADA HCl, MMT+AHA HCl and MMT+3x GABA HCl, described on Table 2.2 in Chapter 2.

Prior to preparing the specimens for the GIC + modified clays, the sample was made by combining the GIC powder (addition or substitution) with 0.5, 1 or 2 wt% of the respective modified clay using a ball mill mixer (IKA Ultra-Turrax® Tube Drive), ball mill tubes (IKA Ultra Turrax BMT-20G tube) and 20-25 glass beads (5mm) for 30 minutes. The samples were then stored in the sealed tube, covered with foil if the clay sample was dyed and left on a roller mixer for 15 to 20 hours after ball milled.

Ball milling is a technique used to grind and blend materials into smaller size helped by the mechanical impact of ceramic, steel or glass balls and is routinely used in the manufacture of GICs. It can be used both in dry and wet systems on a large or small scale[64].

3.2.2 GIC specimen preparation

In all instances the powder sample and water were mixed using a Lustra 8 cement spatula on a waxed paper sheet for glass ionomer cements by Dentsply Sirona supported by a pad of duplicating silicone (Elite Double 32, Zhermark purchased through Henry-Schein) using a folding motion for a period of ~60 seconds. The pliable GIC was then packed into cylinder-shaped moulds taking care to avoid porosity, bubbles, or incomplete packing.

The moulds were made of two parts fabricated from stainless steel thus it could be deconstructed to allow easy removal of the set specimens without breaking or scratching the specimens. A single mould allowed the production of 6 specimens with dimensions of 6 mm height and 4 mm diameter each, for purposes of testing the compressive strength. See Figure 3.1.
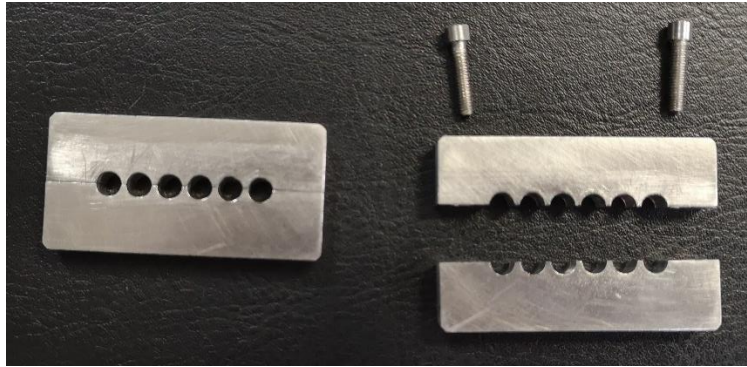
Figure 3.1. Compressive strength specimen mould.

Once the specimens were packed into the mould, this was placed between two plastic sheets, and then put under weight to compact the specimens into the mould (3.898 kg). Once that set up was done, they were allowed to set at room temperature for one hour. After this time, the specimens were then sanded gently using a sandpaper depending on the thickness of the surface #120, #180, #320, #360, or #600 for as long as necessary to get rid to the excess of cement and then #500 or #1200, for approximately 30-60 seconds to attain a smooth surface. Finally, the specimens were placed in a sealed container containing moist tissue paper, with specimens not directly touching the tissue paper, to attain a humid environment, and then stored at 37°C for 7 +/- 1 days prior to mechanical testing.

3.2.2.1   Specimen sets

A first set of specimens was mixed following the instructions from the packaging, similar to how it would be prepared in a dentistry consult room by using 2 spoons of powder (0.2306 g) and 2 drops of water (32 μL) with a resulting powder:liquid ratio of 7.2.

Other sets of specimens were prepared by mixing 0.2368 g of GIC powder weighed using an analytical balance (Sartorius TE64) and 32 μL of deionised water using a pipette (Pipetman Neo, GILSON®) for the desired powder:liquid ratio (7.4:1) suggested in the more specific manufacturer's directions of use for the product[65].

It became apparent during the preparation that the modification of different factors may impact the required powder:liquid mixing ratio. For each testing group, specimens were

prepared with 0.2368 g of GIC or GIC + modified clay respectively and varying the amount of deionised water between 32 µL to 48 µL giving a mixing ratio range of 4.9 to 6.7.

Also, a small set of specimens were prepared to compare the best results reported in the literature while using our own GIC + MMT ADA-HCl (0.2368 g) with three different amounts of deionised water for a powder:liquid ratio range of 7.0 to 7.4.

Lastly, different combinations GIC + modified clays were prepared by mixing 0.2368 g with 36.8 µL for an adjusted powder:liquid ratio of 6.4.

For more detailed information about the materials used to prepare the specimens, specifications about the process and number of specimens prepared, see Table 3.1.

Table 3.1. Detailed specifications about the GIC specimens prepared to then test their mechanical properties.

Set No.	Specimen description	Clay	Clay %	Sub or add	Ball mill	Powder:Liquid (P/L) ratio	n
1	GIC as received from manufacturer	-	-	-	No	7.2	12
2	GIC after ball milling	-	-	-	Yes	7.4	24
3	GIC after ball milling with adjusted P/L ratio to include extra 15% water	-	-	-	Yes	6.4	22
4	GIC + ADA	ADA	2%	Add	Yes	7.4	6
5	GIC + MMT	MMT	2%	Add	Yes	7.4	6
6	GIC + MMT ADA-HCl + 10% extra water	AO ADA-HCl	2%	Sub	Yes	6.7	12
7	GIC + MMT ADA-HCl + 12.5% extra water	AO ADA-HCl	2%	Sub	Yes	6.6	6
8	GIC + MMT ADA-HCl + 15% extra water	AO ADA-HCl	2%	Sub	Yes	6.4	6

9	GIC + MMT ADA-HCl + 17.5% extra water	AO ADA-HCl	2%	Sub	Yes	6.3	6
10	GIC + MMT ADA-HCl + 20% extra water	AO ADA-HCl	2%	Sub	Yes	6.2	6
11	GIC + MMT ADA-HCl + 22.5% extra water	AO ADA-HCl	2%	Sub	Yes	6.0	6
12	GIC + MMT ADA-HCl + 25% extra water	AO ADA-HCl	2%	Sub	Yes	5.9	12
13	GIC + MMT ADA-HCl + 50% extra water	AO ADA-HCl	2%	Sub	Yes	4.9	12
14	GIC + MMT ADA-HCl	AO ADA-HCl	0.50%	Add	Yes	7.4	9
15	GIC + MMT ADA-HCl + 3.75% extra water	AO ADA-HCl	0.50%	Add	Yes	7.1	6
16	GIC + MMT ADA-HCl + 6.25% extra water	AO ADA-HCl	0.50%	Add	Yes	7.0	6
17	GIC + MMT ADA-HCl	ADA-HCl	2%	Sub	Yes	7.4	14
18	GIC+MMT ADA-HCl	ADA-HCl	0.50%	Sub	Yes	7.4	22
19	GIC + MMT ADA-HCl + P/L ratio adjusted (15%)	ADA-HCl	1%	Sub	Yes	6.4	23
20	GIC + MMT ADA-HCl + P/L ratio adjusted (15%)	ADA-HCl	0.50%	Sub	Yes	6.4	23
21	GIC + MMT AHA-HCl + P/L ratio adjusted (15%)	AHA-HCl	1%	Sub	Yes	6.4	22
22	GIC + MMT AHA-HCl + P/L ratio adjusted (15%)	AHA-HCl	0.50%	Sub	Yes	6.4	22
23	GIC + MMT GABA-HCl + P/L ratio adjusted (15%)	3xGABA-HCl	1%	Sub	Yes	6.4	22
24	GIC + MMT GABA-HCl + P/L ratio adjusted (15%)	3xGABA-HCl	0.50%	Sub	Yes	6.4	23

3.2.3 Characterisation

3.2.3.1 Widefield Microscopy (Wf)

This microscopy technique was selected as it would permit characterisation of the fluorescence property of the dyed modified clay samples, then for the purpose of this test a dental cement specimen was prepared using GIC powder that was combined with a dyed clay sample (MMT+AO+ADA HCl) to permit visualisation of the distribution of the clay.

The equipment used was a Widefield 6 (Leica LASX live cell imaging workstation with Leica DFC365FX monochrome CCD camera, 1392x1040 6.45µm pixels, 8 or 12 bits, 21 fps full frame) (Wolfson Bioimaging Facility) was used to explore the distribution of clay within the GIC specimens.

3.2.3.2 Elemental Analysis (EMA)

Samples were sent to be analysed to OEA Laboratories Limited (Cornwall, United Kingdom). All samples were submitted as a powder. This characterisation was done to check if any organic content (our modified clay) was going into the structure of the glass ionomer cement.

3.2.3.3 Small Angle X-Ray Scattering (SAXS)

These measurements were performed using a GANESHA 300 XL (Xenocs) SAXS system with an adjustable sample to detector distance. X-rays were generated using a sealed tube generator with a Cu anode (X-ray wavelength 1.54 Å). Samples were run as powders in between two 7 µm thick mica sheets, held in a custom-built stainless-steel holder, in Medium Angle ($0.015<Q<0.65$ Å^{-1}) and Wide Angle ($0.07<Q<2.8$ Å^{-1}).

The d-spacing measured by SAXS was found by selecting each peak and using the equation (2.2) - presented previously in Chapter 2 - to obtain a real space value in Å.

3.2.4 Mechanical Testing

3.2.4.1 Compressive strength (CS)

Compressive fracture strength is well known to be more sensitive to composition changes of GICs than other mechanical properties. This test is carried out by applying a compressive load to the flat ends of a specimens, see Figure 3.2.
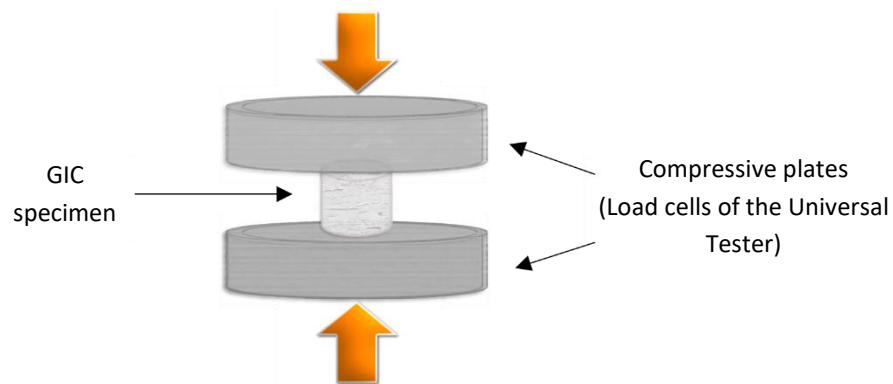
Figure 3.2. Compressive strength measurement set up.

It is calculated in MPa (N/mm^2) according to the equation (3.1) where *F* is the load at fracture and *d* the load in the diameter of the specimen respectively.

$$CS = \frac{4F}{\pi d^2}$$

(3.1)

A Zwick/Roell Universal Tester Z020 with a load cell of 20kN was used with a crosshead speed of 0.5 mm / min. Specimens were placed on their flat side on a stainless-steel platform and compressed by a second, planoparallel stainless steel platform until fracture whereupon the maximum force was recorded.

Any specimens found on fracture to have had internal voids or other imperfections were discarded and the data not used. Any specimens which resulted in imperfect load-displacement curves were also discarded.

3.2.4.1.1 Statistical Analysis

The compressive strength data were analysed using a non-parametric Kruskal-Wallis (KS) test to compare medians. This test was selected as it was ascertained that the data were not normally distributed, and the group sizes were variable owing to the need to exclude specimens that did not meet the inclusion criteria. The Kruskal Wallis test is the non-parametric closest equivalent of the ANOVA (analysis of variance).

3.3 Results

3.3.1 Incorporation of modified clay powders into GICs

3.3.1.1 Sample preparation

The result of ball milling the GIC with the MMT, ADA or modified clay samples: MMT+ADA HCl, MMT+AHA HCl and MMT+3x GABA HCl was a fine powder which was either white or off white, or slightly orange if the clay contained AO, see Figure 3.3.

a)   b)
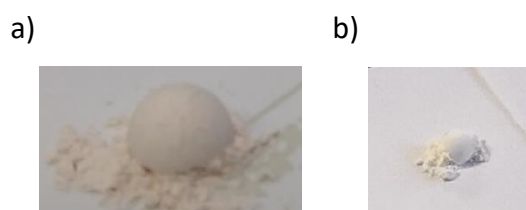
Figure 3.3. a) Powder sample of GIC with 2 wt% MMT+AO+ADA HCl and b) Powder sample of GIC with 2 wt% MMT+ADA HCl. Note the slight orange hue to the powder containing OA, and the off-white appearance of the powder without OA.

3.3.2 GIC specimen preparation

3.3.2.1 Specimen sets

The need to prepare different sets of dental cement specimens arose due to various factors that could be modified and have a direct impact on the mechanical properties of the final specimen. Such as the ball milling process itself as it might alter the GIC powder particle size and/or shape and the addition of a high specific surface area material (clay) that could potentially modify the surface area of the final material. Therefore, an in-depth study was carried out, firstly to ascertain whether ball milling affected the baseline strength of the otherwise unmodified GIC specimens, and secondly, to determine the effect of powder:liquid ratio on CS of GIC with ball-milled powders.

As mentioned in the introduction, published investigations of amino acid modified clays and their effects on properties of GICs used a commercially prepared ADA-montmorillonite and, as such, whereas the amino-acid modified montmorillonite clays described in this thesis were prepared and characterised by the author as described in Chapter 2. It was therefore necessary to ascertain whether these materials provided the same improvement in GIC compressive strength when handled in the same way as in the published studies, that is, without ball mixing or additional water, but rather prepared according to the method reported by Fleming[26].

3.3.3 Characterisation

3.3.3.1 Widefield Microscopy (Wf)

Widefield images of GIC specimen made using dyed clay particles combined using a roller mixer are shown in Figure 3.4. It can be seen that the whole specimen is bright under the fluorescent microscopy which indicates that the particles are well distributed in the cement,

but some points are brighter, this could be a cluster of clay particles that were not well dispersed with the gentle movements of the roller mixer.
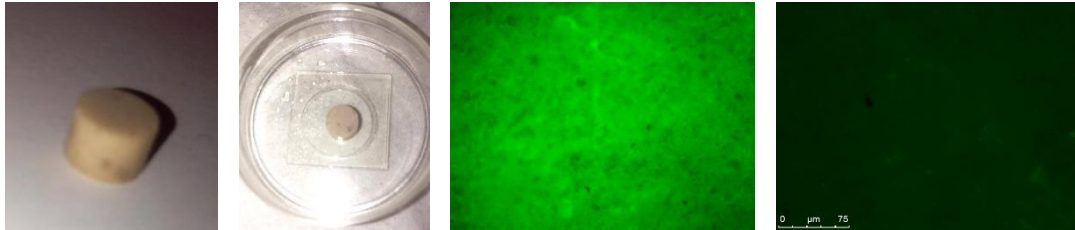
Figure 3.4. Specimen with AO 1% by clay mass. (Scale bar: 0 - 75µm).

3.3.3.2   Elemental Analysis (EMA)

This technique shows the organic content (%N, %C, %H) obtained of the precursors used to prepare the dental cement specimens. The glass ionomer cement (GIC) and clay (MMT) were used as received and the third line corresponds to the clay with 1 wt% AO added, see Table 3.2.

Table 3.2. EMA data for clay samples and GIC before any treatment.

Sample	Experimental Value		
	N %	C %	H %
GIC	<0.01	8.2	1.1
MMT		0.3	1.3
MMT+AO	0.1	1.7	1.2

3.3.3.3   Small Angle X-Ray S (SAXS)

Figure 3.5 presents the data obtained with this technique for the precursors (GIC and MMT) and the GICs with added modified clay, in this instance, two different concentrations of MMT + ADA HCl were analysed, 0.5% and 2%.
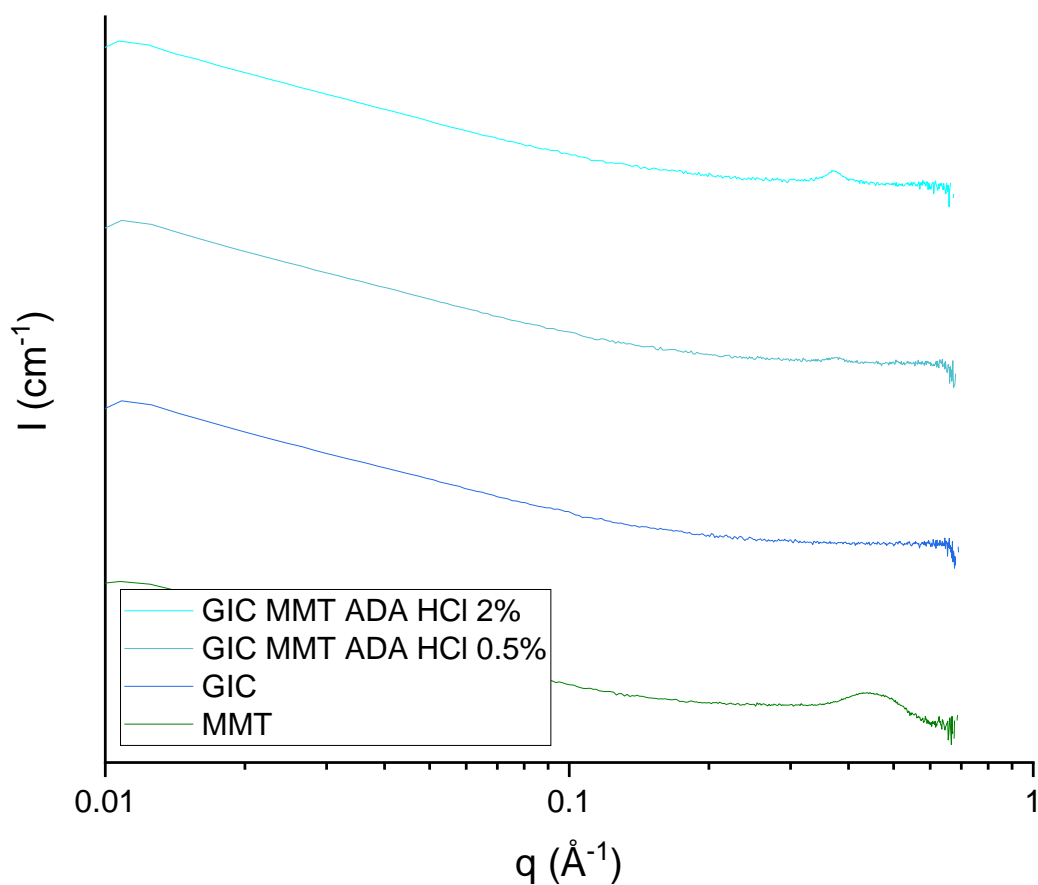
Figure 3.5. SAXS spectra of GIC with clay sample. Graph in Log scale and shifted for clarity.

Table 3.3 shows how the presence of a small amount of modified clay is visible in the SAXS experiments on GIC samples. The pure GIC does not show any peak in the q-range studied, however the samples with MMT added show a small peak that corresponds to the value found for the pure modified clay powder.

Table 3.3. Peak position of GIC + modified clay and precursors.

Precursor	d Space (Å)	Clay Sample	d Space (Å)
MMT	14.3	MMT + ADA HCl	17.1
GIC	No visible peak	GIC + MMT ADA HCl 0.5%	16.7
		GIC + MMT ADA HCl 2%	17.0

3.3.4 Mechanical Testing

3.3.4.1 Compressive Strength (CS)

Detailed information of each set can be found in section 3.2.2.1, different specimens were compressed in the Universal Tester to measure their compressive strength and the results are shown in Table 3.4.

Table 3.4. Compressive strength in MPa and number of specimens made for each set of dental cement.

Set no.	Specimen description	n	Compressive Strength (MPa)		
			Mean	Median	St Dev
1	GIC as received from manufacturer	12	126.3	123.3	21.8
2	GIC after ball milling	24	174.0	170.5	46.6
3	GIC after ball milling with adjusted P/L ratio to include extra 15% water	22	133.6	133.1	22.6
4	GIC + ADA	6	94.4	85.8	29.6
5	GIC + MMT	6	78.4	76.8	13.4
6	GIC + MMT ADA-HCl + 10% extra water	12	104.4	104.5	21.4
7	GIC + MMT ADA-HCl + 12.5% extra water	6	112.7	115.1	13
8	GIC + MMT ADA-HCl + 15% extra water	6	121.9	121.6	8
9	GIC + MMT ADA-HCl + 17.5% extra water	6	108.1	100.2	11.0
10	GIC + MMT ADA-HCl + 20% extra water	6	84.4	77.3	21.1
11	GIC + MMT ADA-HCl + 22.5% extra water	6	91.7	96.6	15.0
12	GIC + MMT ADA-HCl + 25% extra water	12	115.1	119.5	13.9
13	GIC + MMT ADA-HCl + 50% extra water	12	91.4	96.8	17.9
14	GIC + MMT ADA-HCl	9	112.7	115.9	20.2
15	GIC + MMT ADA-HCl + 3.75% extra water	6	113.1	112.6	18.0
16	GIC + MMT ADA-HCl + 6.25% extra water	6	101.1	103.2	31.8

17	GIC + MMT ADA-HCl	14	102.2	97.0	13.0
18	GIC+MMT ADA-HCl	22	144.2	140.8	22.2
19	GIC + MMT ADA-HCl + P/L ratio adjusted (15%)	23	217.0	222.8	32.2
20	GIC + MMT ADA-HCl + P/L ratio adjusted (15%)	23	219.1	216.8	21.9
21	GIC + MMT AHA-HCl + P/L ratio adjusted (15%)	22	220.5	220.9	20.8
22	GIC + MMT AHA-HCl + P/L ratio adjusted (15%)	22	216.0	220.3	22.4
23	GIC + MMT GABA-HCl + P/L ratio adjusted (15%)	22	213.3	217.2	25.6
24	GIC + MMT GABA-HCl + P/L ratio adjusted (15%)	23	202.4	202.8	28.9

3.3.4.1.1 Statistical Analysis

In order to compare the strength of all our dental cement specimens it was important to establish the baseline of the CS presented by GIC without any further process, GIC that has been ball milled, as well as GIC that has been ball milled with adjusted powder:liquid ratio to take into account the higher specific surface area of the GICs containing clays.

Three groups were analysed using KW tests:

Group 1

This analysis was conducted to answer the question: Does milling and adjusting the P/L ratio of the GIC, without any additions, alter the CS?

Table 3.5. Median CS in MPa and statistical comparison of GIC sets.

Set no.	Description	CS (median)	Statistically homogeneous group
1	GIC as received from manufacturer	123	a
2	GIC after ball milling	171	b
3	GIC after ball milling with adjusted P/L ratio to include extra 15% water	133	a

The KW test indicated that set 1 and 3 were statistically indistinguishable whereas set 2 had a significantly higher compressive strength than sets 1 and 3, see Table 3.5.

Group 2

The purpose of analysis was to answer the question: Does modifying the P/L ratio impact the CS of the GICs?

Table 3.6. Median CS in MPa and statistical comparison of dental cement sets varying the amount of water to determine best P/L ratio.

Set no.	Description	CS (median)	Statistically homogeneous group
6	GIC + MMT ADA-HCl + 10% extra water	105	c, d, e
7	GIC + MMT ADA-HCl + 12.5% extra water	115	c, d, e
8	GIC + MMT ADA-HCl + 15% extra water	122	e
9	GIC + MMT ADA-HCl + 17.5% extra water	100	c, d, e
10	GIC + MMT ADA-HCl + 20% extra water	77	c

11	GIC + MMT ADA-HCl + 22.5% extra water	97	c
12	GIC + MMT ADA-HCl + 25% extra water	119	d, e
13	GIC + MMT ADA-HCl + 50% extra water	97	c, d

The KW test indicated that there were no unique sets, which means that there were not any set of specimens statistically significantly different from the rest. Therefore, all sets were statistically indistinguishable from at least one other group, see Table 3.6.

However, set 8 presented the numerically highest compressive strength and this was statistically significantly different from the three sets that presented the numerically lowest CS (sets 10, 11 and 13). This suggests that set 8 was significantly higher than some other specimen sets, and higher but not to a statistically significant degree than the remaining sets.

Set 12 had the numerically second highest CS. Unfortunately, it also had limited statistical significance when compared with other sets. Although, set 12 was statistically significantly higher than sets 10 and 11, it was not the case with the other sets.

Aside from these observations, there were no statistically significant differences between compressive strength of the different specimen sets.

Group 3

This last comparison group analysis was designed to answer the question: Having already considered the ball milling process and adjusted the P/L ratio, does the amount and type of clay make a difference to the final product CS?

Table 3.7. Median CS in MPa and statistical comparison of GIC + modified clay sets.

Set no.	Description	CS (median)	Statistically homogeneous group
3	GIC after ball milling with adjusted P/L ratio to include extra 15% water	133	f
8	GIC + MMT ADA-HCl + 15% extra water	122	f
19	GIC + MMT ADA-HCl + P/L ratio adjusted (15%)	223	g
20	GIC + MMT ADA-HCl + P/L ratio adjusted (15%)	218	g
21	GIC + MMT AHA-HCl + P/L ratio adjusted (15%)	221	g
22	GIC + MMT AHA-HCl + P/L ratio adjusted (15%)	220	g
23	GIC + MMT GABA-HCl + P/L ratio adjusted (15%)	217	g
24	GIC + MMT GABA-HCl + P/L ratio adjusted (15%)	203	g

In this instance the KW test indicated that there are two homogeneous groups: sets 3 and 8 are indistinguishable from one another, and sets 19-24 inclusive are indistinguishable from one another, however, sets 3 and 8 have statistically significantly lower strength than groups 19-24 inclusive, see Table 3.7. This leads to the conclusion that it does not matter the type of modified clay nor the quantity used. 0.5% or 1%, all of them increased the CS compared to the samples with no clay and too much clay (2%). All these observations apply while keeping the ball milling and P/L ratio the same.

3.4 Discussion

The aim of the work presented in this chapter was to determine whether it was possible to enhance the compressive strength of GICs using modified clay particles of high aspect ratio and functionalised with ω-amino carboxylic acids. The preparation and characterisation of these clay particles was described in detail in Chapter 2.

The clay particles were added to a commercial GIC, as to source the appropriate grades and specification of glass and polyacrylic acid to formulate one from first principles is challenging at laboratory scale. Therefore, any addition of clay particles results in an increase in the specific surface area of the resultant GIC powder, since the particles are small and have a higher specific surface area than the glass particles.

Furthermore, the approach taken to combine the clay and glass particles, that of ball milling the combined powders, is likely to have reduced the size and thus increased the surface area of the glass particles. It was therefore considered likely that an additional quantity of water might be required to effectively wet the combined glass and clay particles and to ensure there were not dry and porous areas within the specimens which would reduce the overall strength.

Previous studies of GICs augmented with MMT used a simple and somewhat unclear means of incorporating the clay and the author considers this may not have adequately homogenised the powder blend, and as such the ball milling was considered necessary to better distribute the clay within the glass and was adopted as it is commonly used in the manufacture of these materials.

In addition to that, when we compare the values obtained in Elemental Analysis and SAXS is evident that the addition of modified clays to the GIC structure was successful, as GIC itself did not presented any peak in the spectrum however, with 0.5 wt% of clay a small curve can be seen at 16.7 Å and with 2 wt% it increases to 17.0 Å, this peak appears in the same range than the modified clay itself (MMT ADA HCl) 17.1 Å.

The MMT+ADA used in Fleming's work was a commercial product and, as such, limited information was available to the researchers regarding the clay, on the other hand, the clay used within all the experimental sections of this thesis was provided from a different source as MMT, cleaned, treated and fully characterised in the lab; this gives more information

regarding the clay, but also it makes easier to reproduce the experiments as it doesn't limit the availability of the clay source, once the commercial batch is gone, it would be impossible to get more of it. For comparison purposes it was also necessary to reproduce some of Fleming's experiments to determine whether the same results were observed with this different clay source. The CS values obtained were comparable to the range of value that they reported (87 - 150 MPa)[26] being 112.7 MPa the value obtained using 0.5% added clay, and if the P/L ratio gets adjusted the values were: 113.1 MPa with 3.75% additional water and 101.1 MPa with 6.25% additional water.

The methodology reported by Fleming indicated that they had combined their GIC powder with the clay by hand, to avoid any inhomogeneity in the final product it was decided to use instead a roller mixer. However, after seen the distribution under the microscope (widefield, see section 3.3.3) the decision to use a ball mill mixer as a more appropriate technique was taken. In this way we control the time and force used to mix the powders which resulted in an acceptable level of homogeneity in the formulation as the specimens did not present any indication that could suggest particle agglomeration.

The effect on compressive strength of ball milling the GIC powder on compressive strength of otherwise unmodified (i.e., no clay) GIC, and the effect of adjusting the powder:liquid ratio from 7.4 to 6.4, is shown in Table 3.4, comparing the CS means it can be seen that ball milling the GIC powder results in an increase of 38% from the CS baseline (174 MPa compared with 126 MPa), whereas adding an additional 15% water to adjust the powder:liquid ratio to 6.4 reverts the CS to equivalent to the baseline value (it is only 6% higher, 134 MPa compared with 126 MPa). As shown in Table 3.5 the compressive strength of the unmodified GIC and the GIC that was ball milled and the additional water added, were statistically indistinguishable, whereas the compressive strength of the ball milled GIC without additional water was statistically significantly higher.

The next group of specimens compared were made to determine the amount of water need to get a material that was easy to handle, but remained with good CS. The specimens tested contained GIC + MMT AO ADA-HCl (2 wt%) + different amount of water needed for a P/L adjusted from 6.7 to 4.9. As presented in Table 3.6, there were not statistically significant differences between these sets, despite this, the set that presented the highest numerical strength which was statistically significantly higher than some of the other sets corresponded

to the specimens with 15% extra water, therefore it was selected as the optimal amount of water for adjusting the P/L ratio used for subsequent investigations.

Lastly, a third group of specimens was compared to determine the effect of clay for a fixed P/L ratio in the GIC mechanical properties. The effect on compressive strength of adjusting the powder:liquid ratio to 6.4, as well as incorporating 0.5 wt%, 1 wt% or 2 wt% modified clay (MMT ADA-HCl, MMT AHA-HCl or MMT 3xGABA-HCl) is shown in Table 3.7. In this instance, we could see how the type of clay did not give statistically different results, however 0.5 wt% and 1 wt% produced better CS than no clay or too much clay (2 wt%).

3.5 Conclusion

As we could see within the work done in this chapter, the importance of using the right parameters when preparing a GIC is crucial to obtain better results in the mechanical properties of the material, but it has to be taken into consideration that in the consult room the dentist would not have the equipment to measure specific amounts which will cause variation on every application they make.

Additionally, data comparing the combining process of GIC powder + clay used in this project and previous research was presented, this process impacts the final strength of the dental cements. It is of paramount importance that a filler such as montmorillonite clay sheets is well dispersed within a composite material to effectively enhance strength, and as such it was deemed necessary, as discussed in section 3.4, to affect a more thorough mixing of clay and GIC powder than has been reported in the literature. Ball milling was selected as this is a method used in commercial GIC manufacture and thus would be readily scalable and acceptable from a regulatory as well as manufacturing point of view.

However, it was anticipated that ball milling the clay and GIC powder may also reduce or alter the GIC powder particle size or shape, and this may result in a different required powder: liquid mixing ratio. Therefore, a pilot study was carried out, firstly to ascertain whether ball milling affected the baseline strength of the otherwise unmodified GIC specimens, and secondly, to determine the effect of powder:liquid ratio on CS of GIC with ball milled powders.

These data confirmed the observations made while preparing the specimens, since it had been noticed that GIC's handling properties changed after ball milling, leaving the mix feeling crumbly and dry during the folding and packing process, leading to the finished specimens showing evidence of folds and inhomogeneities. Hence the need to adjust the P/L ratio for the rest of sets.

in the presence of clay, it was observed that to vary the powder:liquid ratio had impact over the CS, and as such it was concluded that an additional 15% water was appropriate for allowing a comparison of the effect of clay on GIC compressive strength without having to allow for a reduction simply due to the manner of combining clay and GIC powder. Presumably to have sufficient water to wet and lubricate all particles and prevent porosity is the most important factor and a small amount of excess water above the optimum is insufficient to result in any untoward impact on the setting reaction.

Improving the compressive strength of the GIC materials is desirable as this would extend the time before such a filling would need replacing, and potentially also allow GIC materials to be used for more challenging types of restoration in the posterior area of the mouth such as larger restoration pieces, multi surface restoration or even casts.

The results presented in this chapter showed that adding a small amount (0.5 or 1% by mass) of modified clay and being aware of the importance of the powder:liquid ratio gives a statistically significant improvement of the compressive strength of the GIC. The chain length of the modifier does not appear to affect the result however it is worth noting that the hydrophobicity of the organoclay increased with the length of the chain (GABA < AHA < ADA) and that could potentially provide some additional interesting properties to the final product and its desired characteristics.

The improved compressive strength of the GIC + modified clay presented in this chapter (203 – 223 MPa) is comparable to the compressive strength of the natural tooth molar enamel (260 MPa) and molar dentine (305 MPa), as well as other dental materials within a range from 250 – 500 MPa.[21]

Chapter 4 Addition of Chlorhexidine to Clay Particles

4.1 Introduction

In Chapter 2 different ω-amino carboxylic acids were added to montmorillonite to create a structure that could potentially be incorporated into dental materials. This idea raised the research question that will be addressed in this chapter: is it possible to layer chlorhexidine in between the clay sheets of montmorillonite, and if so, will this be released when the system comes into contact with an aqueous environment?

Chlorhexidine is a well-known antimicrobial substance that is already used in different products and understanding its interaction with montmorillonite could result in potential interesting applications. These include: wound dressings[66] and/or dental materials such as; silicones, ligatures[67], fillers[62 68 69], implants[70], mouthwash, toothpastes, or gels.

There has been a limited amount of research using montmorillonite and chlorhexidine to test antimicrobial properties following the slow release principle[54 53 71]. The differences in approach between that work and the series of data presented in this chapter are discussed, especially regarding the sample preparation and the steps taken to distinguish free chlorhexidine from chlorhexidine bound to clay.

The objective of the series of experiments in this chapter was to prepare several samples and select the most interesting of the resulting final products; to be added into the development of a more complex material that will be presented within the next chapter of this thesis.

4.2 Materials and Methods

4.2.1 Clay functionalisation with chlorhexidine digluconate (CHX DG)

The clay used was Wyoming montmorillonite, SWy-2 (MMT), which was purchased from the Clay Minerals Society source clays repository at Purdue University $(Si_{7.94}Al_{0.06})$-$(Al_{2.88}Fe_{0.5}Mg_{0.62})O_{20}(OH)_4Na_{0.68}$,[72]. The chlorhexidine digluconate (CHX DG) was purchased from Sigma-Aldrich.

To characterize the precursors, samples were all run using the stated different techniques, however, most of the samples were in powder form with the exception of CHX DG which could cause inconsistent data later due to the presence of differing amounts of water (the material is hygroscopic) for the different spectra. One possible solution was to use chlorhexidine diacetate, which is another salt of chlorhexidine that is a white powder, however this did make it harder to compare data between samples.

Then the challenge faced with CHX DG was that it comes as an aqueous solution. The literature suggests that this substance cannot be isolated as a solid, therefore it has to be purchased as a 20% (w/v) aqueous solution[73]. As the only purpose of using CHX DG powder was to provide us with a reference in different characterisation techniques, some of it was freeze dried to obtain a solid sample. An Alpha 1-2 LD Plus Martin Chris freeze dryer was used. It was put inside the chamber where the temperature remains ~-60 °C and the vacuum ~0.0245 mbar.

Once the aqueous solution was freeze dried, a white solid was obtained (Figure 4.1a) that resulted to be quite brittle and hygroscopic, in line with what the literature suggested. Due to this it was kept well sealed while not in use. It was handled as quickly as possible to run each sample as a powder for each characterisation technique before it absorbs water, see Figure 4.1b and Figure 4.1c.
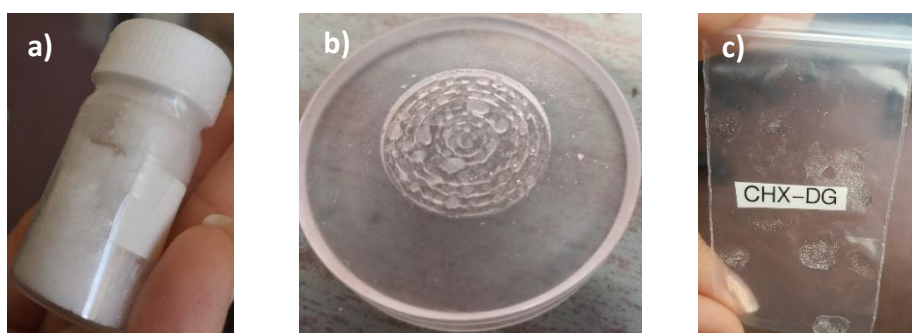
Figure 4.1. a) Freeze dried CHX DG, b) CHX DG on XRD sample holder after running XRD for 2h and c) sample bag with unused CHX DG for IR.

4.2.1.1   Preparation of Different Clay + Chlorhexidine samples

The method to prepare these samples consisted of making a 2% wt clay suspension by adding 20 g of clay to 1 L of deionised water (MilliQ) and leaving it to mix with the assistance of a magnetic stirrer. To ensure a good dispersion, these samples were left on the magnetic stirrer for 24 hours. At this point, the clay powder may still have contained some larger impurities, such as quartz. The sample was therefore allowed to settle for 3 hours and carefully syphoned to exclude the impurities at the bottom of the container avoiding its redispersion. The supernatant was kept as stock and it is considered to contain 20 g of clean MMT.

The different samples were prepared by mixing 180 ml of deionised water (DIW) with 20 ml of the clay stock solution considering that it contains ~0.4 g of MMT and adding, respectively, six different chlorhexidine digluconate amounts needed for 0.3, 0.6, 0.9, 1.2, 1.6 and 1.75 times the clay cation exchange capacity (CEC).

The equation (*4.1*) was used to determine the concentration in units of the clay CEC, where q_m is the maximum adsorption of the monolayer (from mg/g to mmol/100g by using the molar mass in g/mol), z is the valency (in our case z=2), Mw is the molar mass of adsorbed species (value for CHX DG) and CEC is the cation exchange capacity of the clay in mmol/100g (CEC of montmorillonite used in this research project (SWy-2 MMT) corresponds to 84 mmol/100 g[48]).

$$q_{CEC} = \frac{q_m\ z}{M_w\ CEC} \times 100 \qquad (4.1)$$

All samples remained as solutions and were kept constantly stirring throughout the duration of the experiments within this chapter to observe changes and to run tests if necessary.

Furthermore, for the experiments that required samples in powder form, 3 larger dispersions were prepared by mixing 300 ml of deionised water, 300 ml of the stock solution of montmorillonite (~ 6 g clay content) and the required amount of chlorhexidine digluconate solution to obtain 0.3, 0.6 and 1.2 CEC concentrations. These aqueous samples were stirred overnight and left to rest for about 1 to 2 hours. Then, the layer of supernatant (clear phase, see Figure 4.2) was syphoned while the "precipitate" phase was washed to remove any excess

unabsorbed CHX, these washes consisted of the addition of 300 ml more of DIW, stirring and allowing the solution to settle before proceeding to again, syphoning the supernatant and centrifuging the samples at 10.5k rpm to remove as much liquid as possible. These samples were allowed to dry in a vacuum oven at ~60 °C for several days to get a solid sample. Lastly, they were pulverised with a pestle and mortar to get a white/sand/grey fine powder.

Figure 4.2. Layers formed after letting 1.2 CEC sample to settle.

4.2.1.2   Zeta Potential

The measurements were done with the support of the Mann group using a ZETASIZER Nano series instrument (Malvern Instruments, UK) and disposable folded capillary zeta potential cells (Malvern). The point of this was to try and see if there was any correlation between particle charge and colloid stability, as a function of added chlorhexidine concentration. The clay stock suspensions were diluted tenfold to 0.2 wt% for this and chlorhexidine digluconate was added equivalent to 0.3 - 1.75 times the clay cation exchange capacity (CEC).

4.2.2 Characterisation

4.2.2.1 Elemental Analysis (EMA)

This method was chosen as a primary test to check if the chlorhexidine was present in the clay samples. Data was obtained from OEA Laboratories Limited (Cornwall, United Kingdom). All samples were submitted as a powder.

4.2.2.2 Fourier-transform Infrared Spectroscopy (FT-IR)

These data were obtained using a Perkin-Elmer Spectrum 100 FT-IR (PerkinElmer, Waltham, MA, USA) with an Attenuated Total Reflection attachment that allows a powder to be tested, at the teaching labs within the School of Chemistry. The samples were analysed in powder form and tests run in the wavenumber range from 400 to 4000 cm^{-1} and 600 to 4000 cm^{-1} respectively, with a resolution of 8 cm^{-1}.

4.2.2.3 X-Ray Powder Diffraction (XRD)

This analysis was performed using a Bruker (Billerica, USA) D8 Advance Powder X-ray Diffractometer (Cu Kα radiation, wavelength λ = 1.54 Å) at 2θ values of 4° - 35°, with a step size of 0.05°.

The data obtained with this technique had to be corrected due to the presence of a diffuse, broad spectrum signal related to the sample holder. This was done by subtracting the background signal with help of the software EVA (DIFFRAC^{PLUS} Evaluation Package Release 2007).

The d spacing of the peaks was calculated using the equation (2.1) – see 2.2.2.2.

With help of Dr. Annela Seddon, the SAXS data were collected on a Ganesha SAXS/WAXS beamline (Xenocs) with a copper Kα source (λ = 1.54 Å). Samples were loaded into 1.5 mm borosilicate glass capillaries (Capillary Tube Supplies Ltd) and sealed with UV curable adhesive (Norland).

Measurements were made over a q range of 0.015 - 0.65 Å^{-1} and for an exposure time of 3600 seconds. Data were processed in SAXSGUI.

The d space can be calculated using the equation (2.2) – see 2.2.2.3.

4.2.3 Release Test

4.2.3.1 UV-Vis

A Jenway 7315 UV/Visible Spectrophotometer was used to read the absorbance of the solutions (after diluting where necessary) with a wavelength from 198 to 600 nm and a Xenon lamp as light source. To run the samples BRAND® semi-micro cuvettes (BRAND GMBH + CO KG, Wertheim, Germany) were used.

For ensuring the clear and detectable reading of chlorhexidine in solution, the calibration curve presented in Figure 4.3 was made, considering a concentration range from 5 µM to 100 µM.
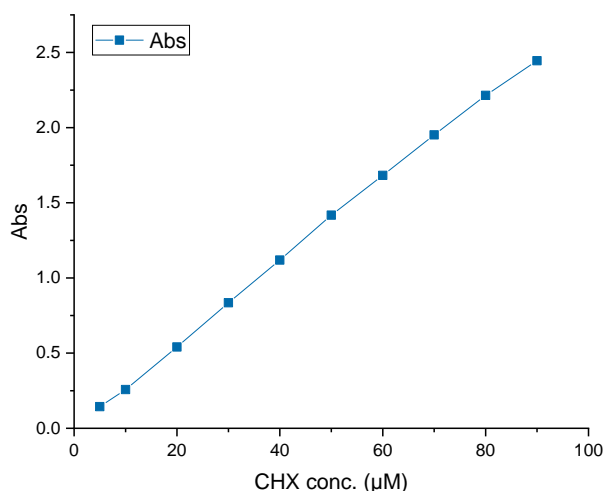
Figure 4.3. UV-Vis calibration curve for chlorhexidine solutions in water (λ = 255 nm)

For samples that required to be centrifuged before the UV-Vis readings a Thermo Scientific™ Heraeus™ Pico™ 21 Microcentrifuge was used.

4.2.3.2   Dialysis

This test was designed to observe the behaviour of the modified clay with different concentrations of chlorhexidine. Samples were checked during the first 8 hours after placing in water and then during subsequent for around a month. Release of CHX was detected in the DIW eluent using UV-Visible spectroscopy at 255 nm.

The experiment consisted of taking 0.5 g of three different treated clays in powder form: 0.3 CEC, 0.6 CEC and 1.2 CEC. These were sealed in 'SnakeSkin' 3.5 kDa pore size dialysis tubing (ThermoFisher Scientific UK Ltd, Loughborough, UK), immersed in 40 ml of deionised water and stirred during the 43 days that this experiment lasted at room temperature to allow soluble material to pass into the water.

4.3   Results

4.3.1 MMT + CHX

4.3.1.1   Sample preparation

As explained in the previous section, MMT was mixed with different amounts of CHX DG. The higher the concentration the less stable the suspensions became. Different concentrations considering the cation exchange capacity (CEC) of the MMT were prepared: 0.3, 0.6, 0.9, 1.2, 1.6 and 1.75. As seen in Figure 4.4, the appearance varies between concentrations, in this case it illustrates two samples that were picked as the most interesting candidates for the release test: 0.6 CEC and 0.3 CEC, and also 0.9 CEC. After being left to stand, it is very noticeable how they change from completely dispersed (Figure 4.4a), after stopping the stirring (Figure 4.4b) and after 5 hours of rest (Figure 4.4c).
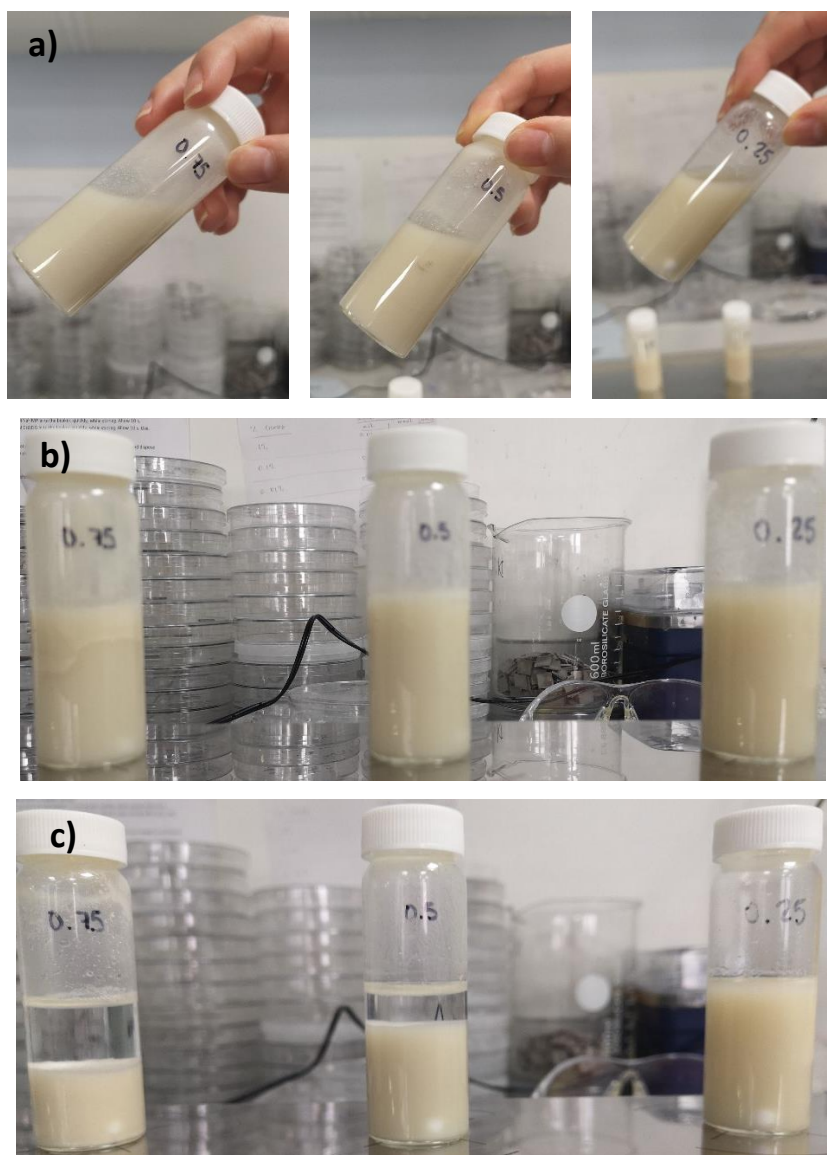
Figure 4.4. Stability of different clay + antimicrobial suspensions at 0.9 CEC, 0.6 CEC and 0.3 CEC. a) right after dispersion, b) separating after stopping the stirring and c) dispersions beginning to settle down after a few hours.

All samples were kept under continuous stirring at room temperature until they needed to be used so the suspensions were as homogenous as possible whenever taking a sample out of their container.

Also, the samples that were used for the dialysis test needed to be in powder form, so they were prepared as described in the previous section and kept carefully sealed in a vial.

4.3.1.2 Zeta Potential

As mentioned in the sample preparation section of this chapter, the higher the concentration of CHX DG in the solution the harder it resulted to keep it well dispersed.

However, is important to mention that all the MMT + CHX samples, even the lower concentration, undergo aggregation, on different levels as can be noticed in different sample images across this chapter (Figure 4.2, Figure 4.4 and Figure 4.6).
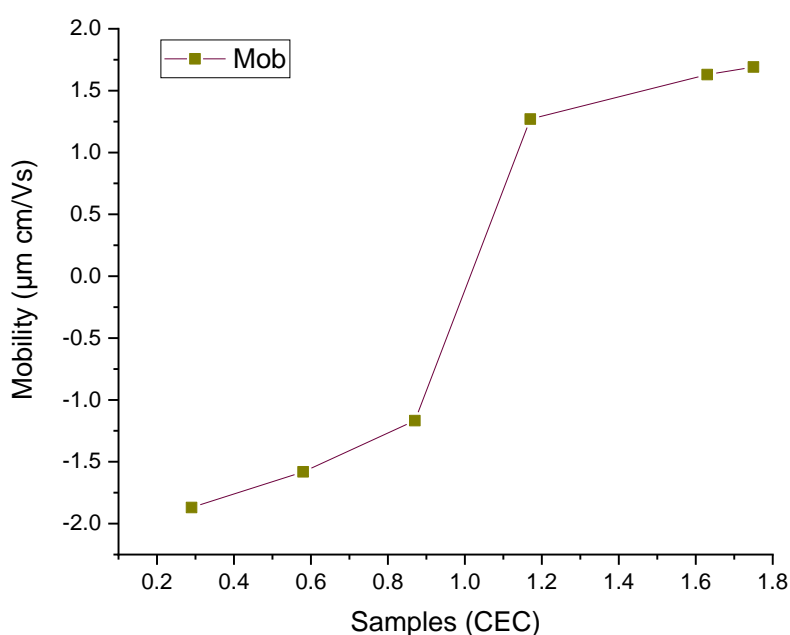
Figure 4.5. Electrophoretic mobility of suspensions of treated clay as a function of CHX content (expressed in CEC)

In principle if enough CHX is added to neutralise the clay (allowing for a charge of 2+ per CHX molecule) and considering that it adsorbs all of it, then the sign of the zeta potential would change from positive to negative. Looking at Figure 4.5, it appears that this change of sign occurs around 1.0 CEC which confirms the effect of the interaction between CHX and MMT.

This also will explain the behaviour noticed in the samples with larger content of CHX where the system seems to collapse when left without stirring, sample 1.6 CEC seemed to form aggregates on the glass even during stirring (Figure 4.6c). All of them were left to settle but the pattern in 1.6 CEC is quite noticeable, see Figure 4.6a and Figure 4.6b.
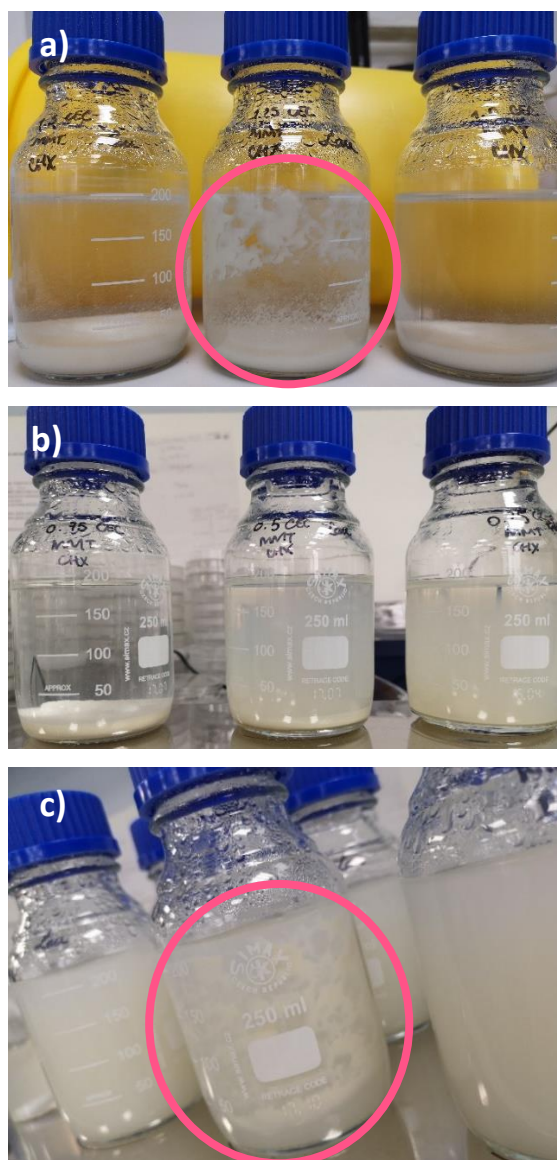
Figure 4.6. a) MMT + CHX DG samples 1.75 CEC, 1.6 CEC, 1.2 CEC after leaving them to settle overnight, b) MMT + CHX DG samples 0.9 CEC, 0.6 CEC, 0.3 CEC after leaving them to settle overnight. and c) all MMT + CHX DG during stirring. (Notice aggregation in sample 1.6 CEC).

4.3.2 Characterisation

4.3.2.1 Elemental Analysis (EMA)

The following tables (Table 4.1 and Table 4.2) show the organic content (%N, %C, %H or %CNH) obtained for the precursors and treated clay samples.

Thanks to this technique it is possible to compare the values of organic content composition of the samples of MMT treated with CHX. As shown in Table 4.1, the experimental values for CHX are close to the predicted values. The clay precursor has a very small organic content which corresponds to its structure. On the other hand, for the treated clays, the organic content and the clay layer spacing seen in SAXS both increase as more CHX is added; this data will be discussed in more detail below in Section 4.4.

Table 4.1. Elemental analysis of precursors.

Sample	Experimental Value			Theoretical Value			d Space (Å)
	N %	C %	H %	N %	C %	H %	
CHX DG	14.7	43.7	6.3	15.6	45.4	6.0	
MMT		0.3	1.3				~10

Table 4.2. Elemental analysis of the different CEC clay samples.

Sample	Experimental Value				d Space (Å) from SAXS
	N %	C %	H %	Total %CNH	
0.3 CEC MMT+ CHX-DG	1.8	3.7	1.7	7.2	14.1
0.6 CEC MMT+ CHX-DG	3.3	6.8	1.6	11.7	14.7
1.2 CEC MMT+ CHX-DG	5.1	10.6	1.8	17.5	15.3

4.3.2.2   *Fourier-transform Infrared Spectroscopy (FT-IR)*

As mentioned in the previous section this technique was used to confirm, in the first instance, that the clay was interacting with the CHX. The spectra of the precursors can be compared with those of CHX treated clay samples.

The distinctive peaks for montmorillonite are situated around 3600 cm^{-1} (-OH of *Al-OH and Si-OH*), 3400 cm^{-1} (most likely to be the -OH stretching of the water in the interlayer)[51], the one around 1630 cm^{-1} (suggests water of hydration in the adsorbent)[52], around 1100 cm^{-1} – 1000 cm^{-1} and 600 cm^{-1} – 500 cm^{-1} (the stretching bands of Si-O-Si and Si-O-Al respectively) and between 950 - 800 cm^{-1} (due to the Al-Al-OH, Al-Fe-OH and Al-Mg-OH interactions).[53] [54] [55] [56]

The distinctive peaks of CHX would be at 3380 cm^{-1} (-NH), 2930 cm^{-1} – 2850 cm^{-1} (-CH$_2$), 1600 cm^{-1} – 1050 cm^{-1} (stretching of the interactions C-N, C-C and C=C)[53] [74] and 1490 cm^{-1} (chlorophenyl group)[75].
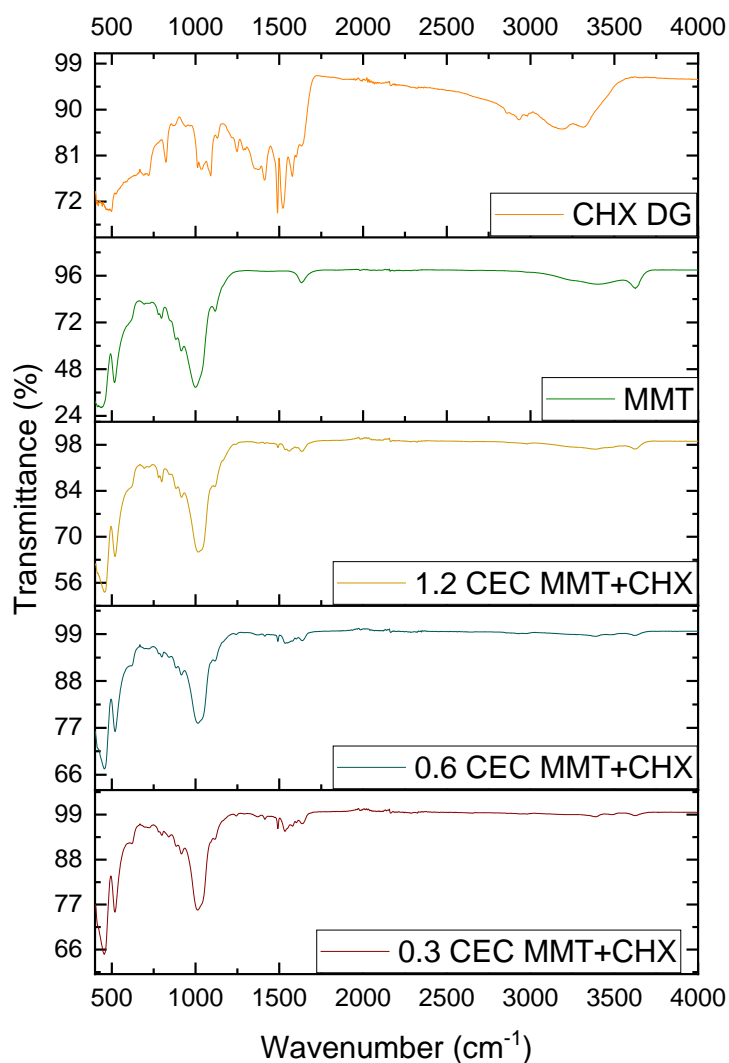
Figure 4.7. All precursors and clay samples IR spectra. Curves have been shifted for clarity.

As seen in Figure 4.7 determining what is happening with our samples is complicated by the fact that the peaks of MMT and CHX DG appear around the same wave number. However, the change in the clay peak around 1630 cm^{-1} reveals a range of weak peaks due to CHX between 1250 - 1750 cm^{-1}. This indicates that the chlorhexidine is present now together with the clay. Also, the disappearance of the broad clay signal around 3000 - 3600 cm^{-1} indicates that there is less H bonding, and therefore, less water in the clay-CHX complexes. and changes

with the -OH interactions happening in the structure This leads to the conclusion that the interspace is now occupied by the molecules of CHX instead.

The use of other techniques will provide more information on how the chlorhexidine could be interacting with the clay stacks but with this one we can confirm the presence of the antibacterial compound in the clay structure.

4.3.2.3   X-Ray Powder Diffraction (XRD)

In Figure 4.8 the spectra of the precursors are compared with the three clay + antimicrobial samples. The most visible feature is the displacement and increase in intensity of the first peak (d_{001}). Also, less visible but interesting is the emergence of a broad peak between 10 ° - 15 ° corresponding with where the CHX DG precursor presents a signal. This data supports the theory of the antimicrobial material intercalating into the clay structure. These changes vary as the concentration of chlorhexidine in the sample increases.
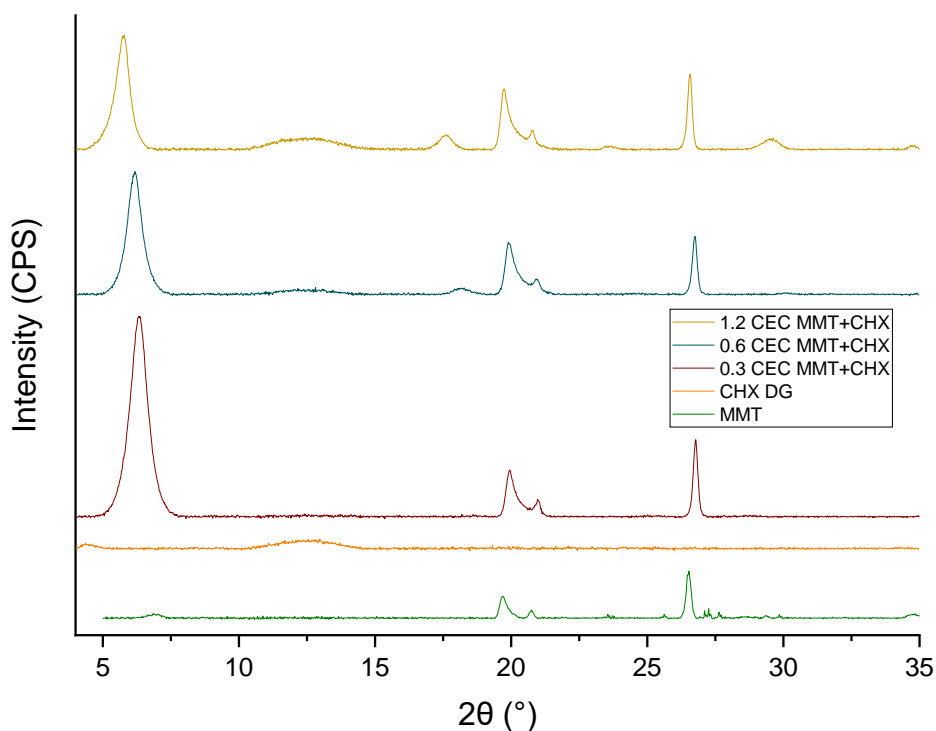
Figure 4.8. XRD spectra of all precursors and clay samples with different concentrations of CHX. Spectra have been shifted for easy comparison.

In addition to the data presented above more information of the stacking and the structure of the clay can be obtained when the d spaces of each peak are compared. Table 4.3 presents those values and despite the visible similarity in spectra between all clay samples, it is noticeable that the d spacing of the first peak (d_{001}) increases along with the appearance of other peaks, this due to the presence of chlorhexidine in the sample.

Table 4.3. Peaks for clay sample and precursors.

Precursor	d Space (Å)	Clay Sample	d Space (Å)
CHX DG	20.2 (broad) 6.7 (broad)	MMT + 0.3 CEC CHX DG	13.9 (sharp) 4.4 (sharp) 4.2 (sharp) 3.3 (sharp)
MMT	12.5 (broad) 4.5 (sharp) 4.3 (sharp) 3.4 (sharp) 2.6 (broad)	MMT + 0.6 CEC CHX DG	14.3 (sharp) 7.0 (broad) 4.8 (broad) 4.4 (sharp) 4.2 (sharp) 3.3 (sharp) 3.0 (broad)

		MMT + 1.2 CEC CHX DG	15.2 (sharp) 7.0 (broad) 5.0 (broad) 4.5 (sharp) 4.3 (sharp) 3.7 (broad) 3.4 (sharp) 3.0 (broad) 2.6 (broad)

Based on the data obtained with this technique it is valid to suggest that CHX molecules are becoming part of the structure and improving its arrangement. This could indicate that these molecules are therefore intercalating in between the clay platelets as the concentration increases, however in addition some of the CHX could also be sitting on top of the clay stacks, see Figure 4.9.

Montmorillonite   **Chlorhexidine digluconate**   **MMT + CHX stack**
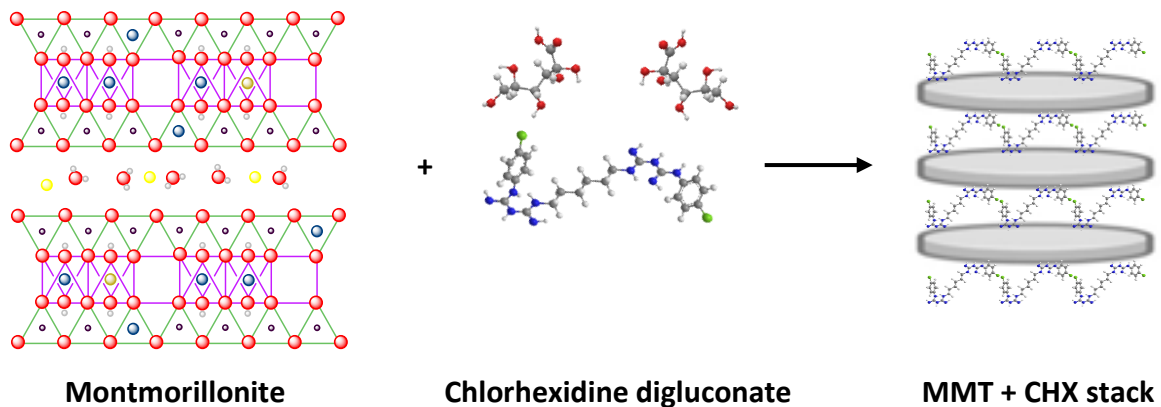
Figure 4.9. Sketch of what the Clay + Antimicrobial samples might look like.

The relationship between d_{001} as a function of the CHX content is shown in Figure 4.10. A gradual increase with CHX content is seen.
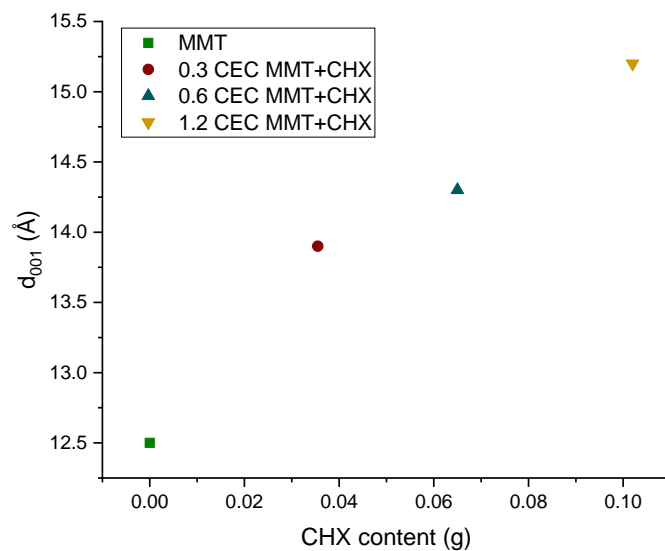
Figure 4.10. d spacing (d_{001} peak) as a function of the CHX content.

4.3.2.4   Small Angle X-Ray Scattering (SAXS)

The purpose of this technique was to focus on the d_{001} peak that was already seen with the XRD spectra but as it was very close to the limits of detection, this technique will be useful to prove if the data was accurate.

In Figure 4.11 we can see the scattering data of the precursors and the three different samples of MMT + CHX. All the peaks were measured to calculate their correspondent d spacing that is shown in Table 4.4.
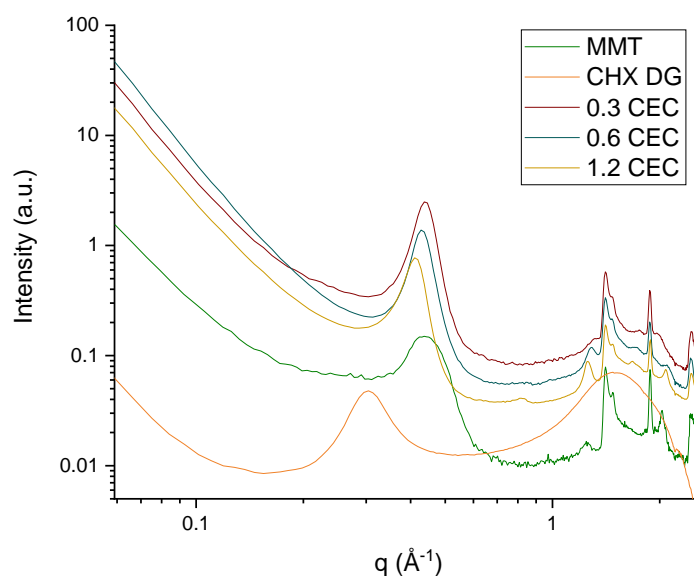
Figure 4.11. SAXS scattering pattern of all samples and precursors. Graph on log-log scale.

Table 4.4. Peak position of all samples and precursors.

Precursor	d Space (Å)	Clay Sample	d Space (Å)
CHX DG	20.7 (broad) 4.2 (broad)	MMT + 0.3 CEC CHX DG	14.4 (sharp) 4.3 (sharp) 3.6 (broad) 3.3 (sharp) 2.6 (sharp)
MMT	14.3 (broad) 5.0 (broad) 4.9 (sharp) 4.4 (sharp) 4.2 (sharp) 3.3 (sharp) 3.1 (broad)	MMT + 0.6 CEC CHX DG	14.7 (sharp) 4.9 (broad) 4.5 (sharp) 4.3 (broad) 3.7 (broad) 3.3 (sharp) 3.0 (broad) 2.6 (sharp)
		MMT + 1.2 CEC CHX DG	15.3 (sharp) 7.7 (broad) 5.0 (sharp) 4.5 (sharp) 4.2 (sharp) 3.7 (broad) 3.3 (sharp) 3.0 (sharp) 2.6 (sharp)

Based on the information obtained for CHX we can consider that it does not present a d_{001} peak, therefore its presence is revealed by the swelling of the clay when these antimicrobial

molecules are added into its layered structure. As more CHX is added, the layer spacing increases.

In Figure 4.12 we compare the scattering pattern of the three different concentrations of MMT + CHX in more detail. In Table 4.5 the d_{001} spacing and the FWHM of each peak (value got with the Integrate Gadget Tool from Origin) are presented. It is interesting that the FWHM of the samples does not change as the concentration of CHX increases, it means that there is no change in the degree of ordering. However, the clay on its own presents a much broader peak which could be considered as a less ordered structure.
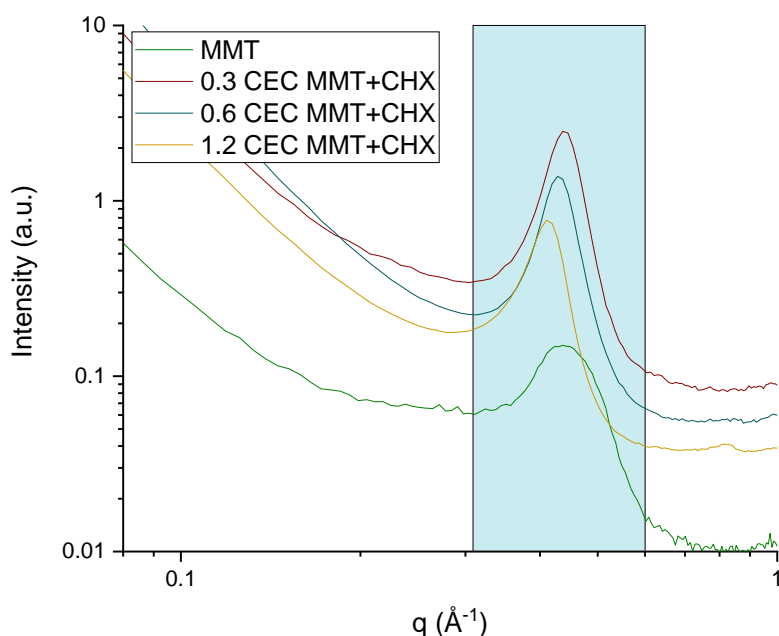
Figure 4.12. SAXS scattering pattern of three different samples of Clay + CHX compared with MMT. d_{001} peak highlighted in blue. Graph on log-log scale.

Table 4.5. Information of d_{001} peak of each sample run in SAXS.

Clay Sample	d_{001} Space (Å)	FWHM ($Å^{-1}$)
MMT	14.3	0.14
MMT + 0.3 CEC CHX DG	14.4	0.06
MMT + 0.6 CEC CHX DG	14.7	0.06
MMT + 1.2 CEC CHX DG	15.3	0.06

4.3.3 Release Test

4.3.3.1 UV-Vis

This technique was initially used as the simplest way to analyse the supernatant of the different concentrations by using a cuvette to determine if the chlorhexidine was being released from the MMT + CHX samples. This was going to be possible thanks to the characteristic absorption peak presented by CHX around 255 nm. Hence, the importance to have the parameters of both precursors as reference. The test became more complicated however when the spectra of MMT seemed to show absorption around the same range of wavelengths as CHX.

Four solutions 1:10 v/v of the different modified clays were run, this samples were prepared by taking 1.5 ml of each aqueous sample: MMT, 0.3 CEC MMT + CHX, 0.6 CEC MMT + CHX and 0.9 CEC MMT + CHX were taken and centrifuged at 21,100 g for 2 h 15 mins. As the peak of MMT was still appearing the supernatant was taken and centrifuged again for another 2.5 h but, the spectrum of MMT was still present.

As an attempt to solve this issue and in addition to the centrifuging, 5 different type of syringe filters were tested to try and separate the remaining clay particles in the supernatant. These were: Whatman® Anotop® 10 with a pore size of 0.02 µm and a non-sterile alumina based membrane; Minisart® NML with a pore size of 0.2 µm and a sterile surfactant-free cellulose acetate (SFCA) membrane, Whatman™ GD/X with a pore size of 0.45 µm and a sterile cellulose acetate (CA) membrane, Filtropur® S with a pore size of 0.2 µm and a polyethersulfone (PES) membrane; and, Millipore Nylon Net filter GNWP with a pore size of 0.2 µm and a hydrophilic nylon membrane.

The solutions tested were: DIW to double check if the filter itself was not releasing anything into the solution filtered; and 60 µM [CHX DG] to see if the filter was letting all of it pass through or if it was retaining some of it in the membrane. In fact, a third sample consisted of 1:10 clay solution but it was only used once due to two reasons: one being because it was noticed that the other filters were catching some of the CHX so there was no need to use it with them and the other because it took hours to filter 1.5 ml (see Figure 4.13) and yet some

of the MMT still managed to pass through, this can be seen in the third bar presented in Figure 4.14.

Figure 4.13. MMT 1:10 passing through Anotop® 10 filter.

The last bar presented in Figure 4.14 corresponds to the total amount of CHX present in the samples filtered. It was interesting to notice how the CHX itself interacted with some of the filters as the intention was to keep the clay out of the supernatant that was going to be used in the UV-Vis reading but still letting the CHX to pass in order to quantify the amount of it released. In fact, all the filters seemed to catch some of the CHX, with the Anotop® 10 and the Filtropur® S (PES) being the ones that allowed most of it to pass.
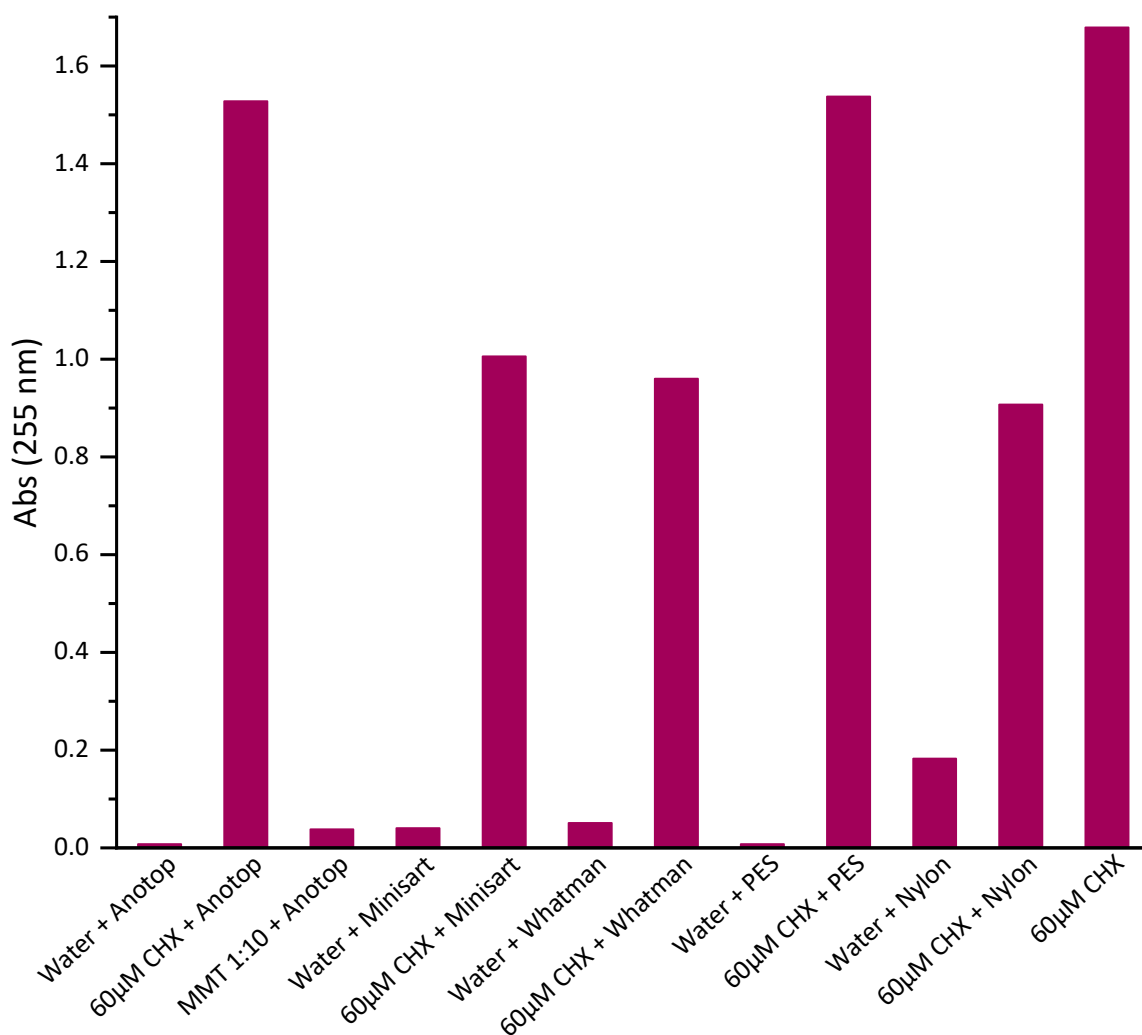
Figure 4.14. Test of the 5 different types of filters.

Actually, upon closer inspection of the data presented in Figure 4.14, the Filtropur® S (PES) seemed to be the best candidate to test with the clay + antimicrobial solution as the water did not show any undesired absorption and the amount of CHX caught by the membrane was very little so 1.5 ml of a 0.9 CEC MMT + CHX solution was filtered and measured to be compared with both precursors' spectra.

Unfortunately, and despite the promising performance of the filter with DIW and antimicrobial, it was not very effective at stopping the MMT to pass into the supernatant sample, as some signs of it can still be seen in the spectra, shown in Figure 4.15. Precursors and Clay + Antimicrobial sample. The blue bar indicates the representative absorption of CHX.

where three samples are compared: 1:10 diluted MMT stock, 60 µM CHX DG solution and one of the medium concentrations of MMT + CHX (0.9 CEC).
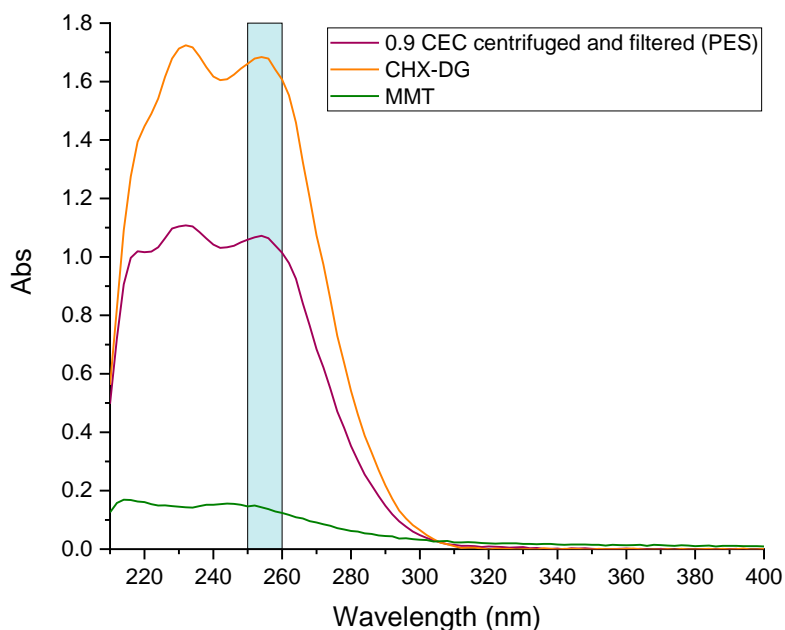
Figure 4.15. Precursors and Clay + Antimicrobial sample. The blue bar indicates the representative absorption of CHX.

Considering that all effort made to eliminate the very small particles of residual montmorillonite in the supernatant of the clay + antimicrobial samples was unsuccessful the conclusion was that any reading obtained from this centrifugation and filtering process was going to result in unreliable data points and it was decided to use dialysis instead to determine the release profile.

4.3.3.2   Dialysis

This experiment involved having the set up shown in Figure 4.16 running for up to 6 weeks. 2 ml were taken from each MMT + CHX dialysis flask, run in the UV-Vis machine and poured back into the medium.
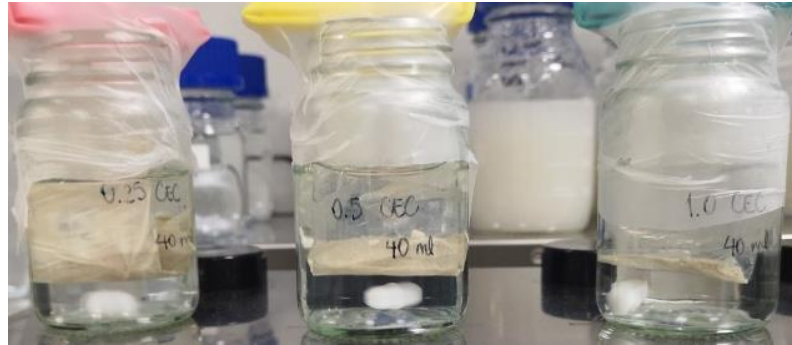
Figure 4.16. Dialysis set-up.

The readings were used to produce the graph in Figure 4.17 where the curve for 0.3 CEC is below the detectable limits and cannot be consider accurate as the values are too low and could be confused with noise. However, the values for 0.6 CEC sample despite being quite low the curve pattern shows that there is a small release (corresponding to 0.06% of the total present) of CHX after 24h, reaching a maximum of 0.2% around day 13 (290h). Lastly, the curve for the sample with the higher CHX content, 1.2 CEC, is showing some release during the first 24 h this corresponds to a 2.4% of the total content. Then, around day 15 (337 h) the curve seems to reach a point of stability and this corresponds to only 3.6% of the total amount of CHX present in the clay sample being released into the aqueous medium.
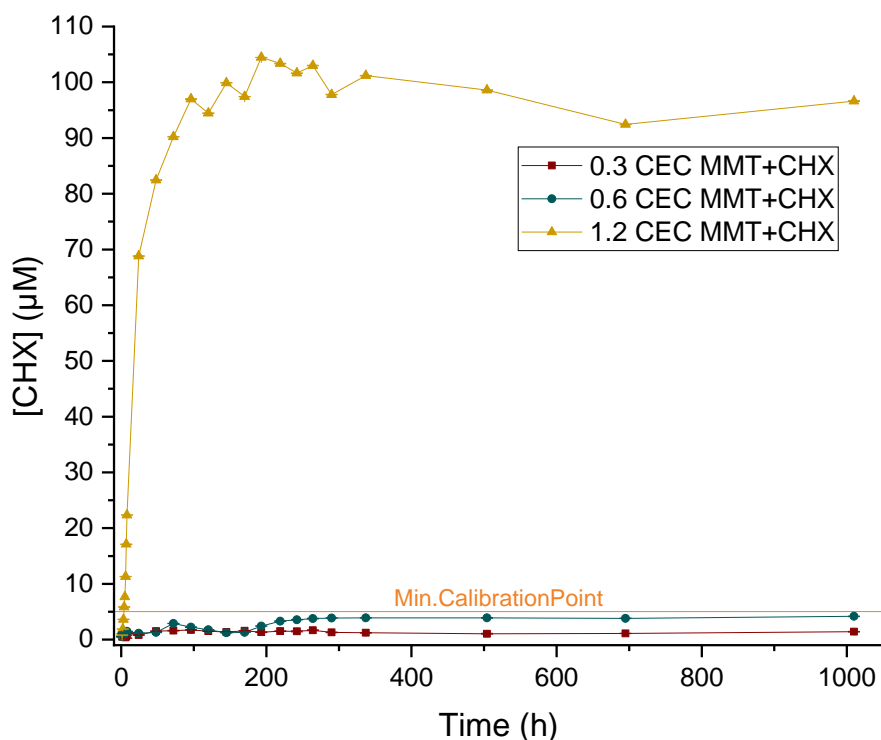
Figure 4.17. All 3 clay samples plus reference line of minimum valuable concentration.

4.4 Discussion

The samples were carefully prepared to determine if some CHX was released. The intention of this was to avoid the presence of any free CHX in the structure. Thus, the readings of the dialysis correspond to an actual release from what was bound to the clay platelets.

This is also supported by the data presented in the elemental analysis report, where the total content of %CNH corresponds to the CHX DG added to the clay. When compared with the initial calculations, see Table 4.6, the numbers are similar, in fact, for the samples where the samples could present free CHX the numbers are slightly lower.

Table 4.6. CHX content in samples used for realising test.

Sample	Theoretical Content		Experimental Content (EMA)
	%MMT	%CHX	Total %CNH
0.3 CEC MMT+CHX-DG	92.9	7.1	7.2

0.6 CEC MMT+CHX-DG	87	13	11.7
1.2 CEC MMT+CHX-DG	79.6	20.4	17.5

If we consider the organic content (CNH%) values obtained by EMA and the theoretical corresponding mass of CHX, then the total content of CHX in 100 g of clay can be estimated leaving the rest as the amount of MMT present in the samples.

In terms of relative volumes of CHX layer and clay layer in a MMT + CHX stack, we need to consider the CHX density of 1.06 g/cm^3 while for MMT the density is 2.7 g/cm^3.

Then, if it forms a one-dimensional stack, we would expect the layer thicknesses to have the same ratio as the respective volumes. The experimentally determined thickness ratios (assuming a single clay platelet is 9.7 Å thick) are given in the final column in Table 4.7. They do increase with CHX content, but the variation is much less than could be expected on the basis of the elemental analysis results. This may reflect how the CHX molecules are able to pack themselves between clay sheets. So, for 0.3 and 0.6 CEC, the structure of the stack does not seem to have a densely packed layer of CHX between clay sheets (as the CHX layer takes up more space than would be expected on the basis of the mass of CHX present), but for 1.2 CEC it looks like it does. In fact, the value for 1.2 CEC is slightly low, which may suggest some of the CHX being present on the outside of the clay stacks.

Table 4.7. EMA content vs SAXS d_{001} spacing of each MMT + CHX sample.

Sample	Relative volume (cm^3)		Ratio of layer thickness	d_{001} Space (Å)			Ratio of layer thickness
	MMT	CHX		Total	MMT	CHX	
0.3 CEC MMT+CHX-DG	34.4	6.7	0.19	14.4	9.7	4.7	0.48
0.6 CEC MMT+CHX-DG	32.2	12.3	0.38	14.7	9.7	5.0	0.51
1.2 CEC MMT+CHX-DG	29.5	19.2	0.65	15.3	9.7	5.6	0.58

Moreover, below 1.2 CEC there is very little to no detectable release of CHX, and even at 1.2 CEC only a small amount of CHX DG was released (less than 5% of the bound CHX). Judging by the release test it may be assumed that the CHX is strongly adsorbed and highly unlikely to leave the structure for the lower concentrations. The small release for the 1.2 CEC sample may reflect a small amount of CHX that is loosely adsorbed to the clay stacks.

The literature suggest that the release is easier for molecules on the external surfaces of the clay stack, whilst any molecule intercalated in the interlayer space of clay is most likely to be strongly adsorbed. To enable the release of intercalated molecules the principle of ion exchange reaction with other cations can be applied, this normally could be done by using a saline solution such as sodium chloride (NaCl)[71] or phosphate buffered saline (PBS)[54][53], this is made more complicated and thereby less desirable in this system as chlorhexidine ion reacts readily with a wide range of ions to form an insoluble precipitate.

However, if the molecule involved is bulky or hydrophobic then simple cations like Na^+ or Ca^{2+} would be insufficient. Depending on the nature of the molecule, it can require other ions with similar or larger molecular size and charge, to assist the release[76].

This is not entirely a disadvantage; this could mean that our system 'Clay + Antimicrobial' will not release all its content in an immediate spike, but instead through a very slow release over a longer period of time, and this property is of use in certain applications.

Both research papers that used PBS also ran the dialysis under a controlled pH of 7.4 and at 37 °C which they explain helped the ion exchange cation. Nevertheless, both studies concluded that a 100% release is impossible because during the equilibrium process, the cations in the interlayers cannot be completely exchanged.

The release test presented in this chapter was not done in any saline solution, and can be explained as following the principle that any ionic adsorption on an ionic surface will be conditioned by the charge determining ions; and specifically the hydrogen ion concentration of the solution, if the solvent is water.[77]

Some other differences can be found in the way samples were prepared within this chapter and the data found in the literature. First the source of chlorhexidine (Figure 4.18a) used. Meng *et al.*[54], Wu *et al.*[71] and Saha *et al.*[53] used chlorhexidine diacetate (CHX DA) in powder

form (Figure 4.18b) while our samples were made using chlorhexidine digluconate (CHX DG) which is a solution (Figure 4.18c).

a)

b)

c)
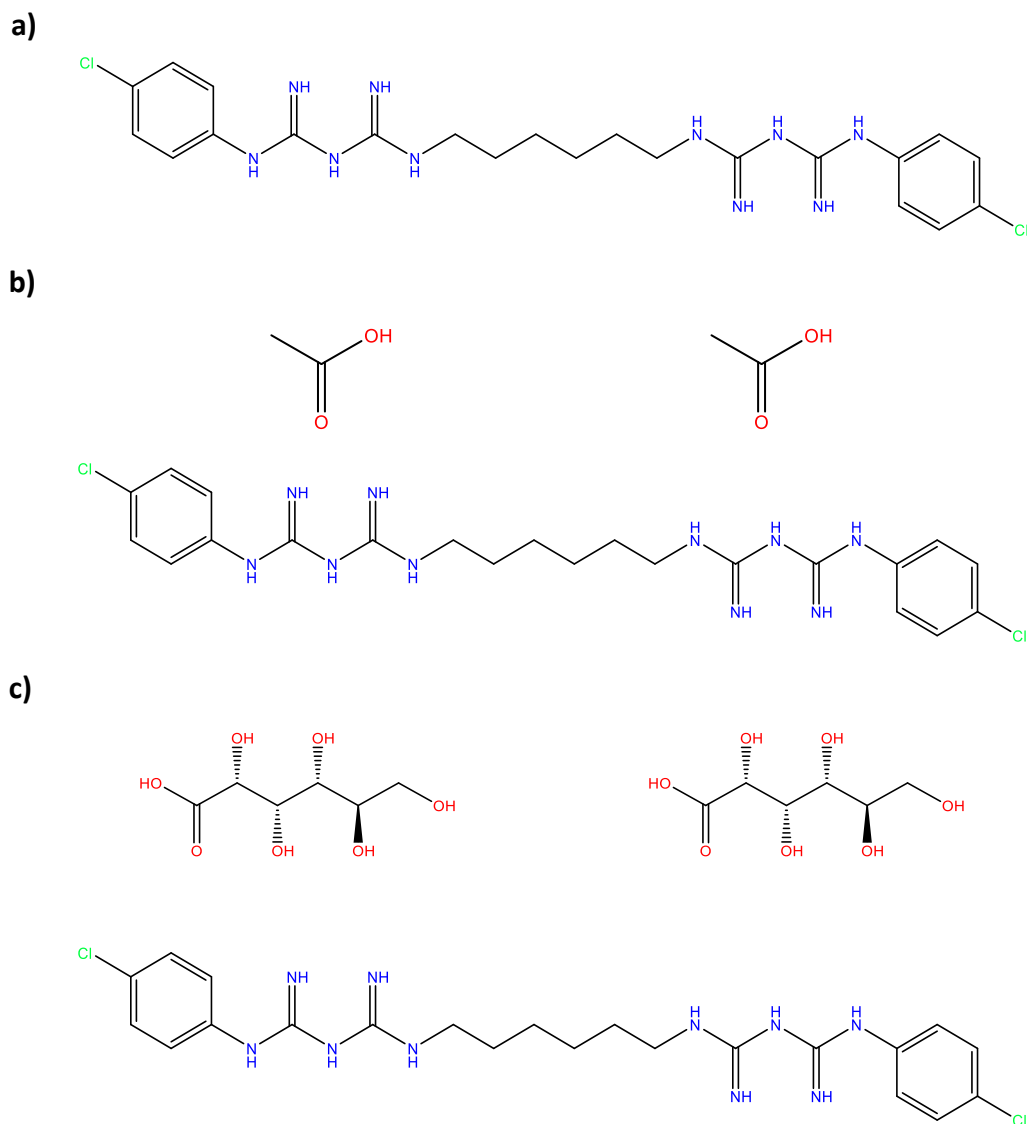
Figure 4.18. a) Chlorhexidine ($C_{22}H_{30}Cl_2N_{10}$), b) Chlorhexidine diacetate ($C_{26}H_{38}Cl_2N_{10}O_4$) and c) Chlorhexidine digluconate ($C_{34}H_{54}Cl_2N_{10}O_{14}$).

To compare these, characterisation techniques were run with samples of both chlorhexidine salts in powder form. Table 4.8 shows the organic content (%N, %C, %H) obtained by elemental analysis for the salts and compared with the estimated of CHX.

Table 4.8. Elemental Analysis of CHX, CHX DA and CHX DG.

Sample	Experimental Value			Theoretical Value		
	N %	C %	H %	N %	C %	H %
CHX DG	14.7	43.7	6.3	15.6	45.4	6.0
CHX DA	21.2	48.1	6.1	22.4	49.9	6.1
CHX				27.7	52.2	5.9

The FT-IR spectra (Figure 4.19) shows signals in the same values, although the shape and intensity of them vary, they can be viewed as the same groups but with slightly different interactions. This makes sense as one presents more groups -OH in its structure.
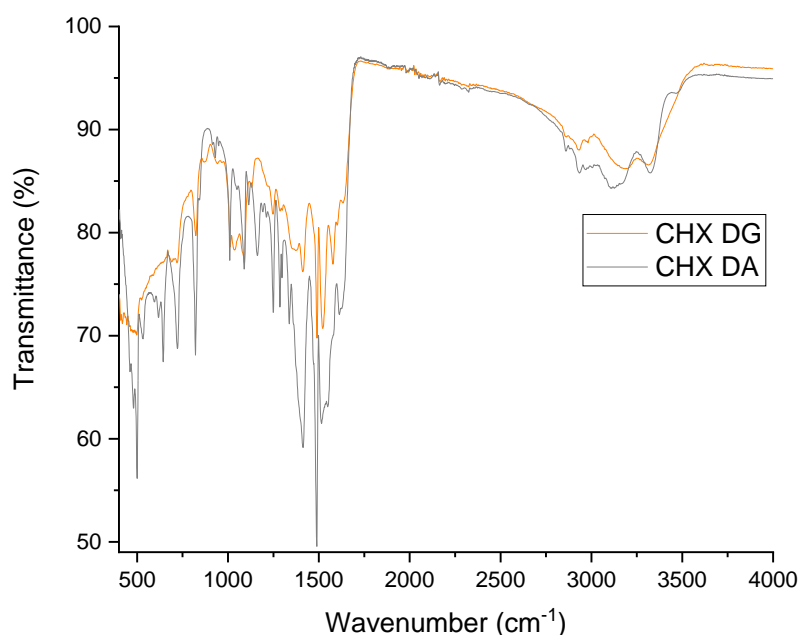
Figure 4.19. Spectra of CHX DA and CHX DG.

Another difference is how the samples were prepared (Table 4.9).

Table 4.9. Sample preparation comparison.

Current work	Meng 2009	Wu 2013	Saha 2014
MMT Disperse ~6 g in 300 ml DIW for 24 h. **MMT+CHX DG** Previous dispersion + 300 ml DIW + CHX for 0.3 CEC, 0.6 CEC, 1.2 CEC, respectively. Stir overnight, settle 1 – 2 h, syphon, washed (+300 ml DIW, stir, settle, syphon), depending on the sample it was washed up to 3 times, centrifuged and dried in vacuum oven at 60 °C. Ground.	**MMT** 1 g dispersed in 30 ml distilled water at room temperature for 0.5 h. **CHX DA** 0.33/1.0/2.0/3.0 g dissolved in 150 ml distilled water at pH 4.1. **MMT+CHX DA** Previous solutions were mixed at 80 °C for 3 h. Centrifuged, and washed once with DIW, dried in vacuum oven at 80 °C for 24 h.	**CHX-Cu** 0.64 g CHX DA dissolved in 30 ml Ethanol. + 0.34 g CuCl2.2H2O stirred at 40 °C for 3 h, filtered, washed (ethanol) and air dried. **MMT+CHX DA** CHX-Cu + MMT in different mass ratios on high speed stirring at 80 °C for 24 h. Precipitated, filtrated, washed with water, and dried in air.	**MMT** 1 g dispersed in 30 ml distilled water at room temperature for 0.5 h. **CHX DA** CHX for 0.2 CEC, 0.5 CEC, 1.0 CEC, 2.0 CEC dispersed in distilled water. **MMT+CHX DA** Previous solutions were mixed with a pH of 4.1 (controlled using H_3PO_4) at 80 °C for 3h at 500 rpm. Cool down, centrifuged, decanted, washed, and dried at 90 °C. Ground.

Table 4.10 presents XRD results to compare the d_{001} spacing for the clays so produced. Meng *et al.* report a well-ordered system[54].The amount of CHX they used ranges from 1.2 to 11 times the CEC. Two steps are seen in the d-spacing, increasing first to around 1.5 nm and the further to around 1.9 nm for their "1:2" sample (which corresponds to a dosage of about 7 times CEC). This probably reflects a different packing of CHX between the clay sheets (such as a single layer vs. a bilayer).

Only a very limited increase in d spacing is seen in the experiments by Wu *et al.*[71]– but it should be noted that they add a complex of CHX and Cu^{2+}, which may reduce the ability of CHX to associate with the clay. The d spacing only increases to around 1.4 nm and there is no trend with further addition of the CHX-Cu complex. One possibility is that only the Cu^{2+} intercalates with the clay, however Cu-MMT has been reported to have a d-spacing of 1.59 nm[78] so it is not clear that CHX has successfully intercalated between the clay sheets.

Saha *et al.*[53] do report an increase of d spacing to 1.48 nm when adding CHX up to 2.0 times CEC, however the XRD peak in their case does not appear very intense, which may suggest that the structures are not very well ordered.

Table 4.10. Relation CHX and d space of d_{001} in the different MMT+CHX systems.

Current work		Meng 2009		Wu 2013		Saha 2014	
Ratio MMT / CHX	d_{001} nm	Ratio MMT / CHX	d_{001} nm	Ratio MMT / CHX-Cu	d_{001} nm	Ratio MMT / CHX	d_{001} nm
Only MMT	1.25	Only MMT	1.53	Only MMT	1.24	Only MMT	1.27
0.3 CEC	1.39	3:1 (~1.2 CEC)	1.51	1:3	1.38	2.0 CEC	1.48
0.6 CEC	1.43	1:1	1.52	1:4	1.39		
1.2 CEC	1.52	1:2	1.93	1:5	1.41		
		1:3	1.94	1:6	1.38		

These studies all proceed to characterise release of the CHX over time and the results are summarised in Table 4.11. Note that all samples here were prepared using CHX amounts in excess of the clay CEC, so quite possibly there was CHX present that was not strongly adsorbed. All studies report a quick release of some of the CHX during the first 24 h and this presumably reflects such loosely bound CHX, as similar release kinetics were seen using just the CHX compound[53].

The Meng study only extends the release study to three days and it is hard to judge whether any long-term, slow release takes place here. In the Wu study there does appear to be release

continuing over a longer time, however no comparison is made with the Cu-CHX complex on its own so it cannot be judged whether the presence of clay brings any benefit here. Finally, the Saha study studies release into a PBS (phosphate buffered saline) solution and there does appear to be a slow, continuing release of CHX here, for the sample that was prepared using CHX equivalent to 2 times CEC.

Table 4.11. Fraction of CHX released within similar time.

Current work		Meng 2009		Wu 2013		Saha 2014	
Time h	% CHX Released for 1.2 CEC	Time h	% CHX Released for 1:2 (~ 7 CEC)	Time h	% CHX Released	Time h	% CHX Released for 2.0 CEC
24	2.4	24	28	6	6	12	20
96	3.4	72	31	24	9	24	24
337	3.6			288	16	180	54

Recall these results were obtained with samples in presence of a considerable excess of chlorhexidine. This is supported by the shape of their d_{001} peaks[53][71], it is evident that the structure was already becoming amorphous, which indicates the CHX is sitting everywhere instead of being nicely packed inside the MMT platelets. Unlike our careful technique to wash the clay very well in order to avoid the presence of any loosely adsorbed CHX, their samples were only centrifuged once, this do not guarantee successful removal from the samples all the possible excess or weakly bound CHX to the structure.

4.5 Conclusion

The MMT + CHX systems studied here could be interesting as a material to see if in this bound form CHX still is effective as an antimicrobial agent. If this were the case the material may find application as a very slow release material or as a coating for surfaces which need to stay free of bacteria.

The preparation route followed by Meng allows for more CHX to be incorporated between the clay sheets (presumably as a bilayer) and the release properties of such a material would be worth investigating further. The results by Saha already indicate that CHX-MMT complexes may have potential as a slow-release vehicle for CHX.

The twist that Wu gave to the composite adding another antibacterial particle was also something to keep in mind, due to the Cu^{2+}, the surface of the clay changed from hydrophilic to hydrophobic. This change is beneficial as it therefore interacts better with the bacteria, it attracts them to the point where the antimicrobial is contained, and then even if the release is slow, it will kill the bacteria trapped there. However, for this material it was not clear to what extent a clay-CHX composite was actually obtained (as opposed to the two materials being present side-by-side in the final samples).

As an example of an application of these type of materials, recently a dimethacrylate-based dental material was developed by mixing more complex systems involving the development of a composite material with an organo-clay (MMT with an ammonium quaternary salt in its composition[79]) and CHX to be incorporated into a resin matrix[80]. This study showed that the clay + CHX systems added an antibacterial release property to the resin while not interfering in the mechanical properties of the material. This supports the idea of our powders as potential addition in materials for this kind of applications.

Chapter 5 Addition of Modified Clays to Alginate hydrogels

5.1 Introduction

This chapter tested a possible application for the materials developed across the different experiments presented within this thesis. Based on the findings in chapter 3, the addition of nanoparticles to certain materials could help improve their mechanical properties.

This leads to question if it would be possible to implement the same idea of a hierarchical structure explored previously but with a different type of polymeric material. Considering the positive interaction of the clay composite with the dental cement that also contains polyacrylic acid in its matrix, it was decided to try and see how a pure (aqueous) polymer matrix, specifically alginate, will react when mixed with the same set of different modified clays.

Similar research has been conducted in the literature where various techniques have been designed for several types of hydrogel-composite materials to be used across different areas. One of these areas that seems appropriate to mention, as it is related to the other applications that have been reviewed in previous chapters, is the biomedical field[81]. Within this field applications range from antimicrobial release materials for dental applications[82] and replacement of damaged cartilage[83] to cancer treatment[84] and wound dressings[85].

These applications rely on the potential for encapsulating other molecules, which results in uses within the biological field[86] [87] such as to reduce the impact of substances on the environment like pesticides[88] or to remove undesired substances, for example, lead[89] or polychlorinated biphenyls[90] from water. It seemed appropriate to produce beads by a dripping method[91] for the purpose of this chapter as the use of such "loaded beads" (the ones that have encapsulated a molecular species) has been reported as immobilized biocatalysts, scaffolds for tissue engineering or for controlled release of the entrapped molecules[92].

How these hydrogels function depends heavily on the way they are prepared, as it has been shown that using different types of alginate, changing the polymer concentration, as well as

varying the type of gelling cation[92] [93] [94] [95] or even temperature[96] all can modify their properties.

There was a undergraduate project student involved early in the development of the idea, the findings of her research project[97] proved helpful and the initial methodology for the hydrogel preparation has been improved upon within this chapter. In short, different concentrations of one of the modified clays from Chapter 2 were added to a sodium alginate solution in order to produce hydrogel beads that were mechanically tested. This was a starting point for what is explored in this chapter where different types of modified clay were added to sodium alginate in order to obtain a hydrogel with the aim of enhancing its mechanical properties.

5.2 Materials and Methods

5.2.1 Preparation of the Hydrogels: Alginate + Modified Clay

The clay used was Wyoming montmorillonite, SWy-2 (MMT), which was purchased from the Clay Minerals Society source clays repository at Purdue University, with a nominal composition $(Si_{7.94}Al_{0.06})$-$(Al_{2.88}Fe_{0.5}Mg_{0.62})O_{20}(OH)_4Na_{0.68}$. Chlorhexidine digluconate (CHX DG) was purchased from Sigma-Aldrich. Meanwhile, the ω-amino carboxylic acids used were: 12-aminododecanoic acid (ADA) (95% Sigma Aldrich UK), 6-aminohexanoic acid (AHA) (≥98.5% (NT) Sigma Aldrich UK) and γ-aminobutyric acid (GABA) (97 % Sigma-Aldrich). Lastly, the sodium alginate (Alg) was obtained from Special Ingredients and calcium chloride $(CaCl_2)$ from Fisher Scientific.

For the purposes of the experiments run within this chapter the modified clays: MMT + ADA HCl, MMT + AHA HCl and MMT + GABA HCl prepared in Chapter 2 (section 2.2.1); and sample MMT + 1.2 CEC CHX prepared in Chapter 4 (section 4.2.1.1) were used to make the hydrogel samples.

5.2.1.1 Preparation of Alginate dispersions

The method to prepare these samples consisted of making a 3 wt% clay suspension and 1 wt% alginate by adding ~0.3 g clay and ~0.1 g of alginate in 10 ml of deionised water (DIW) and mixed using an Ultra Turrax IKA T18 at 13,000 rpm for 5 minutes. To make sure that the dispersion was complete, these samples were left on the roller mixer for 24 hours.

The resulting solution was left to stand for up to 24 hours to ensure there were no air bubbles before being put into the 1 wt% $CaCl_2$ solution to make the different samples using a plastic pipette with the end cut off (Figure 5.1) to get a larger drop and hence larger spheres in the case of the bead samples, or an easier deposit of the solution into the moulds in the case of the disc samples.
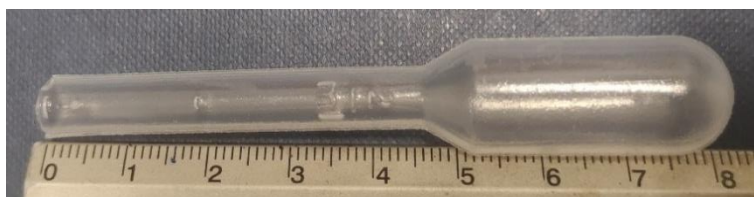
Figure 5.1. Cut pipette to manipulate clay dispersions.

5.2.1.2 Preparation of Alginate beads

The pipette was held above the salt bath to obtain spherical beads. Upon contact with the salt solution, the outside of the drops formed a solid membrane and beads were formed. The beads were left in the salt solution for a week to allow maximum crosslinking and to ensure that the centre of the beads gets solidified. They were then rinsed and stored in deionised water.

5.2.1.3 Preparation of Alginate Discs

In order to characterise Alginate + Clay gel samples in the wet state using XRD, the following sample preparation procedure was devised. Six moulds were made using Elite double 8 duplication silicone (Zhermack) after imprinting the sample holder for XRD samples. In this way, the different alginate dispersions were pipetted into the mould (~2 ml) and left into 200 ml of the salt bath for a week, rinsed and stored in deionized water (Figure 5.8a, moulds in pink).

To prepare the samples for the imaging with SEM, all 6 discs gels were cut into two pieces, and each of those pieces were dried. The first half was put into a SVAC Shel vacuum oven connected to an oil pump and left at 30 °C under vacuum for 3 days whilst the other half was submerged in liquid nitrogen for a few seconds and dried using a Labconco freeze dryer FreeZone 1 for 3 days. All the dried samples were kept sealed to avoid the reabsorption of humidity until they were prepared to be imaged.

5.2.2 Characterisation

5.2.2.1 Differential Interference Contrast (DIC) Microscopy

A drop of each alginate + modified clay dispersion was imaged using an Olympus BX51 optical microscope and Pixelink PL-B62CU colour CCD camera.

DIC microscopy was used to determine whether there was any evidence of interactions between the polymer chains and clay particles considering that the clays used were different to each other.

5.2.2.2 X-Ray Powder Diffraction (XRD)

This analysis was performed using a Bruker (Billerica, USA) D8 Advance Powder X-ray Diffractometer (Cu Kα radiation, λ = 1.54 Å) at 2θ values of 4°-35°, with a step size of 0.05°.

The data obtained with this technique had to be corrected due to the presence of a broad peak related to the sample holder. This was made by subtracting the background signal with help of the software EVA (DIFFRAC[PLUS] Evaluation Package Release 2007).

To calculate the *d* spacing between the layers presented in the materials can be obtained by applying Bragg's Law:

$$n\lambda = 2d \sin(\theta) \qquad (5.1)$$

$$d = \frac{\lambda}{2 \sin(\theta)} \qquad (5.2)$$

5.2.2.3 Scanning Electron Microscopy (SEM)

SEM imaging was carried out using a JEOL JSM IT300 (Japan), and the electron source had an acceleration voltage of 15kV. The detectors in the SEM were a secondary electron detector (SED) and a back scattered electron detector (BED).

Each sample was imaged in cross section and top down by cutting the half disc very carefully with a scalpel, pasting it into the holder and coating it with silver to make it conductive using an Agar High Resolution Sputter Coater. (Figure 5.2)
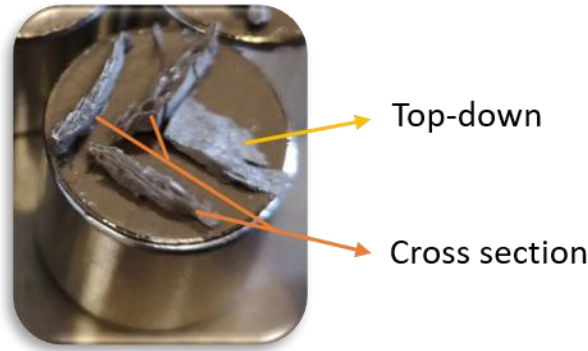
Figure 5.2. Sample preparation for SEM.

5.2.3 Mechanical Testing

5.2.3.1 Compression Test

The compression strength test on spherical bead samples differs from the ones analysed in Chapter 4 where the samples had a cylindrical shape and a much greater hardness, strength and rigidity. A method has been published by Rodriguez *et al*. showing how the shear modulus can be obtained by determining the distortion of a spherical bead under applied stress[98]. This assumes that the volume of the sphere does not change when squashed and the material acts like an ideal rubber which will result in simple shear. With this the following equation is presented as a relation of the force - deformation behaviour to the shear modulus, G'.

$$\sigma_c = \frac{f}{\pi R^{*2}} = G' \left[\left(\frac{R}{R^*} \right)^4 - \left(\frac{R^*}{R} \right)^2 \right] \qquad (5.3)$$

where σ_c is the stress, f is the force applied, R^* is the original equatorial radius, and R is the equatorial radius of the deformed bead after compression. According to the model when a compressive force is applied to the sphere at the poles, the full force is transmitted through the sphere and through every layer that is parallel to the equator. This is a simplified model that can only be applied in situations with small elastic deformations. Experimentally this

approach involves squashing the sphere in between two parallel plates and measuring the resulting change to the equatorial radius (Figure 5.3).
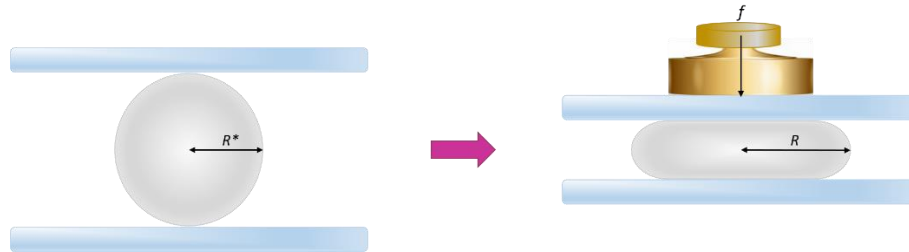

Figure 5.3. Compression Strength Test for a hydrogel bead sample when "squashed".

Groups of three similarly sized hydrogel spheres (beads) were chosen to measure how much their radius varies after the deformation presented due to the application of different weights on top of them in order to apply static stress.

The weights used were taken from a traditional kitchen balance, the range of masses was 10 g to ~ 230 g. To make the calculations correct it is important to consider the dimensions of the glass slides used (obtained by cutting an objective slide in half): ~ 3.7 cm with a mass of ~ 2.45 g.

After getting the 3 similar beads (by weight) they were arranged in an equilateral triangle on the glass slide to run the experiment. Another glass slide was carefully positioned on top of the beads, as in the sketch of Figure 5.4. Finally, a picture of the set up was taken every time a different weight was placed on top.
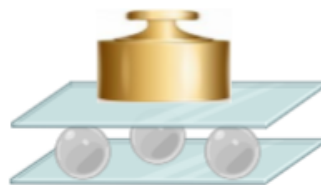

Figure 5.4. Bead arrangement for compression test. (Created with BioRender.com.)

Photographs were taken of the beads corresponding to every change on weight using a Nikon D5100 with a Nikon AF-S NIKKOR 55-200 mm lens and a 36 mm extension tube. To take the pictures Camera Control Pro 2.30.0 M software was used.

As the illumination of the samples was meant to be kept as stable as possible a tripod and several different sources of light were used to create the set-up shown in Figure 5.5.

Figure 5.5. Set-up for compression test pictures.

The size of these beads was determined using ImageJ (Fiji) to analyse the pictures obtained by taking the length of the glass slide as the reference scale and proceeding to measure the rest of the beads before any weight was applied.

5.3 Results

5.3.1 Sample preparation

5.3.1.1   Dispersions

In order to prepare these samples ~0.3 g clay and ~0.1 g of alginate were added into 10 ml of deionised water (MilliQ) and stirred as described in the methods section. There were variations from sample to sample (depending on the surface chemistry of the clays) during this stage due to their ability to interact with water (see Figure 5.6a and Figure 5.6b). Some of them did not remain dispersed when left on the side (Figure 5.6c) and even when they were re-dispersed before using them to prepare samples, a little of the settled clay remained at the bottom of the tube (Figure 5.6d).
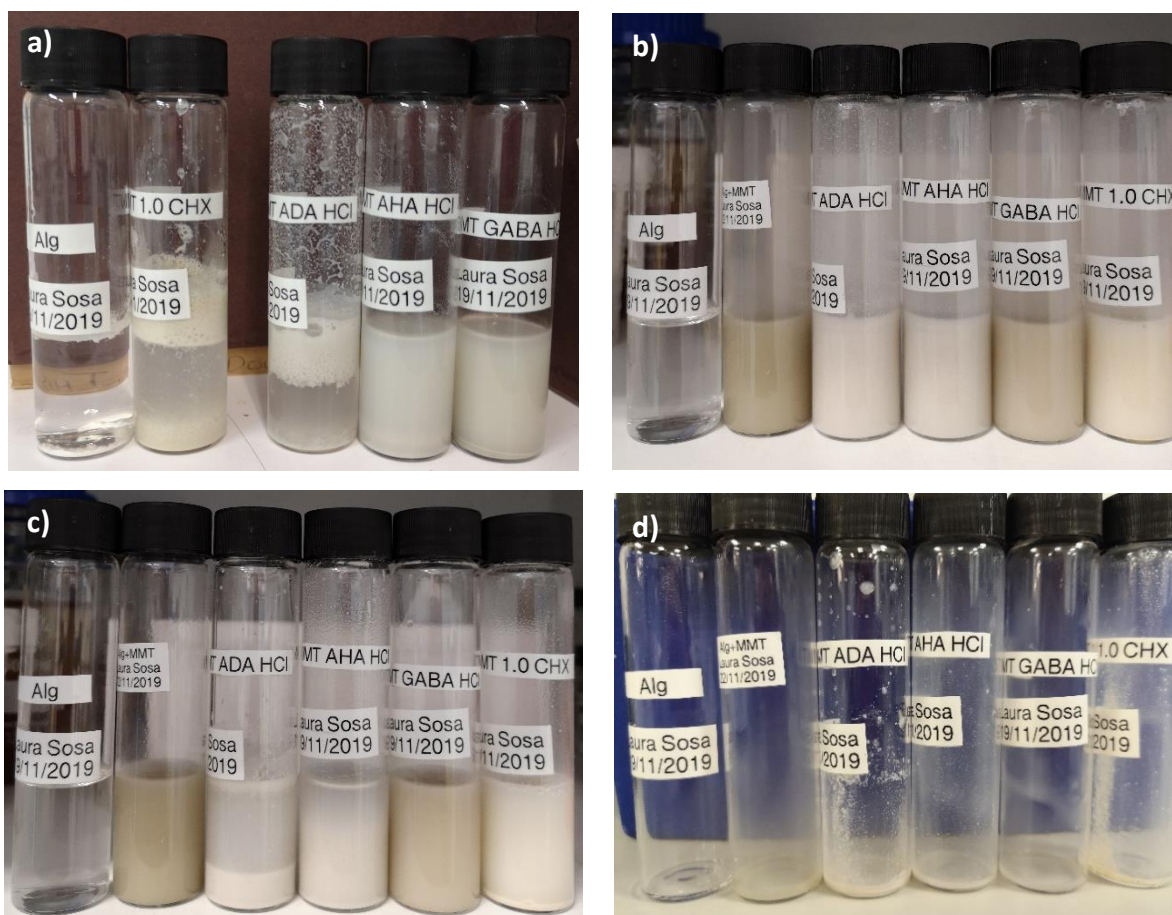
Figure 5.6. Stability of the dispersions: Alg, Alg+MMT 1.2 CHX, Alg+MMT ADA, Alg+MMT AHA and Alg+MMT GABA in panel a) After 5 minutes of Ultra-Turrax. Stability of the dispersions: Alg, Alg+MMT, Alg+MMT ADA, Alg+MMT AHA, Alg+MMT GABA and Alg+MMT 1.2 CHX in panels b) After 24h on the roller mixer, c) after 24 h of standing and d) remaining settled down clay after sample preparation.

5.3.1.2   Beads

These samples were made for mechanical testing purposes. As mentioned in the previous section some of the dispersions needed to be re-dispersed using the vortex mixer before making the beads with the six different samples. (Figure 5.7a). All of them presented different physical characteristics from various colours (Appendix Table 8.1) to size and weight, all these can be seen at the end of the preparation after the rinsing and the beads are stored in DIW. (Figure 5.7b)

Interestingly the sample of Alg + MMT 1.2 CHX after the 7 days of stirring in $CaCl_2$ solution turned cloudy (Figure 5.7c) in contrast with the other 5 samples where the solution remained

clear, this same sample presented some more bubble formation after being rinsed and kept in DIW.

Figure 5.7. a) Six samples during preparation, b) six samples after 7 days, c) Alg + MMT 1.2 CHX beads after 7 days before rinsing.

5.3.1.3 Discs

These samples were prepared for characterisation purposes, so the hydrogel discs required for X-Ray Diffraction were made in the silicone moulds and immersed in $CaCl_2$ solution as shown in Figure 5.8a, then right after the 7 days they were rinsed with DIW and taken for characterisation. They were made in that shape so they can fit in the sample holder as seen in Figure 5.8c.

Finally, in Figure 5.8b it can be appreciated how the discs look when they have been removed from the water environment after a few hours and in Figure 5.8d about a month and a half left without water but in the sealed bag in an attempt to leave them dry for SEM characterisation.

Figure 5.8. a) Silicon moulds for making the hydrogel discs, b) all hydrogel samples after XRD characterization, c) samples in holder for XRD and d) all hydrogel samples after being left outside wet environment for 1.5 months.

The six different discs samples were allowed to slowly dry in a sealed bag, during the time they spent there the disc got a bit "thinner", this absence of water was only causing the structure to collapse. Therefore, to achieve complete dryness, each disc was cut into half across the face. One half was then dried in a vacuum oven and the other half using a freeze dryer.

As Figure 5.9a shows, the vacuum oven treatment resulting a very compact, thin dry disc. On the other hand, the freeze-drying route (Figure 5.9b) allowed more of the original porous structure to be retained, resulting in a visibly thicker sample. It may be worth taking samples straight to the freeze dryer after preparation, possibly resulting in an even "fluffier" product – but this was not pursued here.
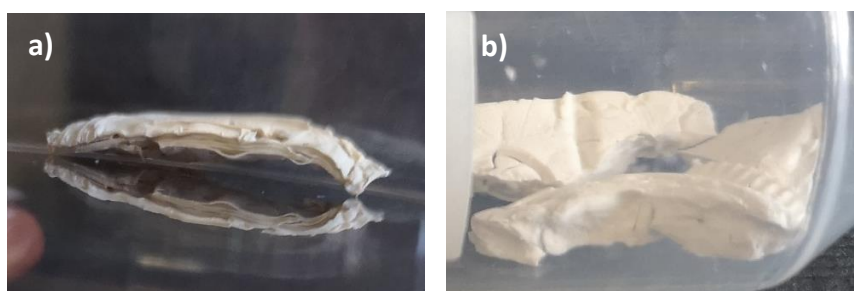

Figure 5.9. Alg + MMT GABA HCl sample: a) dried in vacuum oven and b) freeze dried.

5.3.2 Characterisation

5.3.2.1 DIC Microscopy

One drop of each dispersion was taken and squished between a glass slide and a coverslip to see how they look before the addition of the $CaCl_2$ solution (Figure 5.10). This was challenging especially because some of the modified clays do not disperse very well in water (this applies to the more hydrophobic samples, of clays treated with AHA, ADA and CHX).
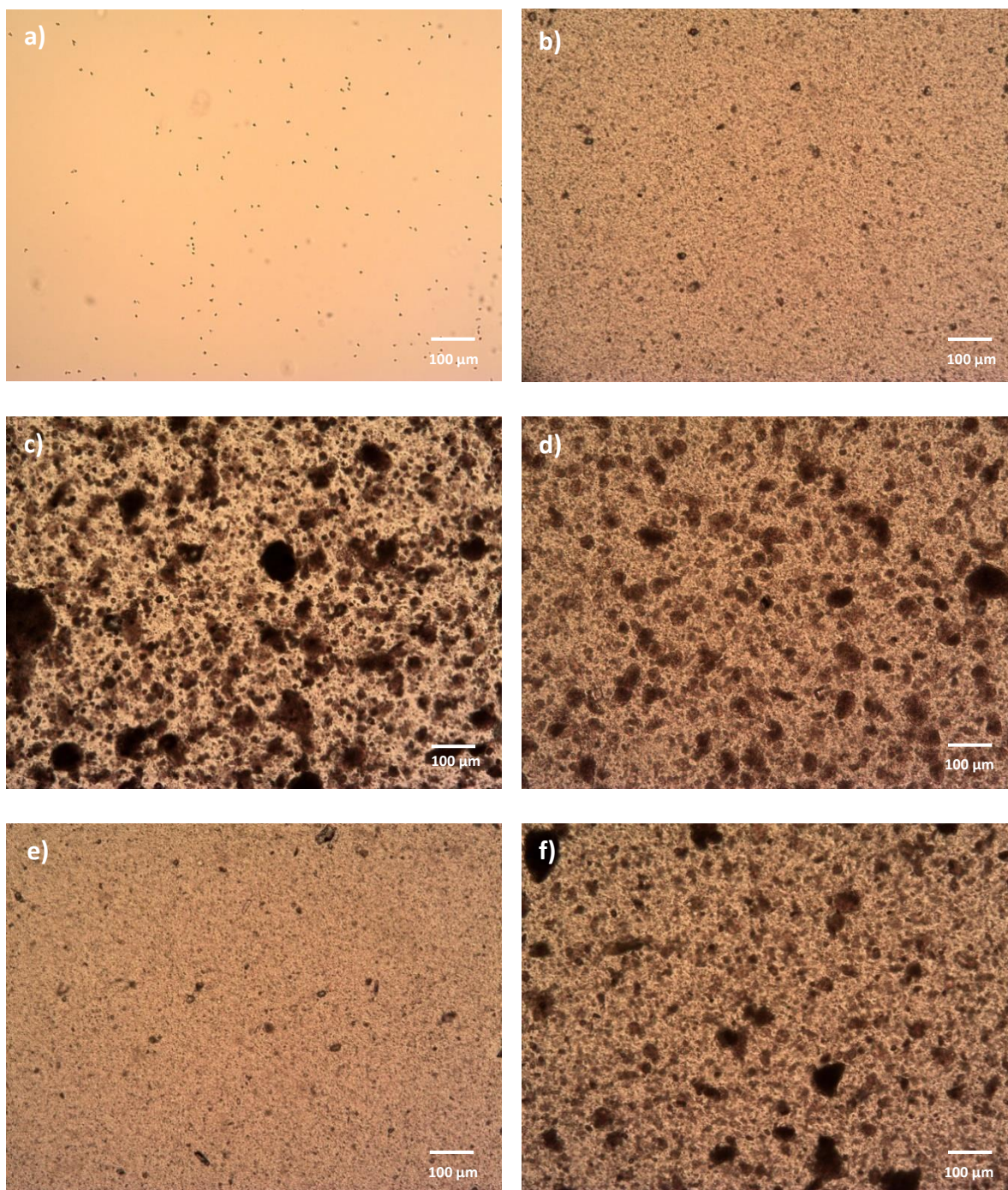
Figure 5.10. DIC of wet samples 1 to 6 at 10x. a) Alg, b) Alg+MMT, c) Alg+MMT ADA HCl, d) Alg+MMT AHA HCl, e) Alg+MMT GABA HCl and f) Alg+MMT CHX.

For purposes of comparison, one drop of MMT dispersed in deionised water (Figure 5.11a) was imaged together with two of the samples already presented in the previous images but this time they were completely dried by leaving them under ambient conditions for ~ 7 months. The reason why it was interesting to image them again was due to how they looked,

even without being gelled this material seemed to have formed a coated surface, however in Figure 5.11b the zones around the edges of the slide presented some "cracks" while the sample corresponding to Figure 5.11c presented a smooth white film on the slide.
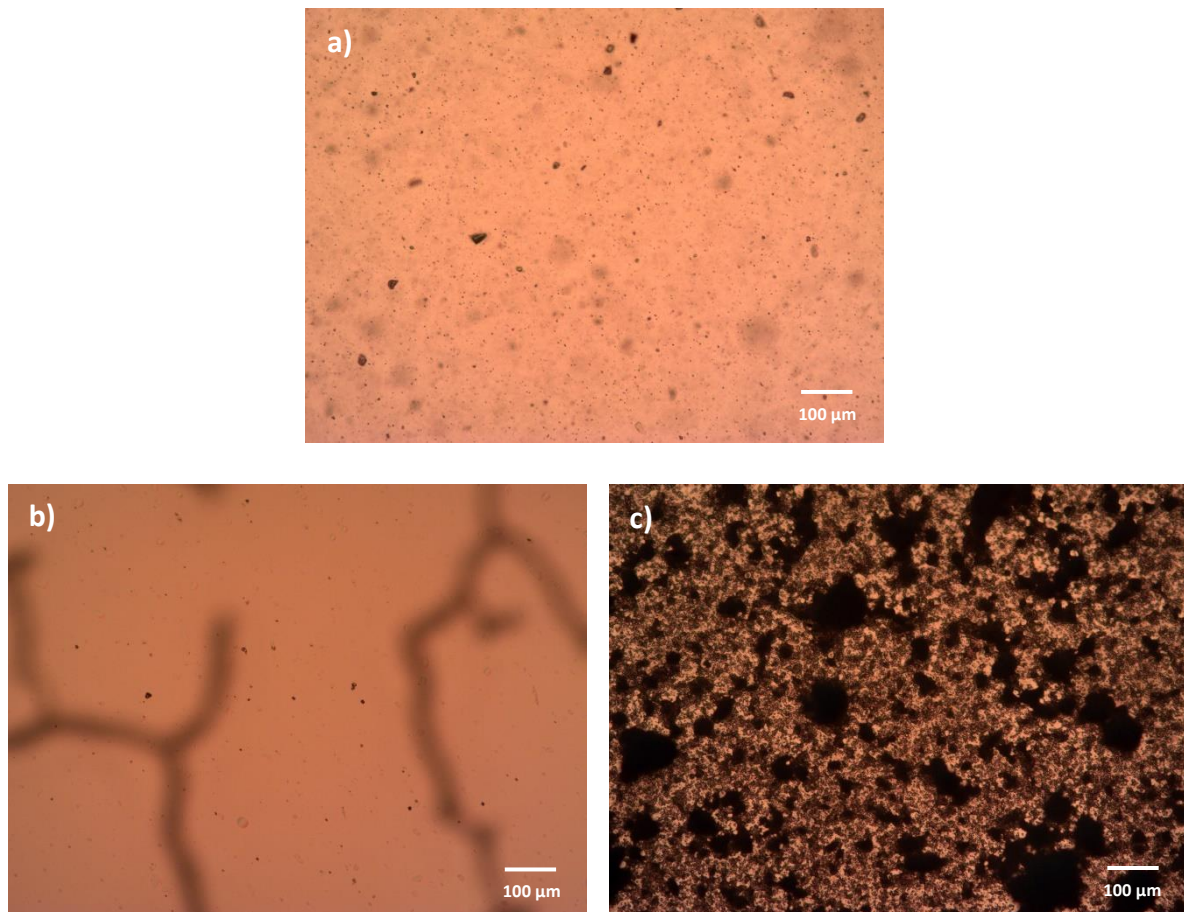

Figure 5.11. DIC of a) MMT dispersion and dried samples b) Alg+MMT and c) Alg+MMT CHX at 10x.

5.3.2.2   X-Ray Powder Diffraction (XRD)

Modified clay powders were discussed in detail in Chapters 3 and 5; for completeness the XRD characterisation spectra before they were mixed with the alginate to make the hydrogels are presented in Figure 5.12. A few observations about these samples are that at high angles (about 20° and above) characteristic peaks appear showing these are all MMT; there is a very well-defined d_{001} peak around 5 – 7 ° for all treated clays while for MMT only this seems to be

a weak (almost imperceptible), broad peak. Additionally, the MMT 1.2 CHX has two additional peaks which correspond to the added CHX in the structure as explained in Chapter 5.
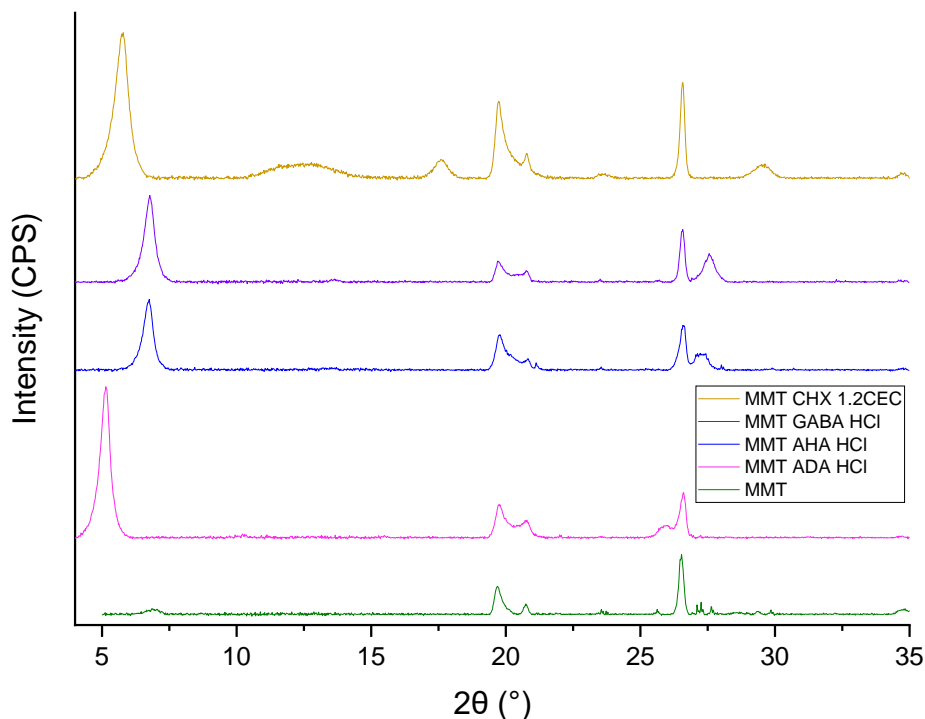

Figure 5.12. XRD spectra of all modified clays used to prepare the hydrogel samples. Spectra have been shifted for easy comparison.

The hydrogel samples were run as wet gel discs in the XRD the spectra obtained are shown in Figure 5.13.

As we can see the Alg gel sample does not present a peak between 4 – 20 °. However, Alg+MMT presented a broad, intense peak instead of the well-defined d_{001} peaks seen with the modified MMTs. The broad peak may be the result of MMT sheets forming disordered stacks interleaved with alginate chains.

It is also noticeable that the peak originally between 4 – 8 ° in the powder samples of MMT + AHA and MMT + GABA displaced when in presence of Alg to align the Alg + MMT ADA first peak.
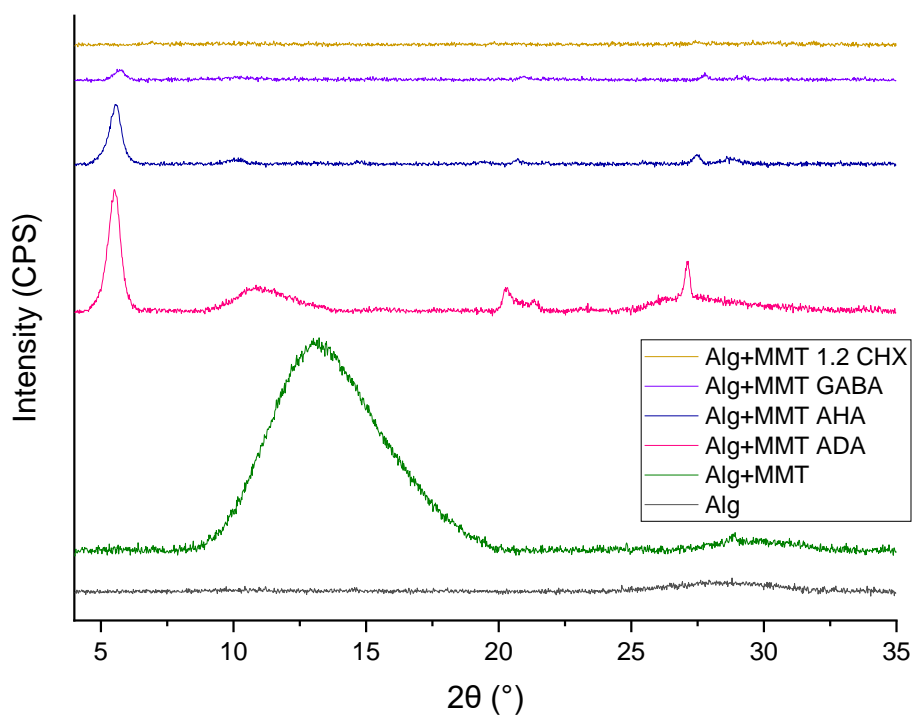
Figure 5.13. XRD spectra of all hydrogel samples (Alg + modified clay). Spectra have been shifted for easy comparison.

Following the equation in 2.2.2.2 the layer spacings of modified clays and hydrogels can be compared, this is summarised in Table 5.1.

Table 5.1. Peaks for gel samples and precursor clays.

Hydrogel Sample	d Space (Å)	Clay Sample	d Space (Å)
Alginate	8.4 (broad) 3.1 (broad)	-	-
Alg+MMT	6.8 (broad) 3.1 (sharp) 3.3 (broad)	MMT	12.5 (broad) 4.5 (sharp) 4.3 (sharp) 3.4 (sharp) 2.6 (broad)
Alg+MMT ADA HCl	16.0 (sharp) 7.9 (broad)	MMT ADA HCl	17.1 (sharp) 4.5 (sharp)

	4.4 (sharp) 4.1 (sharp) 3.3 (broad/sharp)		4.3 (sharp) 3.4 (broad) 3.3 (sharp)
Alg+MMT AHA HCl	15.7 (sharp) 8.7 (broad) 6.0 (sharp) 4.3 (sharp) 3.2 (sharp) 3.1 (broad)	MMT AHA HCl	13.1 (broad) 4.5 (sharp) 4.3 (sharp) 3.4 (sharp) 3.2 (broad)
Alg+MMT GABA HCl	15.2 (sharp) 8.6 (broad) 4.2 (sharp) 3.2 (sharp) 3.1 (sharp)	MMT GABA HCl	13.0 (broad) 4.5 (sharp) 4.3 (sharp) 3.4 (sharp) 3.2 (sharp)
Alg+MMT 1.2 CHX	No visible peaks	MMT 1.2 CHX	15.2 (sharp) 7.0 (broad) 5.0 (broad) 4.5 (sharp) 4.3 (sharp) 3.7 (broad) 3.4 (sharp) 3.0 (broad) 2.6 (broad)

For the ADA MMT modified alginate gel, the d_{001} peak of the modified MMT is clearly visible with only a very small increase of layer spacing compared to the dry clay powder. This can be understood as the result of the long ADA chains being quite hydrophobic and thus the clay is not likely to swell in an aqueous environment.

For the AHA MMT modified gel, once more the clay layering is still visible in the XRD data, but now the layer spacing has increased to 15.7 Å compared to 13.1 Å in the dry clay powder. This is consistent with AHA modified clay being less hydrophobic and allowing some swelling in water.

This trend continues when looking at GABA MMT alginate gel. There is stacking of the clay plates visible in the clay powder XRD. However, in the alginate gel the clay is nearly fully dispersed and the d_{001} peak is only barely visible.

The most remarkable contrast is for CHX modified clay. This shows a number of clear peaks in the dry powder (Figure 5.12), but this structure is totally absent in the modified alginate gel (Figure 5.13). This could either mean that the clay is present but exfoliated into mostly single sheets; or that it is not mixed in properly with the hydrogel (note that this was the sample that dispersed least well, see Figure 5.6).

5.3.2.3 Scanning Electron Microscopy (SEM)

Some samples were harder to image due to the electron density presented, considering that the nature of the hydrogels is not conductive and the surface imaged is not smooth, most of the pictures were taken using a secondary detector (SED) however, when the image was not clear enough a back scattered detector (BED) was used instead.

Most of the structures were visibly different after the drying, and using SEM gave a clear impression of the dispersion of the modified clays in the alginate structure. Also, all samples presented two distinct structures, one corresponding to the interior of the disc and the "skin". The "skin" was avoided in most samples as it interacted more with the environment and it might not be representative of the bulk structure of each sample.

For the purposes of this chapter discs were made to image them in SEM. However, a undergraduate master's project[99] was run in parallel. Ruth Parry imaged some spheres made from Alginate and Alginate + Montmorillonite as shown in Figure 5.14. There is a clear difference in structure where the sphere is made with or without the clay present. In fact, in Figure 5.14b shows evidence of the beads presenting a different structure towards the edge. There is a visible outside layer of about 100 μm thickness and a very thin exterior "skin" on the bead. These images also show the structure is very porous.
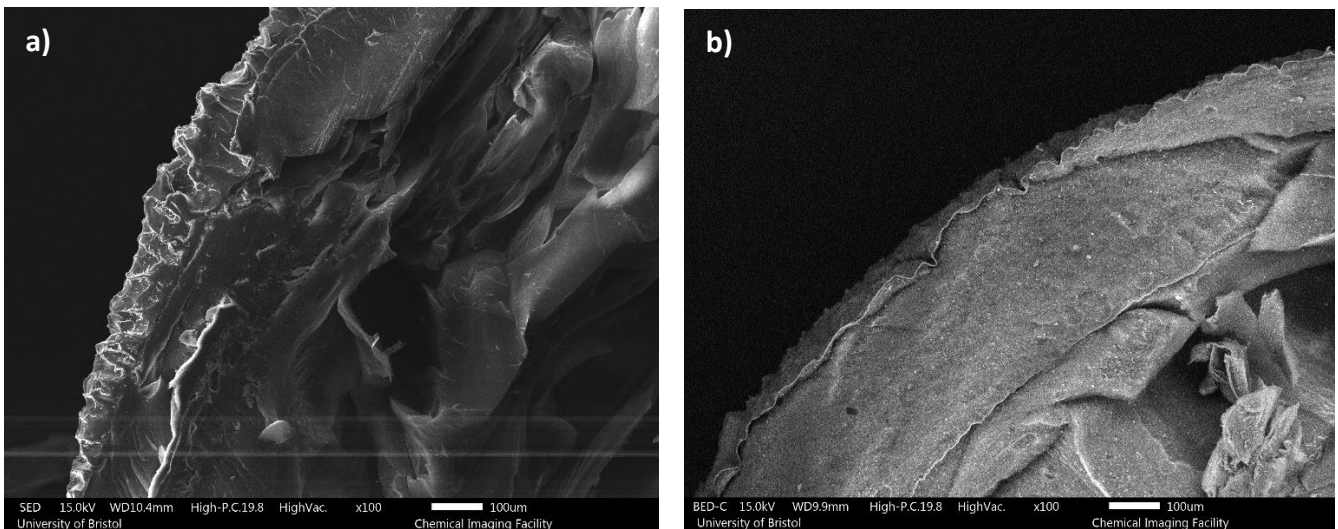
Figure 5.14. SEM of hydrogel beads. a) Alginate and b) Alg+MMT.

In Figure 5.15a and Figure 5.15c the difference between the drying techniques is evident. Freeze drying shows a better defined structure formed by layers of Alginate, whereas the vacuum dried samples show a mostly collapsed structure. However, the porosity does not seem to differ much if we consider only the top-down approach shown in Figure 5.15b and Figure 5.15d maybe due to the structure being the result of the ice crystals within the original material.
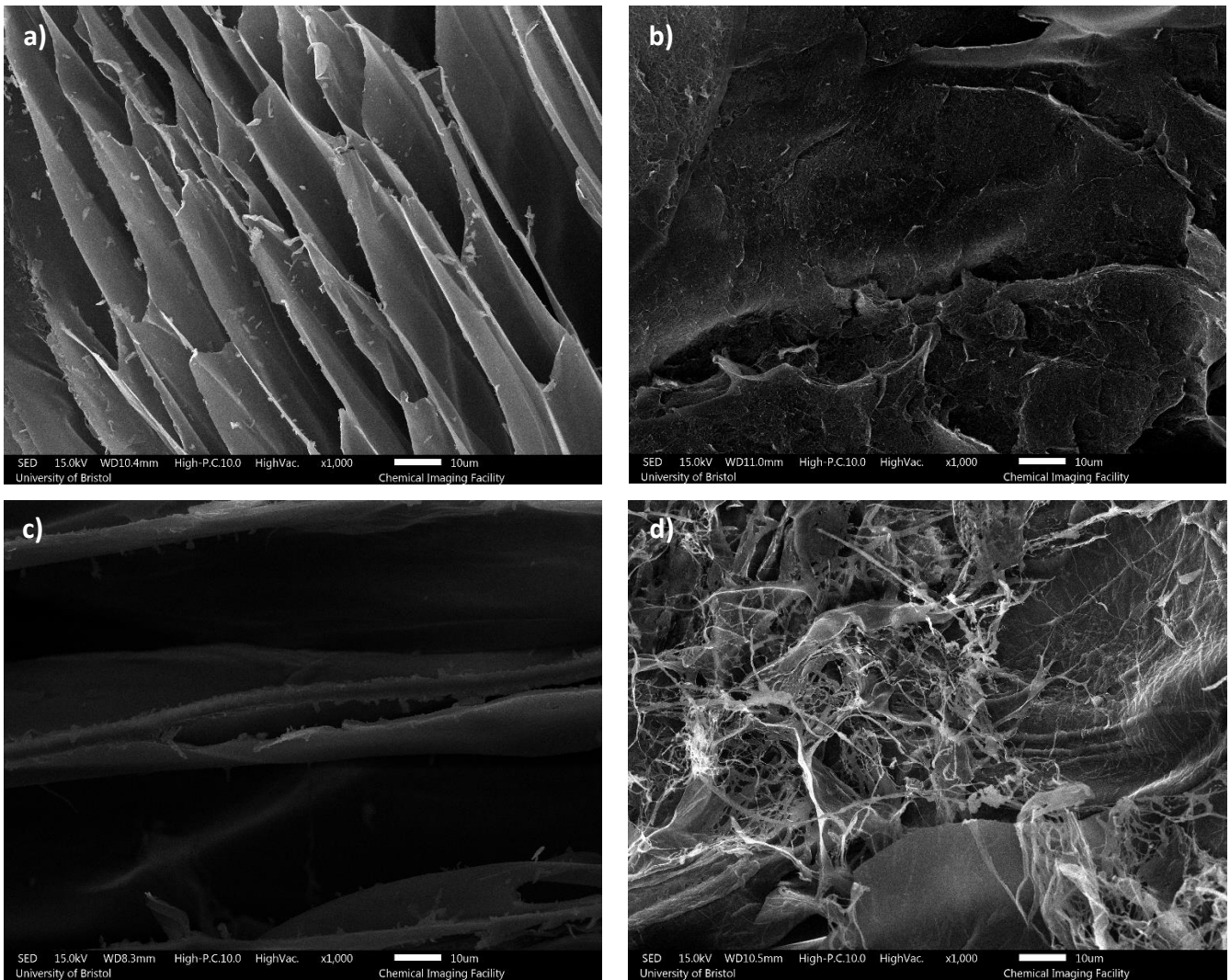
Figure 5.15. Sample 1 - Alginate. a) Freeze dried - Cross section, b) Freeze dried - Top down, c) Vacuum Oven - Cross section and d) Vacuum oven - Top down.

As seen in previous Figure 5.15 the Alginate already presented a well-arranged structure, but this material is not very strong as it easily deforms or breaks when applying some sort of mechanical effort, even by only squashing it by hand, hence the idea of mixing it with modified clays. In Figure 5.16 it is easy to spot fragments of clay (montmorillonite) dispersed on the surface of the alginate layer structure.
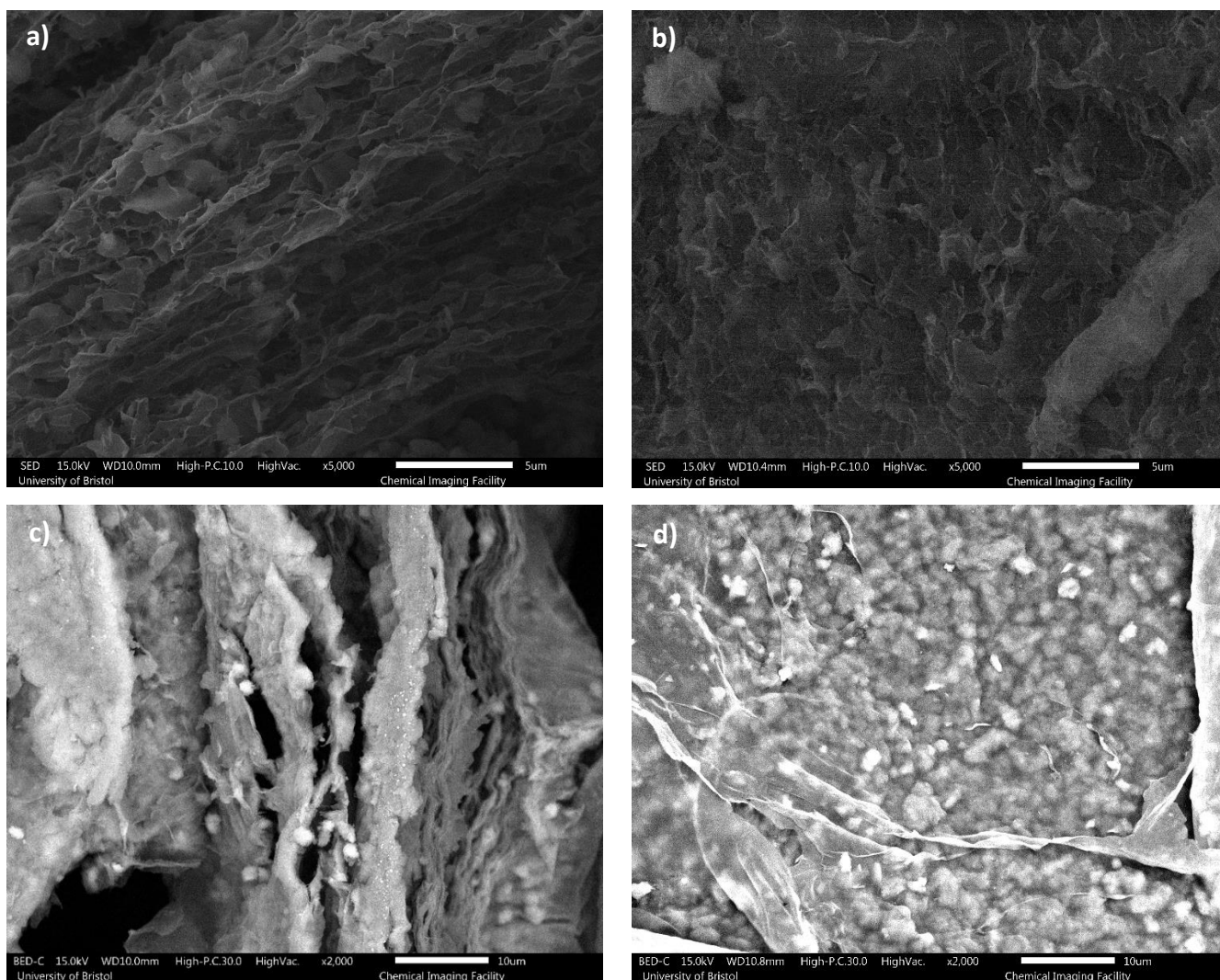
121

Figure 5.16. Sample 2 – Alginate + MMT. a) Freeze dried - Cross section, b) Freeze dried - Top down, c) Vacuum oven - Cross section and d) Top down.

The following three sets of images present the different modified clays interacting with the structure of alginate and how they respond to the drying step. In Figure 5.17 the ADA MMT appears like particles of considerable size (1 – 2 µm) decorating the surface of the alginate. The particles do not seem to be dispersed very evenly but they are present in the system.
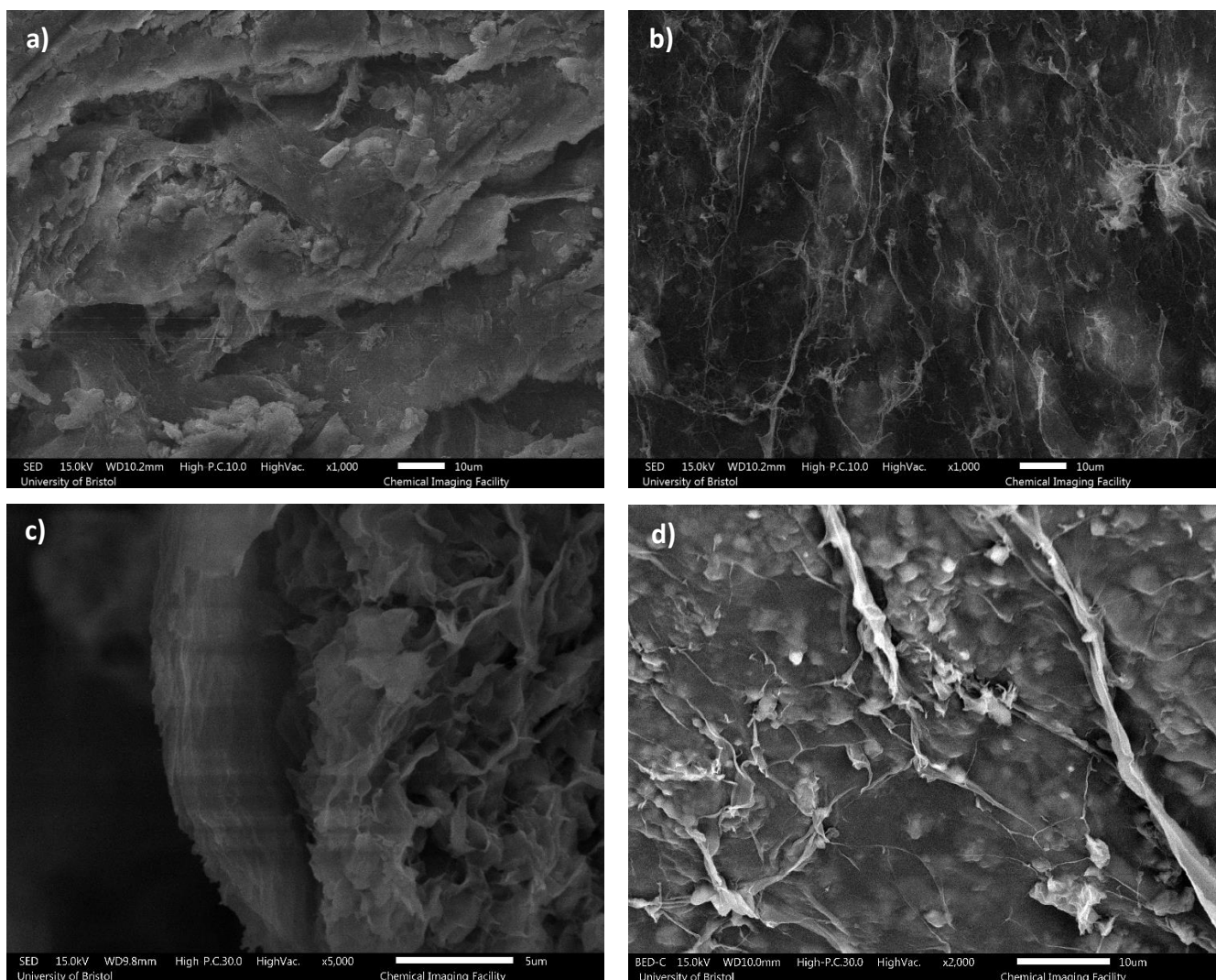
Figure 5.17. Sample 3 – Alginate + MMT ADA HCl. a) Freeze dried - Cross section, b) Freeze dried - Top down, c) Vacuum oven - Cross section and d) Top down.

In Figure 5.18 the clay used is AHA MMT, again it is noticeable that the particles interact with the alginate and how in the dried vacuum samples the sheets of the gel have collapsed (Figure 5.18c).
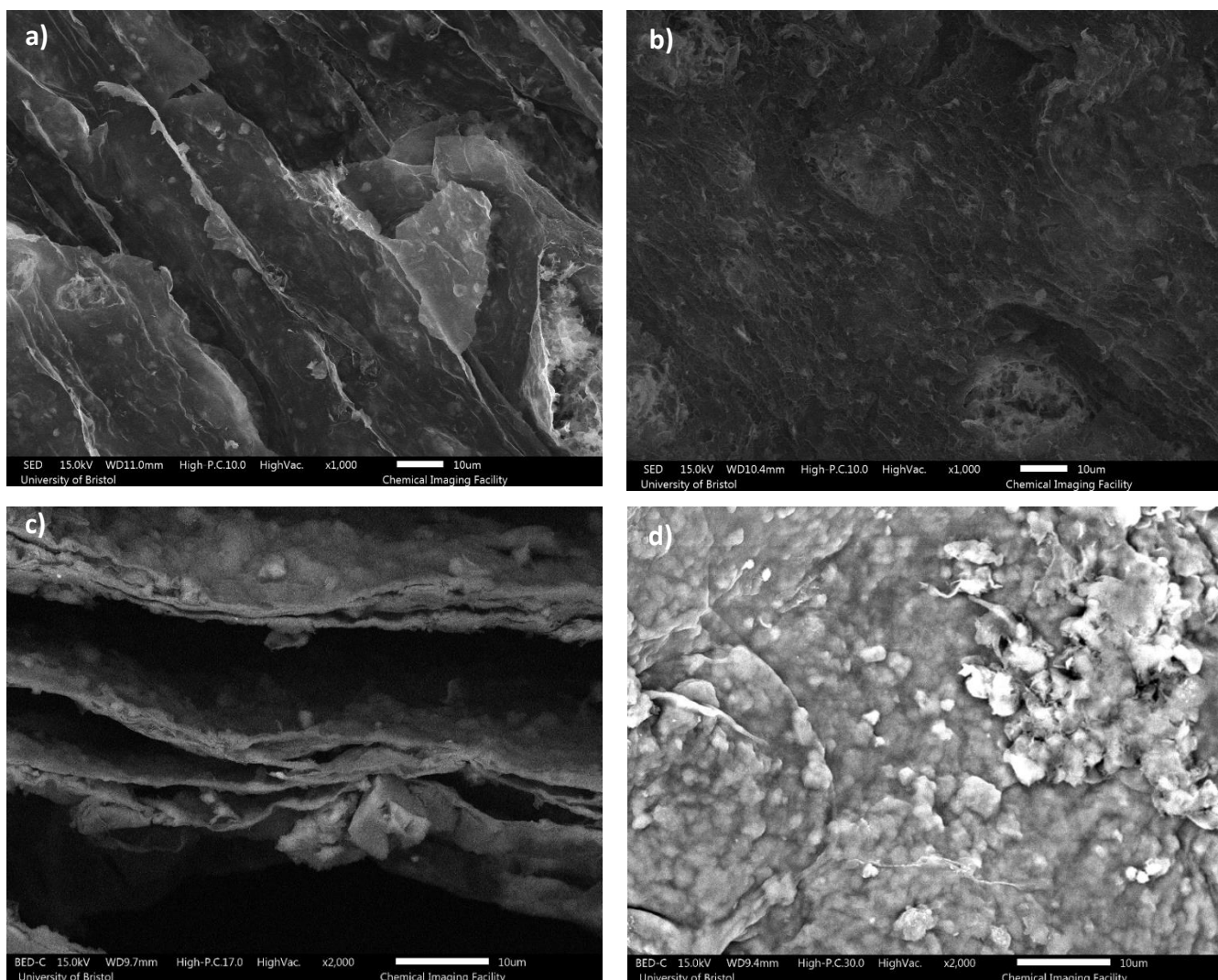
Figure 5.18. Sample 4 – Alginate + MMT AHA HCl. a) Freeze dried - Cross section, b) Freeze dried - Top down, c) Vacuum oven - Cross section and d) Vacuum oven - Top down.

Lastly in Figure 5.19 we have the clay modified with GABA and it looks to be the most "homogenous" decorated alginate gel which make us believe that the GABA MMT is better dispersed. This correspond to their behaviour in water, as the samples with GABA are more hydrophilic therefore, they disperse easier and stay in solution without crashing down or forming clusters.
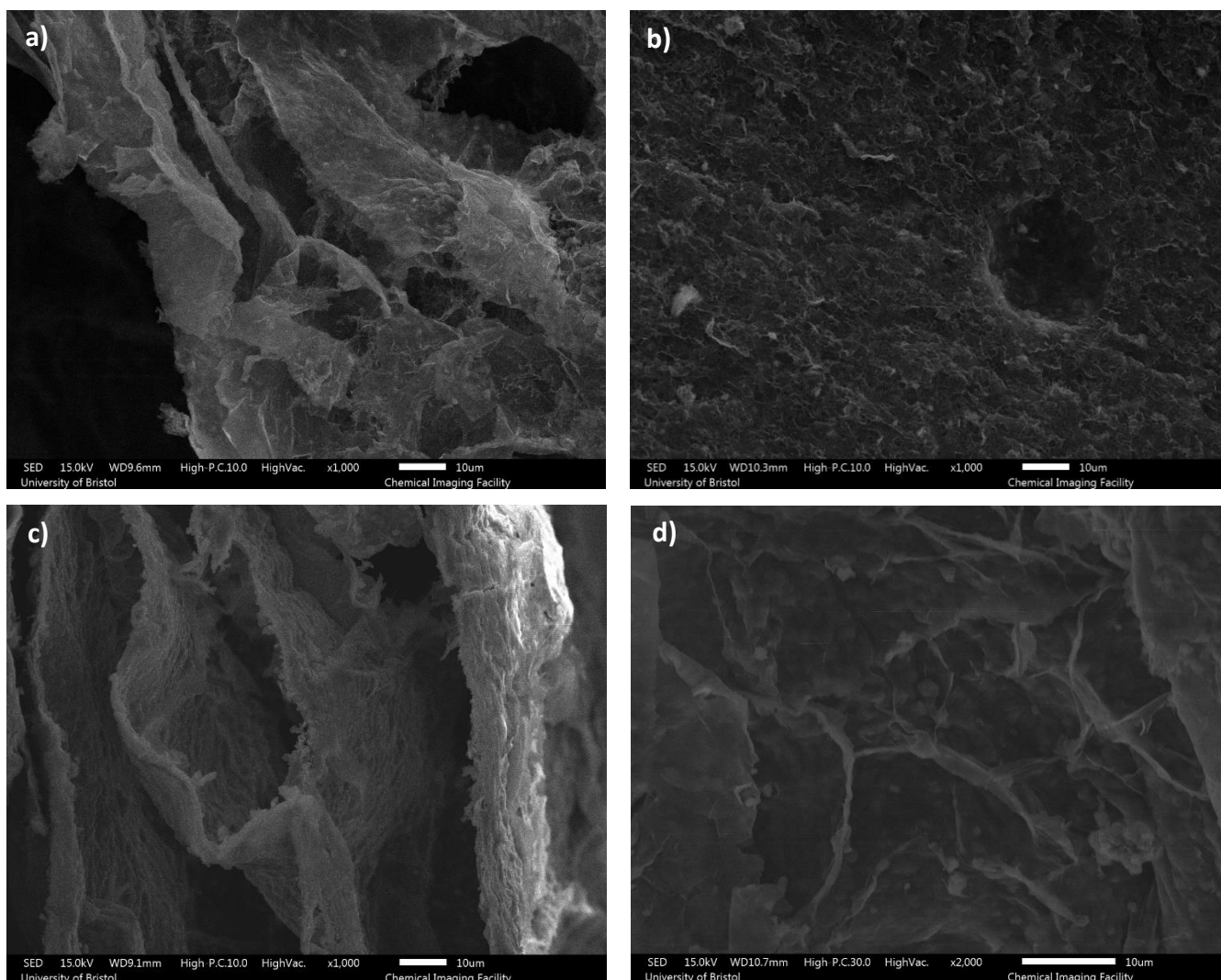
Figure 5.19. Sample 5 – Alginate + MMT GABA HCl. a) Freeze dried - Cross section, b) Freeze dried -Top down, c) Vacuum oven - Cross section and d) Vacuum oven - Top down.

While all the SEM images already presented within this section were taken carefully avoiding the outer skin of the gel samples for the alginate, alginate + clay and alginate + clay modified with ω-aa, Figure 5.21 presents images of the last gel sample correspondent to alginate + clay modified with CHX. In this case the imaging of the disc was made avoiding the borders of the gel (outer skin) as the previous samples however, it also shows images of the skin as the disc seemed to have a white "crust" at the bottom (see Figure 5.20) which presumably is the result of the precipitation of the clay that had formed a sediment during its gelation time.
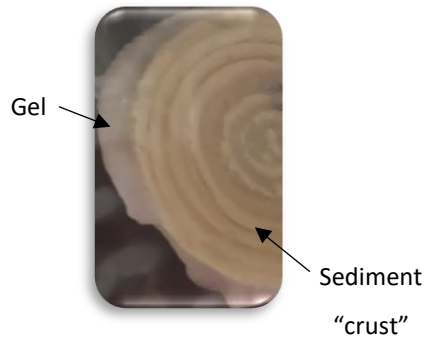
Gel

Sediment "crust"

Figure 5.20. Hydrogel disc sample of Alginate + MMT CHX 1.2.

Then, Figure 5.21a, 21b, 21c and 21d show the structure of the alginate with the clay particles dispersed inside the disc while Figure 5.21e, 21f, 21g and 21h try to lay out the difference on appearance between the gel and the sediment at the bottom. This sediment was not analysed further but looking at the images in addition to the solubility of the modified clay itself, it could be assumed that this sedimented "crust" contains both: clay and alginate, in a way it could be some aggregated clay particles that stick to the disc thanks to the presence of alginate.
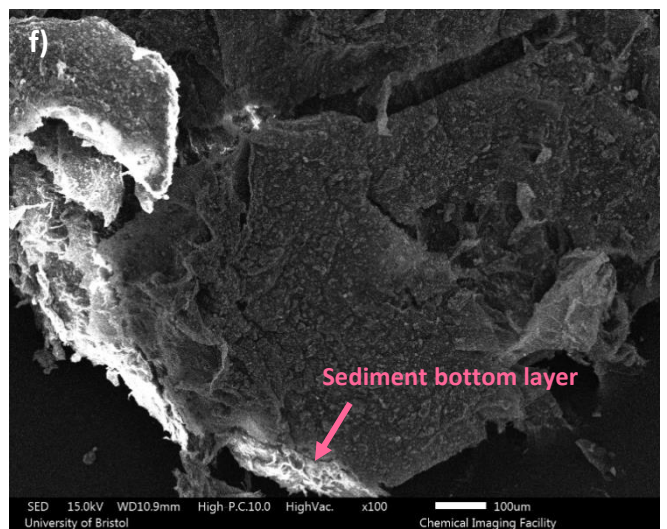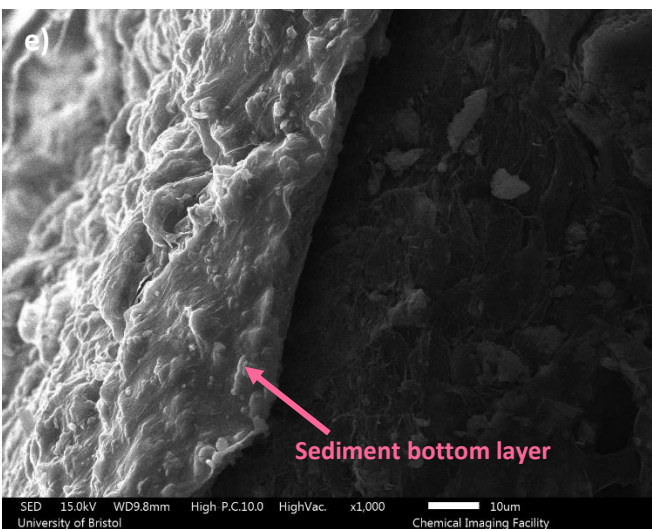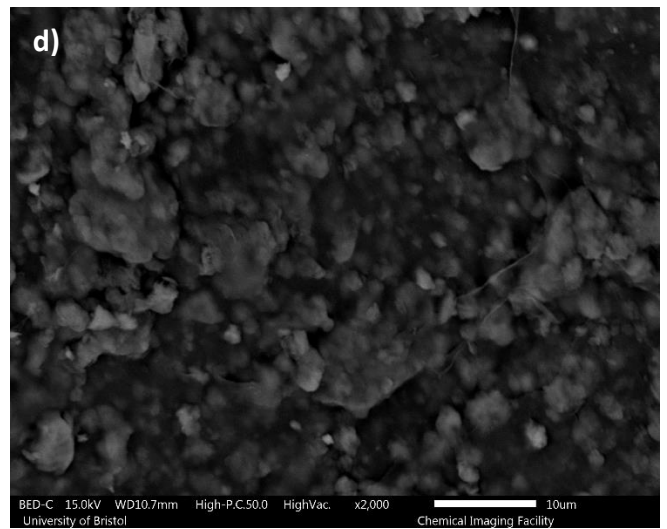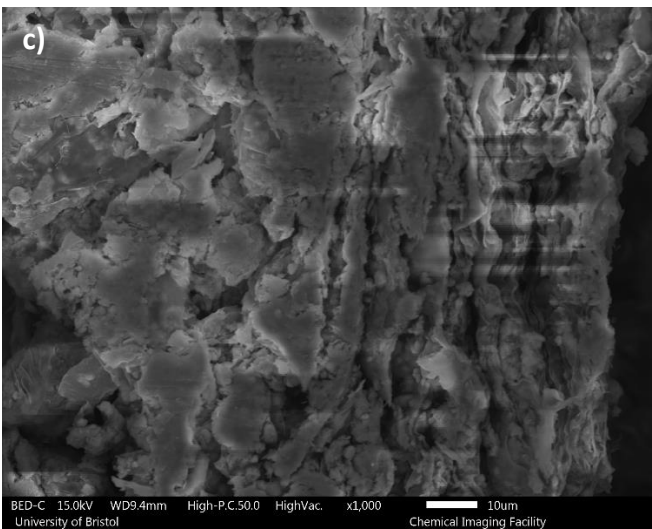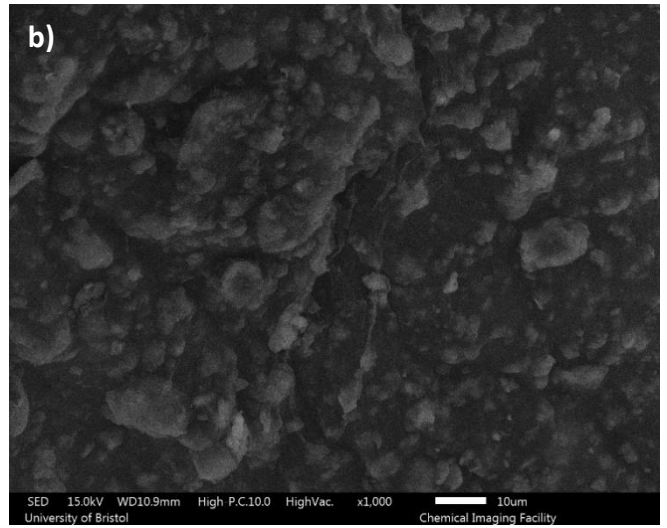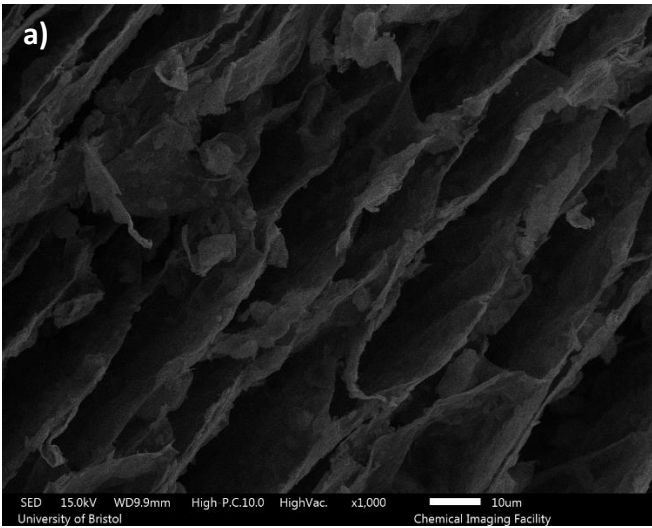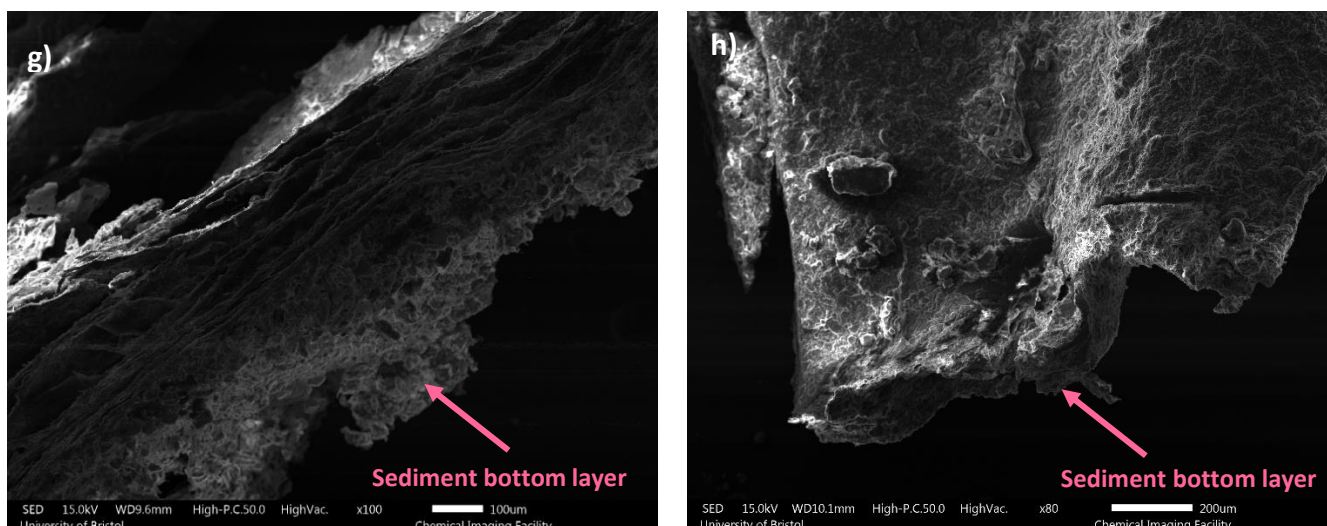
Figure 5.21. Sample 6 – Alginate + MMT 1.2 CHX. a) Freeze dried - Cross section, b) Freeze dried - Top down, c) Vacuum oven - Cross section and d) Vacuum oven - Top down - Next to the outer skin with the sediment. e) Freeze dried - Cross section, f) Freeze dried - Top down, g) Vacuum oven - Cross section and h) Vacuum oven - Top down.

5.3.3 Mechanical Testing

5.3.3.1   Compression Test

As explained in section 5.2.3.1 various sets of three beads were subjected to the compression test by measuring the deformation of the sphere as the weight was increased. As it can be seen in Figure 5.22 the response of the beads was different depending on the sample, some of them present the capacity to recover their shape after the weight has been removed for a few minutes whilst others did not.
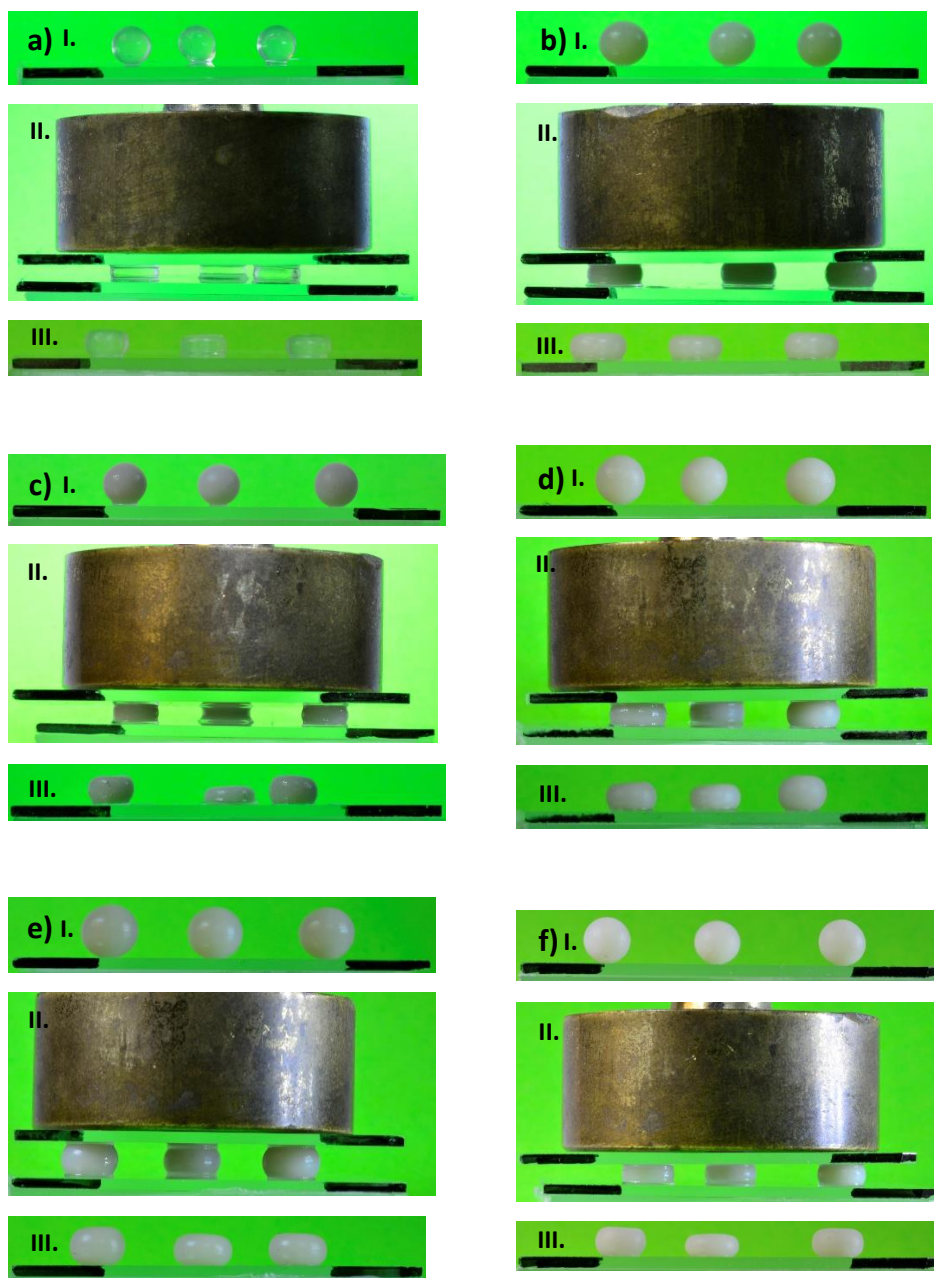
Figure 5.22. Bead appearance during different stages of the experiment. I) before weight applied, II) 100 g on top, III) at the end of compression test of each sample. a) Alg, b) Alg + MMT, c) Alg + MMT ADA, d) Alg + MMT AHA, e) Alg + MMT GABA and f) Alg + MMT CHX.

The results are plotted to allow comparison with equation (*5.3*). Thus, Figure 5.23a shows the performance of the bead correspondent to sample "Alg + GABA MMT", this sample was chosen as it is the one that presents most evidently how the bead behaves whilst being compressed, changing physically from being a well-shaped sphere to a thick small disc. Figure 5.23b was made by using the data up to ≤ 0.8 for the function above it which equates to *(R/R*)*

less than 1.12. With this information its determined that the deformation limit is so low that the rest of our data have a break point above 0.8, the trendline of this fitted data gives us the value of the gradient, G'.
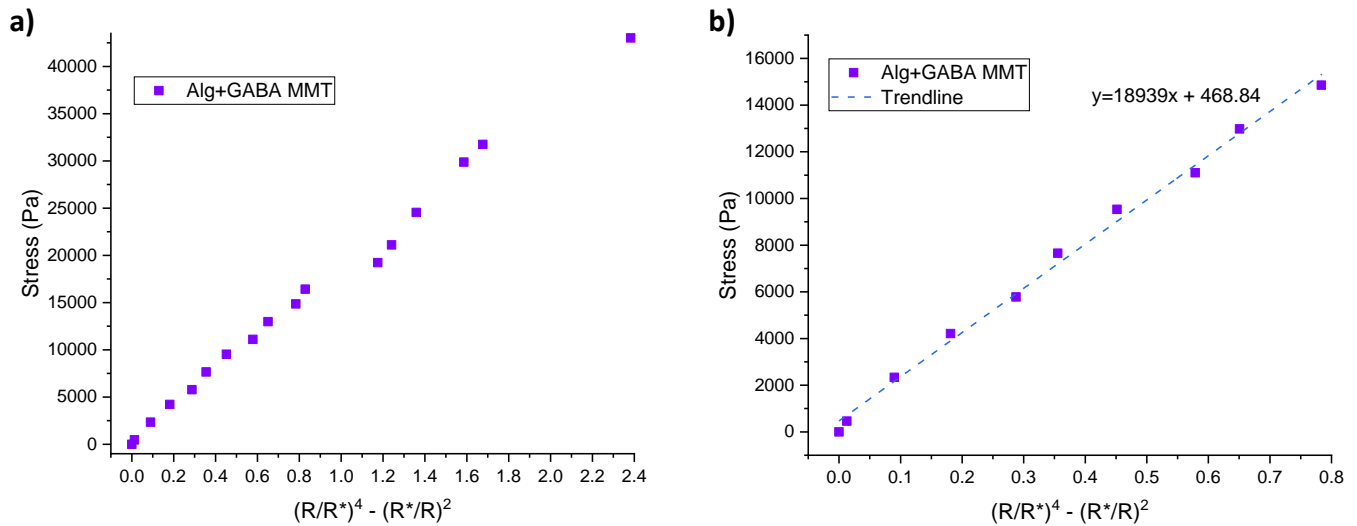
Figure 5.23. Illustrative graph of the mechanical tests results of alginate beads containing modified clays a) whole data set for Alg + GABA MMT and b) deformation limit data to obtain G' in Alg + GABA MMT sample.

Although when calculating the shear modulus (G') presented in Table 5.2 sometimes the results obtained varied significantly from one bead to another within the same sample group. Each ball gives a gradient, and the average is obtained out of the 3 specimens along with the standard deviation, resulting in considerably larger values in some samples, i.e., Alg + ADA MMT. The set of beads of each sample seem different in weight and size between each other as presented in the table below but they do not differ significantly among their own sample group. Based on the average sizes and masses, densities (obtained from these two results) range from 1.0 to 1.2.

Table 5.2. Bead characteristics and shear modulus of each sample. Standard deviation in parentheses and n in square brackets.

Sample	Bead Mass (g)	Bead Size (mm)	Density (g/cm^3)	G' (kPa)
Alginate	0.0299 (0.0036) [18]	3.67 (0.37) [18]	1.15	15.8 (6.0) [3]
Alg+MMT	0.0574 (0.0018) [12]	4.47 (0.33) [12]	1.23	26.5 (2.6) [3]
Alg+MMT ADA HCl	0.0367 (0.0016) [9]	3.89 (0.25) [9]	1.19	26.8 (11.6) [3]
Alg+MMT AHA HCl	0.0484 (0.0022) [9]	4.39 (0.34) [3]	1.1	24.8 (9.1) [3]
Alg+MMT GABA HCl	0.0744 (0.0046) [9]	4.87 (0.33) [3]	1.23	25.1 (5.4) [3]
Alg+MMT 1.2 CHX	0.0378 (0.0011) [9]	4.17 (0.40) [3]	1.0	21.2 (5.7) [3]

5.4 Discussion

It was clear that the addition of modified clays had an impact on the structure of the samples, modifying their capacity to achieve a desired shape as well as altering the shear modulus. The concentration of clay added to the alginate was also important as the beads were spherical; there are reports in the literature, of low concentrations resulting in non-spherical beads while high concentrations can produce beads with a "tail"[92] but this was not observed in this study.

XRD shows that ADA clay does not disperse well in aqueous environment however the other samples all swelled which suggests that they have a good opportunity to interact with the polymer matrix as a result. However, as we have seen in the dispersion images, some other samples also needed to be redispersed before the gel preparation. To see more details about all samples, please see Table 8.2 in the appendix.

Inspecting the shear moduli G' obtained in the compression test, the values vary from sample to sample and the hydrogels containing clay all have higher values than the pure Alginate hydrogel. Given the magnitude of the error bars and the fact that only three beads were analysed per sample, the differences between different clay surface chemistries are not significant. However, the pictures of the mechanical test gave more information to be discussed, see Figure 5.24 and Table 5.4 below.

Considering the deformation presented by the beads at constant volume (neglecting the fact that water content will vary depending on the conditions and time) and assuming that the bead is an isotropic material which is incompressible but presents a homogeneous deformation. The shear modulus G' obtained with the test run in this chapter can be related to the Young's modulus E using the following equation where v is the Poisson's ratio and corresponds to 0.5 due to the type of material[95]:

$$G' = \frac{E}{2(1 + v)} \tag{5.4}$$

$$E = 3G' \tag{5.5}$$

Then the Young's modulus of all the hydrogel samples is presented in Table 5.3.

Table 5.3. Young's modulus of each sample. Standard deviation in parentheses and n in square brackets.

Sample	E (kPa)
Alginate	47.5 (18) [3]
Alg+MMT	79.5 (7.8) [3]
Alg+MMT ADA HCl	80.5 (34.8) [3]
Alg+MMT AHA HCl	74.5 (27) [3]
Alg+MMT GABA HCl	75.2 (16.4) [3]
Alg+MMT 1.2 CHX	63.6 (17.1) [3]

This modulus has been reported in the literature as a number that varies depending on the different factors involved in the gelation stage, the cation used and the concentration of the alginate. Considering $CaCl_2$ the value goes from 46.6 kPa to up to 600 kPa[92 94 100]. The first value is very similar to the one presented by the Alginate hydrogel sample tested in this chapter.

Upon applying a high stress (much larger than that used to obtain G' values in section 5.3.3.1) some beads seem to be more resistant than others. For example, in Figure 5.24, the images presented correspond to each bead sample set under the heaviest weight supported by them. The corresponding set of beads for Alg + MMT GABA seem to be the least deformed of all even under the maximum weight used.
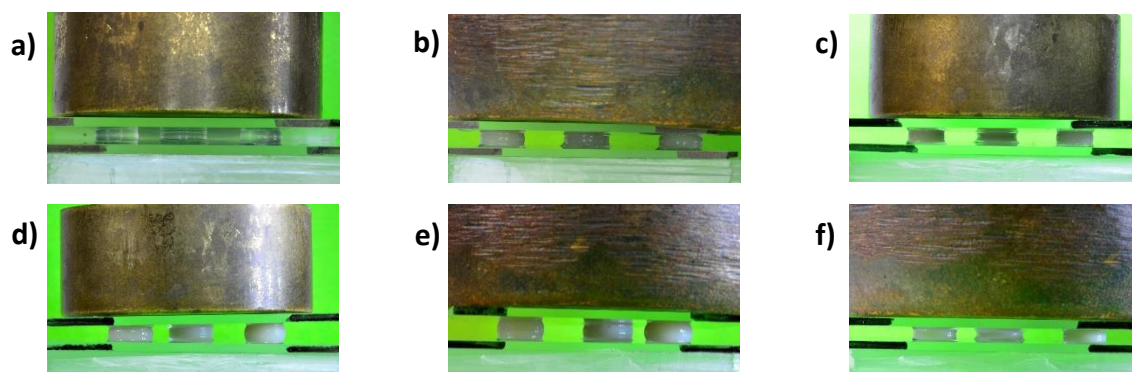

Figure 5.24. Bead appearance under maximum weight supported. a) Alg (~103g), b) Alg + MMT (~230g), c) Alg + MMT ADA (~130g), d) Alg + MMT AHA (~160g), e) Alg + MMT GABA (~230g) and f) Alg + MMT CHX (~230g).

Another detail to point out is how the beads lose water when compressed, for instance, this is evident for some beads in Figure 5.24. In the literature this has been avoided by doing a high compression test with a system immersed in water[92][100], which also helps to allow recovery of the bead shape in some cases.

An interesting observation was made when all the discs prepared for the XRD test had to be kept in DIW to avoid drying further whilst waiting for the equipment to be fixed (overnight). Next day it was very noticeable how during this time most samples almost fully recovered their original shape. This behaviour inspired the idea of taking pictures of the beads a few minutes (~3 min) after removing the weight put on top to measure the compression, see panels labelled III) in Figure 5.22.

Thanks to these sequences of images, it can be seen how some of the beads that contain modified clays "bounced back" from their flattened state to a rounder shape, although none of them recovered the sphere shape completely due to the water content lost. The results are summarised in Table 5.4, which compares how much the bead was deformed, and how much it managed to recover after the compression relative to its initial size. The percentage

of deformation is the increase in diameter vs. its original size once weight was applied, the recovery percentage is how much of the bead diameter bounced back vs. the original bead diameter after weight is removed and the ratio indicates to what extent the bead managed to recover its initial shape.

This ability to recover even after being subjected to the heaviest weight used in this experiment is remarkable, considering that some structures have released a significant amount of their water content. It could be said that the addition of clay has improved the toughness of the material, as it can absorb a lot of energy without breaking.

Table 5.4. Average deformation and recovery of 3 beads per sample.

Sample	% deformation with heavier weight	% recovery after weight removal	% deformation/recovery ratio
Alg	32	19	59
Alg+MMT	23	13	57
Alg+MMT ADA	17	10	60
Alg+MMT AHA	22	13	62
Alg+MMT GABA	22	13	59
Alg+MMT CHX 1.2	29	14	49

In general, it could be said that the clay modified with GABA HCl is the most interesting when combined with the alginate to form a hydrogel, its dispersion looked consistent and did not need to be redispersed which is a great advantage when preparing the gel specimens. This is because they do not create any bubbles in the structure which can affect its performance during the tests. If we compare its SEM (Figure 5.19) it is the most homogeneous of the samples too. Hydrophilic GABA allows good dispersion, good interaction with alginate and avoids forming clay aggregates in the final gel samples. The XRD data (Figure 5.13) suggest only limited stacking of the clay platelets for this sample, which would imply a larger number of reinforcing particles per unit of hydrogel volume.

5.5 Conclusion

This chapter itself could have been a whole new project. However, as part of this thesis, every technique was carefully chosen to obtain as much information as possible, in order to learn more about the material but also identifying achievable goals within the limited time available.

One of the contributions from this research would be the protocol for how to make different hydrogel shapes as in the literature it seems limited to basic ones such as beads, cubes, or cylinders. Here was presented the use of a mould that did not interfere with the gelation stage and let the final gel have more details than just a plain disc. Furthermore, all tests were done at room temperature in air, including the recovery time ("bouncing" behaviour). This expands the relevance of the results as it opens the possibility to have different material designs for multiple applications that do not necessarily run in aqueous environments. Also, the samples were found to tolerate exposure to stress in air for a few hours (while running the characterisation technique) and still being able recover when put back in water.

It is unfortunate that the data obtained out of the compression test are not greatly different from one another, because it makes difficult to prove that the interesting observations made while carrying out the rest of the experimental work done within this chapter are improvements. In particular the MMT GABA addition does seem to improve the ability of the beads to tolerate high applied stress.

If the test done this time did not reveal a clear difference it could mean that different mechanical properties of the gels are being modified but they cannot be measured with this technique. As further work it would be beneficial to do a more detailed rheological characterisation of clay + alginates. Future interesting tests may also include methods to characterise recovery after stress in a more formal way, possibly in presence of water to allow beads to fully recover their shape.

Chapter 6 Conclusions and Future Work

6.1 Conclusions

Clay particles have been used as nanofillers to reinforce or improve properties of polymeric materials. The aim of this research was to develop a hierarchical structured material in which the nanofiller could enhance mechanical properties or add an antimicrobial property to some dental materials. This thesis describes the process to prepare such structures and test them. The experimental work was divided into four sections, on one side chapters 2 and 4 describe the procedure followed to create the modified clay samples that were tested by combining ω-amino carboxylic acids (ω-aa) or chlorhexidine (CHX) with the montmorillonite (MMT) platelets, respectively. On the other side chapters 3 and 5 present the data obtained on mixtures of these modified clays into glass ionomer cement (GIC) or sodium alginate gels (Alg).

The characterisation techniques showed the benefits of following an acid treatment versus a neutral treatment, as an excess of ω-aa was found in the clay samples prepared by the neutral route and the d_{001} spacing changed depending on the parameters varied as well as the definition of the peak. This indicates that for the samples treated by the acid route the ω-aa chains were intercalating in a well-organised way into the platelet structure. To avoid any undesired interaction when adding the modified clay to the GICs and hydrogels the samples used for the application chapters were those obtained using acid treatment. For the same reason the Acridine Orange (AO) was removed from the samples, this dye was only added into some samples in this research to help visualise the state of dispersion and it is not necessary for the purpose of improving the mechanical properties. Lastly, the powders were freeze dried to prevent them from agglomerating.

The challenge faced when mixing clay structures with CHX was to evaluate if the MMT and CHX formed a composite or instead were merely "sitting" side by side. The methodology followed was very cautious trying to avoid unbound CHX in the samples, by thoroughly washing every sample prepared before using them in the dialysis system to test potential release of the remaining CHX. Only one concentration tested showed some release however it only released 5% of the CHX content. This could mean that the CHX was strongly bound to the clay; this is not discouraging as it could mean that materials made with this clay +

antimicrobial composite could present antimicrobial properties for long periods of time due to their retention capacity as a potential slow release or bound antimicrobial system.

For the applications proposed in this project, chapter 3 establishes the results of combining modified clays with a commercial GIC. This research highlights the importance that a filler such as montmorillonite must be well dispersed within a composite material to effectively enhance its final strength, hence the importance of using a ball milling process to achieve this goal. However, considering that this technique noticeably impacted the GIC particle size and shape and the addition of clay particles with different surface area, it was needed to make some adjudgments in the powder:liquid ratio. The required water content was increased by 15% over the commercial formulation to obtain a good quality specimen with appropriate handling properties for use in clinical applications. The specimens produced were tested mechanically with the intention to evaluate their compressive strength; this objective was successfully achieved with CS of the GIC increasing by ~70% irrespective of the manner of pre-treatment of the clay used.

The properties shown above were also found to be transferrable to hydrogel composites made of MMT and sodium alginate, the uses for which have been well established in the literature. One key finding of this research was the improvement in methodology that was used to test and observe the physical properties of these new hydrogels. The use of a mould to create the samples has not been used in the literature before but presents clear advantages as it does not impact the gelation stage and allows for the creation of more complex shapes than previously tested. The findings of the compression test of the bead hydrogels concluded that they were not greatly different from one another, this is unfortunate as it does not explain the interesting observations made while carrying out the rest of the experimental work. The addition of MMT+GABA did seem to improve the ability of the beads to tolerate high applied stress. A last observation is that the experiments were done at room temperature and in open air which suggests that there are potential uses for these gels that do not require their application to be solely under water as was previously reported. The stress recovery shown during these experiments suggests that the gels may be suitable for use for at least a limited time outside of an aqueous environment (longer exposure to air would be expected to result in dry beads).

6.2 Future Work

Compressive strength is not the only parameter that varies when the glass ionomer cement is altered, despite of being a good indicator of success. Other tests such as diametral tensile strength or flexural strength could also be considered to complement the findings of this work, as would characterisation of adhesion to dental hard tissues and setting time parameters. Raman spectroscopy could be used to track every step of the setting process, which would allow comparing the reaction of the unmodified specimen with that involving addition of modified clays.

To have a complete set of modified clays added to GIC, it would be of interest to add the clay sample that contains chlorhexidine to compare if it increases the strength as well; in addition, this sample could be evaluated for its antimicrobial properties. Including a clay with higher CHX content may furthermore result in a (potentially slow and sustained) CHX release. This could be compared with data reported in the literature where researchers had used either clays or CHX.

As mentioned above, for the montmorillonite modified with chlorhexidine testing higher concentrations of it but keeping the cleaning process to avoid lose product that would be easily detached from the clay structure, the purpose is to have a nicely packed amount of CHX in between the layers of the clay that could be released in a "controlled" way instead of just having a lot of excess that would leave the system within the first hours after being placed.

Finally, as indicated at the beginning of chapter 5, the experiments selected were just a few of all the possible techniques that could be used to evaluate the materials. It would be relevant to use a rheometer to quantify the mechanical properties of the alginate gels, in particular given that the compression tests suggest that the addition of modified clays may improve the elastic response of the gels. Furthermore, it would be of worth to repeat the compression experiments whilst keeping the beads submerged in an aqueous environment to compare the "bounce" effect with the experiments carried out in free air.

Chapter 7 Bibliography

1. Theng, B. K. G. Some practical applications of the clay-polymer interaction. in *Developments in Clay Science* vol. 4 153–199 (Elsevier B.V., 2012).

2. IMERYS Transform to perform. Bentonite. https://www.imerys-additivesformetallurgy.com/our-resources/bentonite/.

3. Morgan, A. B. *Polymer-Clay Nanocomposites: Design and Application of Multi-Functional Materials*. (2011).

4. Gul, S., Kausar, A., Muhammad, B. & Jabeen, S. Research progress on properties and applications of polymer/clay nanocomposite. *Polymer - Plastics Technology and Engineering* vol. 55 684–703 (2016).

5. Pircheraghi, G., Nazockdast, H. & Salehi, M. M. The effects of chemical bonding of nanoclay surface modifier and compatibilizer on microstructure development and rheological properties of PP/PP-g-MA/Diamine modified nanoclay. *Polym. - Plast. Technol. Eng.* **50**, 1109–1117 (2011).

6. Liu, C., Tang, T., Wang, D. & Huang, B. In Situ Ethylene Homopolymerization and Copolymerization Catalyzed by Zirconocene Catalysts Entrapped inside Functionalized Montmorillonite. (2003).

7. Schmidt, C. U. & Lagaly, G. Surface modification of bentonites: I. Betaine montmorillonites and their rheological and colloidal properties. *Clay Miner.* **34**, 447–458 (1999).

8. Anusavice, K. J., Shen, C. & Rawls, H. R. *Philips' Science of Dental Materials*. (2012).

9. Rekow, E. D., Fox, C. H., Petersen, P. E. & Watson, T. Innovations in materials for direct restorations: Why do we need innovations? Why is it so hard to capitalize on them? *Journal of Dental Research* vol. 92 945–947 (2013).

10. Rekow, E. D., Bayne, S. C., Carvalho, R. M. & Steele, J. G. What constitutes an ideal dental restorative material? *Adv. Dent. Res.* **25**, 18–23 (2013).

11. Berry, T. G., Summit, J. B., Chung, A. K. H. & Osborne, J. W. HISTORY OF AMALGAM. *J.*

Am. Dent. Assoc. **129**, 1547–1556 (1998).

12. Morrier, J.-J. *et al.* Antimicrobial activity of amalgams, alloys and their elements and phases. *Dent. Mater.* **14**, 150–157 (1998).

13. Sakaguchi, R. L. & Powers, J. M. *Craig's restorative dental materials*. (Elsevier/Mosby, 2012).

14. Barry, T. I., Clinton, D. J. & Wilson, A. D. The Structure of a Glass-Io nomer Cement and its Relationship to the Setting Process. *J. Dent. Res.* **58**, 1072–1079 (1979).

15. Hatton, P. & Brook, I. Characterisation of the ultrastructure of glass-ionomer (poly-alkenoate) cement. *Br. Dent. J.* **173**, 275–277 (1992).

16. Crisp, S., Pringuer, M. A., Wvardlewvorth, D. & Wilson, A. D. Reactions in Glass Ionomer Cements: II. An Infrared Spectroscopic Study. *J. Dent. Res.* **53**, 1414–1419 (1974).

17. Nicholson, J. W., Brookman, P. J., Lacy, O. M. & Wilson, A. D. *Fourier Transform Infrared Spectroscopic Study of the Role of Tartaric Acid in Glass-ionomer Dental Cements*. *J Dent Res* vol. 67 (1988).

18. Prosser, H. J., Richards, C. P. & Wilson, A. D. NMR spectroscopy of dental materials. II. The role of tartaric acid in glass-ionomer cements. *J. Biomed. Mater. Res.* **16**, 431–445 (1982).

19. Smith, D. C. & Ruse, N. D. Acidity of glass ionomer cements during setting and its relation to pulp sensitivity. *J. Am. Dent. Assoc.* **112**, 654–657 (1986).

20. Woolford, M. J. The surface pH of glass ionomer cavity lining agents. *J. Dent.* **17**, 295–300 (1989).

21. van Noort, R. & Barbour, M. *Introduction to Dental Materials*. (2013).

22. Xie, D., Brantley, W. A., Culbertson, B. M. & Wang, G. Mechanical properties and microstructures of glass-ionomer cements. *Dent. Mater.* **16**, 129–138 (2000).

23. Hook, E. R. *et al.* Development of a novel antimicrobial-releasing glass ionomer cement functionalized with chlorhexidine hexametaphosphate nanoparticles. *J. Nanobiotechnology* **12**, (2014).

24. Burrow, M. F. Physicochemical nature of glass-ionomer-based materials and their clinical performance. in *Glass-Ionomers in Dentistry* 25–56 (Springer International Publishing, 2016). doi:10.1007/978-3-319-22626-2_2.

25. Fareed, M. A. & Stamboulis, A. Nanoclays reinforced glass ionomer cements: Dispersion and interaction of polymer grade (PG) montmorillonite with poly(acrylic acid). *J. Mater. Sci. Mater. Med.* **25**, 91–99 (2014).

26. Dowling, A. H., Stamboulis, A. & Fleming, G. J. P. The influence of montmorillonite clay reinforcement on the performance of a glass ionomer restorative. *J. Dent.* **34**, 802–810 (2006).

27. Fareed, M. A. & Stamboulis, A. Nanoclay addition to a conventional glass ionomer cements: Influence on physical properties. *Eur J Dent* **8**, 456–463 (2014).

28. Fareed, M. A. & Stamboulis, A. Effect of nanoclay dispersion on the properties of a commercial glass ionomer cement. *Int. J. Biomater.* **2014**, (2014).

29. Crisp, S., Lewis, B. G. & Wilson, A. D. Characterization of glass-ionomer cements 2. Effect of the powder : liquid ratio on the physical properties". *J. Dent.* **4**, 287–290 (1976).

30. Fleming, G. J. P., Farooq, A. A. & Barralet, J. E. Influence of powder/liquid mixing ratio on the performance of a restorative glass-ionomer dental cement. *Biomaterials* **24**, 4173–4179 (2003).

31. Williams, J. A. & Billington, R. W. Increase in compressive strength of glass ionomer restorative materials with respect to time: a guide to their suitabiHty for use in posterior primary dentition. *Journalof Oral Rehabil.* **16**, 475–479 (1989).

32. Williams, J. A. & Billington, R. W. Changes in compressive strength of glass ionomer restorative materials with respect to time periods of 24 h to 4 months. *J. Oral Rehabil.* **18**, 163–168 (1991).

33. Moshaverinia, A. *et al.* Modification of conventional glass-ionomer cements with N-vinylpyrrolidone containing polyacids, nano-hydroxy and fluoroapatite to improve mechanical properties. *Dent. Mater.* **24**, 1381–1390 (2008).

34. Moshaverinia, A., Roohpour, N. & Rehman, I. U. Synthesis and characterization of a novel fast-set proline-derivative-containing glass ionomer cement with enhanced mechanical properties. *Acta Biomater.* **5**, 498–507 (2009).

35. Cheetham, J. J. The future of glass-ionomers. in *Glass-Ionomers in Dentistry* 125–148 (Springer International Publishing, 2016). doi:10.1007/978-3-319-22626-2_7.

36. Lakhani, N. & Vandana., K. L. Chlorhexidine – An Insight. *Int. J. Adv. Res.* **4**, 1321–1328 (2016).

37. Barbour, M. E., Maddocks, S. E., Wood, N. J. & Collins, A. M. Synthesis, characterization, and efficacy of antimicrobial chlorhexidine hexametaphosphate nanoparticles for applications in biomedical materials and consumer products. *Int. J. Nanomedicine* **8**, 3507–3519 (2013).

38. Lacerda-Santos, R. *et al.* Effect of different concentrations of chlorhexidine in glass-ionomer cements on in vivo biocompatibility. *J. Adhes. Dent.* **18**, 325–330 (2016).

39. Iz, S. G., Ertugrul, F., Eden, E. & Gurhan, S. I. D. Biocompatibility of glass ionomer cements with and without chlorhexidine. *Eur. J. Dent.* **7**, (2013).

40. Talibudeen, O. Complex formation between montmorillonoid clays and amino-acids and proteins. *Trans. Faraday Soc.* **51**, 582–590 (1955).

41. Okada, A. & Usuki, A. Twenty years of polymer-clay nanocomposites. *Macromol. Mater. Eng.* **291**, 1449–1476 (2006).

42. Okada, A. *et al.* Composite Material and Process for Producing the Same. (1990).

43. Okada, A. *et al.* Composite Material and Process for Manufacturing Same. (1988).

44. Fornes, T. D. & Paul, D. R. Formation and Properties of Nylon 6 Nanocomposites. *Polímeros Ciência e Tecnol.* **13**, 212–217 (2003).

45. Kawasumi, M., Kohzaki, M., Kojima, Y., Okada, A. & Kamigaito, O. Process for Producing Composite Material. (1989).

46. Liang, Y., Omachinski, S., Logsdon, J., Cho, J. W. & Lan, T. Nano-effect in in situ Nylon-6 Nanocomposites. *Nanocor® Tehnical Papers* 1–5 (2008).

47. Michot, L. J. *et al.* Phase diagrams of wyoming Na-montmorillonite clay. Influence of particle anisotropy. *Langmuir* **20**, 10829–10837 (2004).

48. Cui, Y. & Van Duijneveldt, J. S. Adsorption of polyetheramines on montmorillonite at high pH. *Langmuir* **26**, 17210–17217 (2010).

49. Usuki, A., Hasegawa, N. & Kato, M. Polymer-clay nanocomposites. in *Advances in Polymer Science* vol. 179 135–195 (2005).

50. Komadel, P. & Madejová, J. Acid activation of clay minerals. in *Developments in Clay Science* vol. 5 385–409 (Elsevier B.V., 2013).

51. Ahmad, M. B., Zin, W. M. & Yunus, W. Synthesis and Characterization of Silver/Clay/Starch Bionanocomposites by Green Method. *Aust. J. Basic Appl. Sci.* **4**, 2158–2165 (2010).

52. Sagar Nayak, P. & Singh, B. K. *Instrumental characterization of clay by XRF, XRD and FTIR. Bull. Mater. Sci* vol. 30 (2007).

53. Saha, K., Butola, B. S. & Joshi, M. Synthesis and characterization of chlorhexidine acetate drug-montmorillonite intercalates for antibacterial applications. *Appl. Clay Sci.* **101**, 477–483 (2014).

54. Meng, N., Zhou, N. L., Zhang, S. Q. & Shen, J. Controlled release and antibacterial activity chlorhexidine acetate (CA) intercalated in montmorillonite. *Int. J. Pharm.* **382**, 45–49 (2009).

55. Martins, M. G. *et al.* Synthesis and characterization of montmorillonite clay intercalated with molecular magnetic compounds. *J. Solid State Chem.* **228**, 99–104 (2015).

56. Liu, H. *et al.* Thermal degradation of organic matter in the interlayer clay-organic complex: A TG-FTIR study on a montmorillonite/12-aminolauric acid system. *Appl. Clay Sci.* **80–81**, 398–406 (2013).

57. Heller-Kallai, L. Thermally modified clay minerals. in *Developments in Clay Science* vol. 5 411–433 (Elsevier B.V., 2013).

58. Solhi, L. *et al.* Poly(acrylic acid) grafted montmorillonite as novel fillers for dental

adhesives: Synthesis, characterization and properties of the adhesive. *Dent. Mater.* **28**, 369–377 (2012).

59. Dowling, A. H. & Fleming, G. J. P. The impact of montmorillonite clay addition on the in vitro wear resistance of a glass-ionomer restorative. *J. Dent.* **35**, 309–317 (2007).

60. Xie, B. Creating Hierarchical Particle Assemblies as Enhanced Fillers for Dental Composite Materials. (University of Bristol, 2015).

61. Bellis, C. A., Nobbs, A. H., O'Sullivan, D. J., Holder, J. A. & Barbour, M. E. Glass ionomer cements functionalised with a concentrated paste of chlorhexidine hexametaphosphate provides dose-dependent chlorhexidine release over at least 14 months. *J. Dent.* **45**, 53–58 (2016).

62. Bellis, C. A. *et al.* Glass ionomer cements with milled, dry chlorhexidine hexametaphosphate filler particles to provide long-term antimicrobial properties with recharge capacity. *Dent. Mater.* **34**, 1717–1726 (2018).

63. Holder, J. Enhancing the Strength of Conventional Glass Ionomer Cements Using Nanomaterials. (University of Bristol, 2018).

64. Duroudier, J.-P. Ball and Rod Mills. in *Size Reduction of Divided Solids* 73–97 (2016).

65. DENTSPLY DeTrey ©. *ChemFil ® Superior Fast Setting Glass-Ionomer Restorative Material Directions for Use English*. (2005).

66. Duckworth, P. F., Rowlands, R. S., Barbour, M. E. & Maddocks, S. E. A novel flow-system to establish experimental biofilms for modelling chronic wound infection and testing the efficacy of wound dressings. *Microbiol. Res.* **215**, 141–147 (2018).

67. Kamarudin, Y., Skeats, M. K., Ireland, A. J. & Barbour, M. E. Chlorhexidine hexametaphosphate as a coating for elastomeric ligatures with sustained antimicrobial properties: A laboratory study. *Am. J. Orthod. Dentofac. Orthop.* **158**, e73–e82 (2020).

68. Takahashi, Y. *et al.* Antibacterial effects and physical properties of glass-ionomer cements containing chlorhexidine for the ART approach. *Dent. Mater.* **22**, 647–652 (2006).

69. Leung, D. *et al.* Chlorhexidine-releasing methacrylate dental composite materials.

Biomaterials **26**, 7145–7153 (2005).

70. Wood, N. J. *et al.* Chlorhexidine hexametaphosphate nanoparticles as a novel antimicrobial coating for dental implants. *J. Mater. Sci. Mater. Med.* **26**, (2015).

71. Wu, Y. *et al.* Long-term and controlled release of chlorhexidine-copper(II) from organically modified montmorillonite (OMMT) nanocomposites. *Mater. Sci. Eng. C* **33**, 752–757 (2013).

72. Michot, L. J. *et al.* Phase diagrams of wyoming Na-montmorillonite clay. Influence of particle anisotropy. *Langmuir* **20**, 10829–10837 (2004).

73. Sigma. *CHLORHEXIDINE DIGLUCONATE 20% Aqueous Solution Sigma Prod. No. C9394*. https://www.sigmaaldrich.com/content/dam/sigma-aldrich/docs/Sigma/Product_Information_Sheet/c9394pis.pdf.

74. Lavoine, N., Tabary, N., Desloges, I., Martel, B. & Bras, J. Controlled release of chlorhexidine digluconate using β-cyclodextrin and microfibrillated cellulose. *Colloids Surfaces B Biointerfaces* **121**, 196–205 (2014).

75. Rema, T., Lawrence, J. R., Dynes, J. J., Hitchcock, A. P. & Korber, D. R. Microscopic and Spectroscopic Analyses of Chlorhexidine Tolerance in Delftia acidovorans Biofilms. *Antimicrob. Agents Chemother.* **58**, 5673–5686 (2014).

76. Jung, H., Kim, H. M., Choy, Y. Bin, Hwang, S. J. & Choy, J. H. Laponite-based nanohybrid for enhanced solubility and controlled release of itraconazole. *Int. J. Pharm.* **349**, 283–290 (2008).

77. Misra, D. N. Interaction of chlsrhexidine digluconate with and adsorption of chlorhexidine on hydroxyapatite*. *J. Biomed. Mater. Res.* **28**, 1375–1381 (1994).

78. Roy, A. & Joshi, M. Enhancing antibacterial properties of polypropylene/Cu-loaded montmorillonite nanocomposite filaments through sheath–core morphology. *Polym. Int.* **67**, 917–924 (2018).

79. Ramadan, A. R., Esawi, A. M. K. & Gawad, A. A. Effect of ball milling on the structure of Na+-montmorillonite and organo-montmorillonite (Cloisite 30B). *Appl. Clay Sci.* **47**, 196–202 (2010).

80. Boaro, L. C. C. *et al.* Antibacterial resin-based composite containing chlorhexidine for dental applications. *Dent. Mater.* **35**, 909–918 (2019).

81. Zhao, Z., Fang, R., Rong, Q. & Liu, M. Bioinspired Nanocomposite Hydrogels with Highly Ordered Structures. *Adv. Mater.* **29**, 1703045: 1–16 (2017).

82. Scholz, M. *et al.* In vitro chlorhexidine release from alginate based microbeads for periodontal therapy. *PLoS One* **12**, 1–19 (2017).

83. Yang, F. *et al.* A Synthetic Hydrogel Composite with the Mechanical Behavior and Durability of Cartilage. *Adv. Funct. Mater.* **30**, 2003451: 1–8 (2020).

84. Surya, R., Mullassery, M. D., Fernandez, N. B. & Thomas, D. Synthesis and characterization of a clay-alginate nanocomposite for the controlled release of 5-Flurouracil. *J. Sci. Adv. Mater. Devices* **4**, 432–441 (2019).

85. Abasalizadeh, F. *et al.* Alginate-based hydrogels as drug delivery vehicles in cancer treatment and their applications in wound dressing and 3D bioprinting. *J. Biol. Eng.* **14**, 1–22 (2020).

86. Chan, E. S., Yim, Z. H., Phan, S. H., Mansa, R. F. & Ravindra, P. Encapsulation of herbal aqueous extract through absorption with ca-alginate hydrogel beads. *Food Bioprod. Process.* **88**, 195–201 (2010).

87. Chan, E. S. *et al.* Effects of starch filler on the physical properties of lyophilized calcium-alginate beads and the viability of encapsulated cells. *Carbohydr. Polym.* **83**, 225–232 (2011).

88. Zhang, H., Shi, Y., Xu, X., Zhang, M. & Ma, L. Structure Regulation of Bentonite-Alginate Nanocomposites for Controlled Release of Imidacloprid. *ACS Omega* **5**, 10068–10076 (2020).

89. Shawky, H. A. Improvement of water quality using alginate/montmorillonite composite beads. *J. Appl. Polym. Sci.* **119**, 2371–2378 (2011).

90. Barreca, S., Orecchio, S. & Pace, A. The effect of montmorillonite clay in alginate gel beads for polychlorinated biphenyl adsorption: Isothermal and kinetic studies. *Appl. Clay Sci.* **99**, 220–228 (2014).

91. Chan, E. S., Lee, B. B., Ravindra, P. & Poncelet, D. Prediction models for shape and size of ca-alginate macrobeads produced through extrusion-dripping method. *J. Colloid Interface Sci.* **338**, 63–72 (2009).

92. Chan, E. S. *et al.* Effect of formulation of alginate beads on their mechanical behavior and stiffness. *Particuology* **9**, 228–234 (2011).

93. Mørch, Ý. A., Donati, I., Strand, B. L. & Skjåk-Bræk, G. Effect of Ca2+, Ba2+, and Sr2+ on alginate microbeads. *Biomacromolecules* **7**, 1471–1480 (2006).

94. Ouwerx, C., Velings, N., Mestdagh, M. M. & Axelos, M. A. V. Physico-chemical properties and rheology of alginate gel beads formed with various divalent cations. *Polym. Gels Networks* **6**, 393–408 (1998).

95. Kaklamani, G., Cheneler, D., Grover, L. M., Adams, M. J. & Bowen, J. Mechanical properties of alginate hydrogels manufactured using external gelation. *J. Mech. Behav. Biomed. Mater.* **36**, 135–142 (2014).

96. Moe, S. T., Draget, K. I., Skjåk-Bræk, G. & Simdsrød, O. Temperature dependence of the elastic modulus of alginate gels. *Carbohydr. Polym.* **19**, 279–284 (1992).

97. Patel, P., Van Duijneveldt, J. & Bartlett, P. Reinforcing Polyanion Networks with Clay Particles. (University of Bristol, 2018).

98. Rodriguez, F., Patel, S. K. & Cohen, C. Measuring the Modulus of a Sphere by Squeezing between Parallel Plates. *J. Appl. Polym. Sci.* **40**, 285–295 (1990).

99. Parry, R. M., Van Duijneveldt, J. & Bartlett, P. Investigation into Surface Area and Dye Adsorption Capacity of Montmorillonite-Polymer Hydrogels. (University of Bristol, 2020).

100. Wang, C. X., Cowen, C., Zhang, Z. & Thomas, C. R. High-speed compression of single alginate microspheres. *Chem. Eng. Sci.* **60**, 6649–6657 (2005).

Chapter 8 Appendix

8.1 Mechanical testing Exclusion Criteria for Chapter 3

In the preparation of dental cements, exclusion criteria were used to reject any specimens unsuitable to be considered in the mechanical testing data collection. The first check-up consisted in inspecting thoroughly every specimen individually for evidence of any visible folding, cracks or voids, in case of finding one or more of these imperfections they got automatically rejected.

Furthermore, any specimens which were visually acceptable prior to the mechanical testing but exhibit irregular load-displacement curves, such as those shown in Figure 8.1c and Figure 8.1d were rejected too, it can be seen how the specimens were inconsistently breaking. In order to be accepted the curve should look like in Figure 8.1a and Figure 8.1b, where the increment occurs gradually and smoothly until reach the breaking point and starts decreasing, this reflects that the material was successfully mixed and packed and hence the measurements obtained could not be affected by any other factor but the force applied to make the specimen collapse.
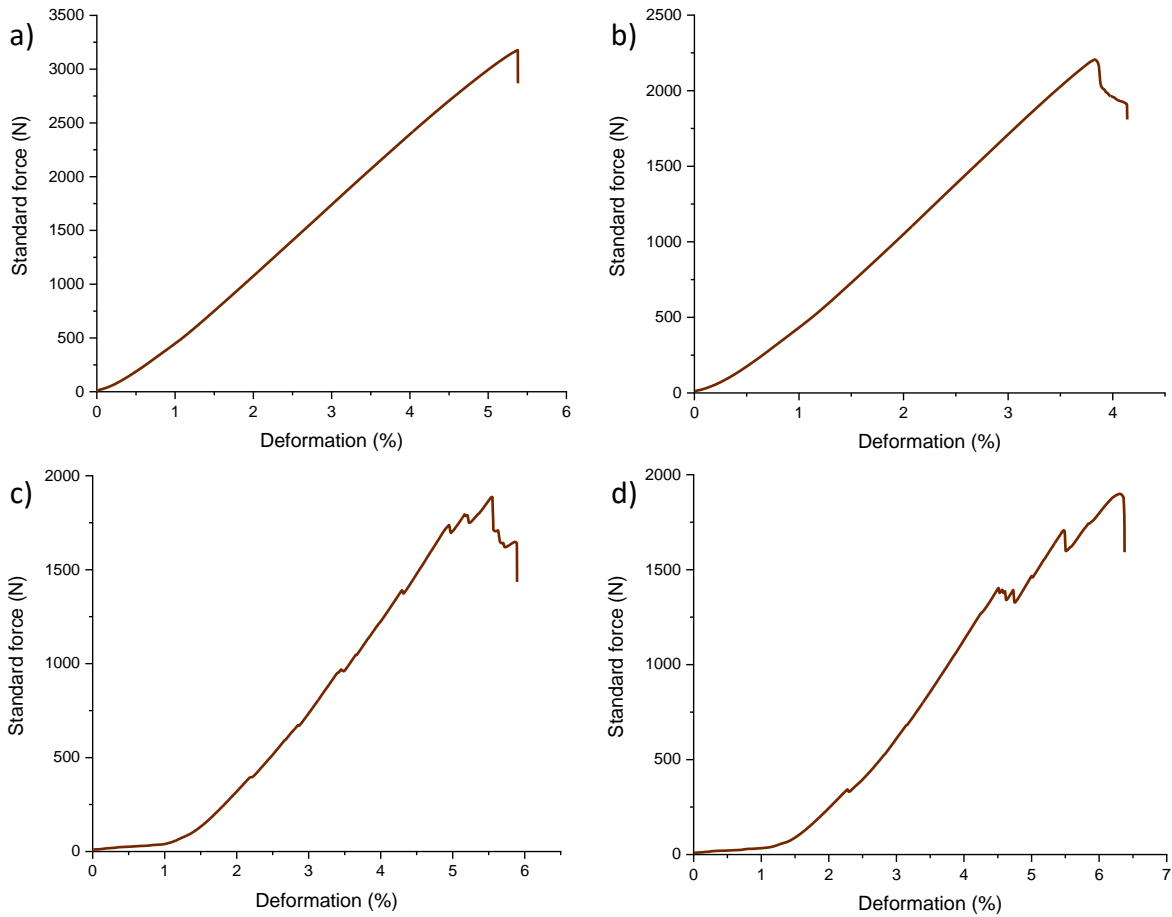
Figure 8.1 Curves extracted from the Universal Test Machine software. a) and b) Specimens accepted after CS test; c) and d) Specimens rejected after CS test.

8.2 Detailed information about Chapter 5 samples

Table 8.1. Colour change variation observed within the different samples.

Sample	Colour
Alginate	Transparent
Alg+MMT	Sand/grey subtone
Alg+MMT ADA HCl	White/light grey subtone
Alg+MMT AHA HCl	White/cream subtone
Alg+MMT GABA HCl	Sand/Cream subtone
Alg+MMT 1.2 CHX	Cream

Table 8.2. Characteristics of six hydrogel samples.

Sample	Dispersion				Bead		Disc		Return to original shape after XRD analysis
	Sediment	Flow	Appearance	Redispersion	Sediment	Appearance	Sediment	Appearance	
Alginate	×	+/+	▪ Easy to handle	×	×	▪ Consistent shape and size	×	▪ Did not get the shape of the mould. ▪ Easy to manipulate to fit in the XRD sample holder.	+/-
Alg+MMT	×	+/-	▪ Must be handled quickly and carefully to avoid imperfections in the final shape.	×	×	▪ Some spheres presented irregular shape	×	▪ Hard to press into the XRD sample holder.	✓
Alg+MMT ADA HCl	✓	-/+	▪ Thick but still fluid therefore easier to handle than Alg+MMT.	✓	×	▪ Consistent shape and size but small	×	▪ Maintained the size of the original mould ▪ Fitted in the XRD sample holder.	N/A
Alg+MMT AHA HCl	✓	-/+	▪ Similar to Alg+MMT ADA but less runny.	✓	×	▪ Consistent shape and size	×	▪ A bit hard to press into XRD sample holder.	×
Alg+MMT GABA HCl	×	-/-	▪ Very thick and "sticky"	×	×	▪ Beads looked "fluffy"	×	▪ Needed to be pressed into the XRD sample holder but easy to do so.	-/+
Alg+MMT 1.2 CHX	✓	+/-	▪ Not as thick as Alg+GABA but also seemed "sticky". ▪ If stirred vigorously it forms foam therefore bubbles in the final shape.	✓	×	▪ Beads had to be picked carefully as some had bubbles.	✓	▪ The disc resulted not being very tall and presented an obvious layer of sediment.	N/A

8.2.1 SEM Images

8.2.1.1 Freeze dried gel samples

| 1 μm | 5 μm | 10 μm |

SED   15.0kV   WD10.4mm   High-P.C.10.0   HighVac.   x100   100um
University of Bristol   Chemical Imaging Facility

100 μm
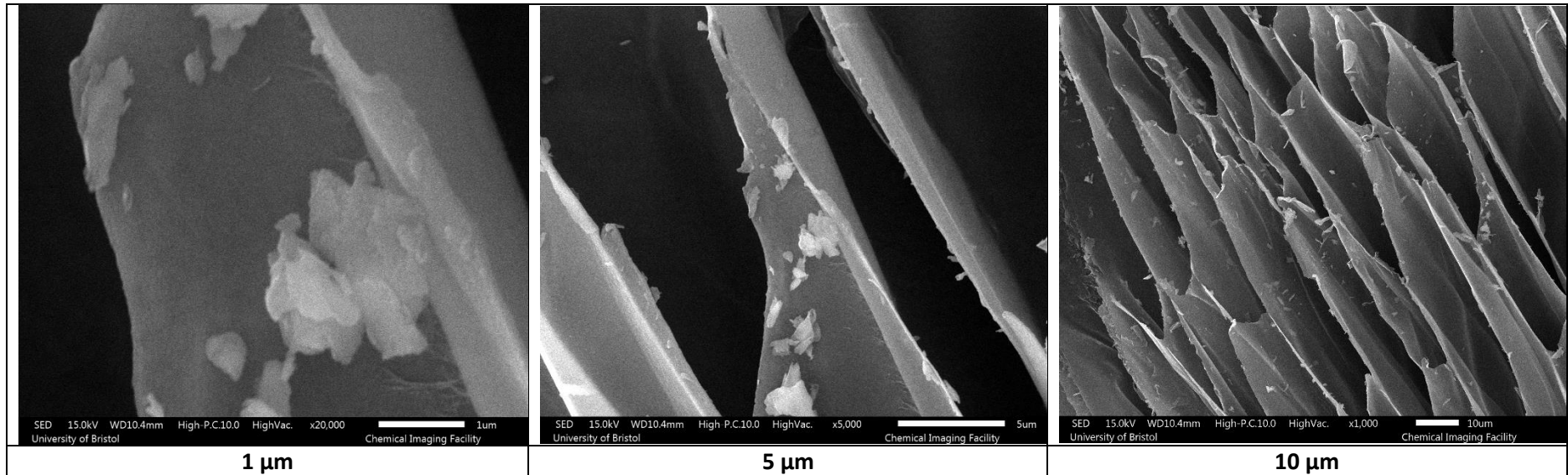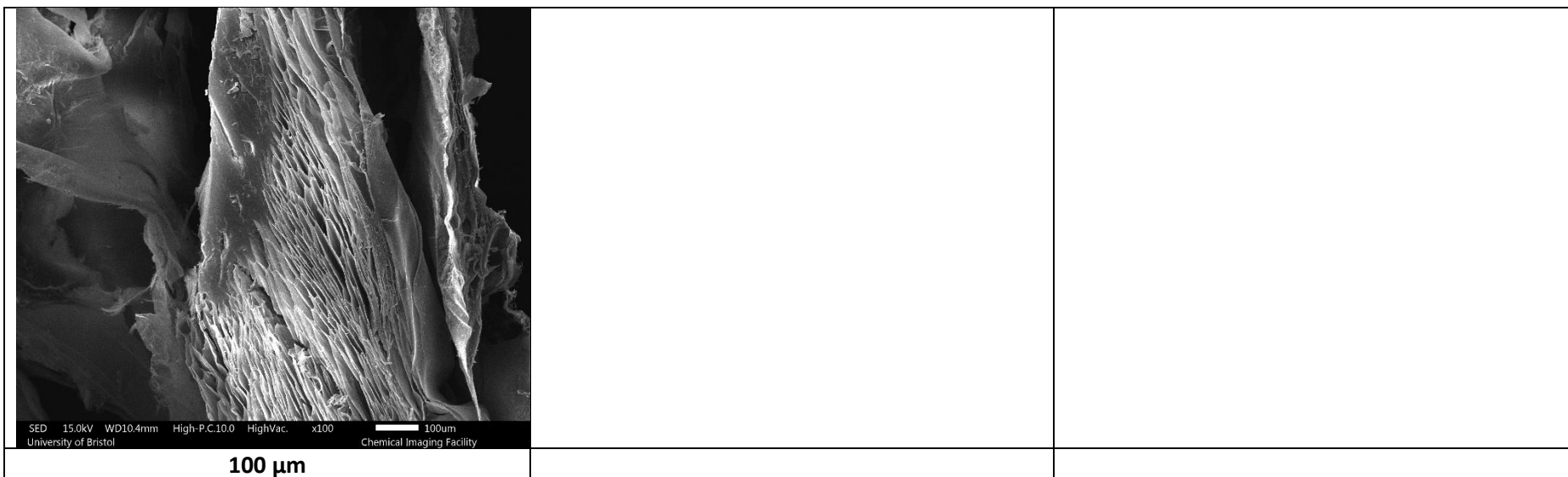
Figure 8.2. SEM images of Alginate (Alg) sample – Cross section.

| 1 μm | 5 μm | 10 μm |
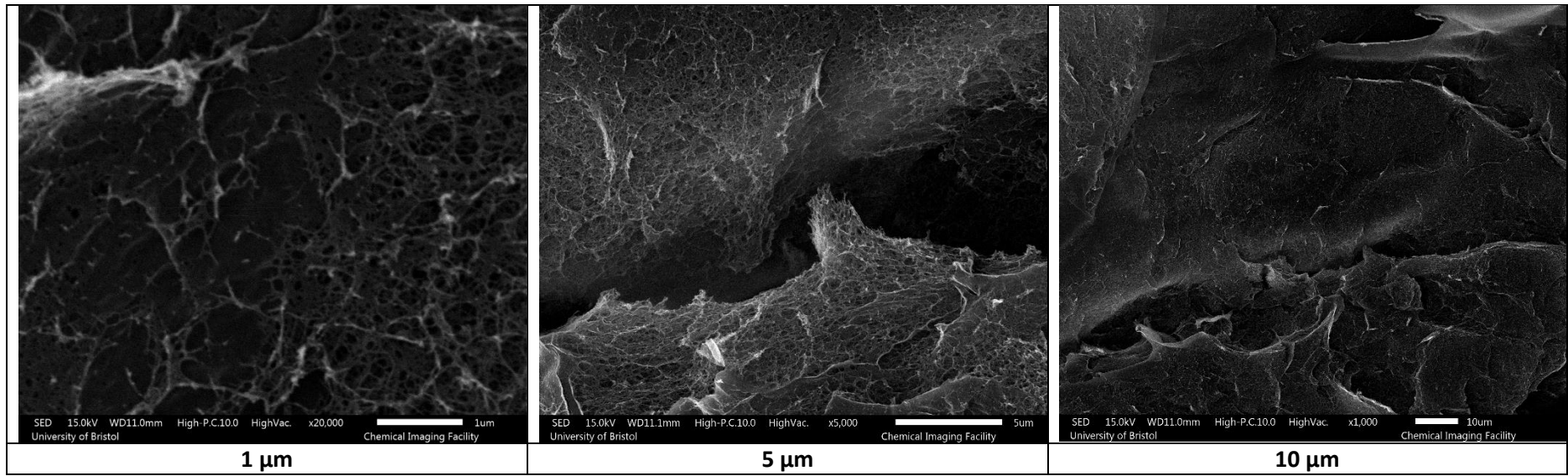
Figure 8.3. SEM images of Alginate (Alg) sample – Top down.

| 1 μm | 5 μm | 10 μm |

| 100 μm | | |
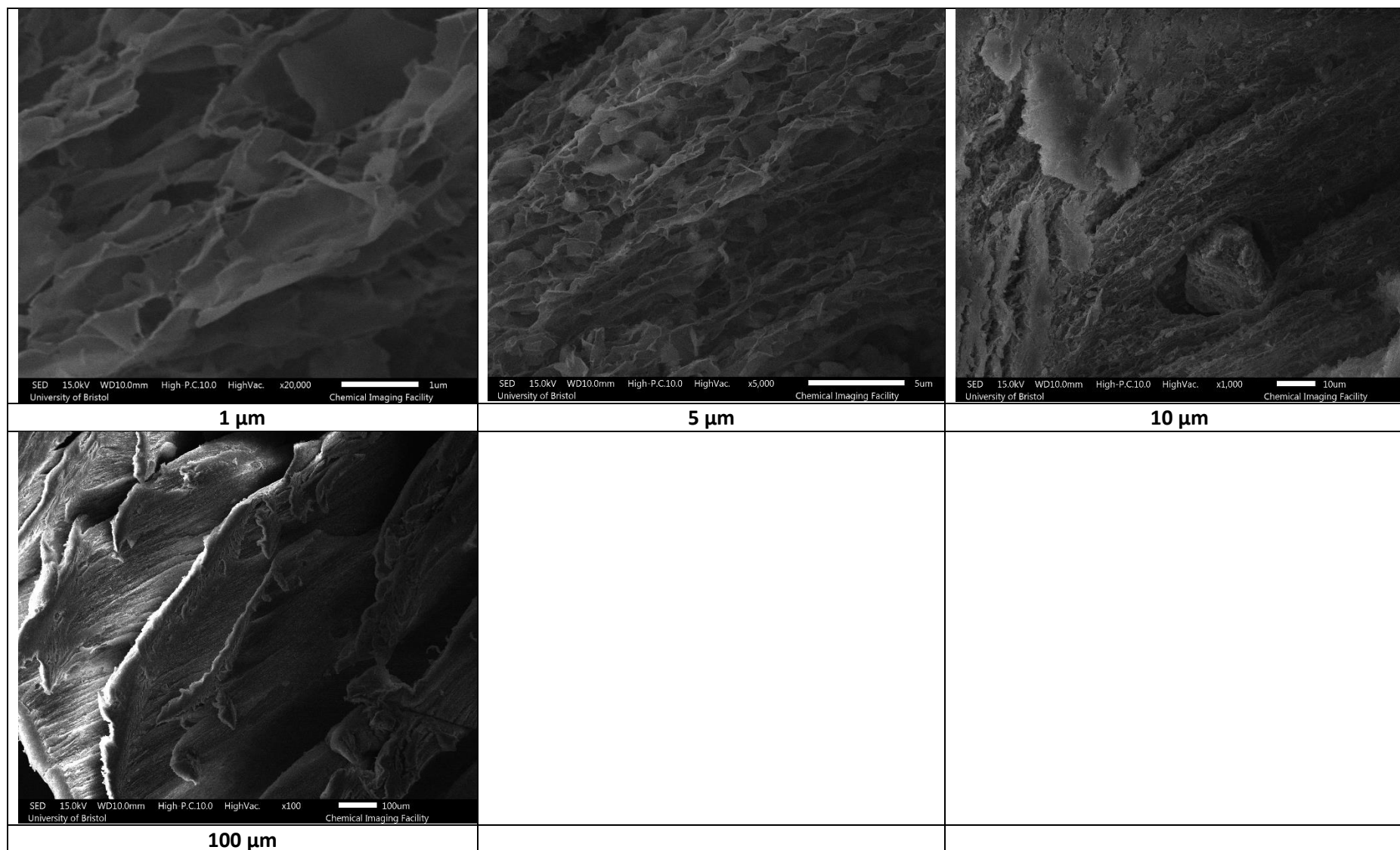
Figure 8.4. Alginate (Alg) + clay (MMT) sample – Cross section.

5 μm

10 μm

100 μm

10 μm

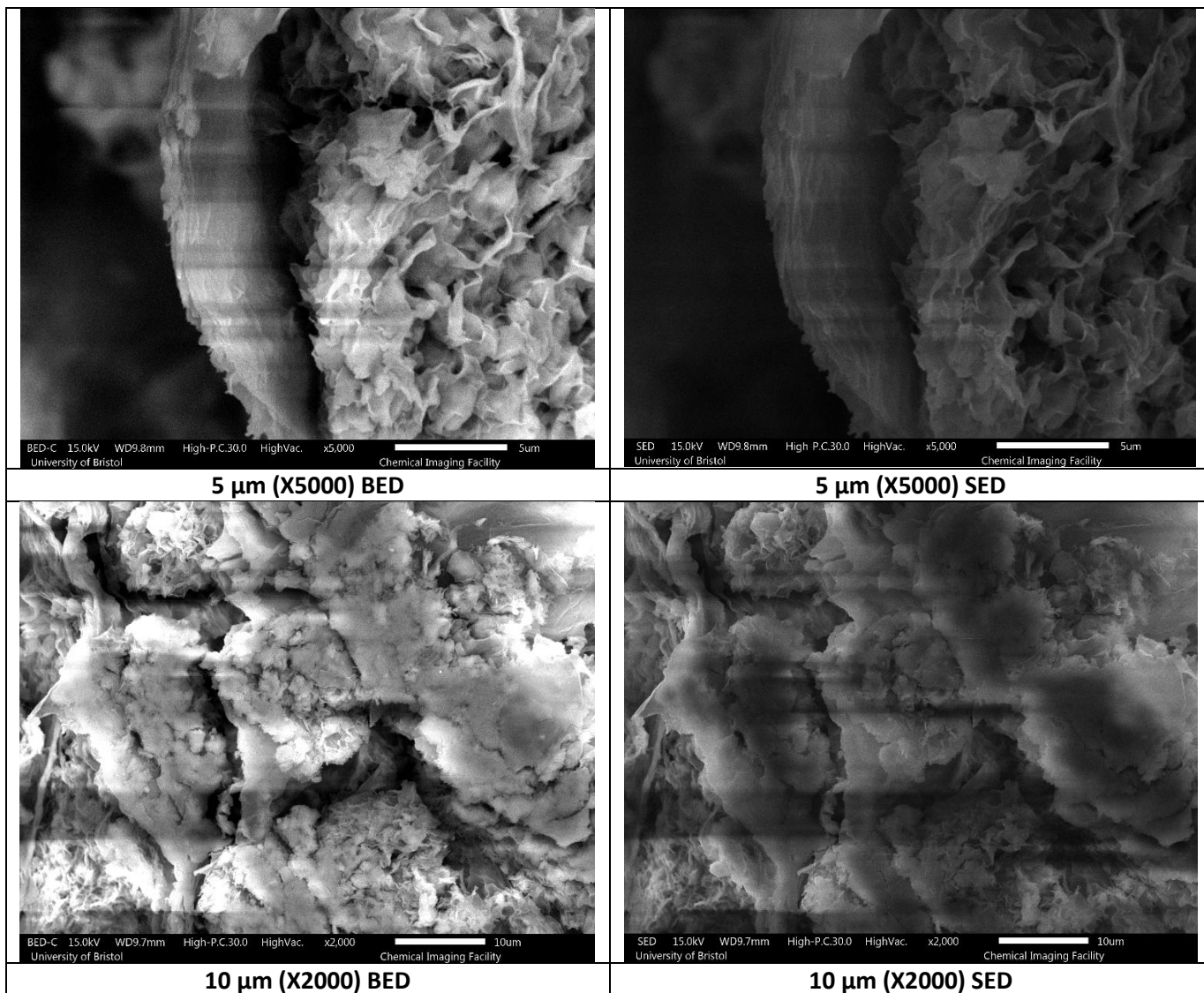**10 μm BED**

10 μm SED

| 5 μm BED | 5 μm SED | |
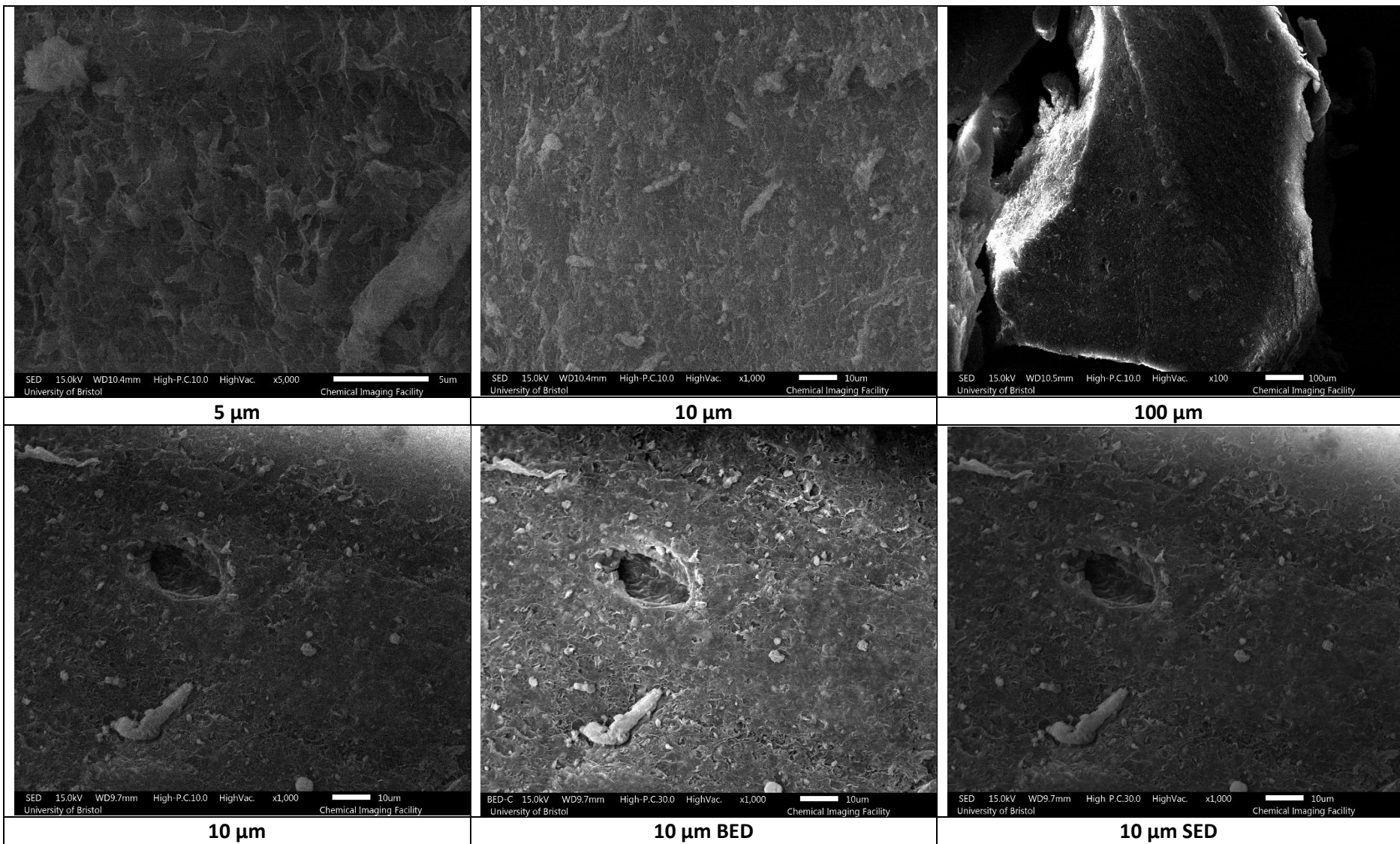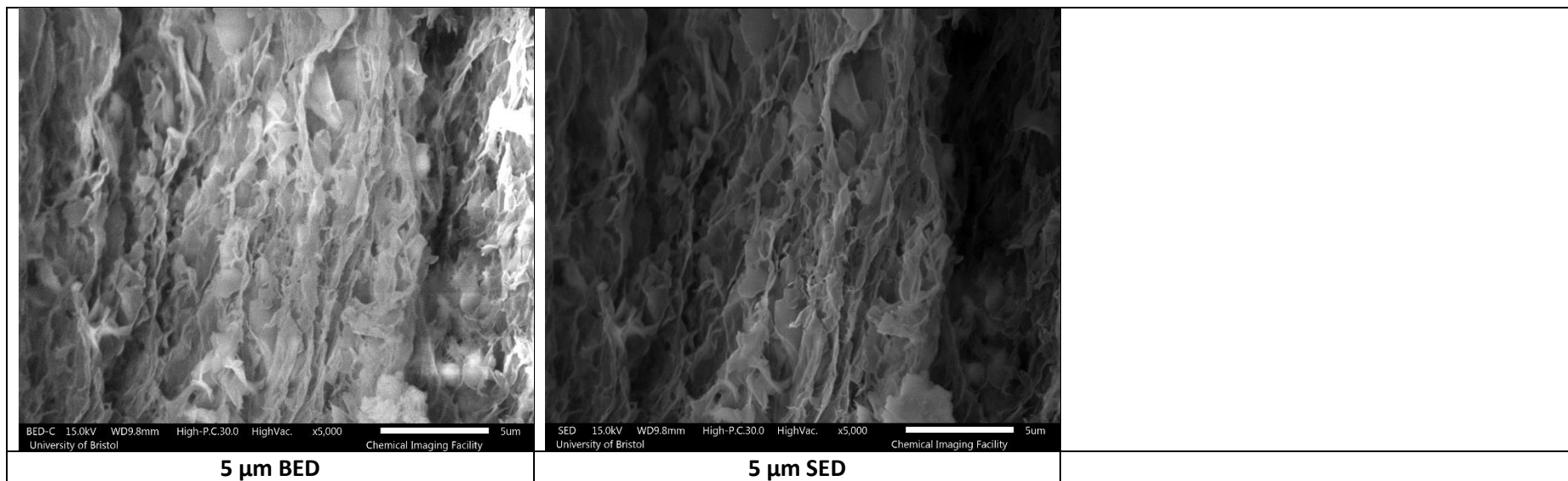
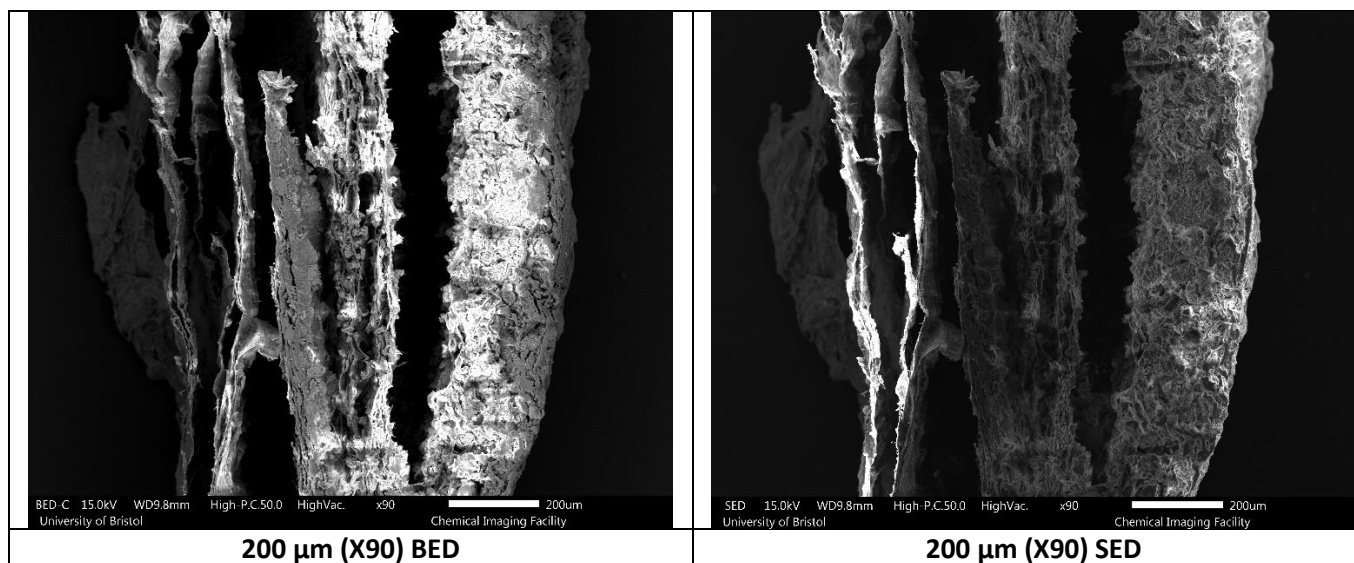*Figure 8.5. SEM images of Alginate (Alg) + clay (MMT) sample – Top down.*
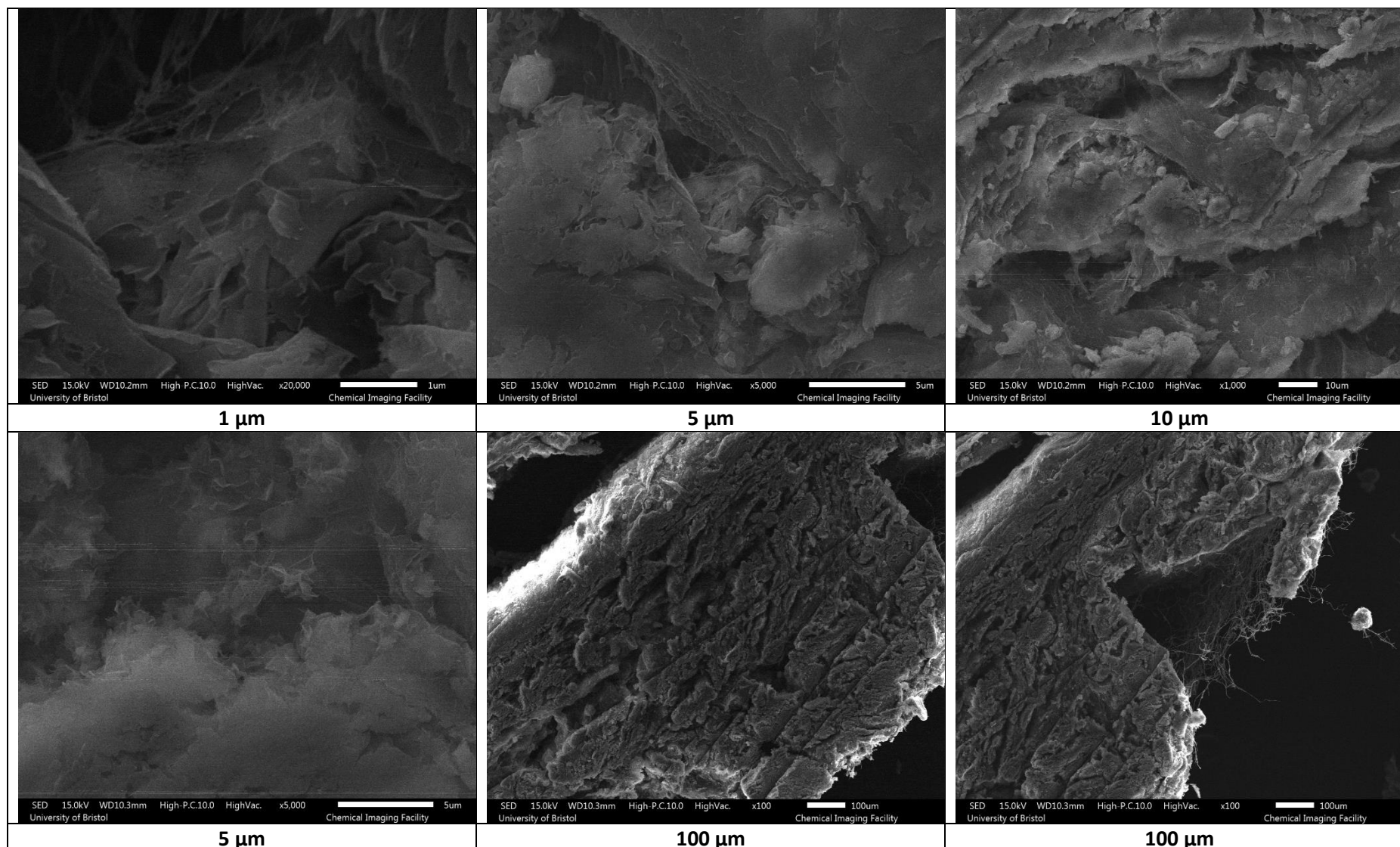
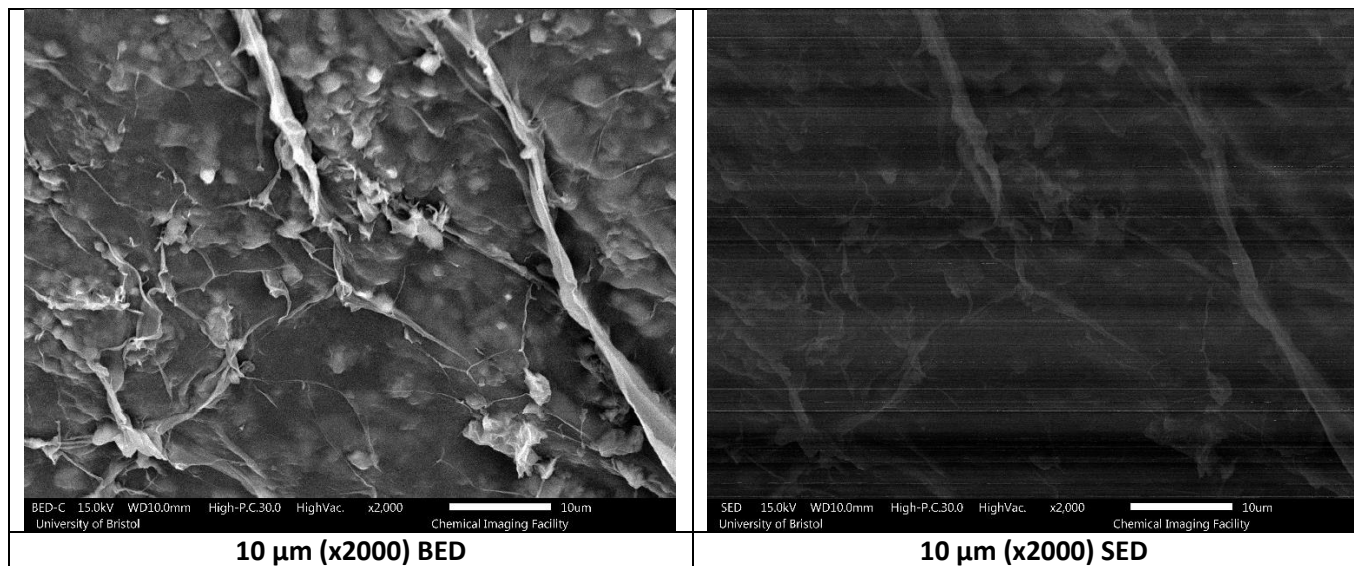*Figure 8.6. SEM images of Alginate (Alg) + modified clay (MMT ADA HCl) sample – Cross section.*
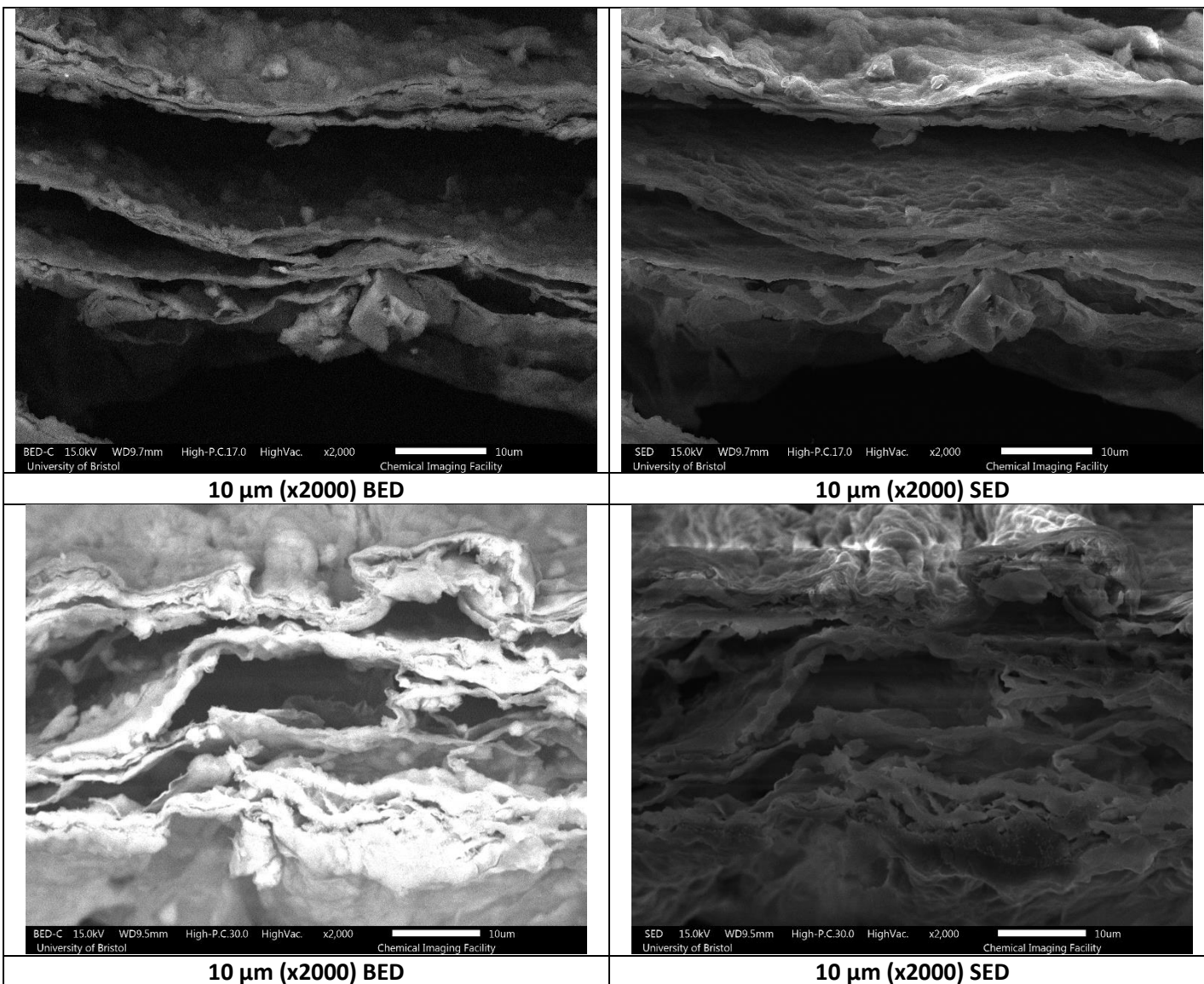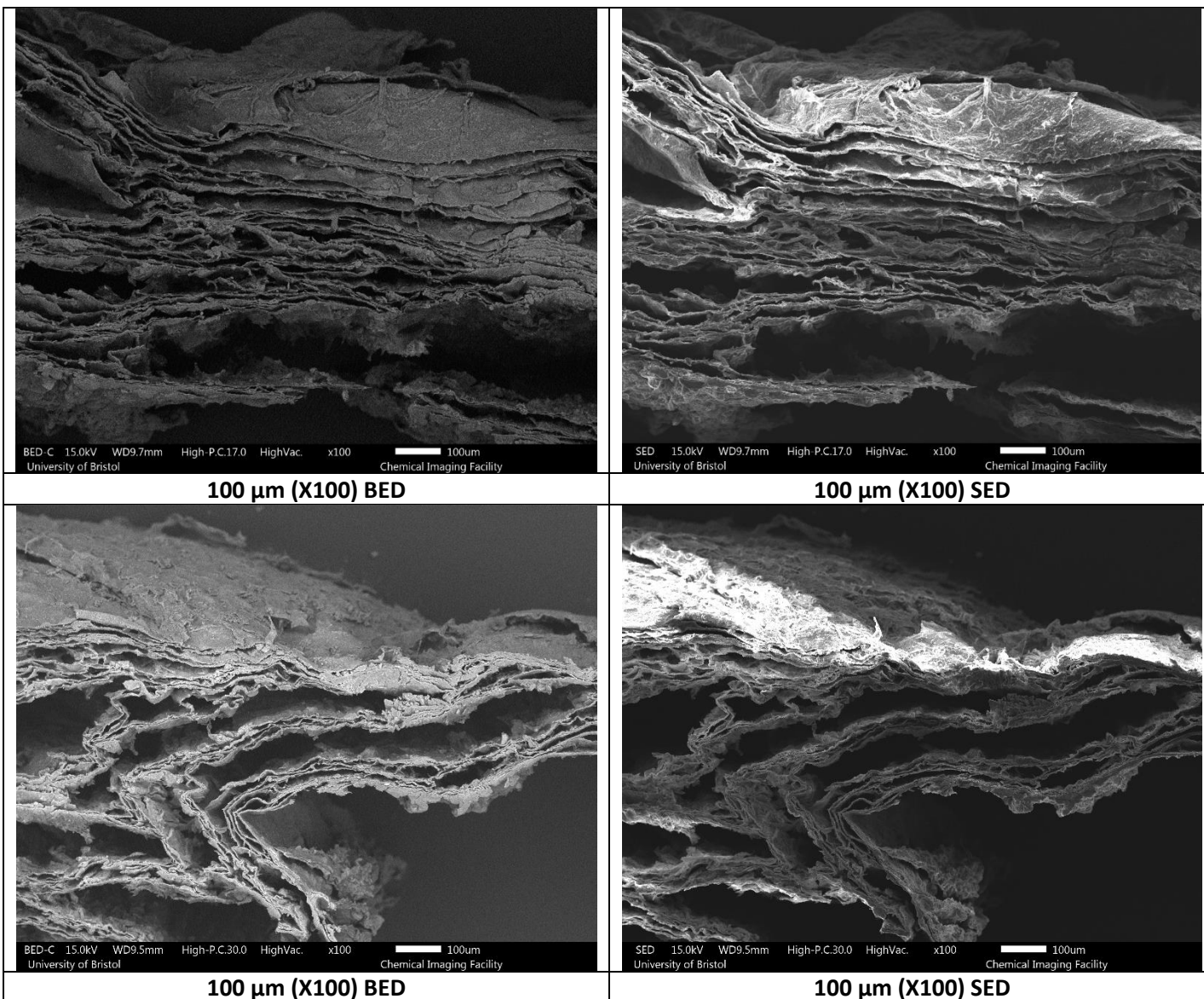
1 μm

5 μm

10 μm

100 μm
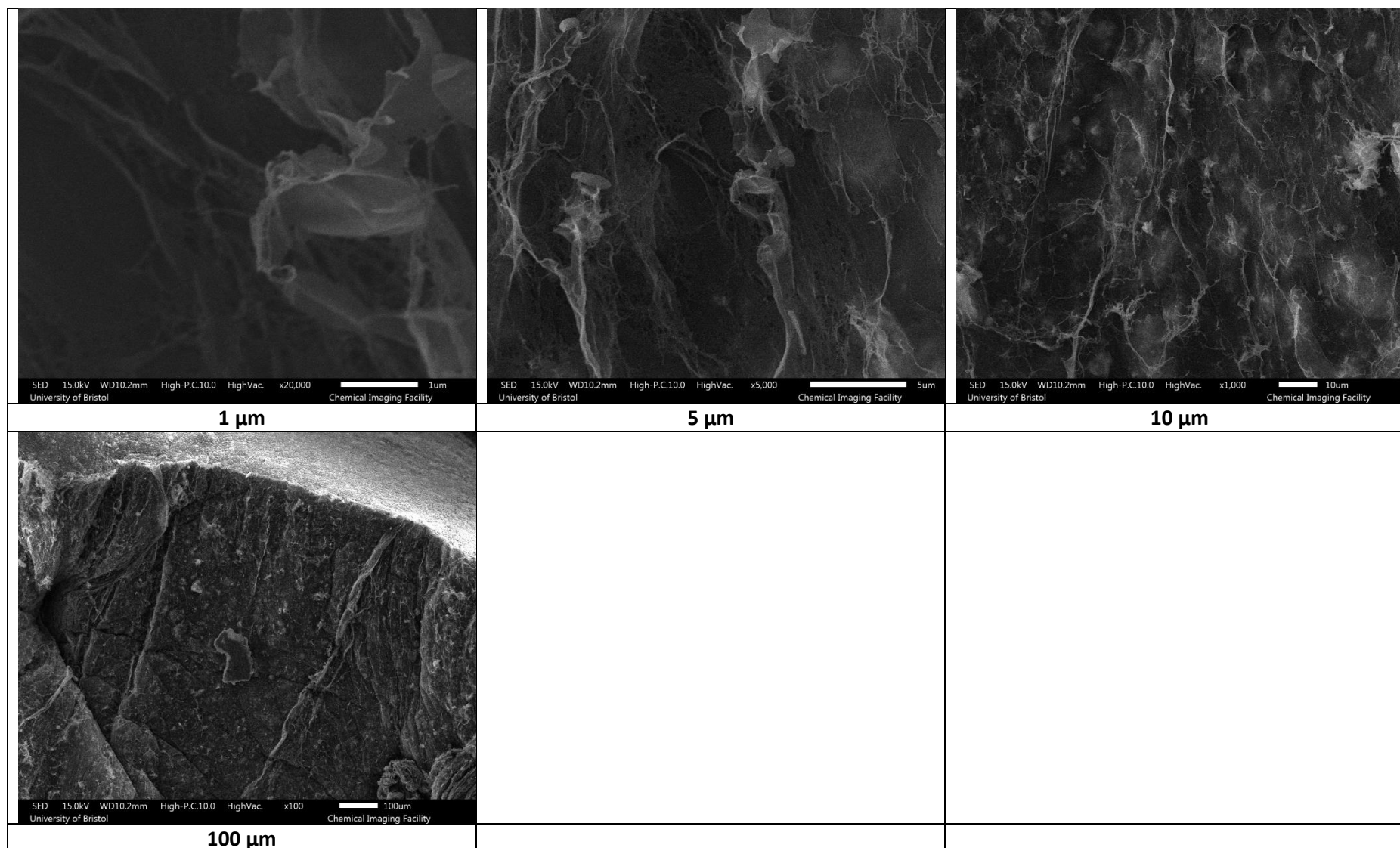
Figure 8.7. SEM images of Alginate (Alg) + modified clay (MMT ADA HCl) sample – Top down.

1 μm

5 μm

10 μm

100 μm

1 μm

5 μm

10 µm	100 µm	
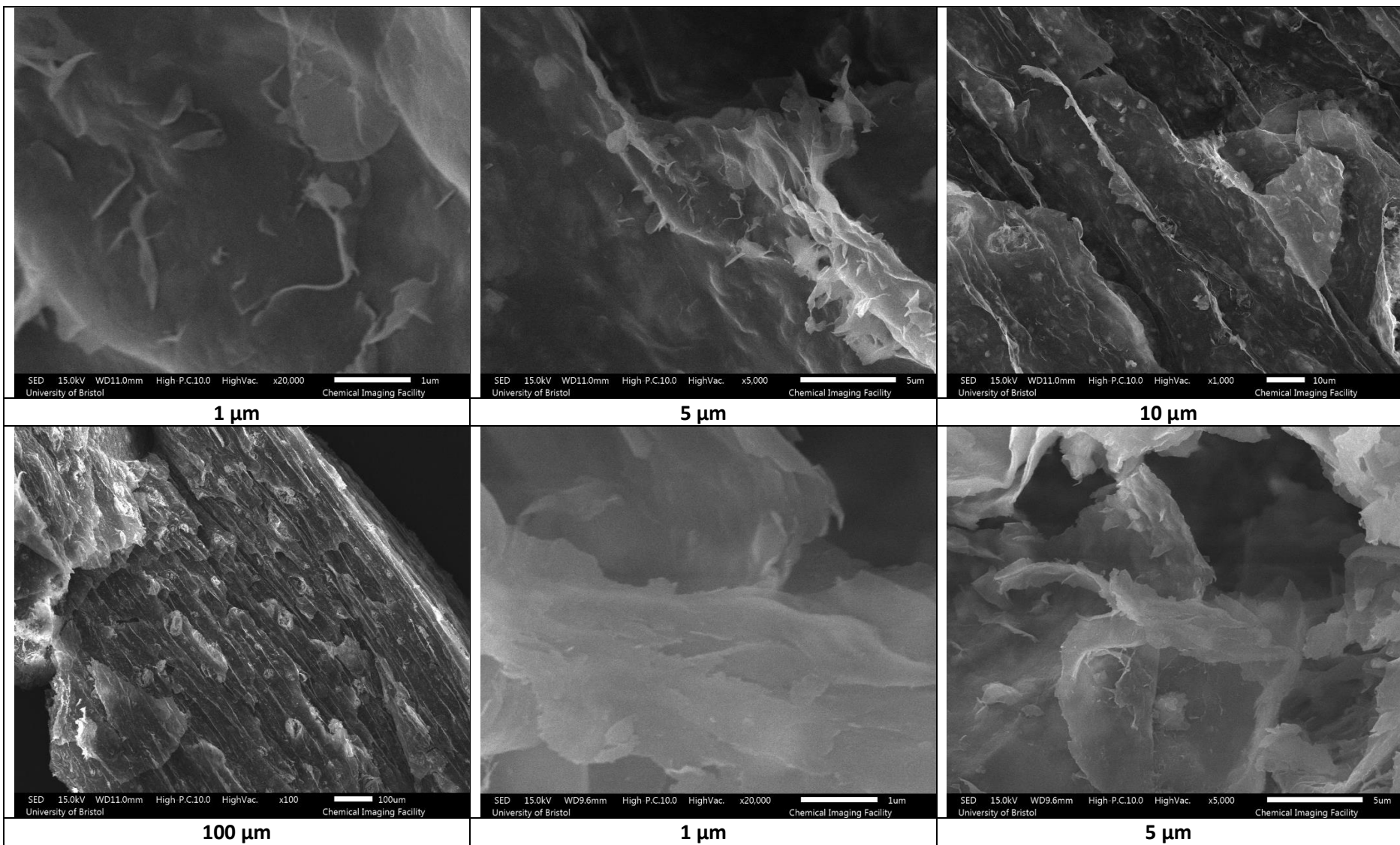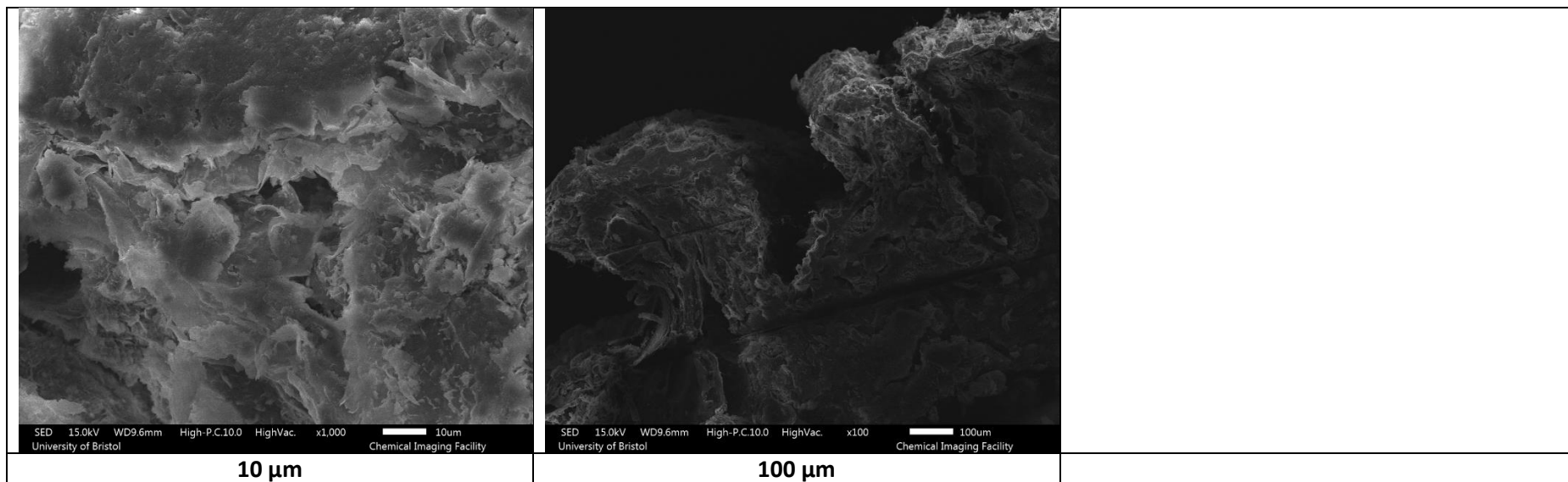
Figure 8.8. SEM images of Alginate (Alg) + modified clay (MMT AHA HCl) sample – Cross section.

1 µm	**5 µm**	**10 µm**
100 µm		
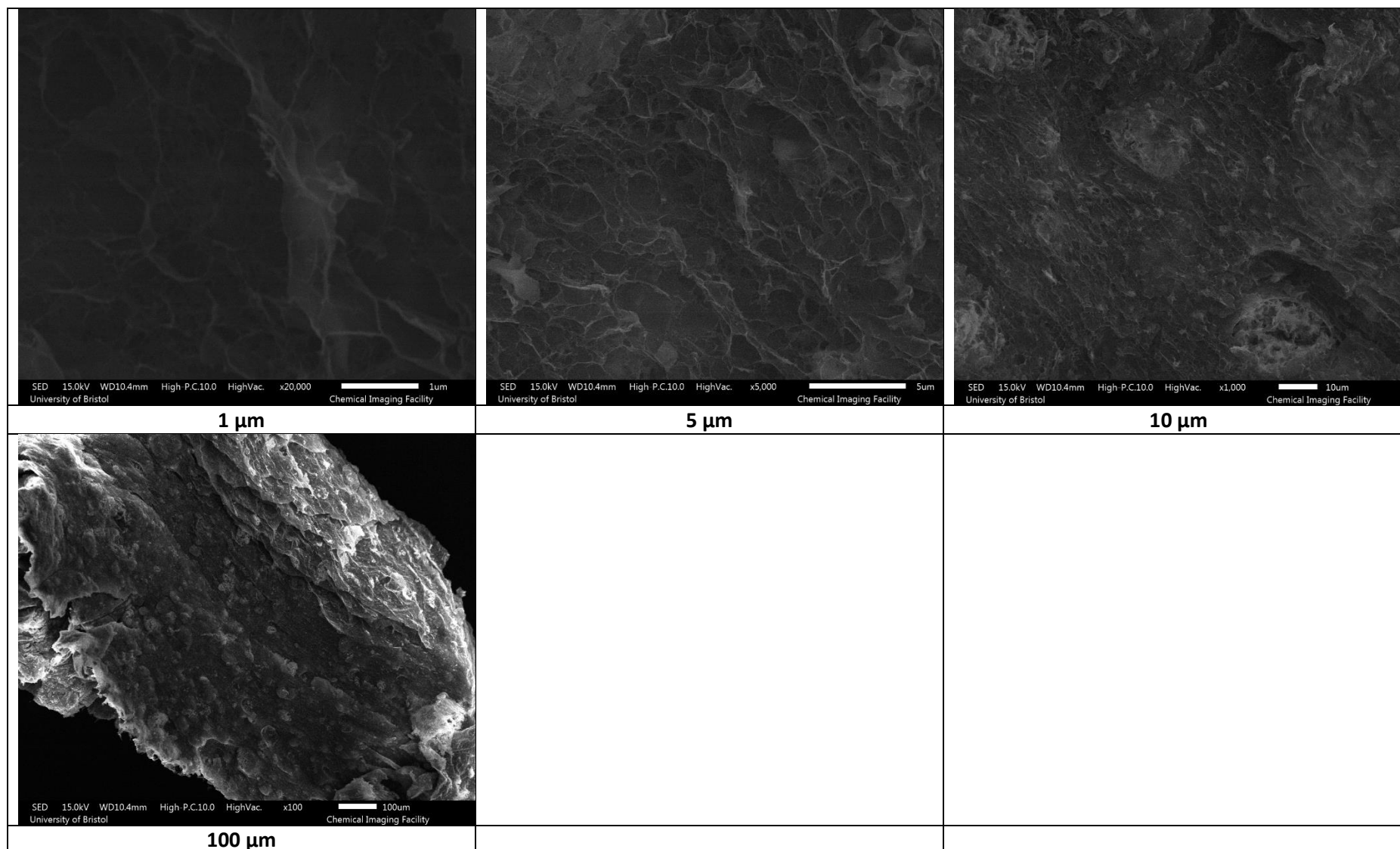
Figure 8.9. SEM images of Alginate (Alg) + modified clay (MMT AHA HCl) sample – Top down..

161

| **1 μm** | **5 μm** | **10 μm** |

| **100 μm** | | |
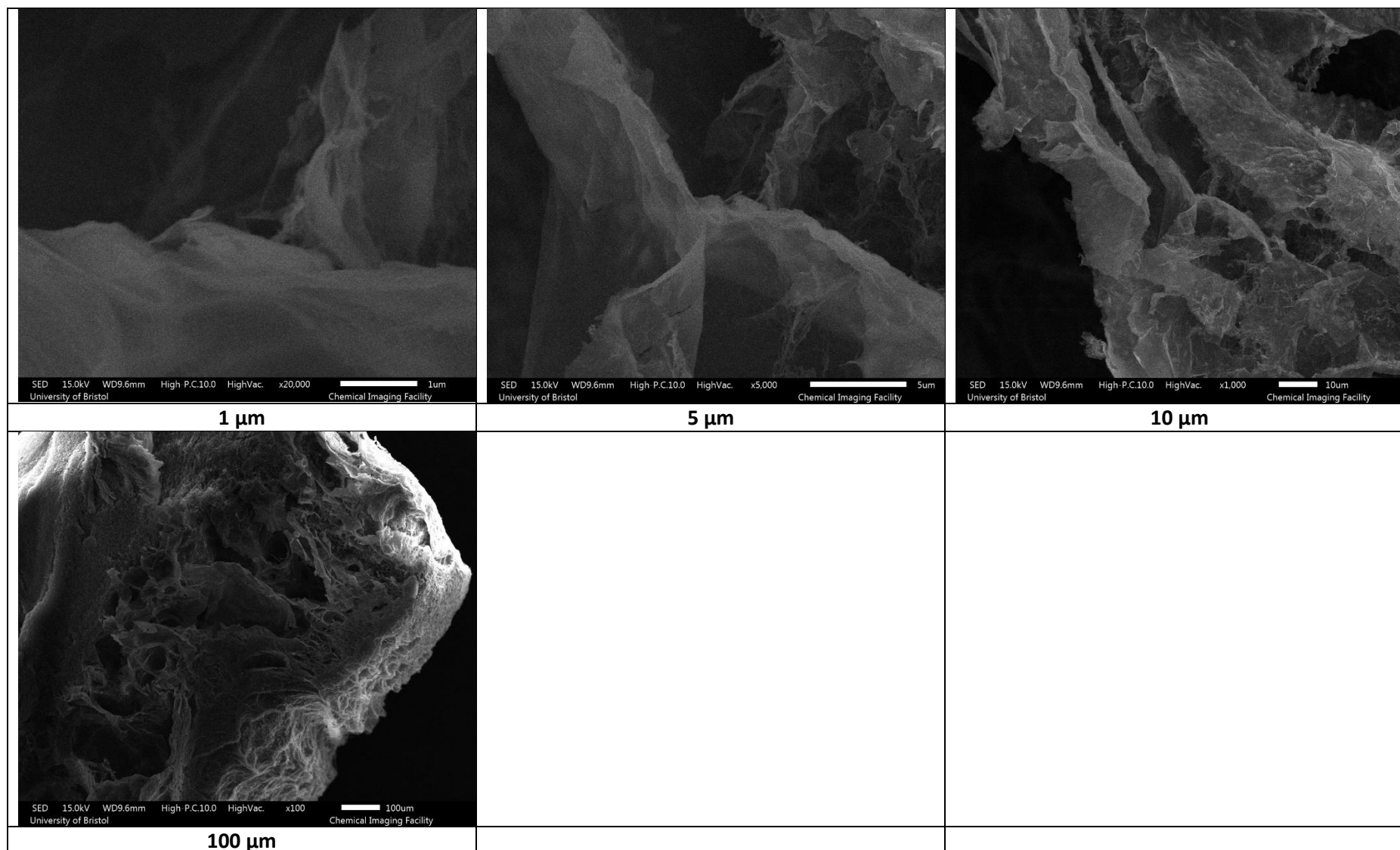
Figure 8.10. SEM images of Alginate (Alg) + modified clay (MMT GABA HCl) sample – Cross section.

| **1 µm** | **5 µm** | **10 µm** |

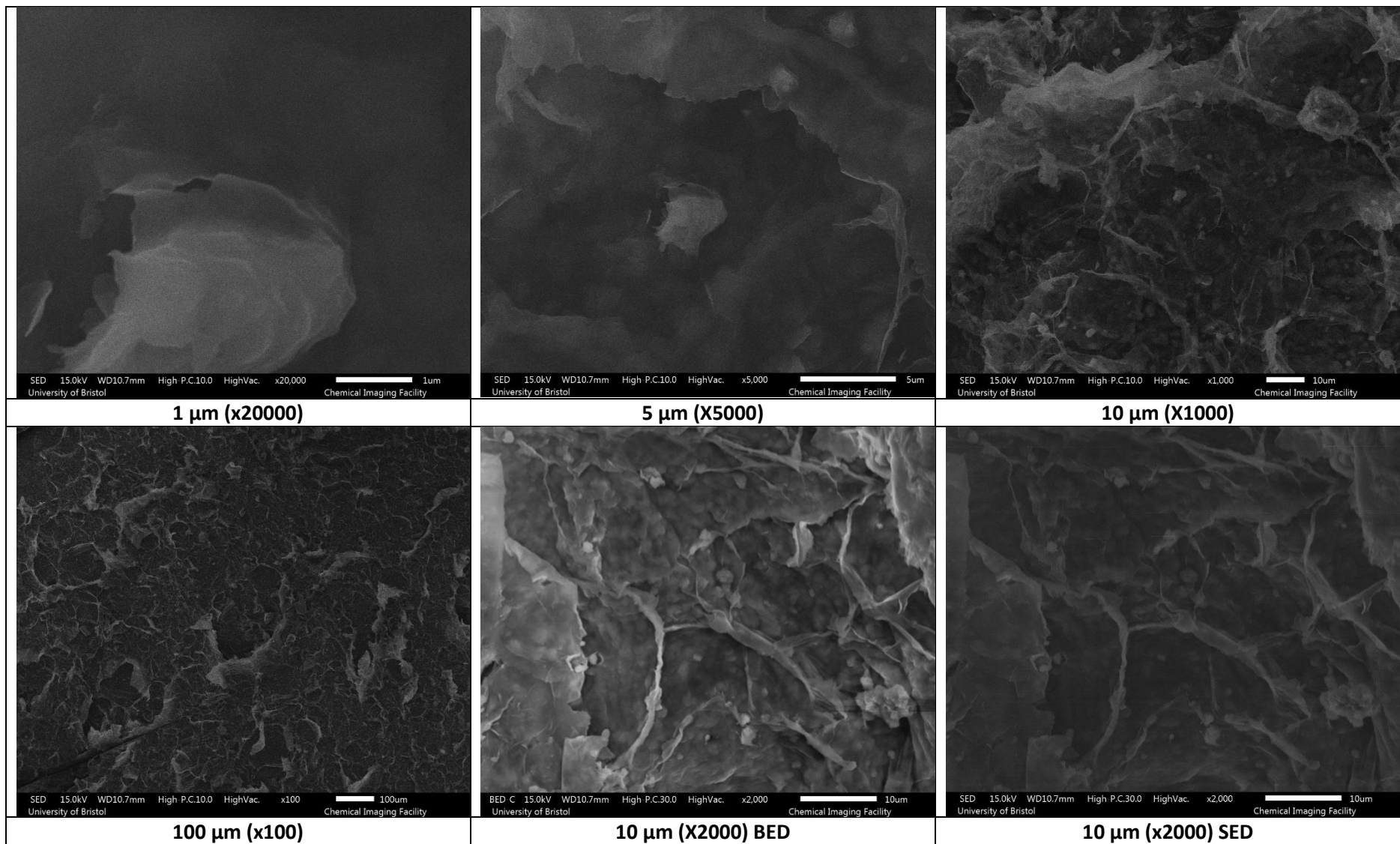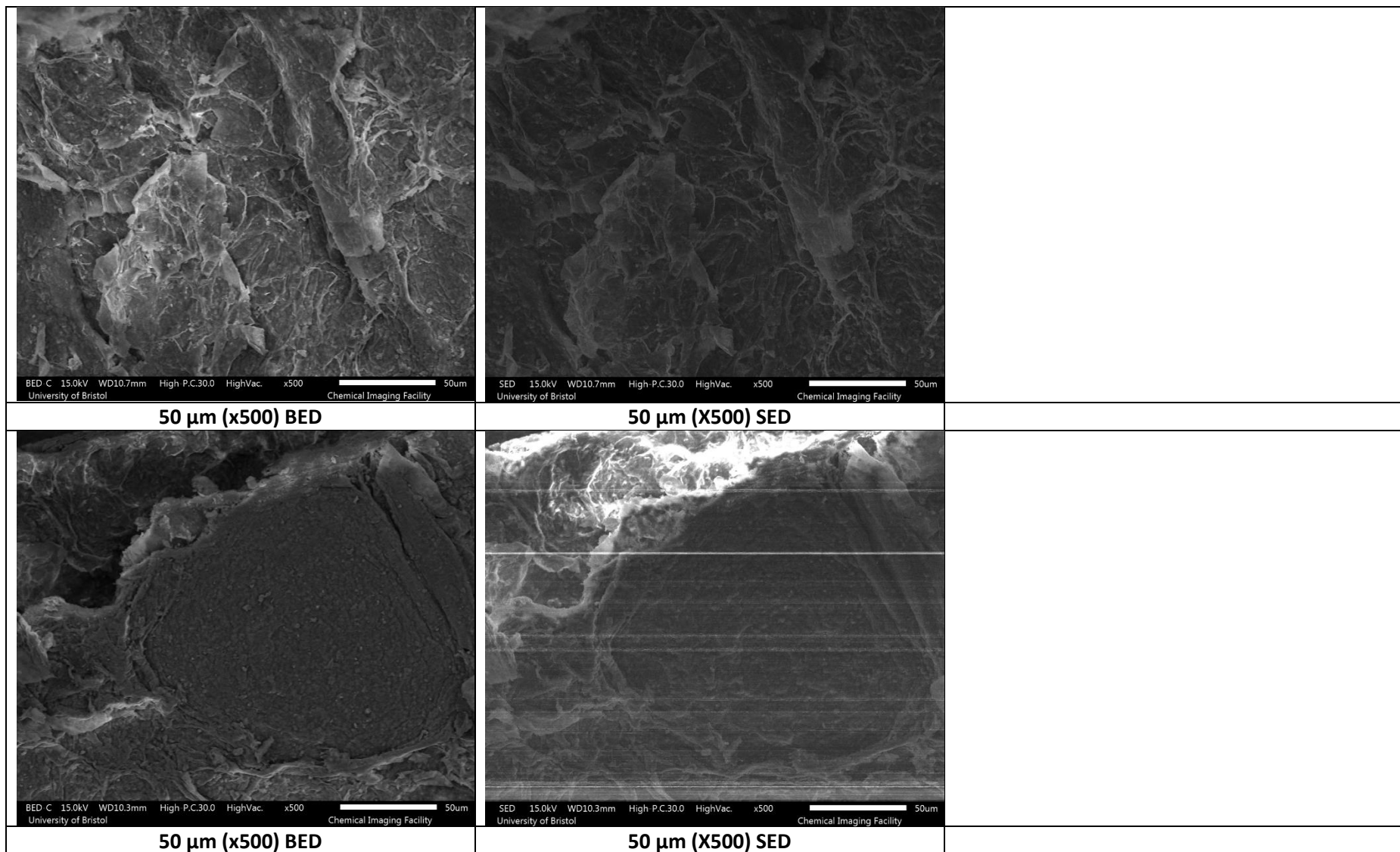| **100 µm** | | |
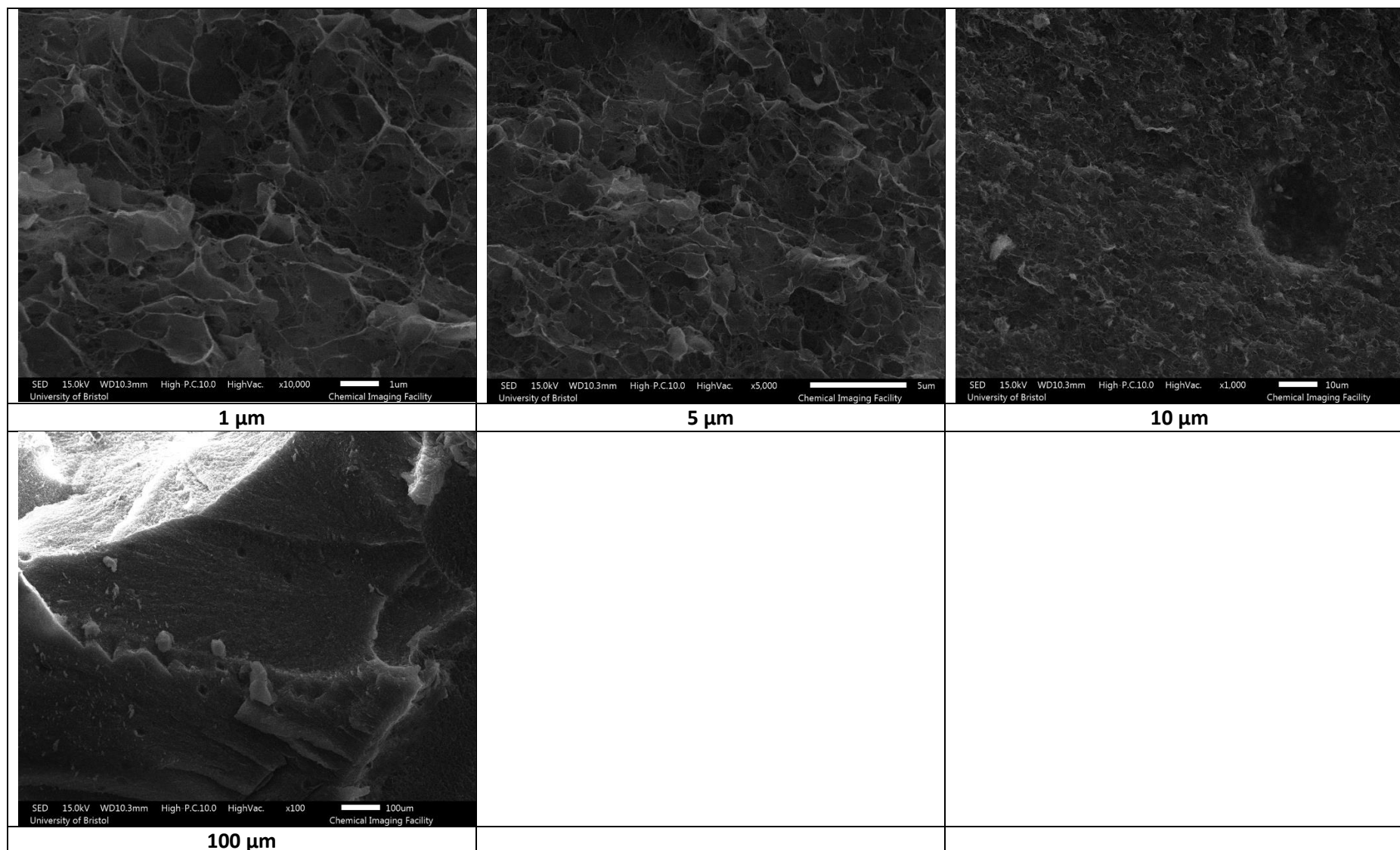
Figure 8.11. SEM images of Alginate (Alg) + modified clay (MMT GABA HCl) sample – Top down.

| 1 µm | 5 µm | 10 µm |
| 100 µm | 10 µm | 100 µm |

100 µm
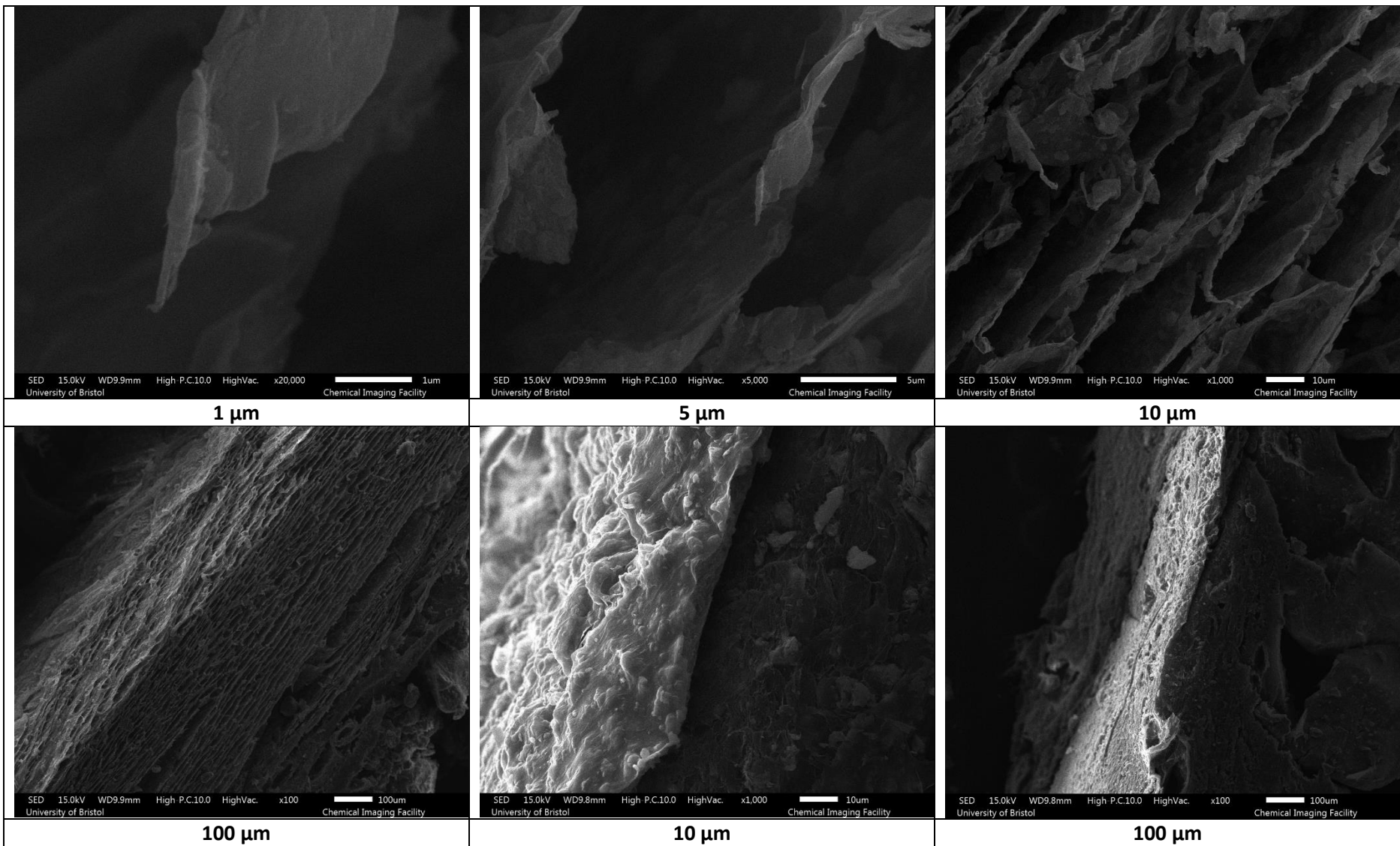
Figure 8.12. SEM images of Alginate (Alg) + modified clay (MMT CHX) sample – Cross section.

1 μm

10 μm

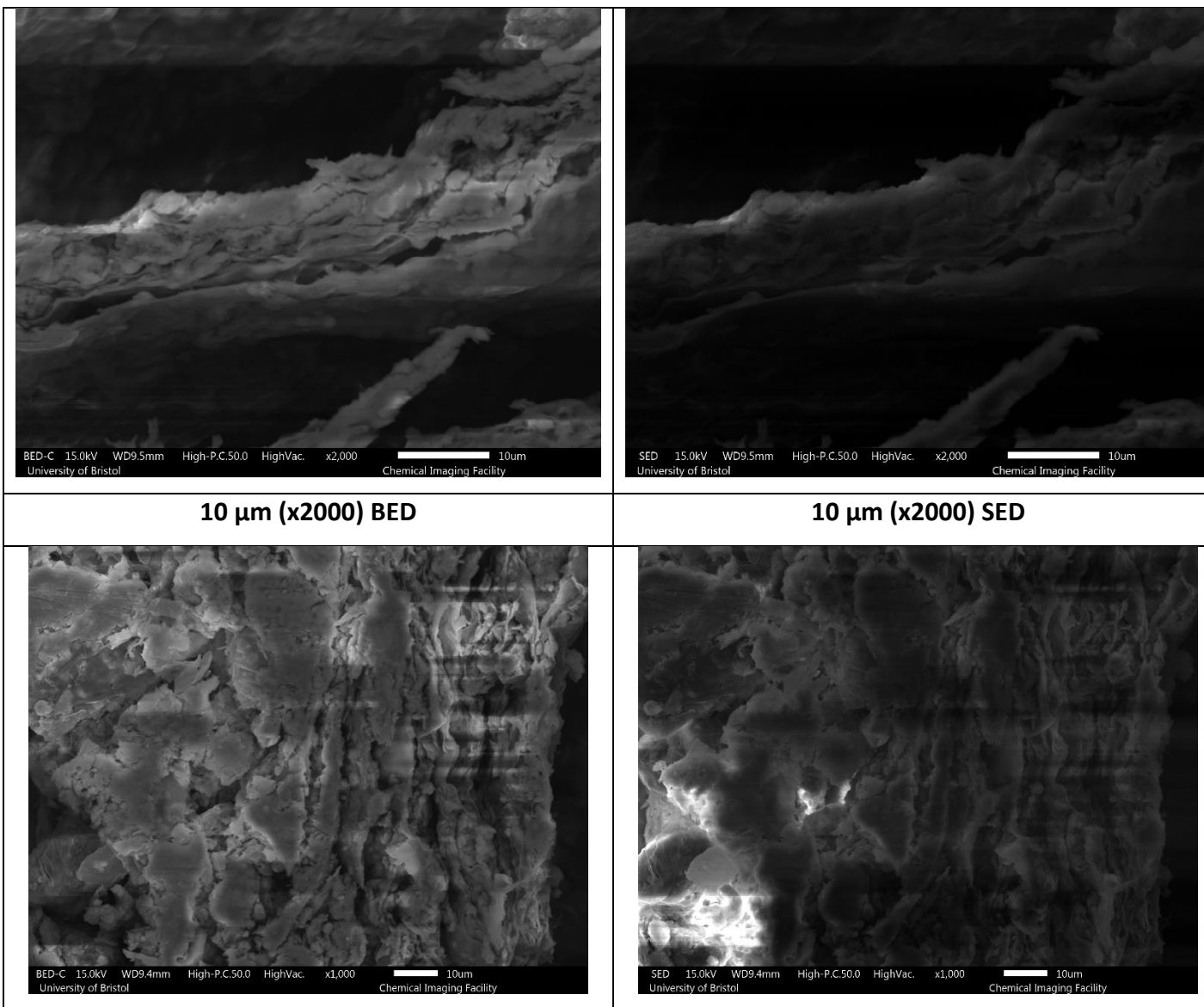**100 μm**
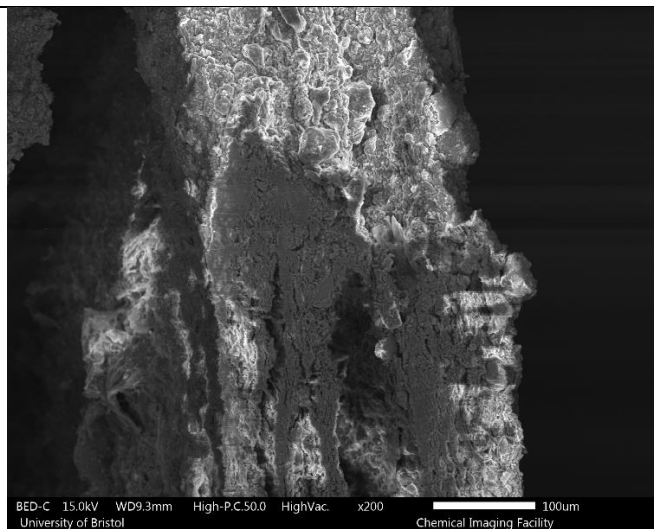
5 μm (X5000)

10 μm (X1000)

100 μm (x100)
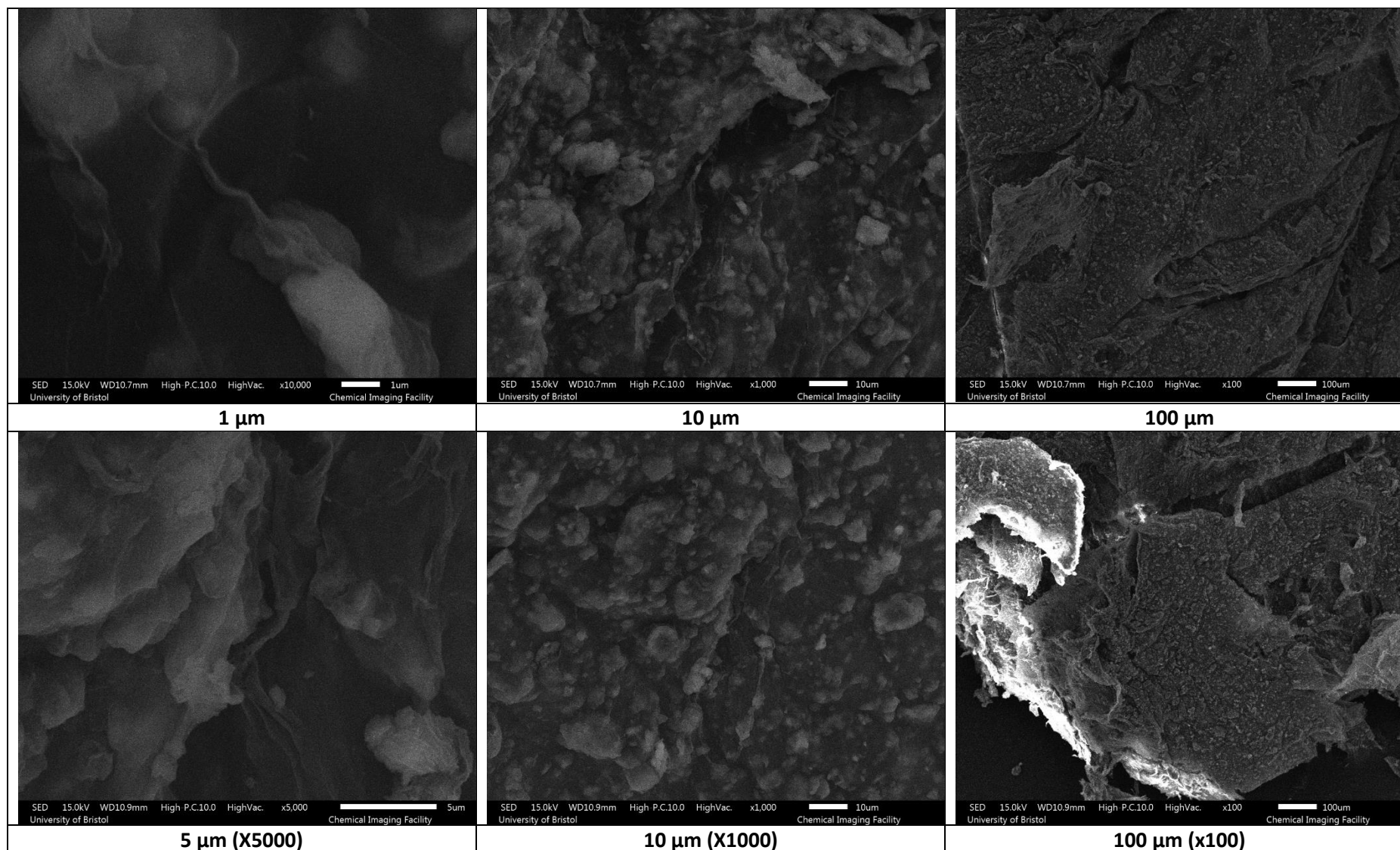
Figure 8.13. SEM images of Alginate (Alg) + modified clay (MMT CHX) sample – Top down.

166

1 μm (x20000) | **5 μm (X5000)** | **10 μm (X1000)**
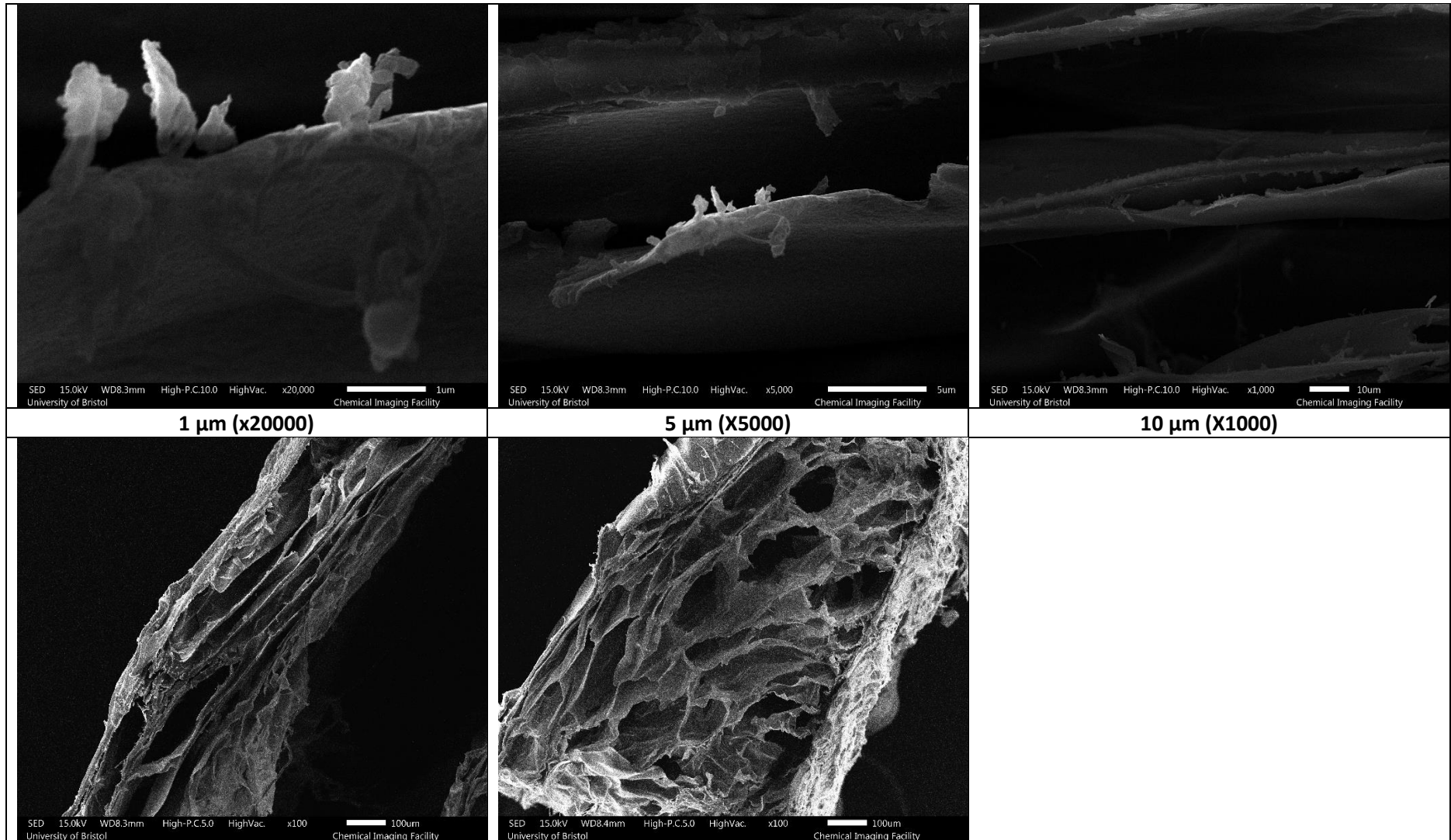
100 μm (x100)	100 μm (x100)	

Figure 8.14. SEM images of Alginate (Alg) sample – Cross section.

1 μm (x20000)	5 μm (X5000)	10 μm (X1000)

| 10 µm (X2000) BED | 10 µm (X2000) SED | 100 µm (x100) |
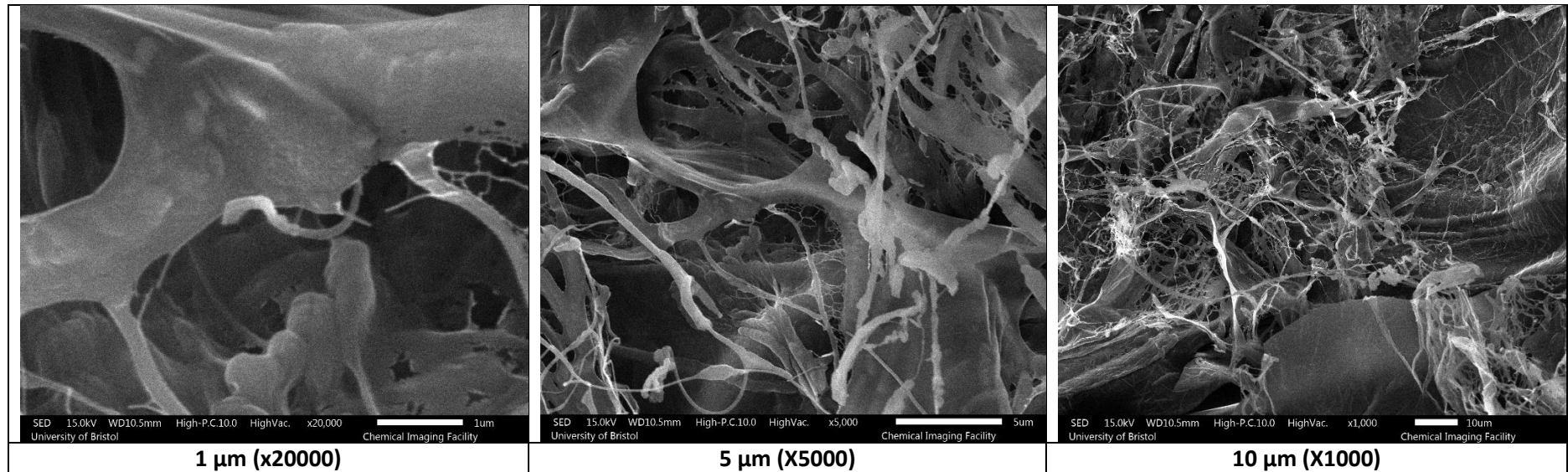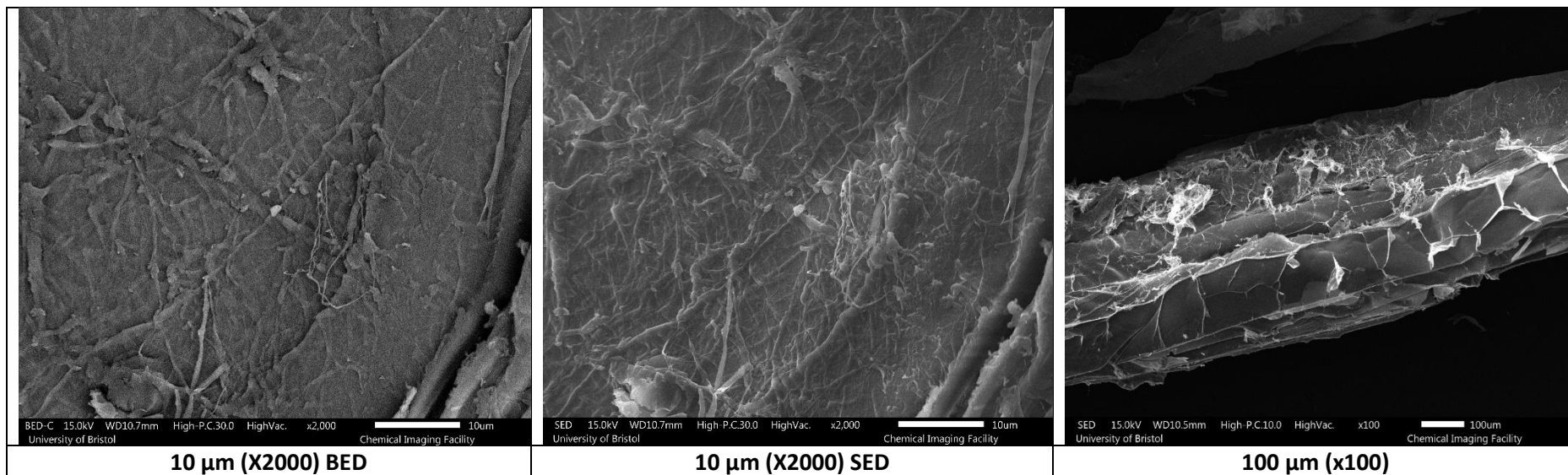
Figure 8.15. SEM images of Alginate (Alg) sample – Top down.

5 μm (X5000) | **10 μm (X2000) BED** | **10 μm (X2000) SED**

100 μm (X100) BED | **100 μm (X100) SED**
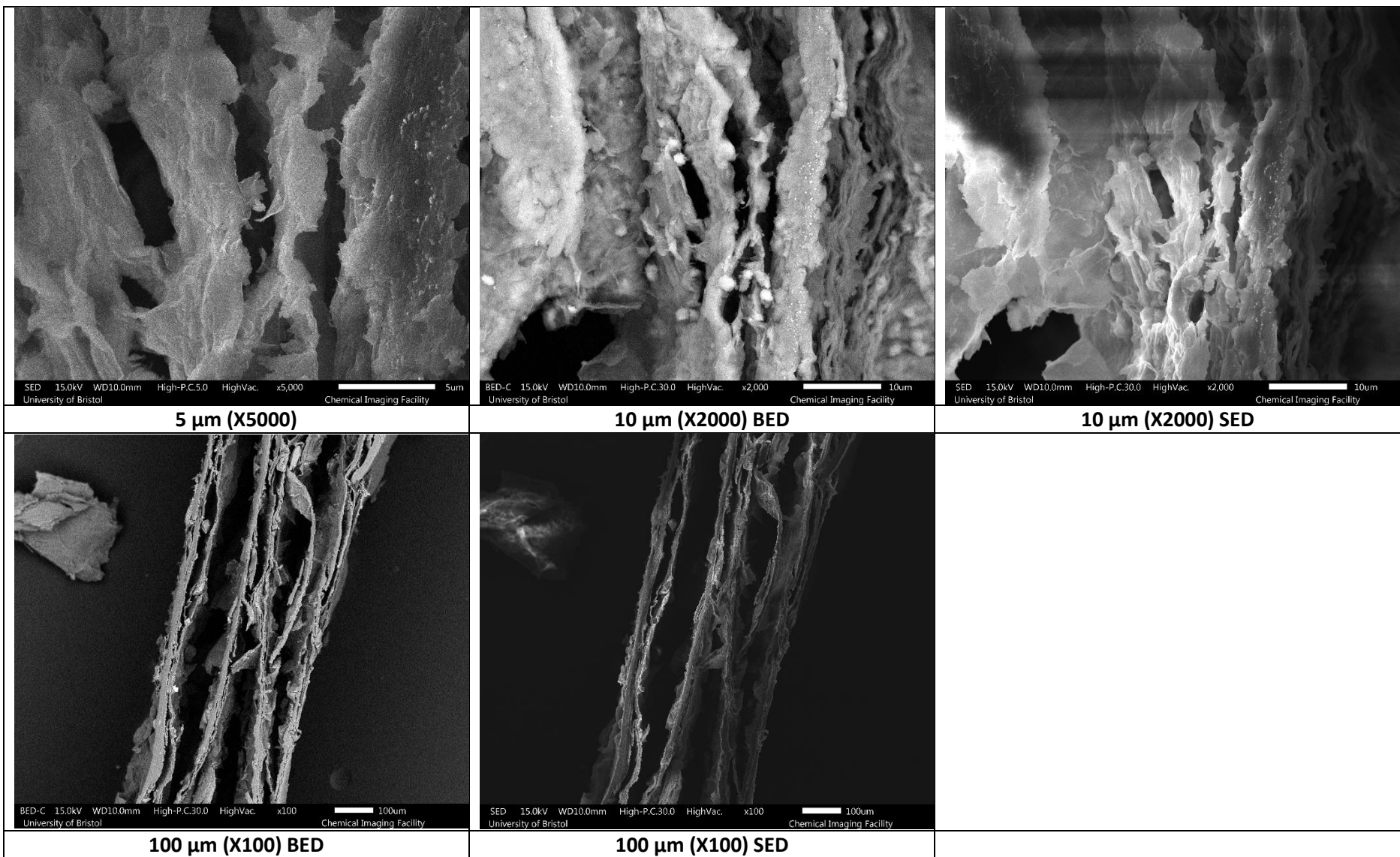
Figure 8.16. SEM images of Alginate (Alg) + clay (MMT) sample – Cross section.

| 10 μm (X2000) BED | 10 μm (X2000) SED |
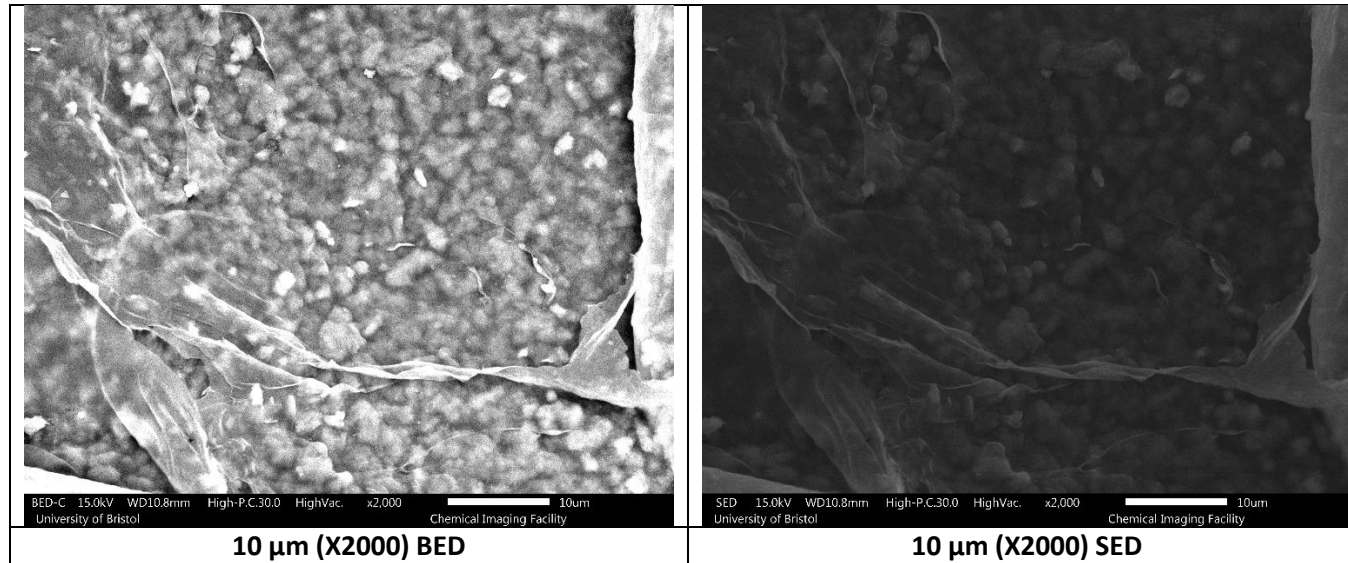
Figure 8.17 SEM images of Alginate (Alg) + clay (MMT) sample – Top down.

5 μm (X5000) BED

5 μm (X5000) SED

10 μm (X2000) BED

10 μm (X2000) SED

| 200 μm (X90) BED | 200 μm (X90) SED |

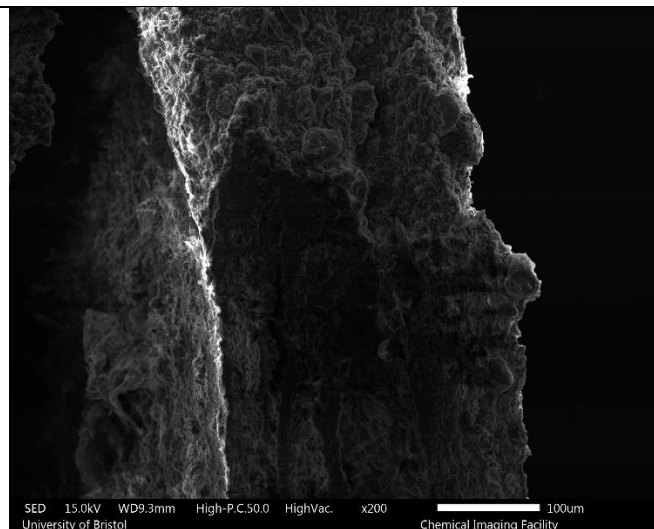*Figure 8.18. SEM images of Alginate (Alg) + modified clay (MMT ADA HCl) sample – Cross section.*

| 10 µm (x2000) BED | 10 µm (x2000) SED |

Figure 8.19. SEM images of Alginate (Alg) + modified clay (MMT ADA HCl) sample – Top down.

10 μm (x2000) BED

10 μm (x2000) SED

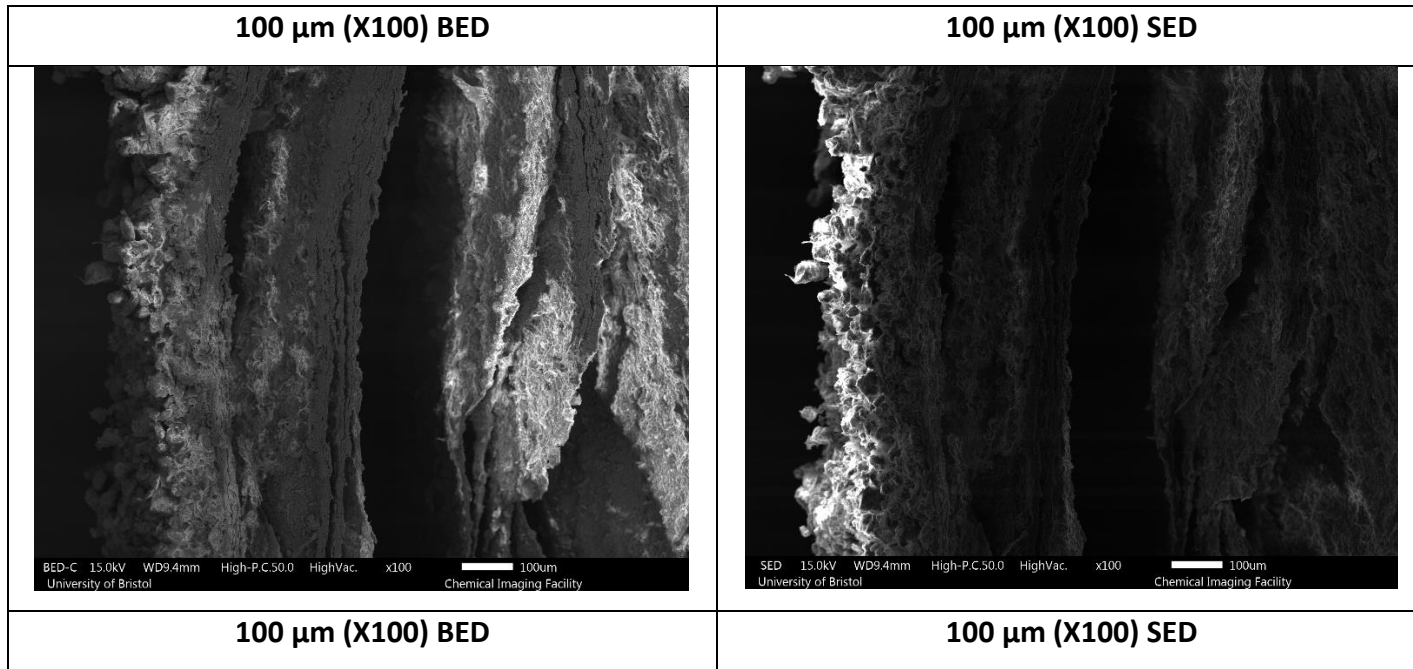**10 μm (x2000) BED**

10 μm (x2000) SED

100 μm (X100) BED
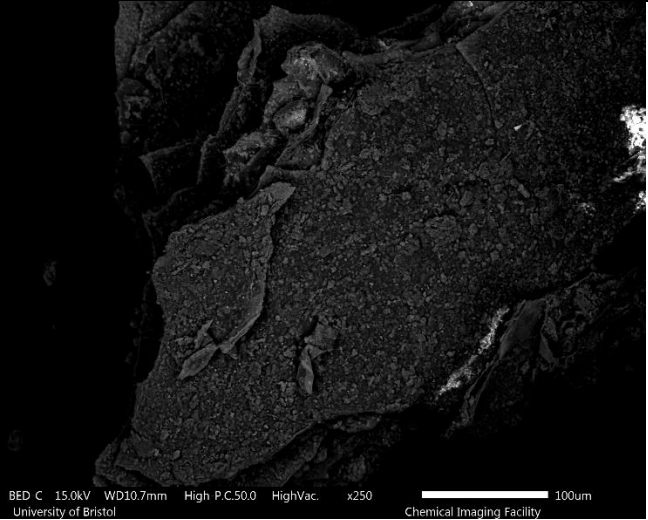
100 μm (X100) SED

100 μm (X100) BED

100 μm (X100) SED

Figure 8.20. SEM images of Alginate (Alg) + modified clay (MMT AHA HCl) sample – Cross section.

10 µm (x2000) BED
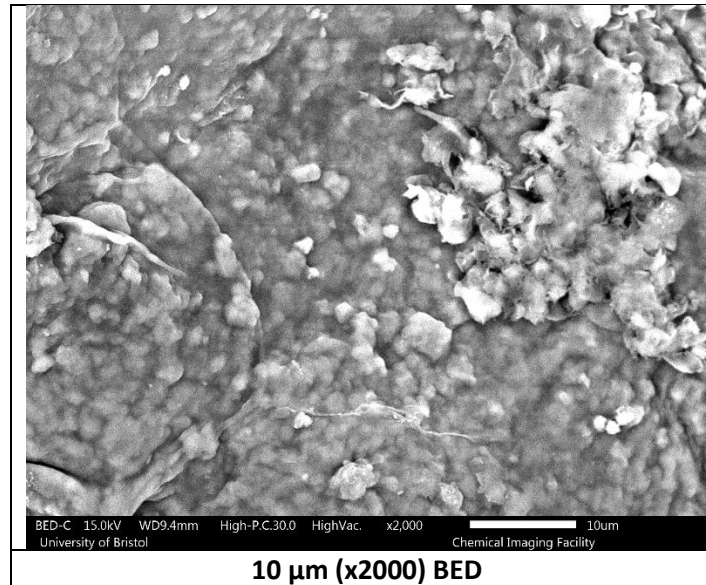
Figure 8.21. SEM images of Alginate (Alg) + modified clay (MMT AHA HCl) sample – Top down.

| 1 μm (x20000) | 5 μm (X5000) | 10 μm (X1000) |
| 100 μm (x100) | 10 μm (X1000) | 100 μm (x250) |
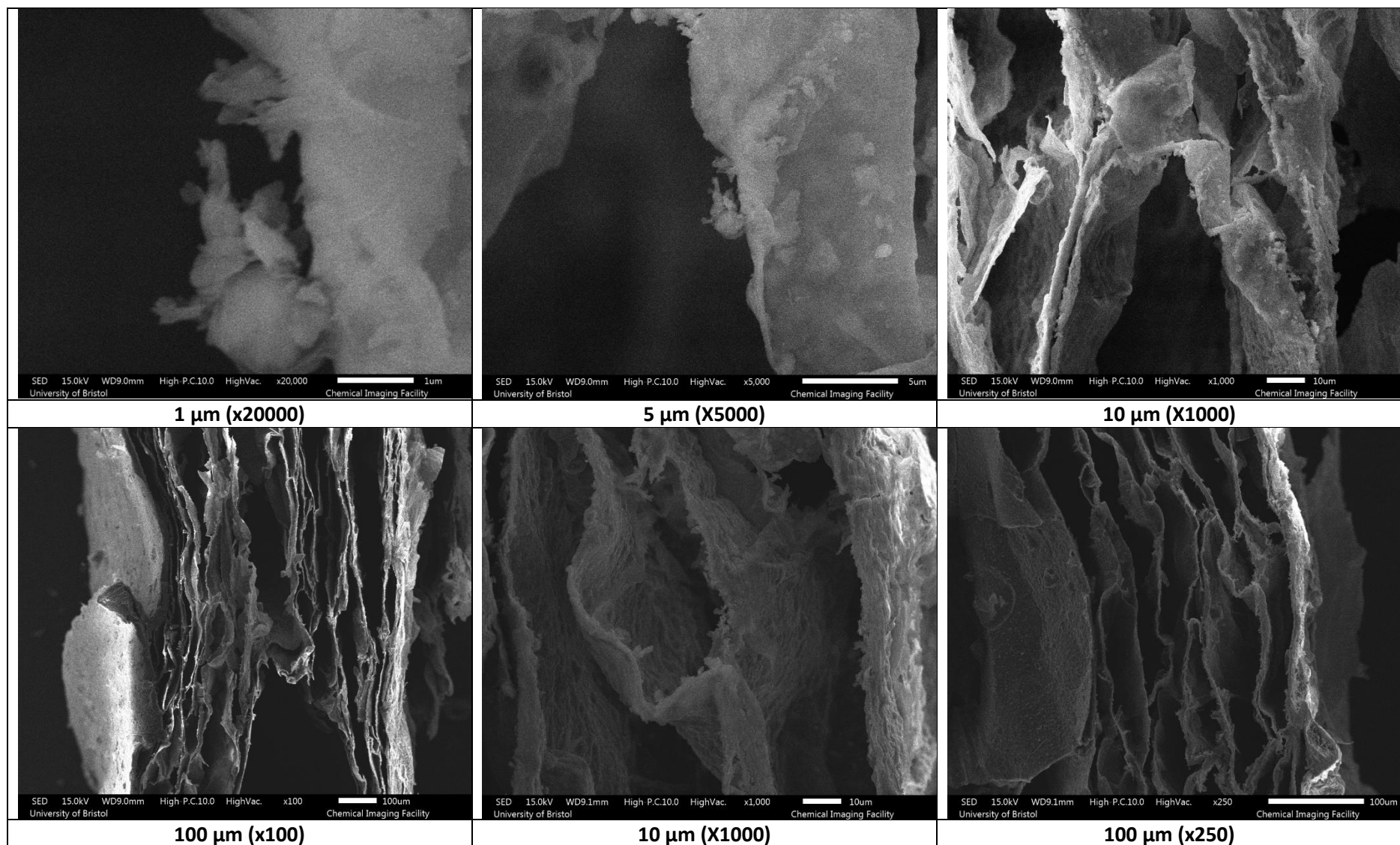
Figure 8.22. SEM images of Alginate (Alg) + modified clay (MMT GABA HCl) sample – Cross section.

1 μm (x20000)

5 μm (X5000)

10 μm (X1000)

100 μm (x100)

10 μm (X2000) BED

10 μm (x2000) SED

50 μm (x500) BED	50 μm (X500) SED
50 μm (x500) BED	50 μm (X500) SED

Figure 8.23. SEM images of Alginate (Alg) + modified clay (MMT GABA HCl) sample – Top down.

10 μm (x2000) BED	**10 μm (x2000) SED**

10 μm (x1000) BED	10 μm (x1000) SED
100 μm (X200) BED	100 μm (X200) SED
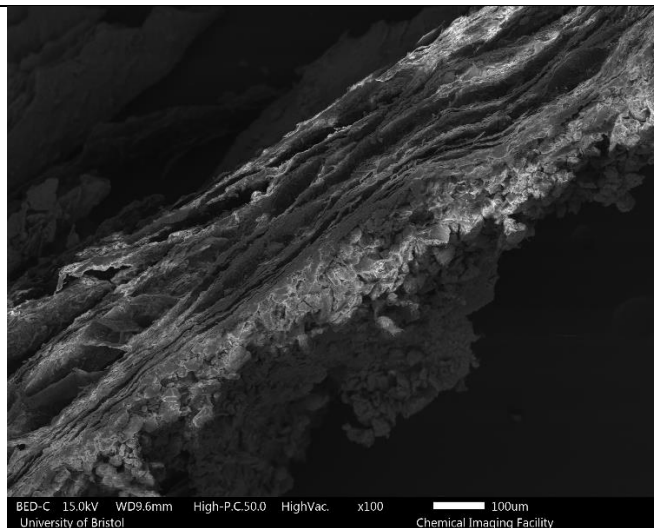
100 μm (X100) BED	100 μm (X100) SED
100 μm (X100) BED	100 μm (X100) SED
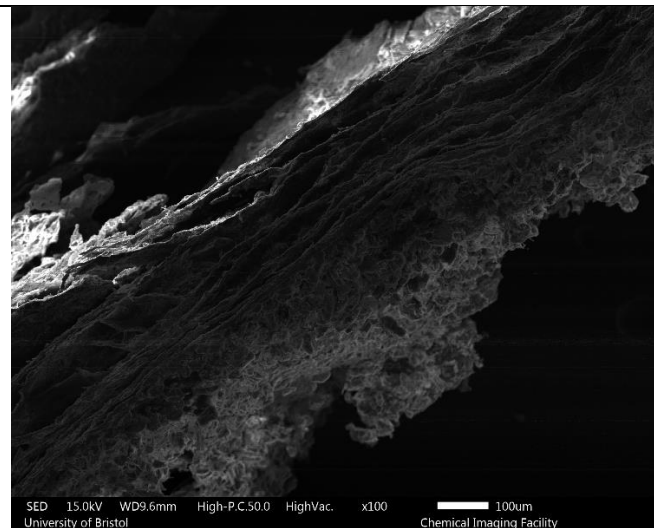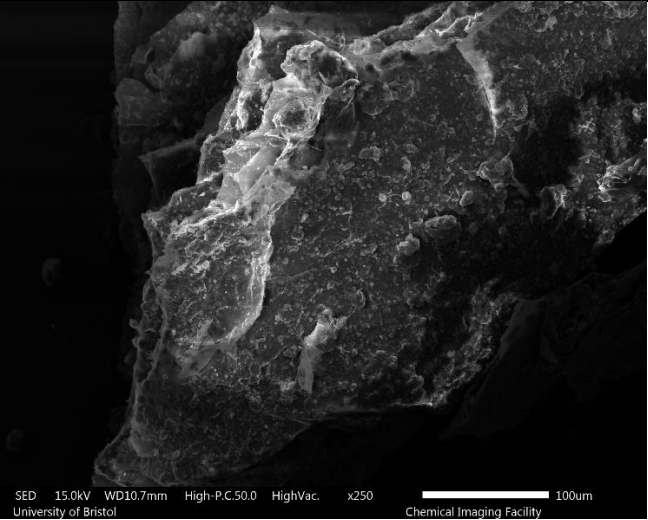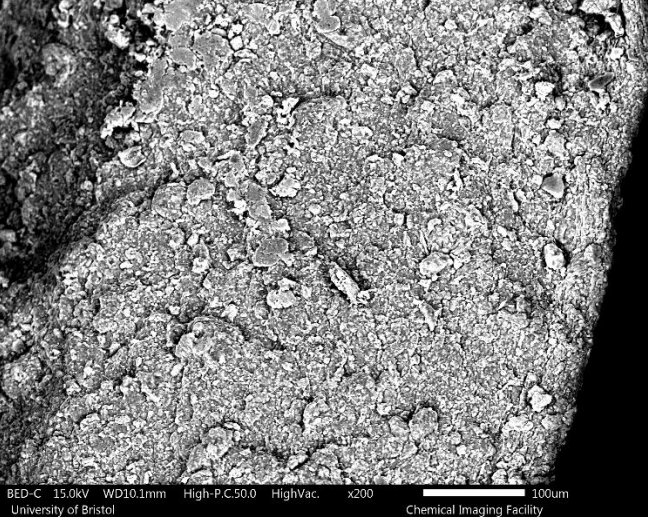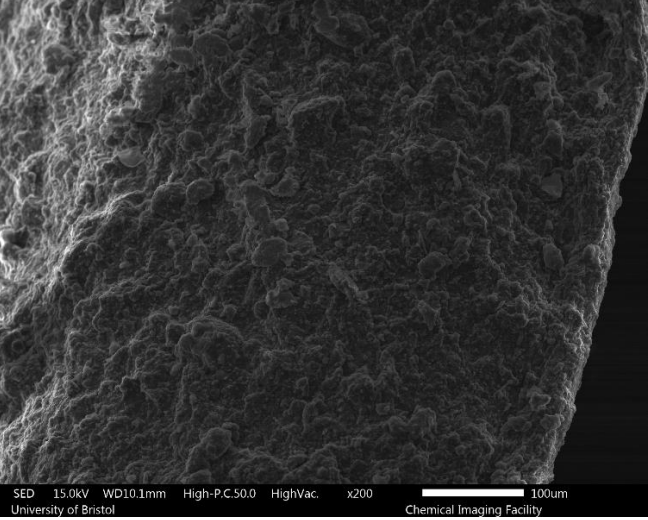
Figure 8.24. SEM images of Alginate (Alg) + modified clay (MMT 1.2 CHX) sample – Cross section.

10 μm (x2000) BED	10 μm (x2000) SED	
		Interlayer
10 μm (x2000) BED	10 μm (x2000) SED	

100 μm (X250) BED	100 μm (X250) SED

100 μm (X200) BED	100 μm (X200) SED

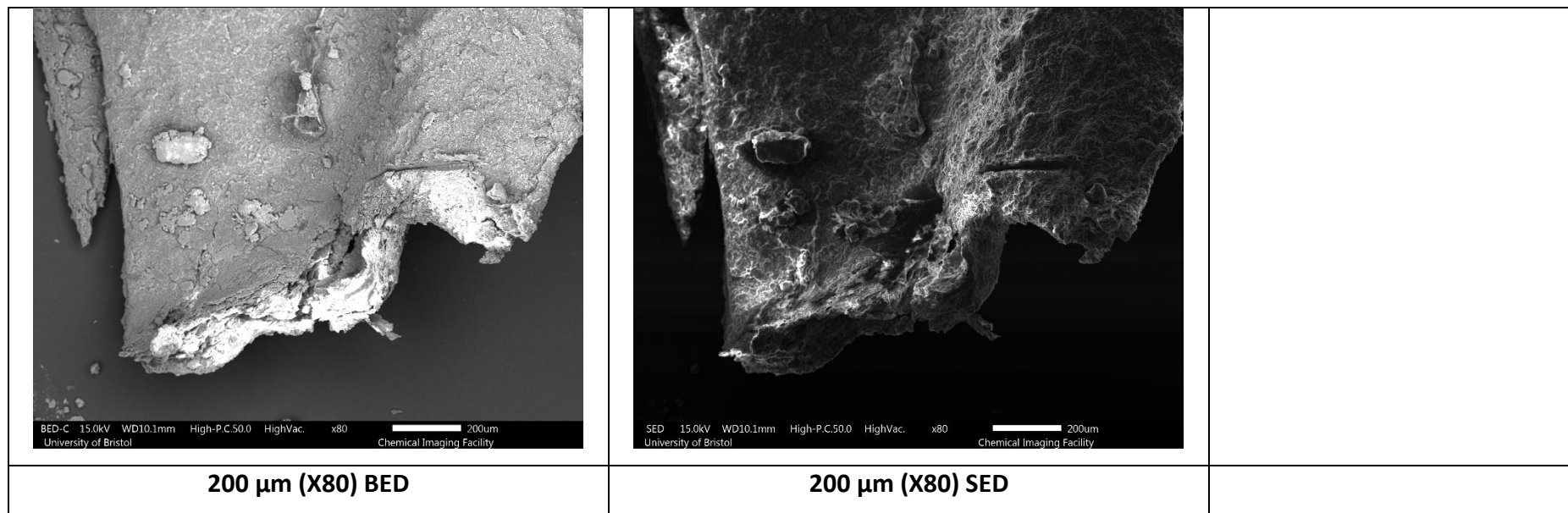| 200 μm (X80) BED | 200 μm (X80) SED | |

Figure 8.25. SEM images of Alginate (Alg) + modified clay (MMT 1.2 CHX) sample – Top down.